UILU-ENG-98-2001

CIVIL ENGINEERING STUDIES
Hydraulic Engineering Series No. 55

ISSN: 0442-1744

Hydraulic Model Study for the Restoration of Batavia Dam, Fox River, Illinois

By

Jonathan T. Armbruster

and

Marcelo H. Garcia

Sponsored by:

**Illinois Department of Natural Resources
Office of Water Resources
(IDNR BIE-9720 S97-171)**

**DEPARTMENT OF CIVIL ENGINEERING
UNIVERSITY OF ILLINOIS AT URBANA-CHAMPAIGN
URBANA, ILLINOIS**

April 1998

Abstract

The Batavia Dam is located in the town of Batavia, Illinois on the Fox River (river mile 56.26). Aging and inappropriate approach flow patterns developed by an upstream island have resulted in structural failure of the dam. The left extreme of the spillway crest has been breached, and significant flow travels overland around the right abutment and down a natural bedrock cascade. The spillway performance, especially during intense storm events, has been deteriorating. The goal of this study was to propose and test rehabilitation and/or replacement dam structures for the Batavia site.

To this end, a 1:30 physical model based on Froude similarity was constructed. The model was calibrated for the existing condition in terms of stage response and flow split characteristics around the upstream island. Detailed stage, velocity, specific discharge, and flow visualization measurements were taken for five flooding event (2, 10, 50, 100, and 500 year flows) in order to fully characterize flow conditions. A baseline, or breach repaired structure, was tested in a similar fashion to provide a comparison benchmark.

Phase two of the research involved design and testing of three alternative dams for the Batavia site. Alternative I added a bathtub spillway to a conventional ogee spillway along the same alignment as the existing structure. Alternative II replaced the existing dam with a rock dam. The final alternative provided a modified ogee spillway with two distinct overflow structures to accommodate the flow approaching from left and right sides of the island. For each of these alternatives, stage, velocity, specific discharge, flow visualization, and general response characteristics of the structures were studied.

Alternative I was found to produce improvements in the upstream approach. Flood stage ratings were comparable to those found for the existing condition. Downstream discharge characteristics were slightly improved. Alternative II provided few hydraulic improvements on-site, and the rock dam promoted higher flood stages. Alternative III resulted in excellent approach and downstream discharge characteristics. Flood stages were reduced for all conditions tested. The potential for development of an undesirable submerged roller for Alternative III was noted.

Based on the study, Alternatives I and III are recommended for candidates as replacements for the Batavia Dam structure. Both of these alternatives produced acceptable and improved hydraulic conditions at the site. The two alternatives offered distinct and competing sets of advantages and disadvantages, and the final selection between them will depend on a weighing of economic, community, and technical priorities. Prior to implementation, continued study and optimization of the chosen alternative is strongly recommended.

Acknowledgements

This research was sponsored by the Illinois Department of Natural Resources, Office of Water Resources. This financial support as well as the advice and contributions of DNR Project Manager, Bill Rice, was greatly appreciated.

Undergraduate research assistants Andy Peabody and Tim King provided vital assistance in each phase of this effort. The success of this study is due, in part, to their hard work and commitment. Thanks is also extended to graduate students Juan Fedele, Andy Waratuke, David Admiraal, Jose Rodriguez, and Juan Gonzalez for their advice and input.

The Civil Engineering Shop provided construction expertise, and their role in this project was greatly appreciated. Their experience, knowledge, and cooperation were instrumental in organizing, building, and perfecting the Batavia Dam model.

This report was submitted by Jonathan Armbruster in partial fulfillment of requirements for the degree of Master of Science in Environmental Hydrology and Hydraulic Engineering in Civil Engineering at the Graduate College of the University of Illinois at Urbana-Champaign in May 1998.

Table of Contents

List of Tables

Table

List of Figures

Figure

1. Introduction

1.1 Background

Batavia Dam is located on the Fox River, Kane County, Illinois, at river mile 56.26 in the town of Batavia. Figure 1.1 shows the relative location of the town of Batavia within the state of Illinois along with an aerial photo inset of the site. Figure 1.2 shows a photograph of the Batavia Dam in its current condition.

The History of the Dam begins in the early 1800's when water ponded by the dam was used to operate a saw and grist mill. Records from 1916 show a concrete dam with a modified ogee shape in the east channel connecting Island 193 to the east bank of the Fox River. A 1934 survey reports a dam height of 5.8 feet and a spillway length of 328 feet. A 1946 survey places the spillway crest elevation at 665.09 feet above mean sea level.

In the early 1970's, the spillway at Batavia Dam began experiencing structural problems. A report prepared by the Illinois Department of Transportation states: "The west end appears today as being anchored in the rock side slope of island 193. Moderate flow tends to skirt this end of the spillway and form a cascade on the rock slope. The east end abutment which was surveyed in 1934 as a V-shaped concrete retaining wall appears to have completely collapsed on one leg of the V, exposing the retained fill to tailwater action. Some shallow portions of concrete are broken off of the crest of the dam. Undermining of the east end and abutment, which was noted subsequent to the 1974 writing of this report, has continued and resulted in the collapse of a 15 foot section of the crest. It is estimated that extensive work is now needed to restore the structure." (Illinois Department of Transportation, 1974)

Since 1974, extensive work has been done at Batavia Dam to keep the spillway operational, including a 1978 study conducted by IDOT to reconstruct the Dam. However, most of the remedial work has been of a temporary nature, and the spillway performance, particularly during intense storm events, has not been appropriate. At the same time, there are increasing doubts over the structural integrity of the dam. Clearly, a permanent solution needs to be found for this serious problem.

1.2 Objectives

A physical model of the Fox River has been constructed in the Hydrosystems Laboratory of the Civil Engineering Department at the University of Illinois. A 1 to 30 scale model based on Froude similarity allows for investigation of over 1200 feet of the Fox River in the laboratory's newly constructed model basin.

Research objectives for this study can be summarized in three distinct steps. First, the selected river area must be scaled and modeled correctly within the laboratory environment. Second, once the model is constructed, it must be calibrated to assure that it correctly reproduces prototype flow characteristics. During the calibration phase, data will be collected to better describe and understand the existing conditions on-site. Using this information, the final objective will be to design, construct, and test alternative dam configurations. At the conclusion of this research, a recommendation will be made as to how the Batavia Dam may be successfully rebuilt and/or rehabilitated.

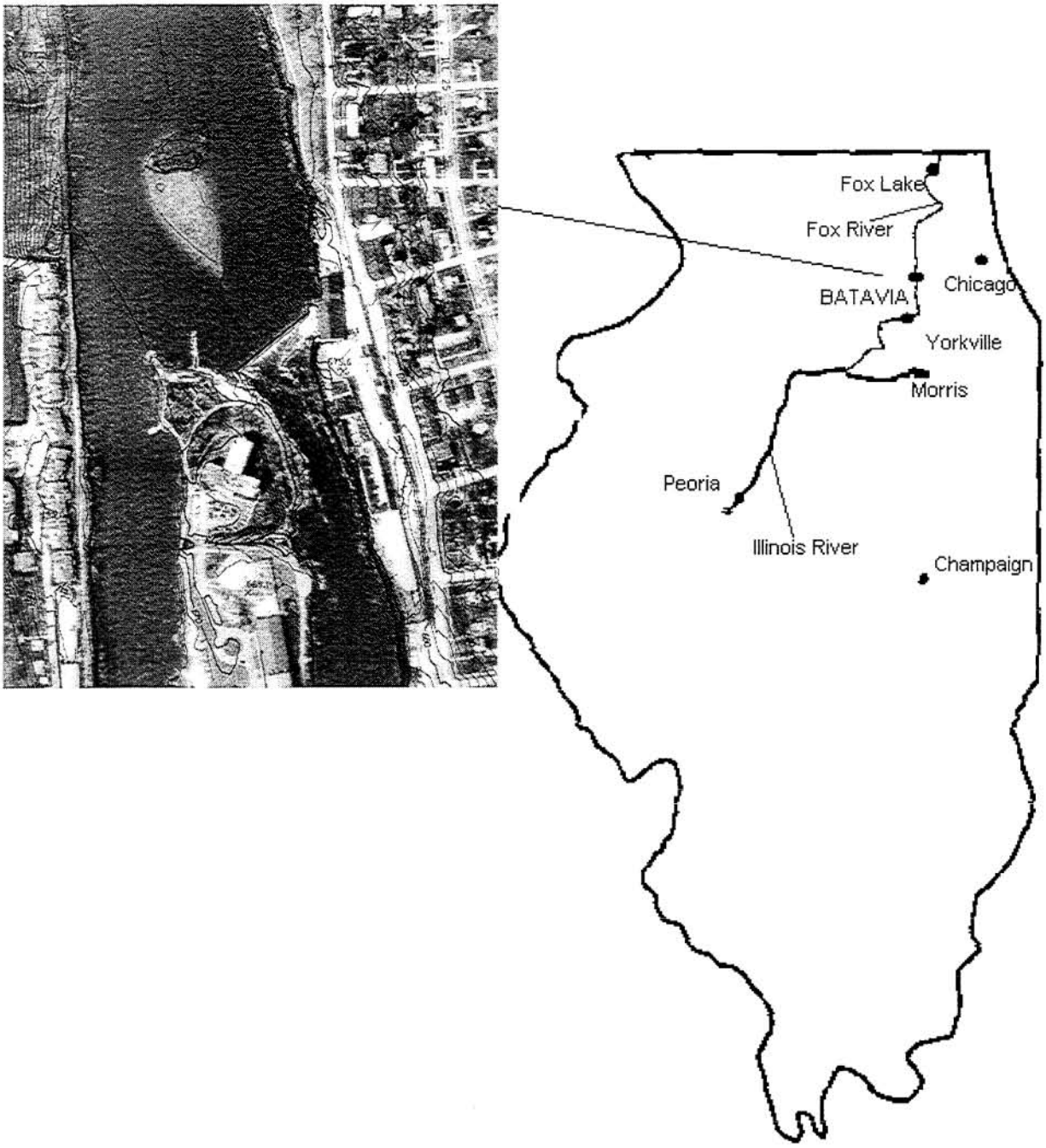

Figure 1.1. Location of Batavia Dam with aerial photo inset

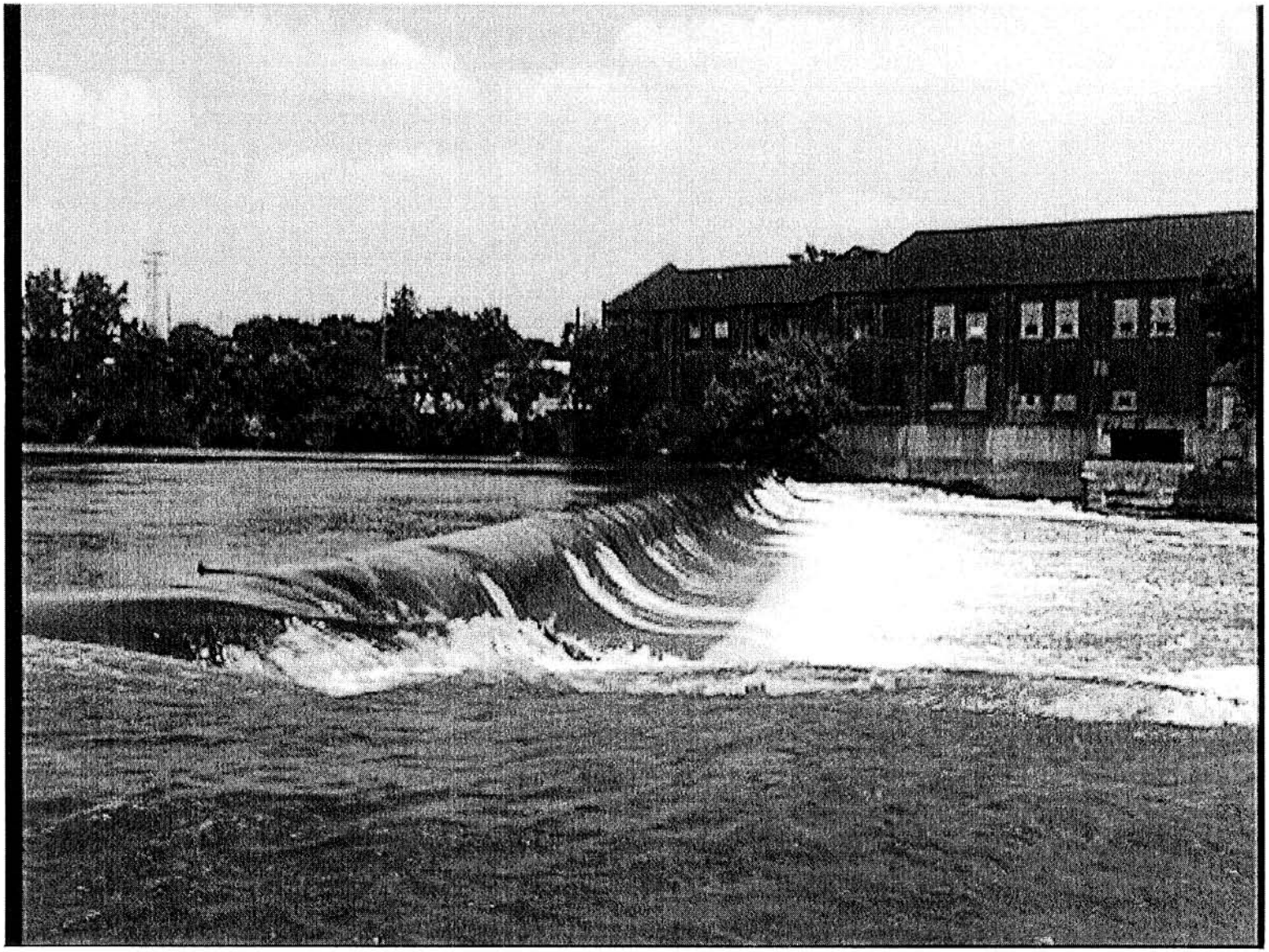

Figure 1.2. Existing Batavia Dam spillway (6/28/97)

2. Model Design and Construction

2.1 Principles for hydraulic modeling of open channel flow

Any hydraulic modeling study is based on the principle of similitude; in general, similitude is the indication of a relationship between two phenomena. In the case of this research, the relation is that of a full-scale flow through an open channel (The Fox River) and the flow through a hydraulically similar, yet geometrically smaller, model of the open channel.

For hydraulic similarity to exist, however, more than just geometric similarity between model and prototype must be preserved. It is also necessary that both model and prototype streamlines be geometrically similar: this is termed kinematic similarity.

Yet a third type of similarity is necessary to allow for accurate hydraulic modeling: dynamic similarity indicates that the force distribution between the two flows is such that at corresponding points in the flow, identical types of forces have the same direction and are proportional in magnitude. In addition, the model and prototype force magnitude ratio must have the same value at all sets of corresponding points between the two flows. In order to attain dynamic similarity two conditions must be met. First, the aforementioned kinematic similarity must exist. Second, the flow must have a similar mass distribution.

The strict requirements of hydraulic similarity can be simplified and summarized through dimensional analysis; the analysis provides dimensionless groups which must be duplicated between geometrically similar flows. When gravitational forces are dominant, as in most open channel situations, similarity can be established by equating the model and prototype ratio of inertial forces to gravitational forces. This ratio is expressed in the dimensionless number known as the Froude number:

$$F = \frac{V}{\sqrt{gH}} \qquad 2.1$$

where V is the mean flow velocity, g is the gravitational acceleration, and H is the mean flow depth.

Other forces important in open channel flow are viscous (frictional) in nature. The role of these forces can be expressed as the ratio of inertial forces to viscous forces. This ratio is known as the Reynolds number:

$$R = \frac{VH}{\nu} \qquad 2.2$$

where ν is the kinematic viscosity of the fluid. Strictly speaking, the model and prototype Reynolds number must be equal. However, satisfying both the Froude and Reynolds law is impractical for open channel flow studies. Thankfully, if both model and prototype flows are within the turbulent regime, the role of frictional forces between model and prototype can be assumed near equivalent. Hence, the Froude law is sufficient to develop an accurate hydraulic model.

A geometric length scale of 1 to 30 was chosen to satisfy facility space constraints. Using the Froude Law, the prototype/model parameter ratios are quantified with the following similitude relations.

$$L_r = \frac{L_p}{L_m} = 30 \quad (2.3)$$

$$A_r = L^2{}_r = 900 \quad (2.4)$$

$$T_r = L^{1/2}{}_r = 5.5 \quad (2.5)$$

$$V_r = L^{1/2}{}_r = 5.5 \quad (2.6)$$

$$Q_r = L^{5/2}{}_r = 4929.5 \quad (2.7)$$

Here, the subscript m and p refer to the model and prototype respectively. The subscript r is used to represent a ratio where:

L_r = Length ratio

A_r = Area ratio

T_r = Time ratio

V_r = Velocity ratio

Q_r = Flow ratio

2.2 Model basin

The Fox River/Batavia Dam Model required the design and construction of a large model basin. The basin infrastructure (walls, "channels," and piping) were designed as a permanent addition to the Hydrosystems Laboratory to allow for future modeling efforts.

Total basin dimensions, including head and tailwater channels, are approximately 49 x 37 feet. Water enters the model through a 3 foot head channel. Exiting flow fills a tailwater channel before leaving the basin over a leaf-gate and into the laboratory's drainage channels. The walls are of poured concrete, 3 foot tall, 8 inches thick, and reinforced with #3 rebar. Figure 2.1 is a drawing of the basin.

2.3 Water supply and flow measurement

Hydraulic flow is maintained through a recirculating system. Water is pumped from the laboratory sump into the constant head water tower outside the lab. From here, flow travels through a fourteen inch diameter pipe to the model. At this point, flow branches into two eight inch pipes leading to diffuser manifolds within the model basin head channel. The eight inch pipes are equipped with valves for controlling flow into the model. Water travels through the model before entering the tailwater channel and spilling over a leaf-gate into the laboratory's drainage channel. The channel conveys the flow to the laboratory sump.

Flow metering is accomplished through the use of a Dall Flow tube installed in the fourteen inch diameter pipe upstream of the model basin. The tube is connected to a manometer filled with manometer blue fluid having a specific gravity of 1.75. The metering system was calibrated in-situ using the laboratory's weighing tanks. The calibration curve has been include in Appendix I (Figure AI.1).

2.4 Topographic modeling

In order to properly construct a hydraulic model, the river topography must be reproduced within the laboratory environment with great accuracy. This procedure was facilitated by field surveys conducted by the Illinois Department of Natural Resources between April 1996 and March 1997. In all, topographic data for over 30 river cross sections were made available in AutoCAD format. These survey were easily manipulated and scaled to provide plots of full (model) scale templates of river cross sections.

These template plots were overlaid and cut from 20 gage sheet metal with a pneumatic "nibbler". This effort required cutting over 800 linear feet of sheet metal. Within the basin, along the proper transects, 16 gage sheet metal L-brackets were fastened to the floor. The proper elevation for each topographic template was determined with a survey level. The templates were then fastened to the floor brackets with an electric spot welder. Figure 2.2 is a drawing of the model basin showing the location of the cross section templates used in construction of the model. Figure 2.3 is a photograph showing several installed templates.

The topographic templates provided a guide for pouring and contouring of a concrete "cap" representing the river bottom. Of course, the spaces between the cross-sections required preparation prior to pouring concrete. Usually, these spaces are filled with cinder block, sand, gravel, or some such combination. The size of this model made these conventional fill materials expensive and impractical. Therefore, it was decided to build a sheet metal form work between the sections to support the concrete as well subsequent water and live loads. This innovative technique, suggested by the UIUC Civil Engineering Shop, required the construction of "pan" structures out of sheet metal. These pans were spot-welded in place between the cross-sectional templates. A 2x4 column placed beneath the pan provided direct load path to the floor. The "pan and column" technique, though somewhat time consuming, provided a stable form for the pouring of a 2 inch concrete cap. Figure 2.4 is a photograph showing the installation of the metal pans.

2.5 The "soft" section

The goal in this investigation is to test as many design alternatives as possible in the shortest period of time. Simply put, the more alternatives tested, the more likely the optimum design will result. Ideally, the area around the dam would be soft and mutable to allow for rapid changes to channel configuration. At the same time, the channel must be strong and rigid enough to resist hydraulic forces and allow for practical testing. The "soft" section is an attempt to attain the best of both worlds: a rigid channel which can be rapidly modified and replaced.

This has been accomplished by building a steel frame which can be removed by the 10 ton capacity crane available within the lab. In effect, this allowed for the removal of an entire portion of the river bed. The 14 foot square soft section contained the Batavia Dam and the surroundings most likely to be modified in any rehabilitation design. The area represented 176,400 square feet of river area. Two identical steel frames were constructed from 8" C-channel sections. These frames were designed to withstand lifting under the full weight of construction materials. Each corner was equipped with a

leveling jack and lifting iron. The leveling jacks assured that the frame would return to the same place and elevation each time. Sheet metal cross-sections were attached to the steel frame. Between the sheet metal contours, large EPS foam blocks were cut to fit using a hot wire cutter. This material was more expensive than the sheet metal (pans) used previously, but construction was completed in a fraction of the time. A concrete cap was placed over the Styrofoam to form the final river bed channel. Figure 2.5 is a figure showing the relative location of the "soft" section within the Fox River model.

2.6 Modeling the Batavia Dam

2.6.1 Survey data

Illinois Department of Natural Resources' surveys included four cross sections to be used in modeling the dam: upstream side of dam, crest of dam, toe of dam, and downstream side of dam. This data, in conjunction with photographic and historical information concerning the dam's cross – sectional shape, were used for modeling purposes.

2.6.2 Dam breach

The left extreme of the Batavia Dam suffered a considerable breach. In this region, flow conditions were so severe that a complete field survey was impossible. For this reason, it was necessary to model the breach using the available data and engineering considerations.

The location of the breach has been marked in Figure 2.2. The breach was estimated to be approximately 58 feet long. During low flow conditions, it was known that the majority of the river flow passed through the breach; at these times, the intact spillway was inactive. This flow condition was observed during a large portion of the third week of July, 1997. Using data from the Geneva gaging station, it was possible to ascertain that the flow for this period was approximately 800 cfs.

Knowing this information, the breach was modeled as a broad crested weir having an equivalent elevation. Theory available for broad crested weirs (Hwang et al., 1987) allowed for an estimation of the breach elevation. These calculations are summarized in Appendix I (Calculation AI.1). The breach, therefore, was modeled as a broad crested weir extension of the existing dam having a elevation above sea level of 661.81 feet. The breach was then roughened with gravel to more accurately simulate existing field flow conditions.

2.6.3 Movable bed modeling downstream of breach

Flow conditions downstream of the dam breach did not allow for adequate field survey. In order to model the river bottom here, a movable bed was employed. This area has been marked on Figure 2.2.

Movable bed modeling consists of the placement of an appropriate sediment within the study area. The model flow then displaces the sediment and forms a representation of the river bottom. Obviously, the selection of the correct model sediment is necessary to properly model sediment transport.

Physical movable-bed modeling is as much an art as it is a science, and different criteria have been developed over the years by different schools. Herein, a criterion previously used with some apparent success for solving sedimentation problems in Midwest rivers with the help of movable bed models is

used (Parker et al., 1988). It involves the bed shear velocity, u_*, which quantifies flow-induced bed shear stress, and the sediment fall velocity V_s, in a quiescent fluid. These two parameters are indicative of the expected hydraulic behavior of the sediment material making up the river bed. The criteria used in this study to scale the sediment is, therefore, given by:

$$\left(\frac{u_*}{V_s}\right)_m = \left(\frac{u_*}{V_s}\right)_p \tag{2.8}$$

For a previous model study conducted on the Fox River by the University of Illinois Hydrosystems Laboratory (Freeman and Garcia, 1996), sediment samples were collected by the Urbana office of the USGS. These samples were analyzed for particle size distribution. It was determined that, for the Fox River downstream of low-head dams, a realistic D_{50} was approximately 13 millimeters. This information, along with flow characteristics at the location being model, were considered in the determination of correct sediment type and size to be used in modeling. These calculations are summarized in Appendix I (Calculation AI.2). Results indicated that a quartz sediment having a D_{50} of approximately 1 mm could be used at this location for movable bed investigation on the Fox River.

Figure 2.6 is a photograph of the modeled dam breach and movable bed section of the model prior to flow incidence.

Figure 2.7 shows the completed Fox River / Batavia Dam model following design and construction.

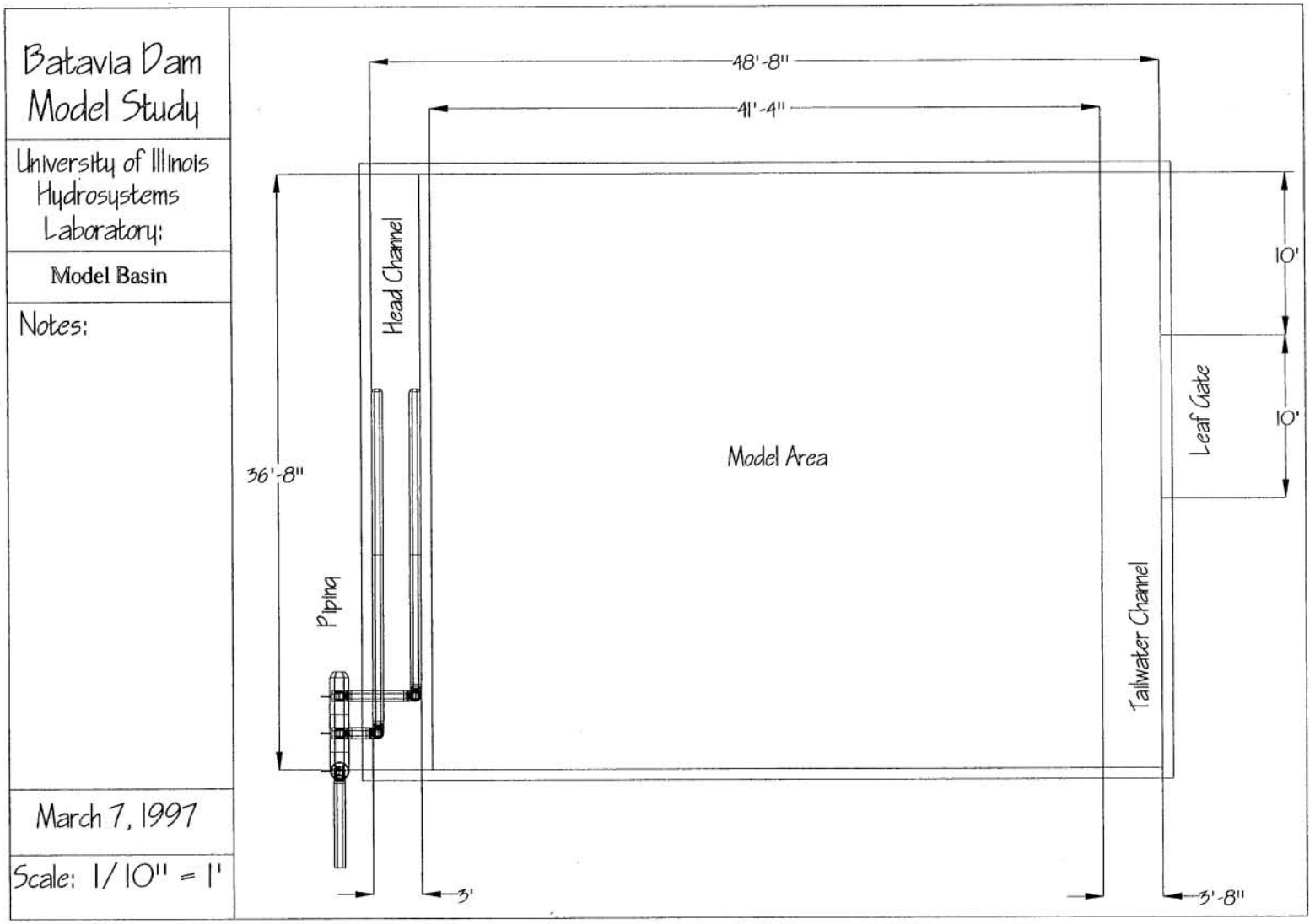

Figure 2.1. University of Illinois Hydrosystems Laboratory model basin

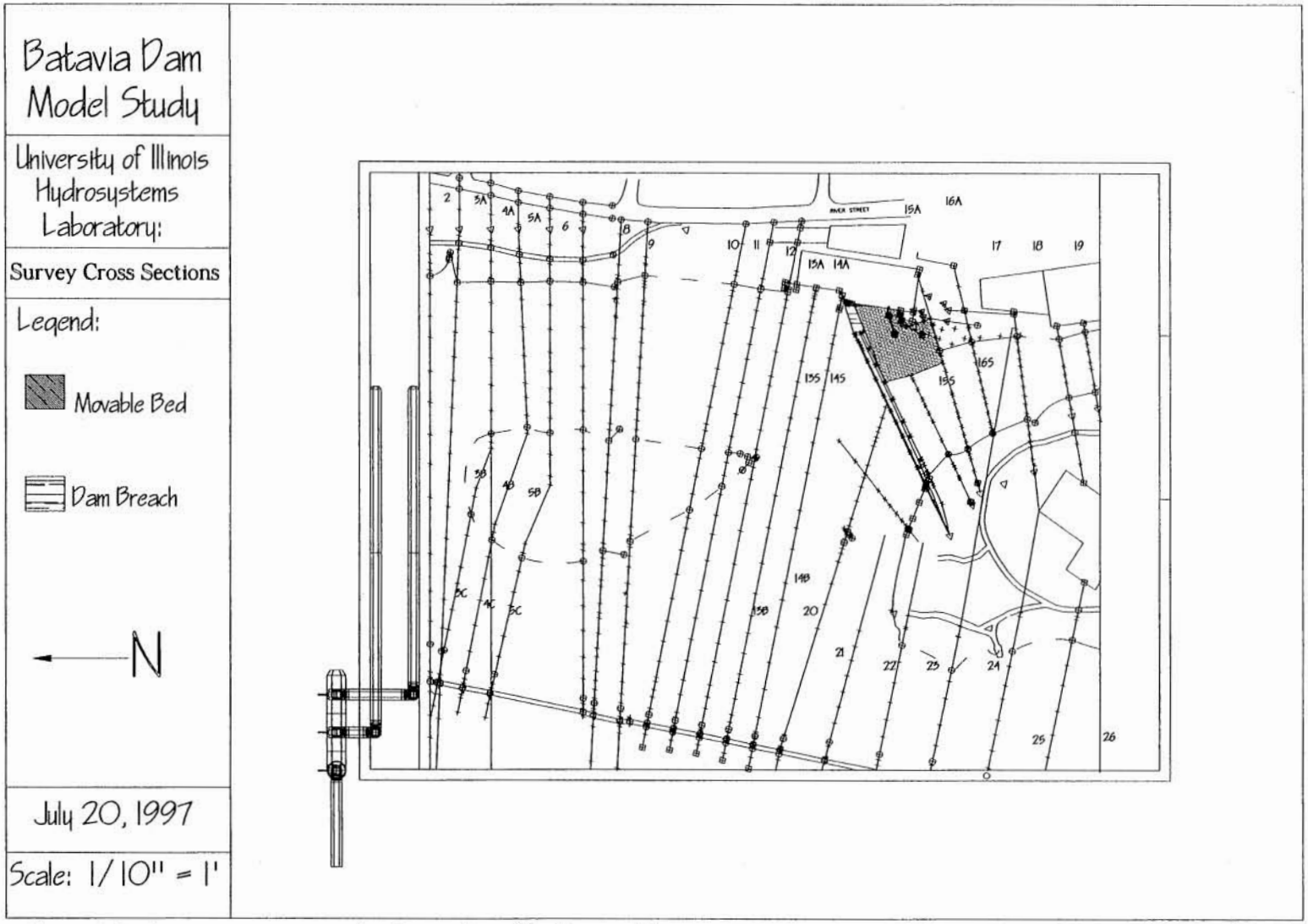

Figure 2.2. Survey cross section used in Batavia Dam/ Fox River model

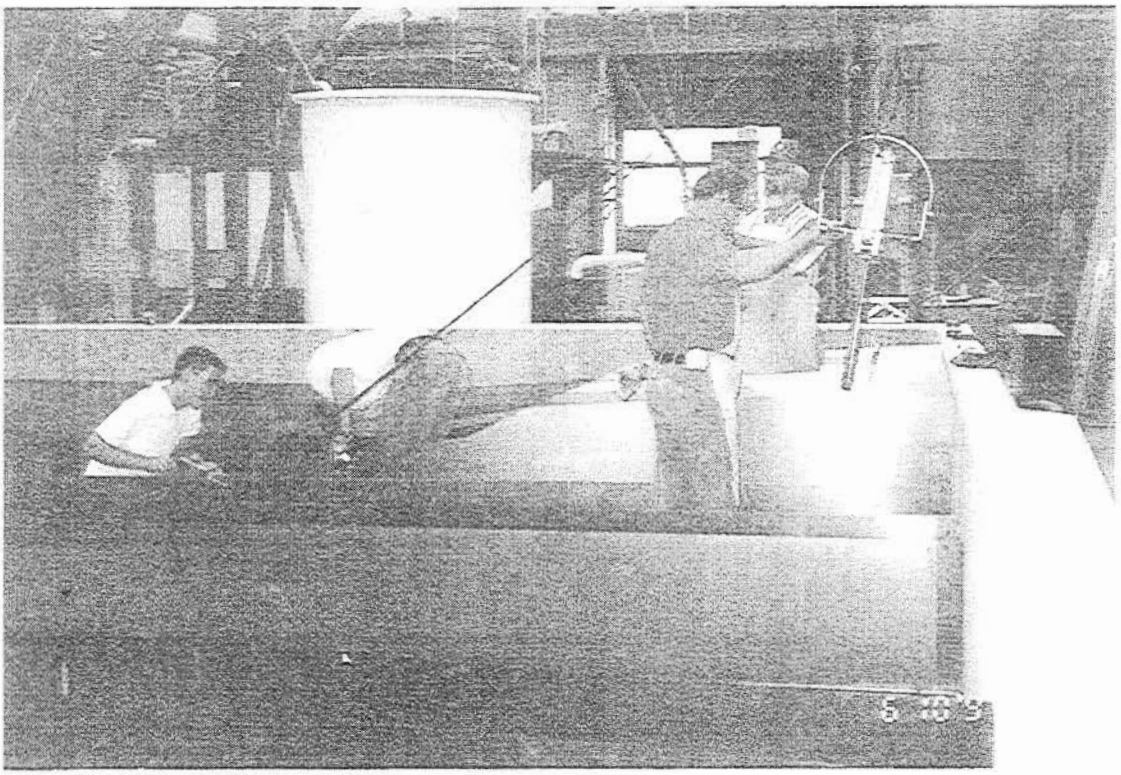

Figure 2.3. Installation of topographic templates

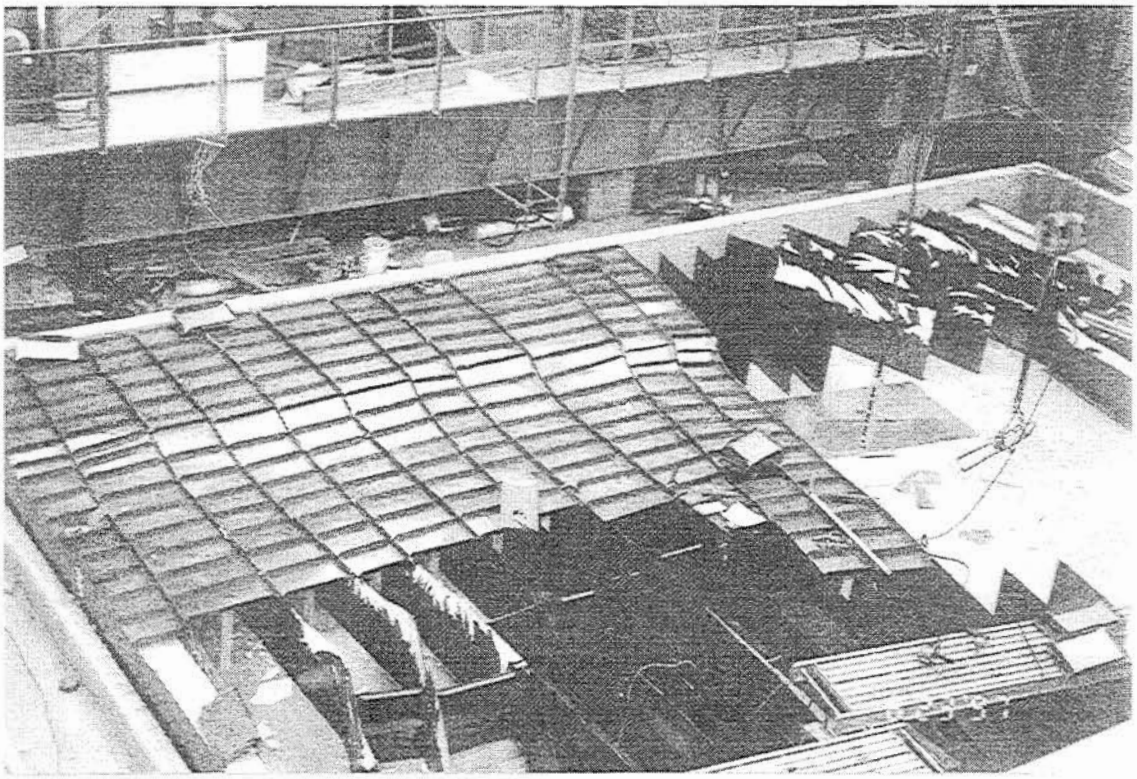

Figure 2.4. Installation of inter-template metal "pans"

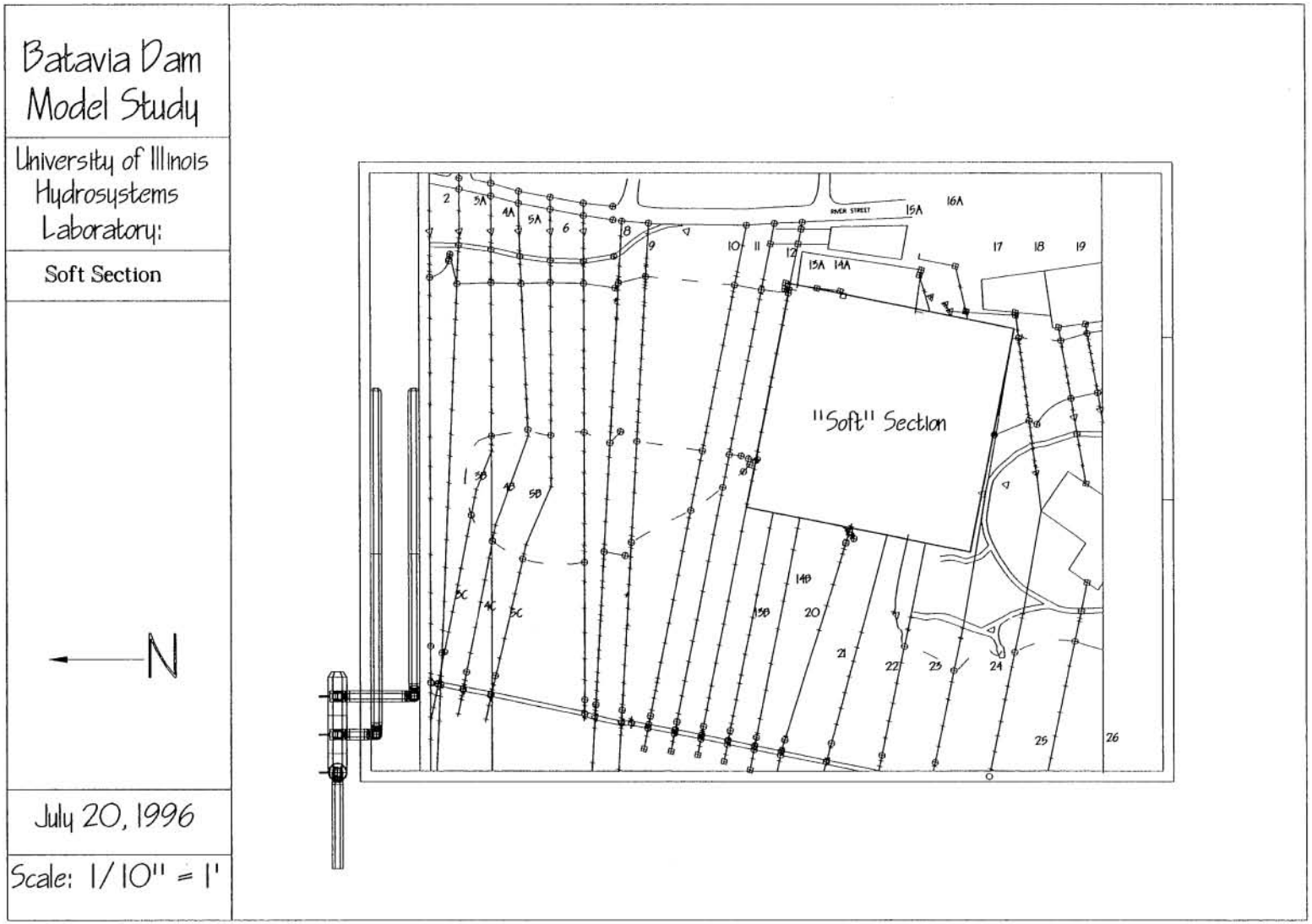

Figure 2.5. Batavia Dam model - Location of "soft" section

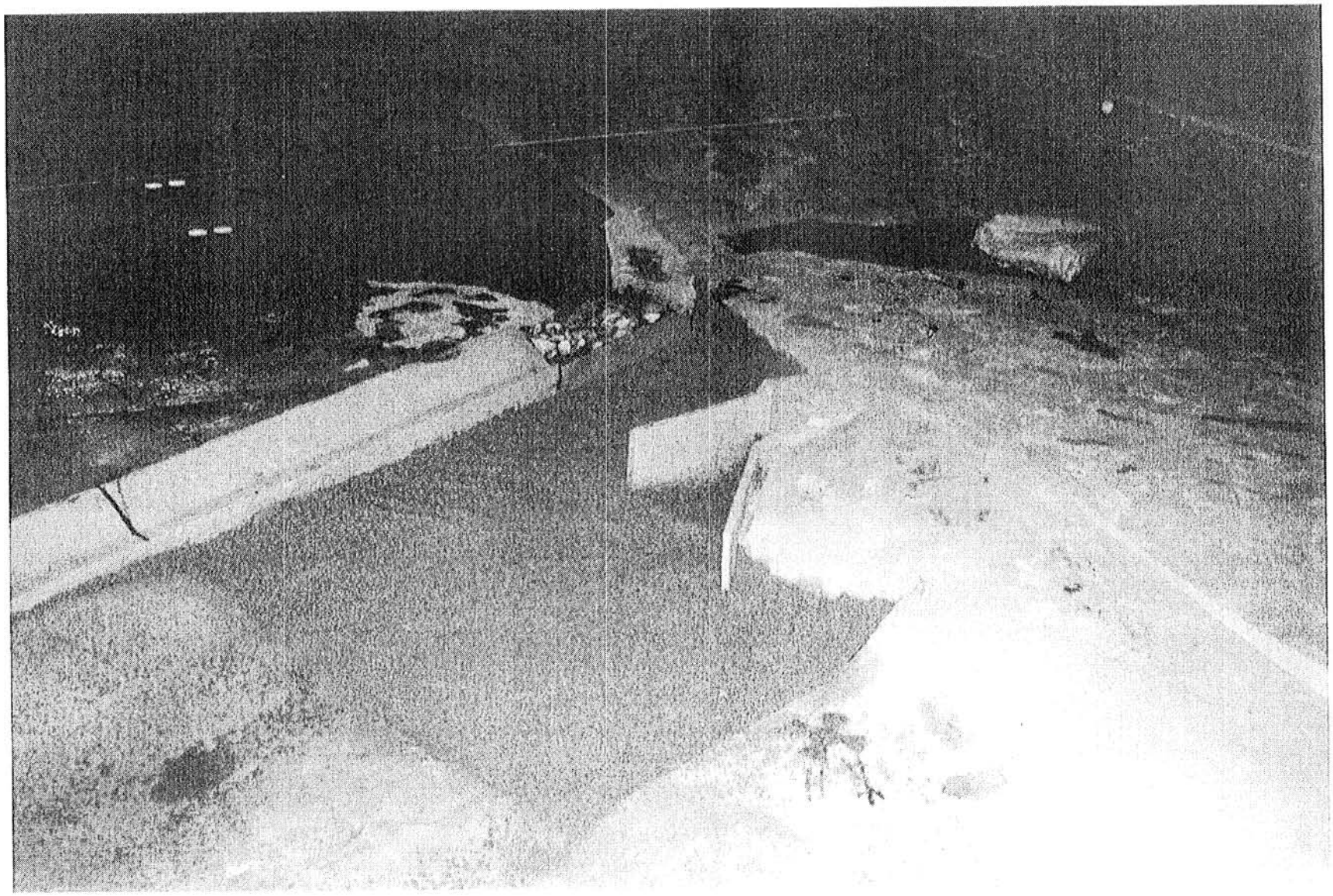

Figure 2.6. Model dam breach and movable bed section

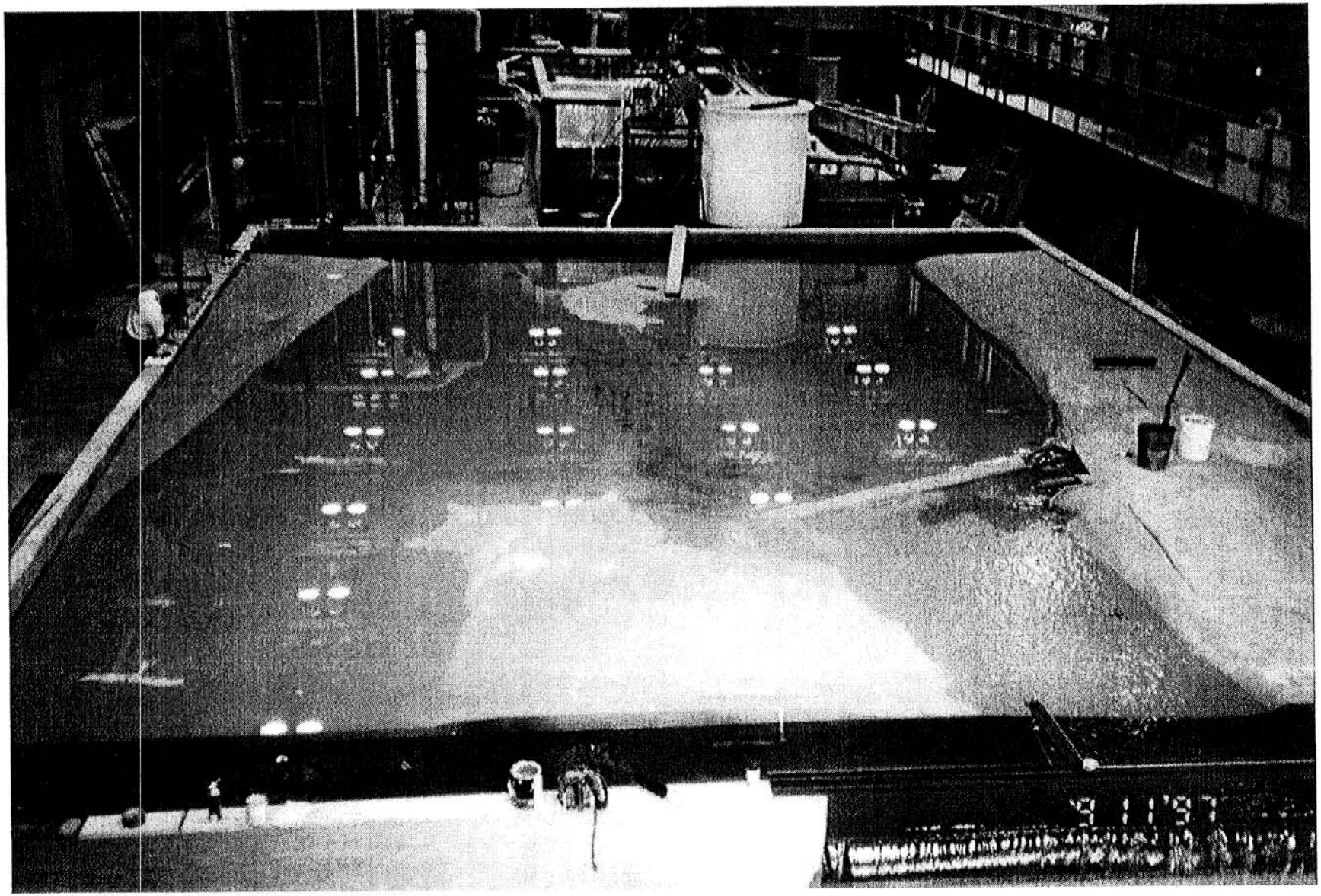

Figure 2.7. Completed Batavia Dam model following design and construction

3. Model Calibration and Flow Characterization

3.1 Model testing flows

The initial step in the calibration phase was the determination of flow magnitudes which best characterize the hydraulic response of Fox River in the vicinity of Batavia Dam. In the design and evaluation of a hydraulic structure, a broad range of flow conditions must be considered. Of primary concern in this study was the response of the structure and river during high flow flooding conditions. Average and low flow conditions were also investigated to insure that the structure operated in a an appropriate manner, offering sufficient aesthetic merit, and minimizing stagnation.

FEMA had completed a study on the Fox River which provides predictions of flow conditions in terms of recurrence intervals (FEMA, 1981). The main flows chosen for investigation in this study have been outlined in Table 3.1.

Table 3.1. Primary flows used in investigation of the Fox River at Batavia Dam

Expected Flows for Fox River at Batavia (FEMA,1981)		Model Parameters	
Recurrence Interval (yr)	Flow (cfs)	Scaled Flow (cfs)	Manometer Displacement (in)
2	5700	1.16	4.91
10	8500	1.72	10.91
50	12500	2.54	23.60
100	13500	2.74	27.52
500	17630	3.58	46.94

Several other flows were used during various stages of the investigation in order to better characterize the response of the model. These include the 1 year flood (4200 cfs), the 5 year flood (7800 cfs), and the 20 year flood (10050 cfs) as defined by FEMA (1981). The only field data available for this study were collected by the Urbana office of the USGS on February 23, 1997. Field investigation indicated the flow at this time was 6062 cfs. This flow was used during the calibration phase of the model and is hereafter referred to as the "calibration" flow.

3.2 Stage-flow relations – Existing condition

3.2.1 Collection of stage data

In order to verify and characterize the response of the model to the above flow conditions, it was necessary to collect detailed stage (water surface elevation) data. Complicated flow patterns induced by the island, peninsula, and breached hydraulic structure were expected to result in considerable variation in stage for any given cross section within the river. Therefore, numerous stage measurement stations were necessary to sufficiently characterize the stage response of the model. In all, thirteen measurement stations were chosen. The location of these stations have been illustrated

on Figure 3.1. The measurement stations have been labeled with letters A through I with A being the extreme most upstream measurement station and I being the extreme most downstream measurement station. Each letter represents a single river cross section (see Figure 2.2) taken approximately perpendicular to the flow direction. In cases where more than one measurement station was defined along the same survey cross section, the labels have been numbered (D1, D2, D3, etc.).

The procedure used to collect the stage data was as follows. First, at each measurement station, the elevation of the bed was determined using a survey level through comparison with the laboratory benchmark used in construction. A point gage was mounted on a movable aluminum beam which spanned the area being studied. Following establishment of a given flow condition, the point gage was used to measure the depth of water at the measurement station. Adding the depth of water to the bed elevation provided the stage. Then, these values were converted to prototype scale in order to allow for simple comparison to field and computer generated data.

3.2.2 Tailwater stage and HEC-RAS modeling

Upstream of the dam, the water surface elevation is controlled directly by the structure. However, the tailwater elevation is generally governed by the backwater effects from downstream river conditions. Of course, it is impossible to incorporate all downstream conditions within a laboratory model. For this reason, the tailwater elevation must be controlled as a boundary condition via the tailgate. In order to properly set the elevation, stage data downstream of the structure must be available. These data are generally obtained through field investigation and/or computer modeling.

In the case of this study, no field data downstream of the structure within the scope of the model were available. Therefore, it was necessary to rely on a computer model to develop a tailwater elevation boundary condition as a function of flow. The Illinois Department of Natural Resources had developed a HEC-RAS model of the Fox River. In general, this computer model required the input of river cross-section topography, roughness, known flow conditions, and hydraulic structures. The software preformed backwater calculations to arrive at water surface elevations for various flows. This allowed for the development of rating curves for various cross sections along the river. The resulting rating curve for survey section 45.94.06A at river mile 56.245 was selected as the downstream boundary condition. This section was chosen to coincide with stage measurement station I. For each flow, knowing both the elevation of the bed at station I and the boundary condition water surface elevation, it was possible to compute the required depth of flow. These data have been summarized in Table 3.2. The tailgate was then adjusted to cause the depth at station I to match that predicted by the computer model.

One difficulty with this technique was that it relied solely on the result of the HEC-RAS computer model. This, in itself, would not be detrimental if the accuracy of the computer model was verified. However, lack of field data on the Fox River at Batavia did not allow for verification and calibration of the computer model. As a result, the tailwater boundary condition is not wholly dependable. However, the results of the computer model have been accepted as sufficiently accurate to set the tailwater boundary condition.

Table 3.2. Tailwater boundary condition at measurement station I as defined by HEC-RAS

Recurrence Interval (yr)	Bed Elevation (ft above sea level)	Stage (HEC-RAS) (ft above sea level)	Flow Depth (ft)	Model Depth (ft)
2	653.52	661.92	8.4	0.28
10	653.52	663.42	9.9	0.33
50	653.52	665.52	12.0	0.40
100	653.52	666.12	12.6	0.42
500	653.52	667.92	14.4	0.48

3.2.3 Stage data results

The data collected during investigation of the physical model's stage-flow response are included in Appendix II (Table AII.1). Stage data for the primary investigation flows at the measurement stations have been converted to field scale and are summarize in Table 3.3. The final row of the table presents the average upstream pool stage response across the eleven upstream measurement locations. This averaged rating curve is presented as Figure 3.2.

Table 3.3. Stage data results – Existing condition

Flood Year	2	10	50	100	500
Flow (cfs)	5700	8500	12500	13500	17630
Gage Location	Stage (ft above sea level)				
A	667.48	668.38	669.19	669.37	670.27
B1	667.63	668.38	669.25	669.55	670.66
B2	667.40	668.24	668.93	669.20	670.16
C1	667.53	668.37	669.09	669.27	670.20
C2	667.25	668.12	668.93	669.08	669.92
D1	667.31	668.33	669.68	669.74	670.52
D2	667.58	668.63	669.23	669.50	670.22
D3	667.54	668.23	669.01	669.28	670.39
E	667.30	667.78	668.59	668.74	669.88
F	667.73	668.36	669.17	669.26	670.19
G	667.45	668.14	668.89	669.16	670.03
H	662.00	663.80	665.39	666.02	668.06
I	661.92	663.42	665.40	666.12	667.92
AVERAGE	667.47	668.27	669.09	669.29	670.22

3.2.4 Stage calibration and HEC-RAS comparison

One method of model verification is to compare stages developed in the model for a given flow to those that have been measured in the field.

In the case of this study, there were no field stage data available. As a result, it was necessary to again rely on the results from HEC-RAS computer model runs. Six river cross sections were chosen to compare the model's stage response to HEC-RAS modeling. These river cross sections were

chosen to correspond to the following gage measurement stations: A, B, D, E, H, I. The first three sections characterized stage response upstream of Batavia Dam while the last two sections characterized stage conditions downstream of Batavia Dam.

Running of HEC-RAS required the development of two distinct models, one for the upper reach (upstream of Batavia Dam) and one for the lower reach (downstream of Batavia Dam). In both cases, the computer model boundary condition was a specified known flow-stage relation at the downstream end of the reach. For the upper reach, an estimated rating curve (Army Corps of Engineers, 1978) for Batavia Dam was the input. For the lower reach, an estimated rating curve (Army Corps of Engineers, 1978) for the lower dam was the input.

The HEC-RAS model provided rating curves with respect to the eight FEMA (1981) flooding conditions for the selected river sections. It was a simple matter to plot the average of the model stage response investigation (see Table 3.3) against the average of these computer generated curves for comparison purposes. This comparison has been included on Figure 3.2.

Several summary remarks concerning this stage comparison have been made. First, results indicated that the model responded with stages higher than those predicted by HEC-RAS modeling. This discrepancy appeared to be on the order of one-half to one foot in field scale (0.033 feet in model scale). This variation can be accepted in light of the fact that calibration of the HEC-RAS computer model was impossible due to a lack of reliable field data. If calibration were possible, river cross section roughness (Manning's n) in the computer model would be adjusted to provide results matching field measurements. Underestimated (uncalibrated) values of roughness parameters could easily result in a lower computer-predicted stage. Also, the HEC-RAS model is sensitive to input boundary conditions. Inaccuracy in the boundary rating curve could be responsible for the stage discrepancy.

Measurement results downstream of the dam (gaging location H and I) match computer model results well. This, however, was expected as tailwater stage conditions were set using HEC results.

3.3 Flow visualization – Existing Condition

3.3.1 Time lapsed confetti photography study

In order to better understand the approach flow to the Batavia Dam, two flow visualization studies were completed. An accurate understanding of flow patterns was essential to the successful design of Batavia Dam replacement structures. The first study utilized 35 mm time lapsed photography. Two second timed exposures were taken of model flow seeded with paper confetti. Upon development, the photographs provided motion streaks representing the path taken by the flow. In this way, through still photography, it was possible to capture the essence of flow motion within the model. Figure 3.3 is a sample photograph showing the flow split around Duck Island for the calibration flow.

3.3.2 Dye tracer study

The presence of an island directly upstream of the dam complicated approach flow patterns considerably. Confetti studies revealed a strong flow spilt upstream of the island followed by vortex shedding in both the right and left channels and a considerable wake structure downstream of the

island. In order to fully capture, study, and understand these phenomena, a video study was performed. For this effort, a dye tracer, potassium permanganate, was applied. A dye injection system was constructed with three injectors mounted in each the right and left channel. Digital video was taken from above and upstream to examine flow splitting, and approach flow conditions. Some general conclusion for the various flow magnitudes are discussed below.

2 year flood – 5700 cfs

The flow orientation and patterns developed by the 2 year flood (5700 cfs) are presented in Figures 3.4 and 3.5. These photographs are still frame captures taken from the video data collected during the dye tracer study.

Figure 3.4 shows the flow split around Duck Island. Several distinct characteristics were observed. First, the rightmost (looking upstream) dye plume showed the role the dam breach played in flow development. This plume traveled rapidly, tightly hugging the bank. Most the flow in this area entered the river downstream of the dam directly through the breach itself. The next two plumes, moving from right to left, helped to characterize the complicated flow patterns developed as the flow split around the island. Strong vortex shedding was observed along the right edge of the island. This vortex phenomena appeared to be stable in location but oscillate slightly in strength. In general, the vortex action resulted in a mixing of the two plumes downstream of the island bulk. On the left side of the island, a strong vortex action was not visible. Here, the dye plume originating at the head of the island traveled in a cross river orientation until it was slung around the island by the rapidly moving, more central flow. Again, the two plumes closest to the island were observed to undergo mixing just downstream of the island. The leftmost plume showed the flow in this region to be low in velocity. Here, the flow hugged the bank and remained separated from the main body of the flow approaching the dam. This plume was observed to enter the still pool on the left side of the peninsula before slowly and circuitously crossing the dam in the region of the low retaining wall.

Figure 3.5 depicts the approach flow immediately upstream of the Batavia Dam. Here, three separate bands of dye were visible. The strong effect of the island wake was visible in the sharp band of clear water which separated the dye originating form the left and right sides of the island respectively. For the 2 year flow, these two flow sources showed very little mixing. The central band represented mixed flow from the two dye injectors to the right and closest to the Island. The rightmost band of dye had its source directly from the rightmost dye injector and was caused by the heavy concentration of flow through the breach. In general, it was observed that the central portion of the dam received relatively less flow than the right and left sides of the structure. The breach concentrated a large portion of the right channel flow on the far right side while the wake effects of the island forced most of the flow from the left channel to attack the dam on the far left side.

10 year flood – 8500 cfs

Figures 3.6 and 3.7 show some results of the dye tracer study conducted for the 10 year flood. Conditions here were similar to those described above for the 2 year flood. Although not visible in

Figure 3.6, vortex shedding from the right side of the island was again prominent. The rightmost dye plume behaved in a similar manner, traveling directly to the breach. In general, the 10 year flood developed visibly more mixing than experienced in the 2 year flood. However, the wake effects of the island continued to cause the left and right extremes of Batavia Dam to pass the majority of the flow while the central portion of the dam took only a relatively small portion of the flow.

50 year flood – 12500 cfs

Figures 3.8 and 3.9 show the 50 year flood. Here, the mixing effect of the right vortex was particularly visible. The strength of the flow on the right side was strong enough to break into the wake of the island. On the left side, the flow showed a curling motion in its approach to the dam. A strong division between left and right flow was still visible as shown in Figure 3.9 in the form of a distinct band of clear water separating the two dye tracts. This division was observed to oscillate across the central portion of the dam. The left and right extent of the dam continued to pass the majority of flow .

100 year flood – 13500 cfs

The results from the 100 year flood are shown in Figures 3.10 and 3.11. This flow showed some unique characteristics. The curling motion in the left channel began further upstream than observed for other flows, and the flow tended to hook around the island before approaching the dam. Conditions in the right channel remained similar to those previously discussed; however, the strong vortex on the right promoted some upstream mixing between left and right channel flows. Still, in general, the two flow sources remained distinct and were separated by the island wake clear water. This region of separation did show erratic oscillation across the central portion of the dam. The left and right extremes of the dam continued to take the brunt of the flow; however, the central region of the dam was more active than for lower flow conditions.

500 year flood – 17630 cfs

Figures 3.12 and 3.13 characterize the results of the dye tracer study for the 500 year flood event. This flow magnitude demonstrated considerable unpredictability over several runs. In some cases upstream mixing between left and right channel flows was high. For other runs (as shown in Figures 3.12 and 3.13) the wake effect of the island kept the flows strongly separated. At this flow, vortex shedding was observed to periodically develop in the left channel. The mixing characteristics of the flow appeared to be dependent on the frequency, intensity, and interaction between the left and right channel vortex shedding. Generally, the central portion of the spillway was observed to be much more actively involved in passing considerable portions of the flow at this highest flow condition than at any other flows investigated.

3.4 Flow split, velocity, and discharge characteristics – Existing condition

3.4.1 Flow split field data and calibration goal

On February 23, 1997, the Urbana office of the USGS collected field data for use during the calibration phase of this study. This field effort aimed at characterizing the flow split around Duck Island. The flow magnitude was found to be 6062 cfs. Flow through the left (looking downstream) channel was found to be 3695 cfs (61%) while flow through the right channel was found to be 2332 cfs (39%).

The effect of the island on flow patterns played a prime role in this study. It was, therefore, important that field flow split conditions were properly reproduced within the modeling environment. Three investigations were conducted within the model to verify the model flow split response for the calibration flow (6062 cfs).

3.4.2 Flow split as determined by velocity profile integration method

The first technique used to analyze the flow split around duck island relied on the use of a mini propeller velocity meter. This meter consisted of a propeller sensor mounted parallel to the direction of flow. The sensor output a voltage proportional to the velocity of flow driving the propeller. The meter was calibrated against the Hydrosystems Laboratory's ADV (Acoustic Doppler Velocimeter). The calibration curve for the sensor has been included in Appendix II (Figure AII.1). Following calibration, the meter was coupled to a Laboratory computer in order to automate data acquisition. For each velocity measured, data acquisition occurred for a period of two minutes at a frequency of five hertz (600 data points). This procedure was found to be acceptable for the determination of an average velocity at any given point.

The meter was used to evaluate velocity profiles at representative locations of the flow. These locations were chosen by dividing the left and right channel into flow "lanes." These flow lanes have been marked on Figure 3.14. For each lane, the central velocity profile was measured and taken to represent the average velocity condition across the lane. Knowing the width of a given lane as well as the vertical velocity measurement interval, it was a simple matter to integrate the velocity profile over the area in order to determine the volumetric flow rate through the lane. Figures 3.15 through 3.20 summarize the velocity profile data collected in the left channel, lanes 1-6. Table 3.4 provides the result of the velocity profile study.

Table 3.4. Velocity profile investigation summary

	Width (ft)	Specific Discharge (cfs/ft)	Discharge (cfs)
Lane 1	1.5	0.0337	0.051
Lane 2	1.5	0.0727	0.109
Lane 3	1.5	0.0706	0.106
Lane 4	1.5	0.0704	0.106
Lane 5	1.5	0.0868	0.130
Lane 6	1.83	0.119	0.218
		Total Flow Left Channel	0.719

Following collection of the above data, a comparison between field and model results was made. Table 3.5 indicates that, within the model, 58.5% of incoming water flowed through the left channel. This represented a discrepancy of only 2.5% from measurements taken in the field. This discrepancy was acceptably within the limits of procedural error. These results indicated that the model properly reproduced field flow splitting characteristics.

Table 3.5. Field to model flow splitting comparison – Velocity profile method

	Field	Model
Total Flow (cfs)	6062	1.23
Left Channel (cfs)	3695	0.719
Percent of Total Flow	61.0%	58.5%

Note: Field conditions as determined during 2/23/97 USGS field survey

Irrevocable equipment failure precluded a similar velocity profile investigation in the right channel. For this reason, two other techniques for the evaluation of flow splitting were applied in order to confirm the above results.

3.4.3 Flow split as determined by confetti image velocimetry

A confetti study was completed in order to more thoroughly characterize the flow around Duck Island. This technique depended on the use of the Laboratory's digital video camera. Confetti was released within the flow and filmed from above. Following collection of this video data for each flow lane, software post-processing was completed in order to track the movement of a confetti particle frame by frame through time. Knowing the time between frames and the total distance traveled by the particle, it was a simple matter to determine the average velocity of particle motion. Tracking a number of particles across a given lane allowed for the determination of an average surface velocity over the lane. The data collected for all thirteen flow lanes have been summarized in Table AII.2 and Table AII.3 in Appendix II.

In order to develop some approximation of flow through a lane, the area of the flow across a lane was needed. This information was obtained from an AutoCAD representation of the river cross section. Knowing the stage across the section for the calibration flow, the software provided a direct calculation of flow area.

A true calculation of flow through a lane would have required information on the average velocity across the lane. The confetti tracking technique only provided a rough estimate of average surface velocity. However, the product of flow area and average surface velocity was accepted as a surrogate providing some indication of "flow contribution." The final results of the confetti testing are summarized in Table 3.6.

The total flow contributions from the left and right channel were used as a basis for calculating the percentage of flow traveling through the left and right channels. These calculations and a comparison to field measurements are summarized in Table 3.7. This analysis indicated that the left channel was receiving approximately 6% more flow than suggested by field measurements. These

results suggest that, within the limits of approximations made in this technique and in light of results developed during the velocity profile investigation (section 3.3.2), the model provided adequate flow splitting characteristics.

Table 3.6. Summary of flow contribution from left and right channel – Confetti method

Lane	Average Surface Velocity (fps)	Flow Area (ft^2)	Flow Contribution (cfs)
Left Channel			
1	0.29	0.26	0.07
2	0.32	0.47	0.15
3	0.35	0.49	0.17
4	0.37	0.48	0.18
5	0.43	0.56	0.24
6	0.40	0.53	0.21
		Total Left Channel	1.03
Right Channel			
1	0.31	0.09	0.03
2	0.32	0.33	0.10
3	0.26	0.46	0.12
4	0.26	0.43	0.11
5	0.16	0.36	0.06
6	0.19	0.26	0.05
7	0.17	0.16	0.03
		Total Right Channel	0.50
		Total Flow Contribution	1.53

Table 3.7 Field to model flow splitting comparison – Confetti image velocimetry

	Field		Model	
	Flow (cfs)	Percent	Flow (cfs)	Percent
Total Flow Contribution	6062	100.0%	1.53	100.0%
Left Channel Contribution	3695	61.0%	1.03	67.2%
Right Channel Contribution	2332	38.5%	0.50	32.8%

Note: Field conditions as determined during 2/23/97 USGS field survey

3.4.4 Flow split as determined by transect method

The purchase of a new electromagnetic velocity meter allowed for a third investigation of the flow split around Duck Island. The procedure here was similar to that followed in the velocity profile integration method (section 3.3.2). However, the magnetic meter did not allow for sufficient vertical resolution to provide for accurate measurements of velocity profiles. Hence, a central velocity at each location was measured and used as an representation of an average velocity. Also, the magnetic meter measured velocity in 2 dimensions. In this case, the positive x direction was taken downstream and parallel to the walls of the model basin. Measuring both the x and y velocity vector components allowed for the determination of the direction for the total velocity vector. In order to facilitate data

collection and instrument setup, a new measurement transect parallel to the y direction of the coordinate system was chosen. In the left channel, the six flow lanes previously used were repeated; while, in the right channel, five new measurement lanes were chosen. Figure 3.21 illustrates the location for these measurements. In this case, the velocity component perpendicular to the transect (x-direction) multiplied by the flow area of the lane was used to evaluate the flow across the lane.

The data collected for this investigation are included in Table AII.4 in Appendix II. The results of the transect flow split investigation are summarized in Table 3.8 below, and Table 3.9 again compares the results with field measurements.

Table 3.8. Summary of flow contribution from left and right channel – Transect method

Lane	Average X velocity (fps)	Flow Area (ft^2)	Flow Contribution (cfs)
Left Channel			
1	0.31	0.26	0.08
2	0.28	0.47	0.13
3	0.29	0.49	0.14
4	0.33	0.48	0.16
5	0.33	0.56	0.19
6	0.32	0.53	0.17
		Total Left Channel	0.87
Right Channel			
1	0.26	0.67	0.18
2	0.20	0.49	0.10
3	0.20	0.39	0.08
4	0.19	0.29	0.06
5	0.16	0.18	0.03
		Total Right Channel	0.44
		Total Flow Contribution	1.31

Table 3.9 Field to model flow splitting comparison – Transect method

	Field		Model	
	Flow (cfs)	Percent	Flow (cfs)	Percent
Total Flow Contribution	6062	100.0%	1.31	100.0%
Left Channel Contribution	3695	61.0%	0.87	66.7%
Right Channel Contribution	2332	38.5%	0.44	33.3%

Note: Field conditions as determined during 2/23/97 USGS field survey

The above results agreed well with the two previous flow split investigations. The variability of technique and repeatability of results indicated that the hydraulic model adequately reproduced the flow split observed in the field.

The magnetic meter allowed for quantification of both magnitude and direction of velocity within the model. The flow split was found to be best illustrated graphically by considering the specific

discharge (velocity multiplied by flow depth) observed at each of the transect measurement locations. Figure 3.21 presents the results. Here, both the x and y components were applied to determine the current velocity and direction. The length of the graphical vector is proportional to the "strength" of flow at the particular location.

3.4.5 Point velocity and downstream specific discharge measurements

The flow trends observed qualitatively through dye tracer visualization were confirmed through point measurements of velocity using the 2-D electromagnetic velocity probe. These investigations provided further understanding of the flow field in the river. The data collected in this phase of the project are presented in Table AII.4 of Appendix II. Figures 3.22 through 3.26 graphically present velocities measured for the 2, 10, 50, 100, and 500 year floods respectively.

Velocities at location B1 show the upstream impact of the breach; velocities at this location were, on average, two and a half times greater than those observed at the cross river counterpart measurement location, B2. It was postulated that closing the breach would decrease these velocities considerably, and this hypothesis was tested during investigation of the baseline condition (Section 3.6.4.).

For low flow (2 year flood) velocities measured at location C1 were directed toward the breach and left-central side of the dam. As flow increased in magnitude, a rotation of this velocity vector was observed. For high flows, the velocity in the central portion of left channel (C1) was directed toward the central right side of the structure. A similar trend was recognized at location D2. In fact, measurements for the 500 year flood showed flow at D2 as directed cross river and toward the low retaining wall along the peninsula. This measurement, however, did exhibit considerable and erratic oscillation in orientation from left to right. These observations confirmed those made during dye tracer investigation. Left to right channel mixing increased with flow magnitude, and the central portion of structure was more active at high flows.

Measurements at location F indicated flow directly over the structure with an increase in velocity for each increase in flow magnitude. The vector for the 500 year flow event showed a rotation toward the peninsula. This result, in conjunction with the measurements at D2, helped to quantify the role the low retaining wall had in passing considerable flow during extreme flood events.

Measurements at locations D1 and E were influenced considerably by the breach. The largest velocities were observed at location E. For the 2 year flood, a velocity of 4.27 ft/s was recorded; at the 500 year flood condition, the velocity increased to 5.77 ft/s. The direction of the velocity vector at location E clearly indicated the indispensable role the downstream wing-wall played in protecting the bank.

Measurements in the right channel (C2, D3, and G) indicated that, in general, the flow is not directed at the main body of the Batavia Dam. The island wake structure prevented direct flow to the dam. This result supported the dye tracer observation that flow in the right channel often took a circuitous path , flowing overland on the peninsula and over the low retaining wall.

Downstream measurements at H and I quantified velocities in the downstream channel. Velocity at H was greater than I. This was attributed to the considerable flow being directed away from the breach and toward location H by the wing-wall. The wing-wall was also responsible for the orientation of the velocity vectors at H and I. For higher flows, with greater flow concentrated through the breach, the vectors were observed to rotate into alignment with the wing-wall and toward the right of the channel. Table 3.10 provides a field scale summary of the point velocity data.

A more thorough understanding of the downstream flow patterns can be grasped by plotting specific discharge values along a downstream transect. In this case, five velocity measurements were made along a downstream transect. Simultaneously, the depth of flow was measured using a point gage. The product of the velocity and the depth provided a measure of the specific discharge (cfs/ft) which allowed for a quantification of flow strength and direction at each point. The results are presented graphically in Figures 3.27 to 3.31 for each flow magnitude. A summary of the data taken during experimentation is included in Table AII.4 of Appendix II. Table 3.11 provides a summary of the data in field scale.

For the 2 year flood, flow within the downstream channel is well distributed with maximum specific discharge in the center of the channel (points 2 and 3). The 10 year flood increased flow over the peninsula. This was reflected in the increased discharge at location 4. A similar trend is recognized for the 50 year flow. Also, flow through the breach and deflected by the wing-wall increased, rotating the velocity vectors along the left bank toward the right of the channel. Location 2 generally experienced discharge values greater than location 1. This was attributed to the strong wing-wall current which shielded location 1 while concentrating flow at location 2. Measurable flow developed at location 5 for the 100 year flood. This flow contribution increased for the 500 year event.

3.5 General response characteristics – Existing condition

3.5.1 Movable bed breach response

The bed downstream of the dam breach was found to be highly mobile. Directly at the toe of the breached spillway, 4-6 inches of scour was observed. In field scale, this would correspond to 10-15 feet of sediment removed. This result characterized the capacity of the river to remove sediment. However, in reality, the extent of scour on-site would have depended upon the geologic conditions. Historical boring investigations (Raymond International Inc, 1978) indicated that bedrock would have been encountered prior to removal of 15 feet of bed material. In general, the movable bed response showed good agreement with surrounding topography. Figure 3.32 shows the scour hole developed by flow through the breach. A comparison to the initial condition can be achieved by examining Figure 2.6.

3.5.2 Spillway hydraulic jump characteristics

The hydraulic jump characteristics for the primary investigation flows were observed and photographed. Some general comments are documented below.

For the 2 year flood, flow tended to shoot from the spillway toe, and the resulting jump was weak and undulating. The 10 year flood resulted in a strong, well formed jump at the toe of the

Table 3.10. Summary of field scale point velocity measurements – Existing condition

Flow (cfs)	5700		8500		12500		13500		17630	
Gage	Current (ft/s)	Angle (deg)	Current (ft/s)	Angle (deg)	Current (ft/s)	Angle (deg)	Current (ft/s)	Angle (deg)	Current (ft/s)	Angle (deg)
A	Insufficient Depth		Insufficient Depth		1.51	-44.03	1.09	-28.69	1.41	-38.77
B1	Insufficient Depth		2.26	4.12	2.67	-16.11	2.74	-11.01	3.63	-3.13
B2	Insufficient Depth		0.99	-1.04	1.10	-10.39	1.13	-12.93	1.37	-13.67
C1	1.96	4.76	2.80	4.06	3.84	-10.83	4.03	-12.67	4.46	-5.57
C2	0.94	12.17	1.17	8.88	1.10	-0.94	1.30	3.97	1.61	-9.67
D1	1.68	1.23	2.13	-0.97	2.78	-15.03	2.82	13.12	3.53	-7.63
D2	1.24	32.54	0.64	34.59	1.82	13.21	2.01	22.66	1.46	-39.99
D3	Insufficient Depth		Insufficient Depth		0.27	28.30	0.50	19.09	0.53	-28.30
E	4.27	7.03	5.05	3.90	5.56	-7.84	5.50	-10.98	5.77	-3.41
F	1.23	26.19	1.76	19.18	2.53	1.38	2.63	11.46	3.29	-8.84
G	Insufficient Depth		0.27	3.81	0.39	-10.78	0.58	11.22	0.62	-25.82
H	3.45	1.50	4.19	0.25	4.02	-10.60	3.64	66.57	5.75	-7.04
I	2.81	5.89	3.55	7.02	4.05	-5.89	4.14	-6.01	4.20	4.68

Table 3.11. Summary of field scale specific discharge downstream of structure – Existing condition

Flow (cfs)	5700		8500		12500		13500		17630	
Station	Flow (cfs/ft)	Angle (deg)	Flow (cfs/ft)	Angle (deg)	Flow (cfs/ft)	Angle (deg)	Flow (cfs/ft)	Angle (deg)	Flow (cfs/ft)	Angle (deg)
5	Insufficient Depth		Insufficient Depth		4.43	37.97	19.87	32.36	58.05	30.02
4	31.23	21.38	70.38	23.75	96.00	12.24	91.14	8.37	79.25	19.25
3	39.49	18.38	54.31	23.75	69.32	7.03	76.04	5.05	86.30	15.19
2	36.03	11.49	56.81	23.75	68.58	1.85	73.56	0.17	79.79	9.46
1	21.25	6.84	28.28	23.75	42.05	-6.04	42.18	-6.05	58.39	4.09

spillway. Flow for the 50 year flood submerged the spillway toe. In this situation, the jump formed on the spillway and was generally strong. The 100 year flood resulted in increased spillway submergence. The hydraulic jump tended to be submerged with visible surface disturbance resulting from the submerged roller. The 500 year flood raised tailwater conditions to near crest submergence. The jump for this flow was again submerged.

3.6 Investigation of baseline condition

3.6.1 Description and motivation

Within this report, the term *baseline condition* refers to the Batavia Dam as it was originally designed and constructed. In short, this condition was achieved by patching the breached section of the dam along the left abutments in order to return the structure to its original form.

Analyzing this condition allows for an approximation of the river response to the original structure as designed and constructed. Prediction of this response may be necessary for permitting purposes, and it provides a second benchmark against which to compare alternative design responses.

It is important to keep in mind that when the original dam was built, Duck Island was smaller.

3.6.2. Model stage response – Baseline condition

The data collected during investigation of the physical model's baseline stage response are included in Appendix II (Table AII.5). Stage data for the primary flows at the measurement stations have been converted to field scale and are summarized in Table 3.12. The final row of the table provides the average upstream pool stage response across all upstream measurement locations. This average rating curve is presented in Figure 3.33.

Table 3.12. Stage data results – Baseline condition

Flood Year	2	10	50	100	500
Flow (cfs)	5700	8500	12500	13500	17630
Gage Location	Stage (ft above sea level)				
A	668.14	668.95	669.79	669.85	670.66
B1	668.32	669.16	669.73	669.79	670.57
B2	668.24	668.81	669.56	669.89	670.46
C1	668.13	668.76	669.45	669.63	670.29
C2	667.97	668.60	669.35	669.68	669.95
D1	668.51	669.41	670.13	670.40	671.00
D2	668.24	668.96	669.62	669.83	670.52
D3	668.20	668.98	669.67	669.79	670.66
E	668.65	668.98	669.79	669.88	670.63
F	668.27	668.87	669.59	669.92	670.40
G	668.05	668.65	669.55	669.58	670.30
H	662.12	663.29	665.42	666.38	668.36
I	662.04	663.12	665.25	665.91	667.92
Average	668.25	668.92	669.66	669.84	670.49

The above results clearly indicated that flow stage increased with breach closure. Stage was observed to increase as much as 0.77 feet for low flows (2year) to 0.27 feet for high flows (500 year flood).

3.6.3. Dye tracer flow visualization – Baseline condition

A tracer study was preformed on the baseline condition in order to compare approach flow conditions to those observed for the existing condition. By this stage in the research, the outline of the island and peninsula had been painted in a darker color and instrumentation rails had been added to the model. The silhouette of the island, in particular, helped to accentuate the role it had in flow development.

2 year flood – 5700 cfs

The flow dye patterns developed for the baseline condition under the influence of the 2 year flow are presented in Figures 3.34 and 3.35.

Figure 3.34. shows the flow split around Duck Island. Closing the breach seemed, at this qualitative level, to have little effect on the flow development. The rightmost dye plume (looking upstream) continued to travel directly along the bank and toward the location of the closed breach. The two plumes to the right of the island showed considerable mixing under the influence of vortex shedding. The vortex on the right appeared at the same location observed for the existing condition. Plumes on the left side of the island also showed little variation from observations made for the existing condition.

Figure 3.35 shows the approach flow directly upstream of the structure. Dye continued to show strong concentration on the left and right of the dam with more diffuse and mixed dye in a central band of flow. For the baseline case, the clear water divide between left and right flow was not as evident. However, the division of flow paths was observed to maintain the same location as found in the existing condition. The extreme left and right portions of the structure continued to pass the majority of the flow.

10 year flood – 8500 cfs

Figures 3.36 and 3.37 provide still frame captures of the dye tracer study conducted for the 10 year flow. Again, dye tracer patterns showed little variations from those described for existing conditions. One new phenomena was observed to occur in the left channel at the downstream end of the island. Here, it appeared that a large eddy had developed, creating a bulb of dye which grew with time and filled the still pool left of the peninsula. Faster moving water at the tail of the island tended to pull dye from this bulb and convey it over the structure on the far left near the low retaining wall.

50 year flood – 12500 cfs

Figures 3.38 and 3.39 show results from the baseline dye tracer study for the 50 year flow. In this case, the eddy in the left channel helped to promote mixing of flow with the right channel. A clear divide between left and right flows was not as visible in this case. In the existing condition (Figure 3.9)

it was obvious that the breach played a large role in pulling flow from the right channel toward the right extreme of the structure. For baseline conditions, the absence of the breach resulted in a more active passage of the dye flow over the center of the structure.

100 year flood – 13500 cfs

The dye tracer patterns developed by the 100 flood are provided in Figures 3.40 and 3.41. Here, the vortex shedding in the right channel was quite apparent, Also, the eddy in the left channel resulted in a bulb of dye spreading into the left channel as described for the 10 year flow. This result was somewhat different from those observed for the existing condition (Figure 3.10). There, left channel flow tended to curl to the right across the island tail as if drawn to the breach.

500 year flood – 17630 cfs

Figure 3.42 and 3.43 characterize the results of the dye tracer study for the 500 year flood event. Again, right channel mixing was increased with the patching of the breach. Also, the two plumes left of the island continued to show a curling motion toward the left of the channel. Mixing between left and right flow was more pronounced for the baseline condition, and a clear water division was not so distinctly defined as for the existing condition (Figure 3.13).

3.6.4. Flow split, velocity, and discharge characteristics – Baseline condition

The flow patterns observed qualitatively through dye tracer visualization were quantified using the 2-D electromagnetic velocity meter.

A study of the baseline flow split around the island was conducted under the same procedure described for the existing condition. The data taken during this phase of study have been summarized in Table AII.6 in Appendix II, and the field scale results are summarized graphically in Figure 3.44. These results showed minor but interesting variations from those observed previously. In the left channel (looking downstream) the magnitude of the specific discharge values remained essentially the same as found for the existing condition. The orientation of the vectors at measurement stations 5 and 6, however, showed some slight change (compare to Figure 3.21). For the existing condition, the angle of orientation was more sharply directed toward the breach. Specific discharge magnitudes in the right channel were slightly lower in magnitude than those measured for the existing condition. This may be a result of the dye tracer observation that breach closure appeared to decrease the draw of flow from the right channel toward the left extreme of the dam. The decrease in specific discharge along the right transect resulted in a flow split with a slightly increased weight (1%) in the right channel. For practical purposes, it can be stated that breach closure had little to no impact on observed flow split.

Data taken during collection of point velocity measurements are included in Table AII.6 in Appendix II. Field scale results are summarized graphically in Figures 3.45 through 3.49 and in Table 3.13. In all flow cases, velocities at measurement locations D1 and E decreased significantly with breach closure. Also, the effect of closing the breach was felt at locations B1 and C1. At these stations, the velocity was decreased, though to a lesser extent. For low flows (2 and 10 year), orientation of the

velocity vector at C1 was rotated away from the breach. Velocities at point F experienced an increase for the baseline condition. This was expected because closure of the breach resulted in higher heads, and thus flow rates, over the spillway crest. Measurements in the right channel generally showed a slight increase in magnitude. For low flows (2 and 10 year), the orientation of the vector at C2 was observed to be rotated away from the structure, reflecting the absence of the breach's ability to pull flow from the right channel. Downstream measurement location H showed a decrease in velocity magnitude and an orientation more aligned with the bank rather than the wing-wall. This was attributed to the loss of flow previously concentrated through the breach and directed by wing-wall toward location H. Flow was more evenly distributed by the unbroken crest, and a greater quantity of flow was forced over the peninsula. In the existing condition, a large portion of the flow volume was directed by the wing-wall toward the opposite shore. In essence, location I was shielded from high velocities by the current generated by the wing-wall. In the baseline condition, however, the strong flow off the peninsula and an even distribution across the downstream channel subjected location I to higher velocities.

Downstream specific discharge measurements are included in Table AII.6 in Appendix II. Figures 3.50 through 3.54 provide the field scale results graphically, and Table 3.14 summarizes the data. The downstream discharge for the baseline condition exhibited two major difference from those observed during testing of the existing condition. First, breach closure resulted in an increased flow over the peninsula, causing increased discharge at measurement locations on the right side of the channel. This was particularly evident at location 3 and 4 where both magnitude and orientation of the specific discharge reflected increased overland flow. The second observed variation from existing conditions was at locations 1 and 2. As described above, for the breached condition, the wing-wall tended to generate a strong current which shielded the left bank (location 1) from high velocities while directing large flows at location 2. Closing the breach decreased this current and allowed for more evenly distributed discharge; the result was a considerable increase in specific discharge measurements at location 1 with a decrease at location 2. These findings were summarized as follows. In the existing condition, two opposing currents control downstream flow development: one from the wing-wall directed breach flow, and the second from the peninsula overland flow entering on the right of the channel. Closing the breach for the baseline condition resulted in a diminishing of the wing-wall current while strengthening the peninsula current. The resulting downstream flow pattern was slightly skewed toward the left bank.

3.6.5. General response characteristics – Baseline condition

The hydraulic jump characteristics observed for the baseline condition were similar to those described for the existing condition (Section 3.5). Breach closure resulted in considerably less turbulent flow along the left abutment, and jump development in this region was consistent with the remainder of the spillway. For this case, the movable bed downstream of the closed breach exhibited little to no scour.

Table 3.13. Summary of field scale point velocity measurements – Baseline condition

Flow (cfs)	5700		8500		12500		13500		17630	
Gage	Current (ft/s)	Angle (deg)	Current (ft/s)	Angle (deg)	Current (ft/s)	Angle (deg)	Current (ft/s)	Angle (deg)	Current (ft/s)	Angle (deg)
A	Insufficient Depth		0.30	-14.04	0.31	-35.54	0.42	-19.98	0.82	-14.04
B1	0.81	-10.30	1.68	-2.46	2.10	-5.91	2.22	-2.79	2.75	-7.54
B2	Insufficient Depth		1.16	-12.53	1.27	-15.61	1.19	-10.46	0.42	-30.96
C1	1.65	-6.89	2.24	-7.87	3.21	-5.81	3.44	-7.54	4.08	-12.25
C2	1.05	-1.97	1.23	-1.68	1.36	-3.05	1.68	-9.26	1.93	-14.04
D1	1.14	-10.06	1.44	-8.64	1.99	-11.51	2.24	-8.33	2.40	-12.58
D2	1.04	13.07	1.18	23.43	1.78	21.37	1.16	-10.78	1.49	-29.05
D3	Insufficient Depth		0.31	-10.01	0.75	-9.69	0.37	-11.31	0.55	-19.03
E	1.35	-9.21	1.89	-7.67	2.53	-10.27	2.76	-8.66	3.19	-13.41
F	1.55	7.37	2.30	3.60	3.05	-3.05	3.00	9.69	3.29	-6.31
G	0.26	56.31	0.69	6.01	0.76	13.71	0.66	15.95	0.74	1.40
H	2.25	12.03	2.75	4.89	3.23	8.04	3.43	8.17	3.25	-1.59
I	2.73	4.92	4.06	4.59	5.61	4.43	5.60	1.66	5.59	0.92

Table 3.14. Summary of field scale specific discharge downstream of structure – Baseline condition

Flow (cfs)	5700		8500		12500		13500		17630	
Station	Flow (cfs/ft)	Angle (deg)	Flow (cfs/ft)	Angle (deg)	Flow (cfs/ft)	Angle (deg)	Flow (cfs/ft)	Angle (deg)	Flow (cfs/ft)	Angle (deg)
5	Insufficient Depth		Insufficient Depth		3.71	-16.11	6.08	50.83	41.93	30.80
4	24.24	28.81	54.71	21.96	120.72	24.68	120.84	24.66	113.02	20.81
3	40.37	27.04	59.06	32.50	71.88	18.89	78.36	19.74	88.81	13.39
2	33.77	11.05	46.04	17.04	57.74	13.80	59.90	11.86	71.75	5.55
1	21.11	3.12	36.40	5.61	62.53	2.18	63.00	2.92	68.83	-0.41

Figure 3.1. Stage measurement locations

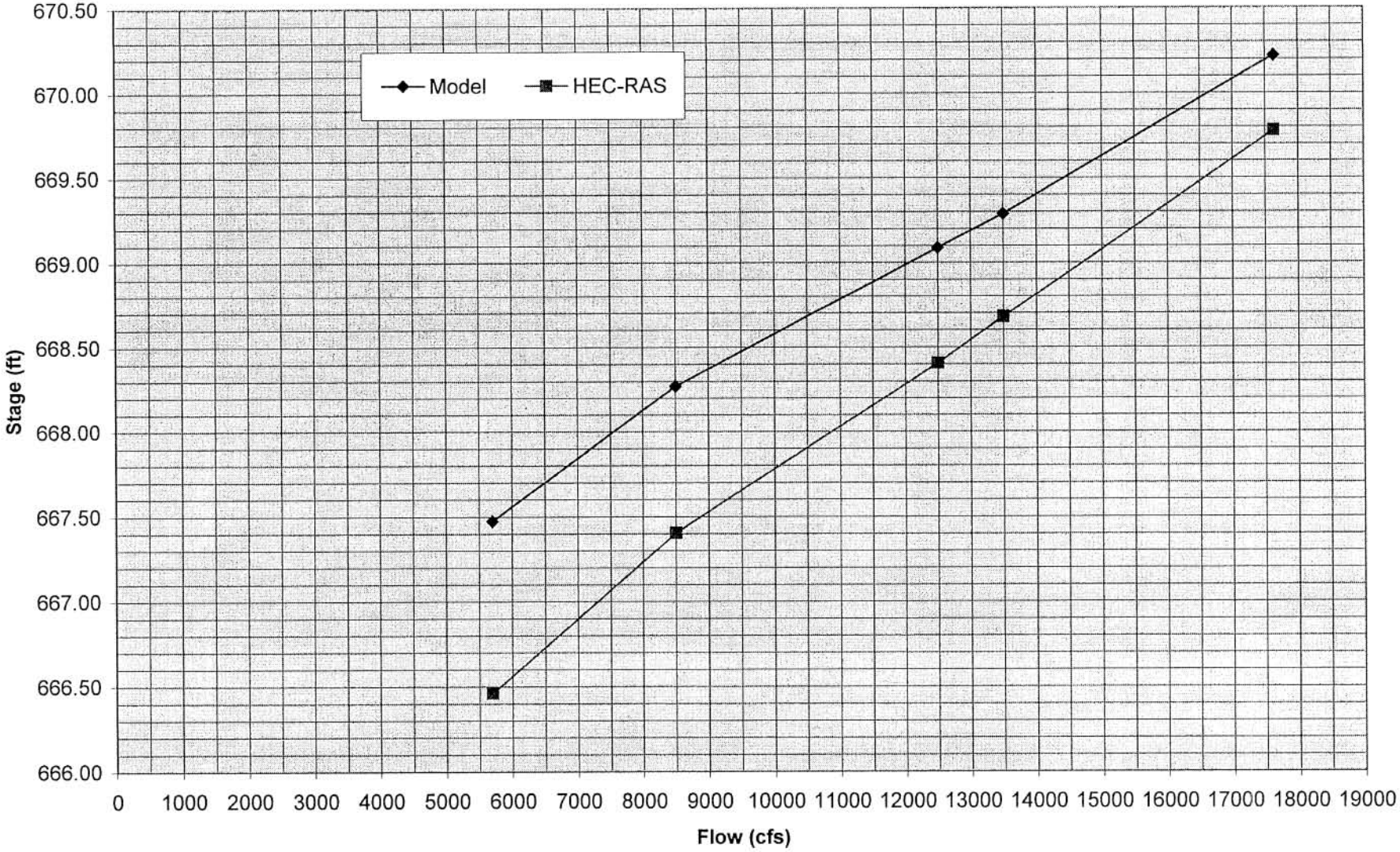

Figure 3.2. Averaged upstream pool stage response - Existing condition

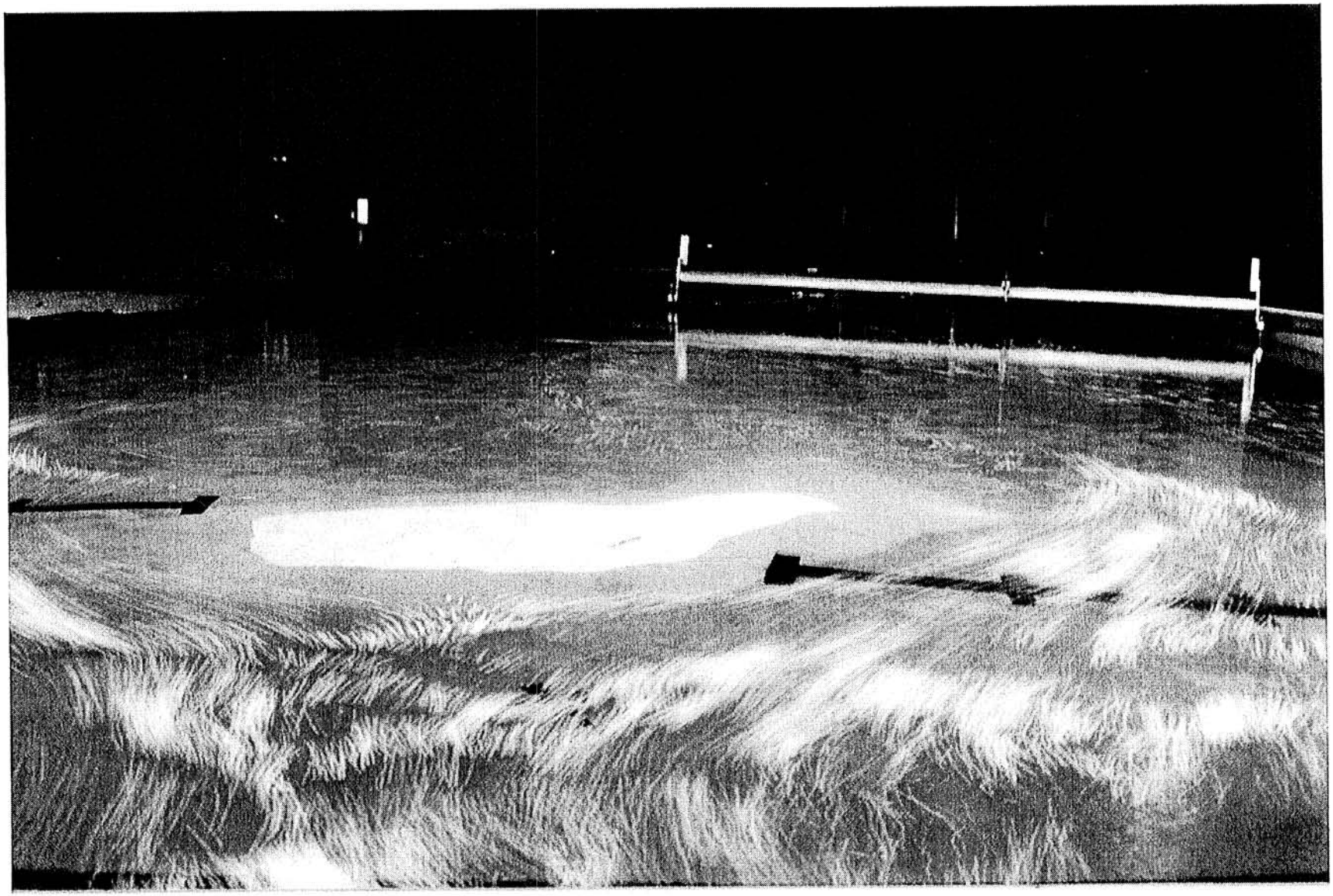

Figure 3.3. Visualization of flow split around Duck Island using time lapsed confetti photography

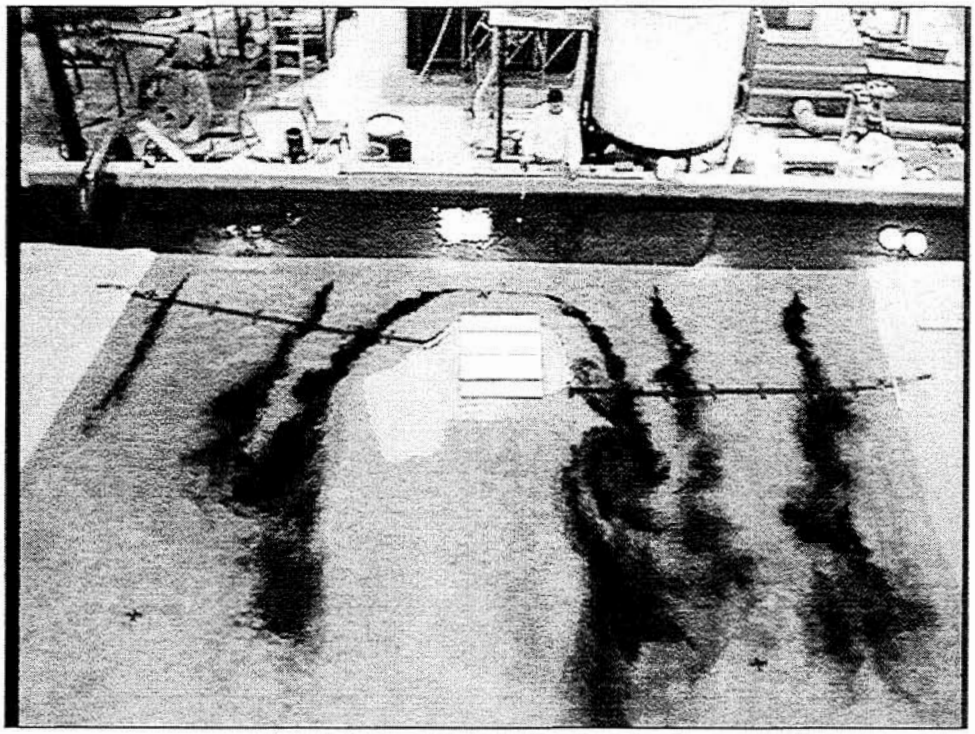

Figure 3.4. Existing condition - Visualization of flow split around Duck Island - 2 year flood (5700 cfs)

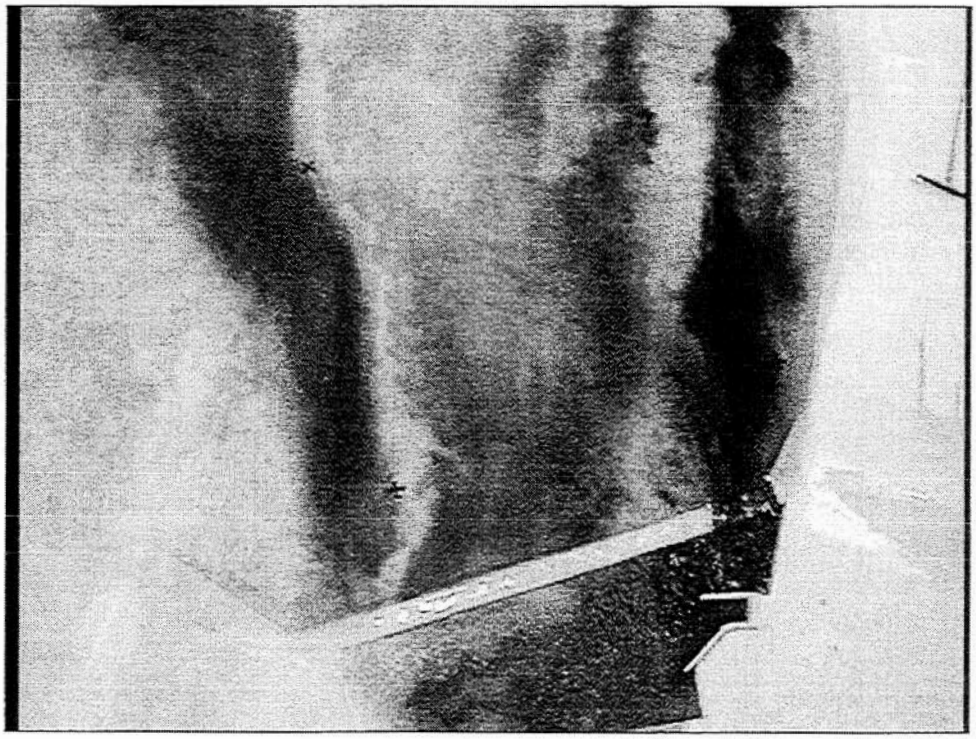

Figure 3.5. Existing condition - Visualization of Batavia Dam approach flow - 2 year flood (5700 cfs)

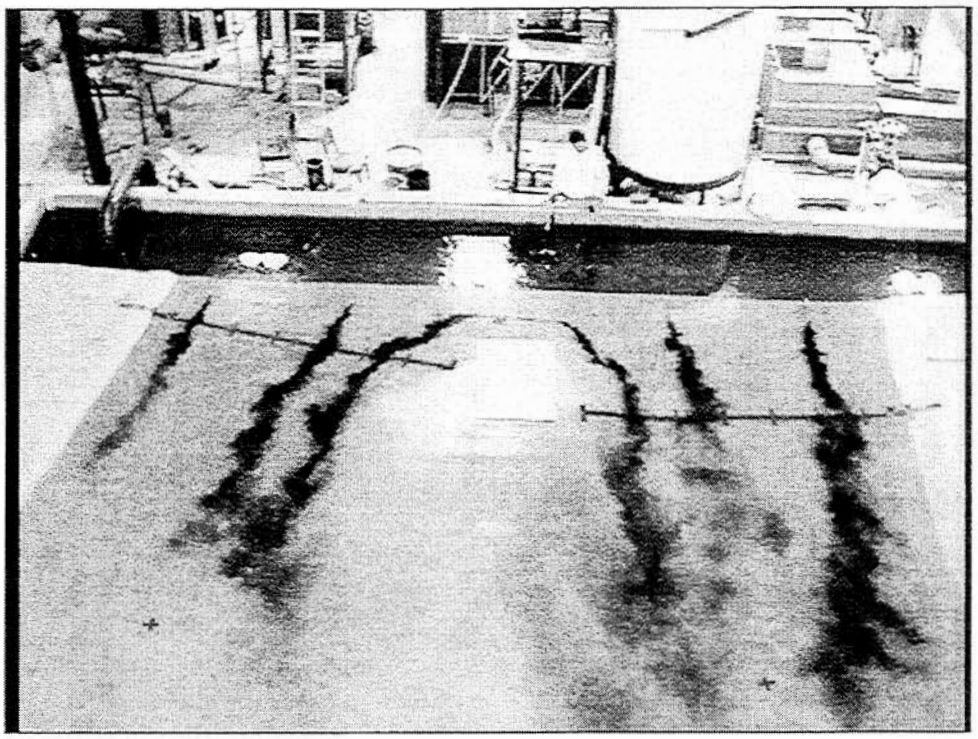

Figure 3.6. Existing condition - Visualization of flow split around Duck Island - 10 year flood (8500 cfs)

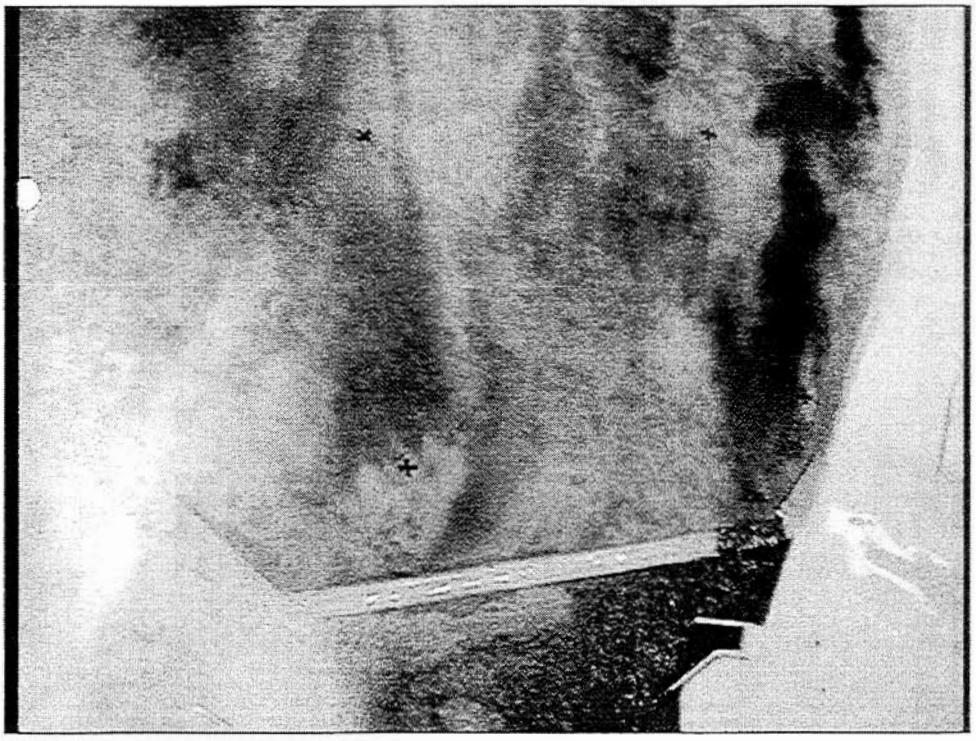

Figure 3.7. Existing condition - Visualization of Batavia Dam approach flow - 10 year flood (8500 cfs)

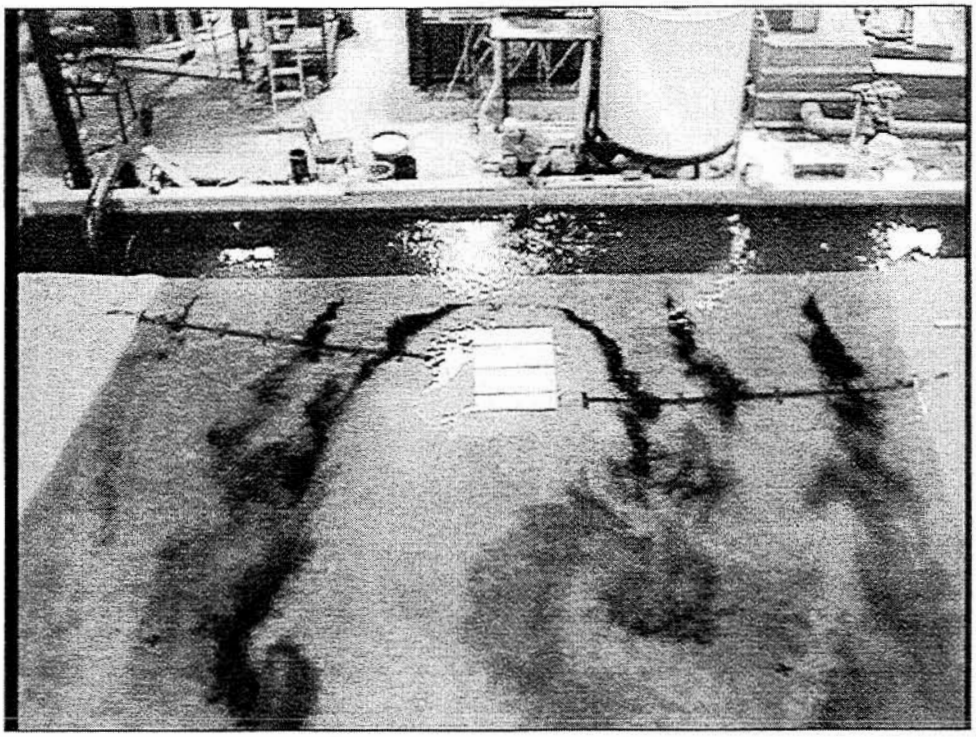

Figure 3.8. Existing condition - Visualization of flow split around Duck Island - 50 year flood (12500 cfs)

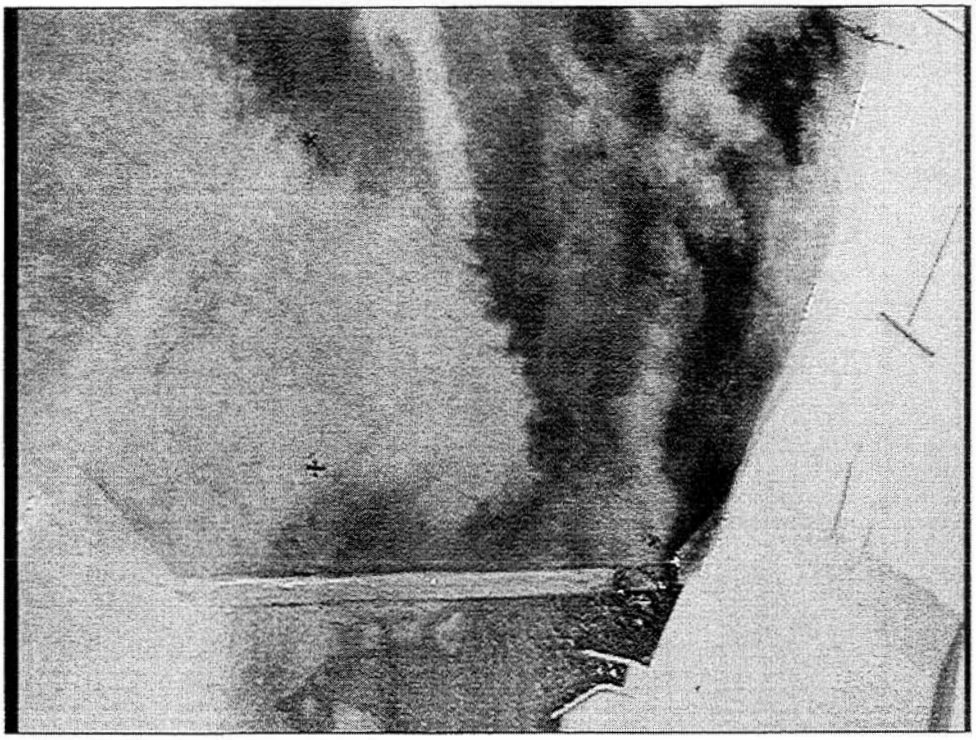

Figure 3.9. Existing condition - Visualization of Batavia Dam approach flow - 50 year flood (12500 cfs)

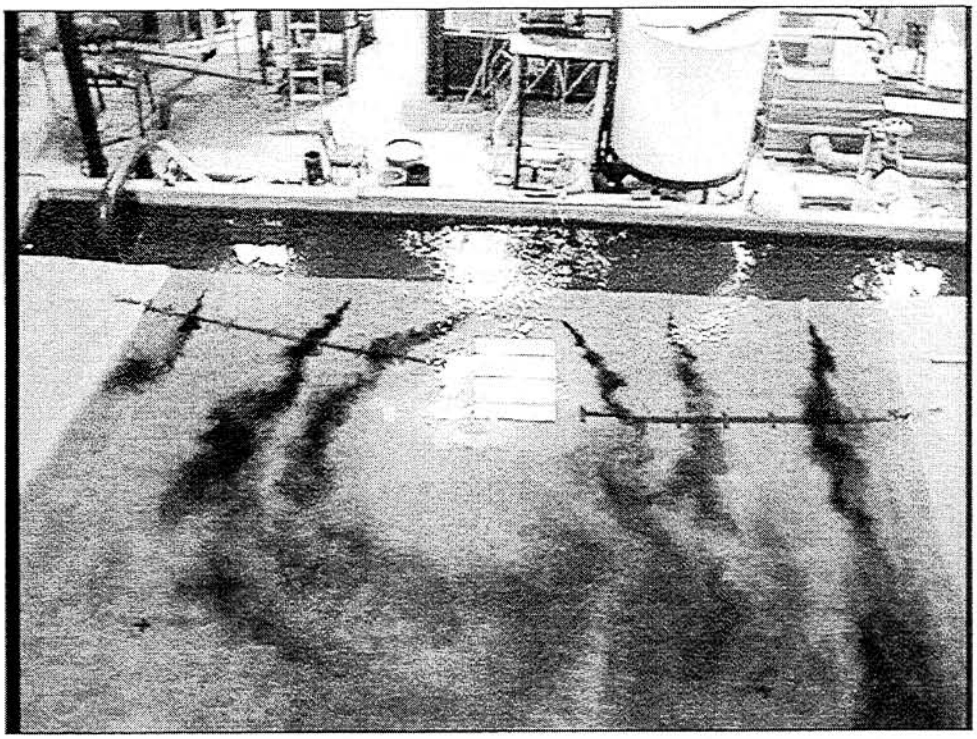

Figure 3.10. Existing condition - Visualization of flow split around Duck Island - 100 year flood (13500 cfs)

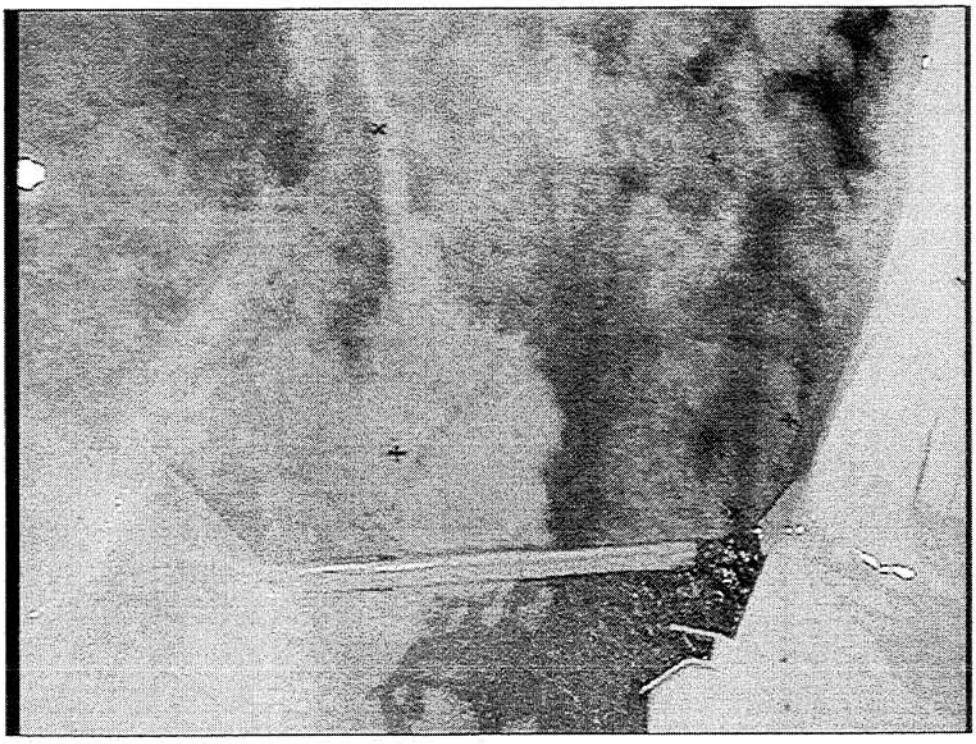

Figure 3.11. Existing condition - Visualization of Batavia Dam approach flow - 100 year flood (13500 cfs)

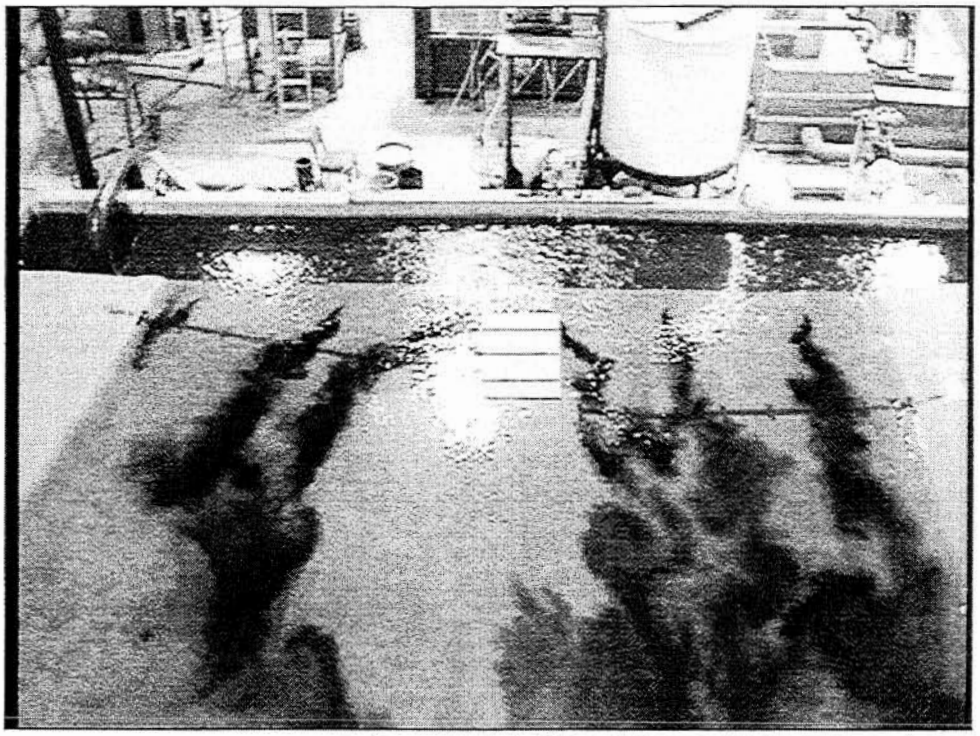

Figure 3.12. Existing condition - Visualization of flow split around Duck Island - 500 year flood (17630 cfs)

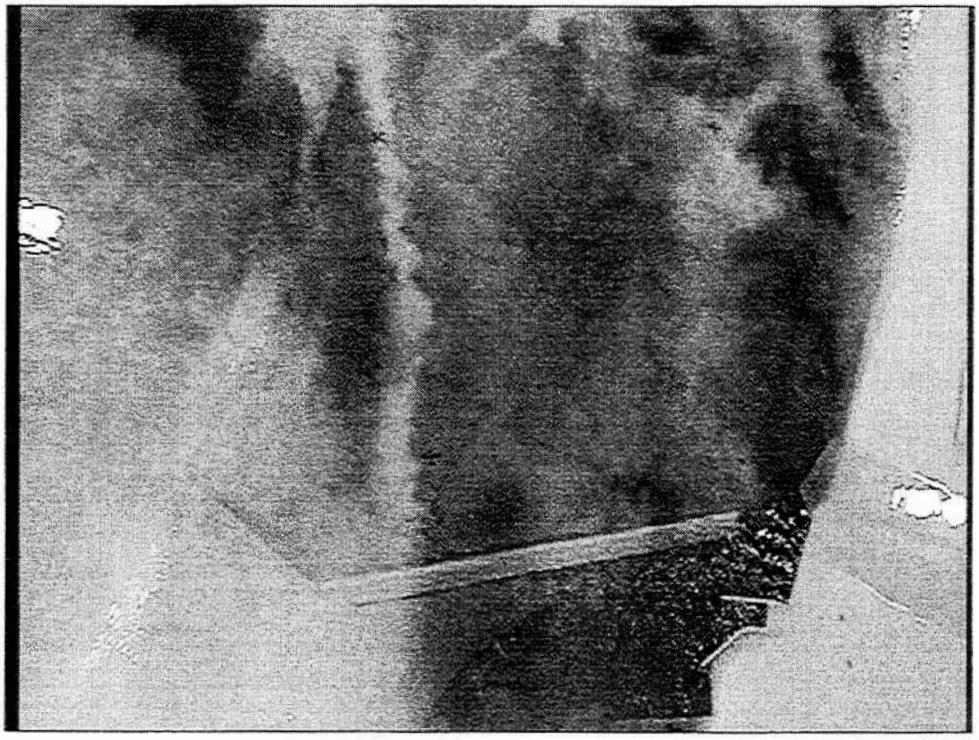

Figure 3.13. Existing condition - Visualization of Batavia Dam approach flow - 500 year flood (17630 cfs)

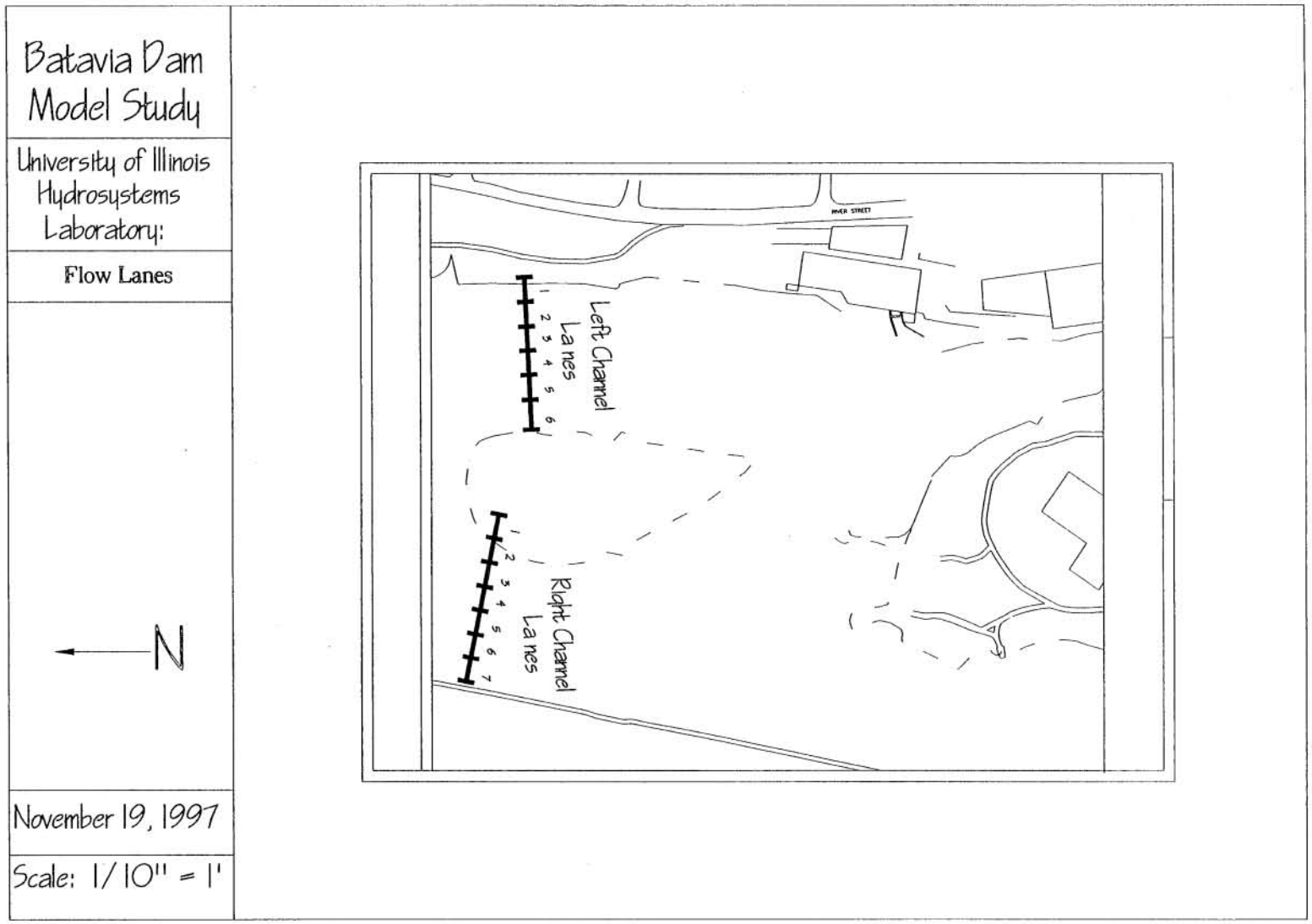

Figure 3.14. Flow lanes used in analysis of flow split around Duck Island

	Gage Reading (ft)	Depth (ft)	Average Voltage (V)	Velocity (fps)	Flow Contribution (cfs/ft)
Bed	1.683	0.000	0.00E+00	0.00	0.00E+00
	1.709	0.026	5.26E-02	0.24	3.12E-03
	1.715	0.032	4.88E-02	0.23	1.39E-03
	1.739	0.056	6.24E-02	0.27	5.92E-03
	1.745	0.062	5.94E-02	0.26	1.58E-03
	1.769	0.086	6.02E-02	0.26	6.23E-03
	1.785	0.102	6.36E-02	0.27	4.26E-03
	1.799	0.116	6.00E-02	0.26	3.72E-03
	1.808	0.125	7.05E-02	0.29	2.49E-03
Surface	1.825	0.142	*	*	5.05E-03
				Specific Discharge	3.37E-02
				Flow (cfs)	5.06E-02

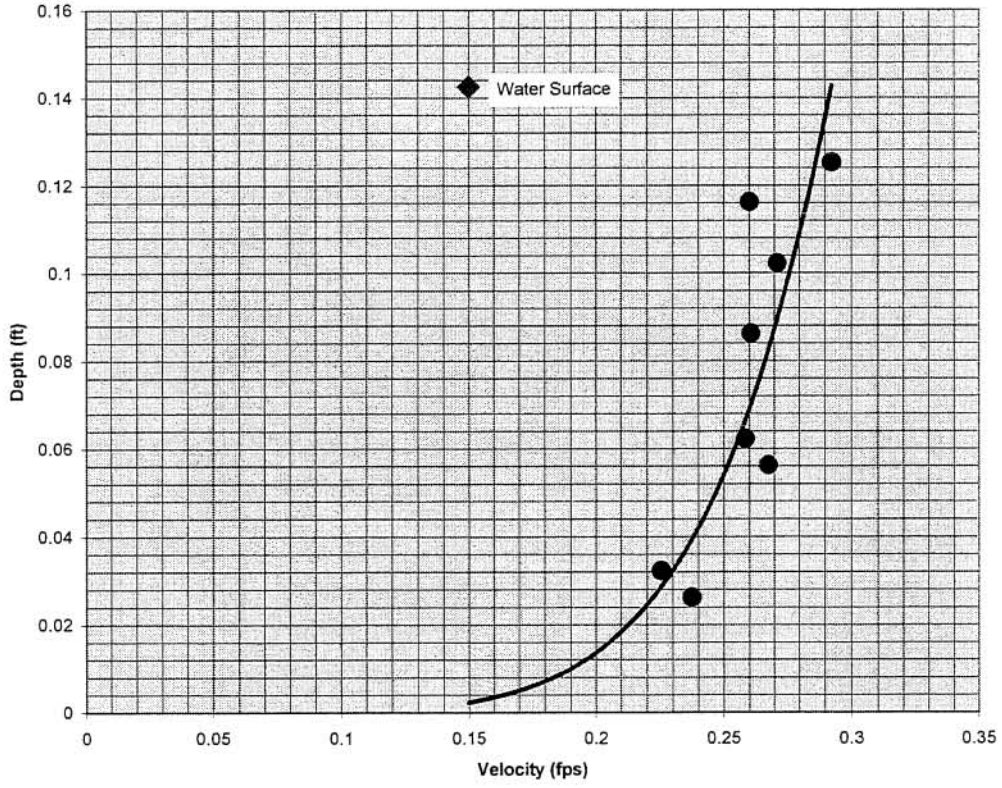

Figure 3.15. Left channel - Lane 1 velocity profile

	Gage Reading (ft)	Depth (ft)	Average Voltage (V)	Velocity (fps)	Flow Contribution (cfs/ft)
Bed	1.523	0.000	0.00E+00	0.00	0.00E+00
	1.549	0.026	3.76E-02	0.19	2.51E-03
	1.579	0.056	5.34E-02	0.24	6.47E-03
	1.609	0.086	5.27E-02	0.24	7.16E-03
	1.639	0.116	5.72E-02	0.25	7.34E-03
	1.669	0.146	5.57E-02	0.25	7.48E-03
	1.699	0.176	6.26E-02	0.27	7.73E-03
	1.729	0.206	5.31E-02	0.24	7.61E-03
	1.759	0.236	5.96E-02	0.26	7.47E-03
	1.789	0.266	5.69E-02	0.25	7.65E-03
	1.809	0.286	5.45E-02	0.24	4.94E-03
Surface	1.835	0.312	*	*	6.38E-03
				Specific Discharge	7.27E-02
				Flow	1.09E-01

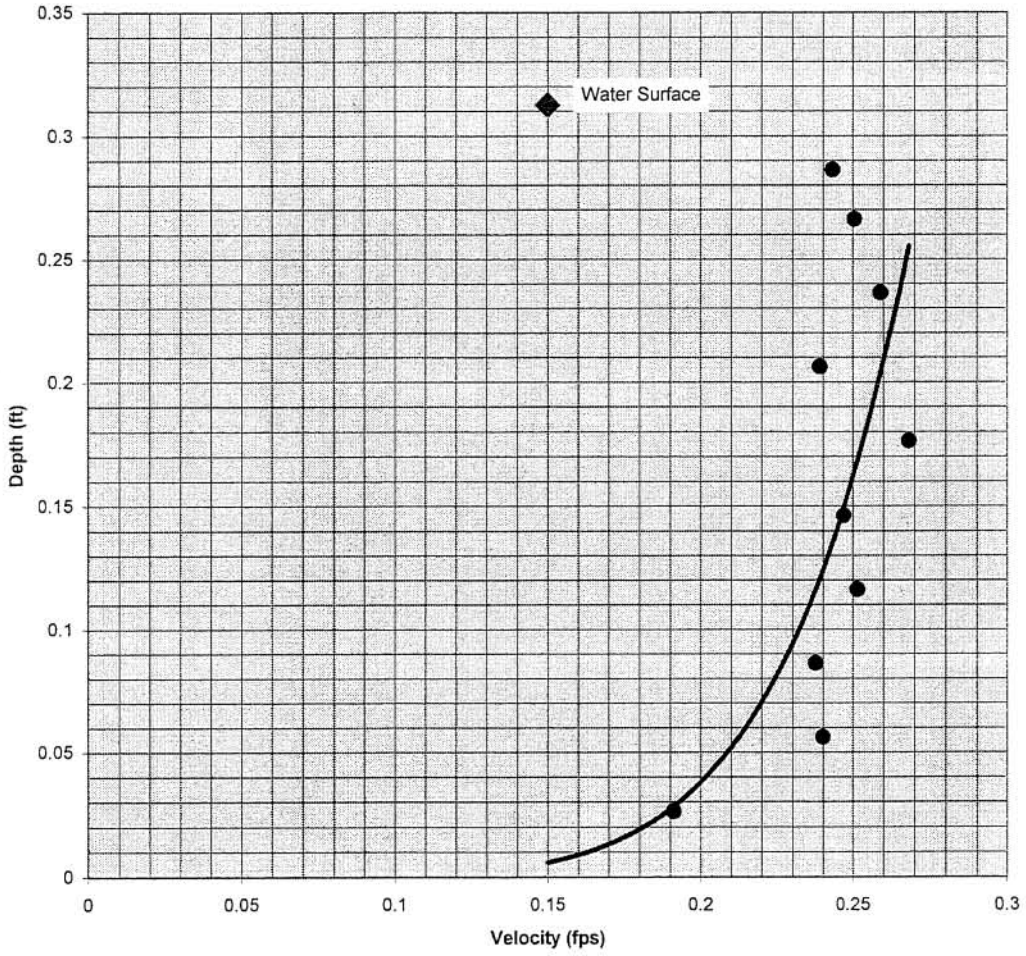

Figure 3.16. Left channel - Lane 2 velocity profile

	Gage Reading (ft)	Depth (ft)	Average Voltage (V)	Velocity (fps)	Flow Contribution (cfs/ft)
Bed	1.543	0.000	0.00E+00	0.00	0.00E+00
	1.569	0.026	4.53E-02	0.21	2.82E-03
	1.605	0.062	5.66E-02	0.25	8.36E-03
	1.630	0.087	5.67E-02	0.25	6.25E-03
	1.655	0.112	5.70E-02	0.25	6.26E-03
	1.680	0.137	6.09E-02	0.26	6.43E-03
	1.705	0.162	5.51E-02	0.25	6.35E-03
	1.730	0.187	6.10E-02	0.26	6.35E-03
	1.755	0.212	6.10E-02	0.26	6.58E-03
	1.780	0.237	6.02E-02	0.26	6.55E-03
	1.812	0.269	5.58E-02	0.25	8.13E-03
Surface	1.838	0.295	*	*	6.49E-03
				Specific Discharge	7.06E-02
				Flow (cfs)	1.06E-01

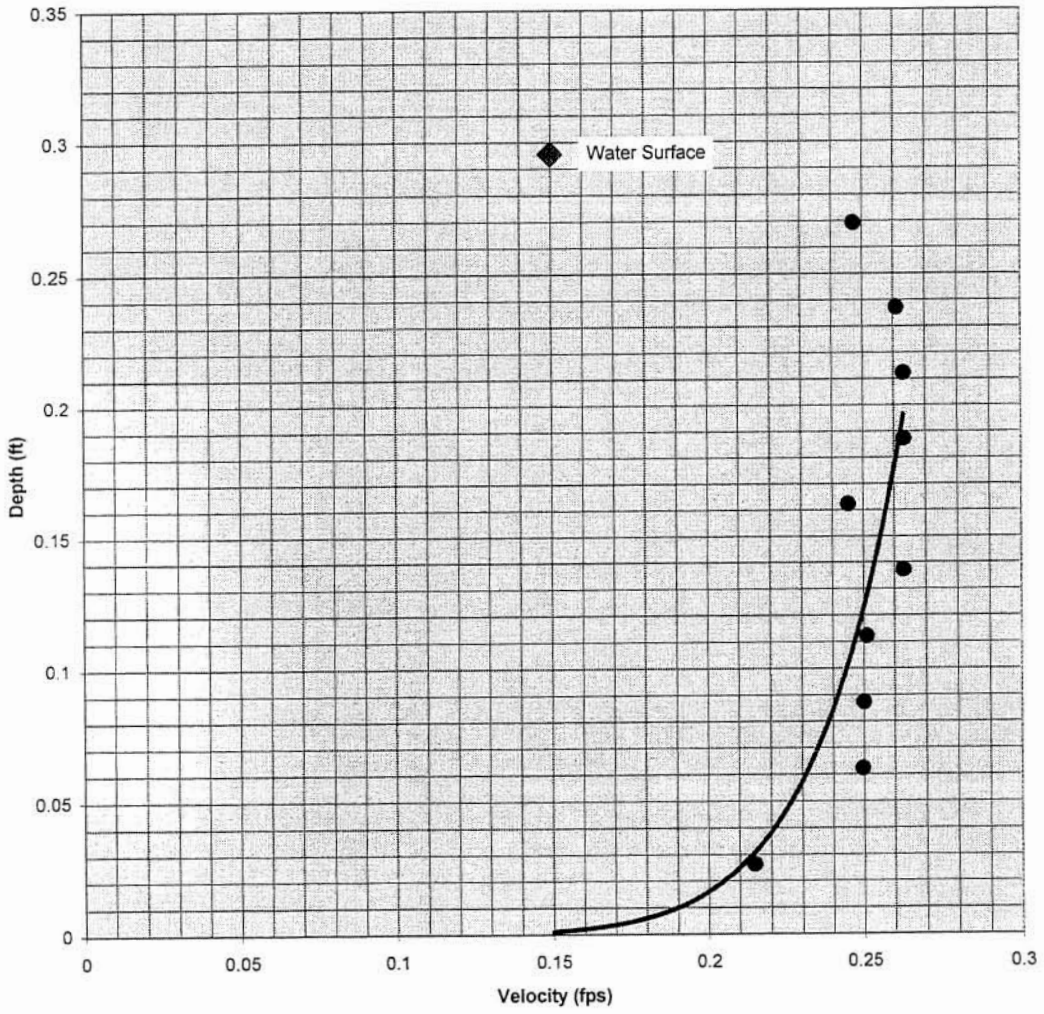

Figure 3.17. Left channel - Lane 3 velocity profile

	Gage Reading (ft)	Depth (ft)	Average Voltage (V)	Velocity (fps)	Flow Contribution (cfs/ft)
Bed	1.555	0.000	0.00E+00	0.00	0.00E+00
	1.581	0.026	4.73E-02	0.22	2.90E-03
	1.607	0.052	5.44E-02	0.24	6.03E-03
	1.632	0.077	5.60E-02	0.25	6.13E-03
	1.658	0.103	5.26E-02	0.24	6.31E-03
	1.684	0.129	5.93E-02	0.26	6.44E-03
	1.709	0.154	5.69E-02	0.25	6.36E-03
	1.735	0.180	6.51E-02	0.28	6.85E-03
	1.761	0.206	5.59E-02	0.25	6.81E-03
	1.786	0.231	5.51E-02	0.25	6.16E-03
	1.824	0.269	5.95E-02	0.26	9.57E-03
Surface	1.850	0.295	*	*	6.79E-03
					7.04E-02
					1.06E-01

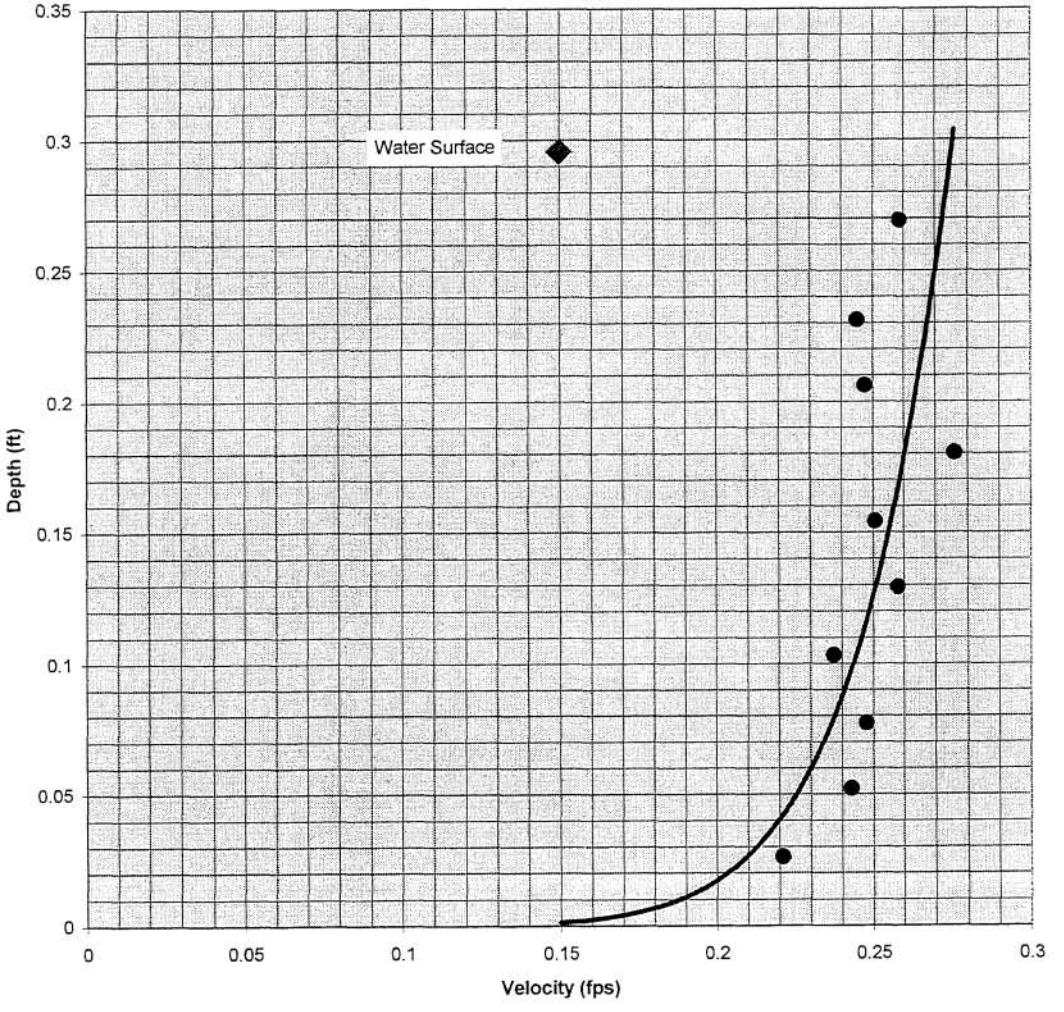

Figure 3.18. Left channel - Lane 4 velocity profile

	Gage Reading (ft)	Depth (ft)	Average Voltage (V)	Velocity (fps)	Flow Contribution (cfs/ft)
Bed	1.490	0.000	0.00E+00	0.00	0.00E+00
	1.516	0.026	4.38E-02	0.21	2.76E-03
	1.550	0.060	5.32E-02	0.24	7.64E-03
	1.584	0.094	5.54E-02	0.25	8.25E-03
	1.619	0.129	6.02E-02	0.26	8.87E-03
	1.653	0.163	6.00E-02	0.26	8.86E-03
	1.687	0.197	5.97E-02	0.26	8.83E-03
	1.721	0.231	6.33E-02	0.27	9.01E-03
	1.756	0.266	6.04E-02	0.26	9.31E-03
	1.789	0.299	6.10E-02	0.26	8.66E-03
	1.821	0.331	5.56E-02	0.25	8.16E-03
Surface	1.847	0.357	*	*	6.48E-03
				Specific Discharge	8.68E-02
				Flow (cfs)	1.30E-01

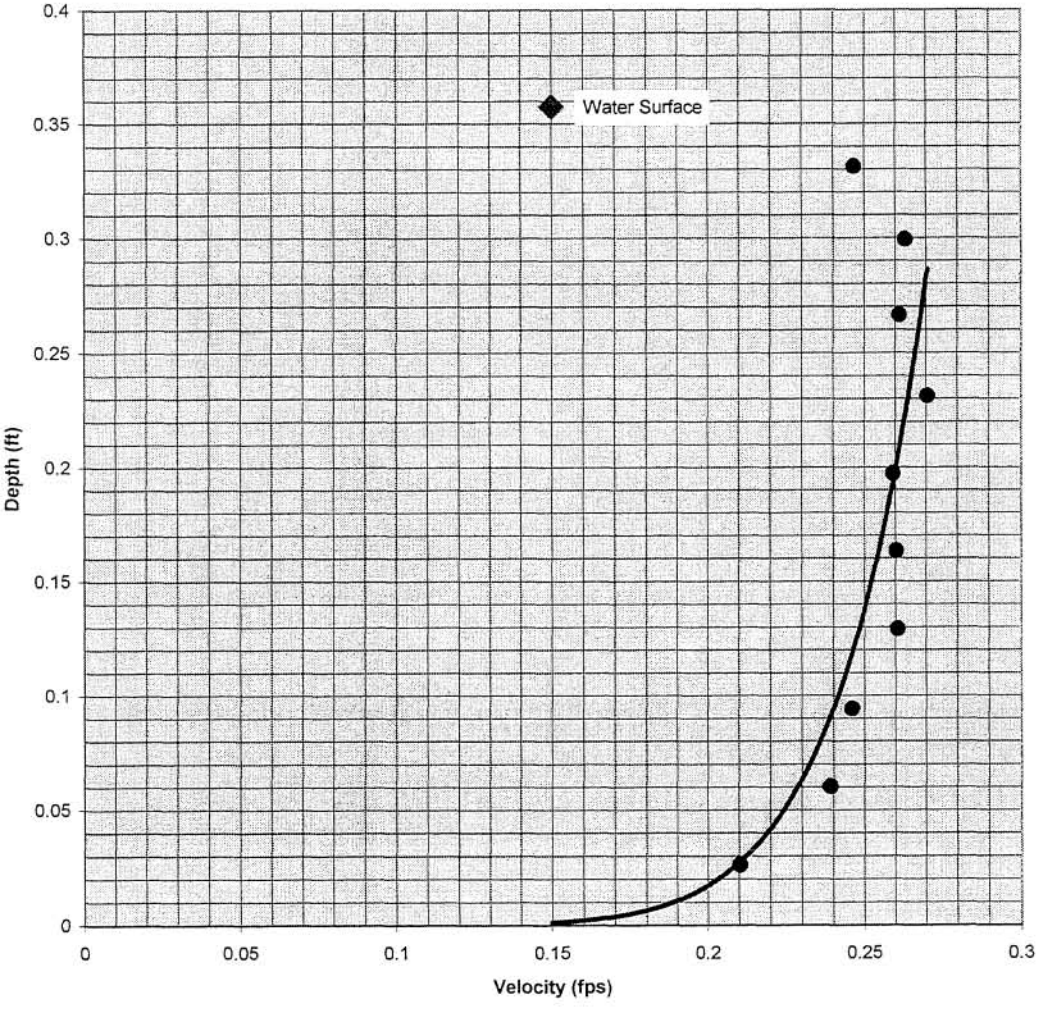

Figure 3.19. Left channel - Lane 5 velocity profile

	Gage Reading (ft)	Depth (ft)	Average Voltage (V)	Velocity (fps)	Flow Contribution (cfs/ft)
Bed	1.494	0.000	0.00E+00	0.00	0.00E+00
	1.520	0.026	6.74E-02	0.28	3.72E-03
	1.552	0.058	7.87E-02	0.32	9.62E-03
	1.585	0.091	8.51E-02	0.34	1.08E-02
	1.617	0.123	8.81E-02	0.35	1.09E-02
	1.650	0.156	9.37E-02	0.36	1.17E-02
	1.682	0.188	9.27E-02	0.36	1.16E-02
	1.715	0.221	9.26E-02	0.36	1.19E-02
	1.747	0.253	9.47E-02	0.37	1.16E-02
	1.780	0.286	9.73E-02	0.38	1.23E-02
	1.821	0.327	9.19E-02	0.36	1.50E-02
Surface	1.847	0.353	*	*	9.41E-03
				Specific Discharge	1.19E-01
				Flow (cfs)	2.18E-01

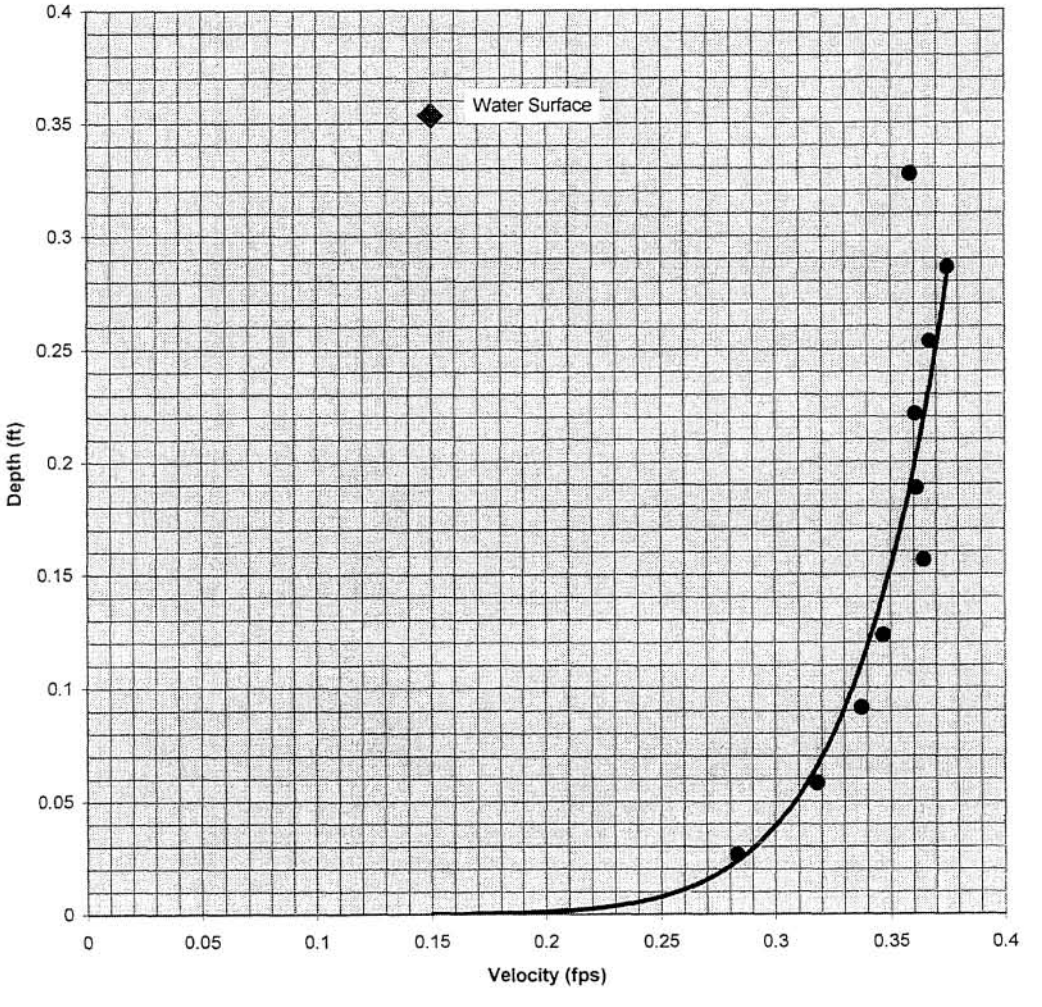

Figure 3.20. Left channel - Lane 6 velocity profile

Batavia Dam Model Study

University of Illinois Hydrosystems Laboratory:

Existing - Flow Split

Specific Discharge Key

× ⟶ = 10 cfs/ ft

63% = % total flow (cfs)

January 25, 1998

Scale: 1/10" = 1'

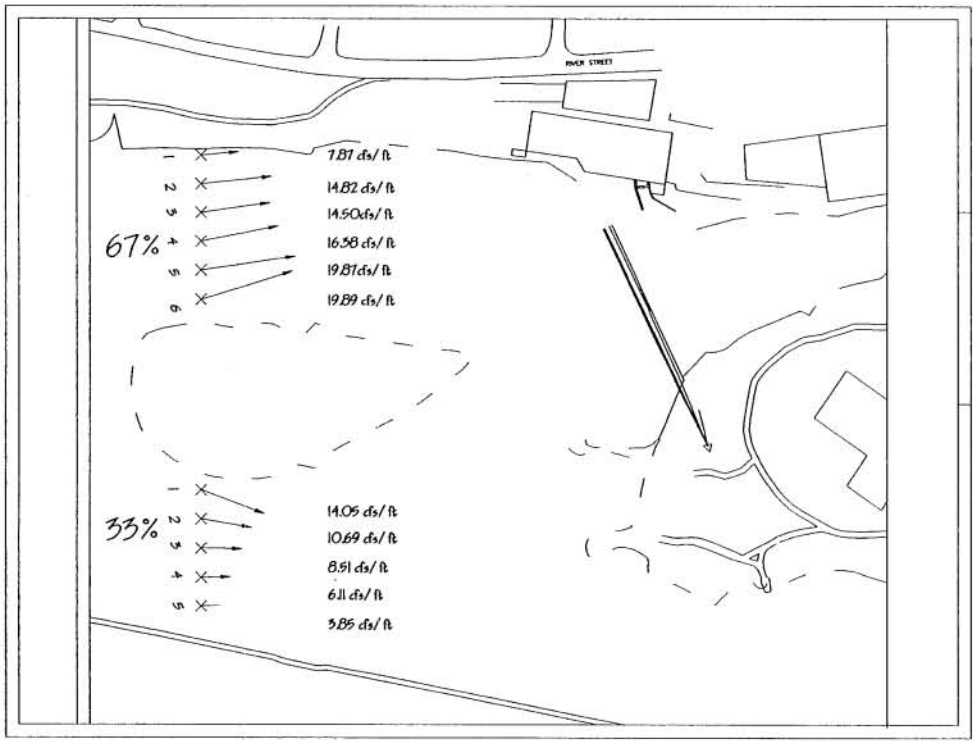

Figure 3.21. Existing condition - Specific discharge flow split around Duck Island - Calibration flow (6062 cfs)

Batavia Dam Model Study

University of Illinois Hydrosystems Laboratory:

Existing - Velocity
2 year flood

Velocity Key

→ = 5 ft/s

I.D. = Insufficient depth

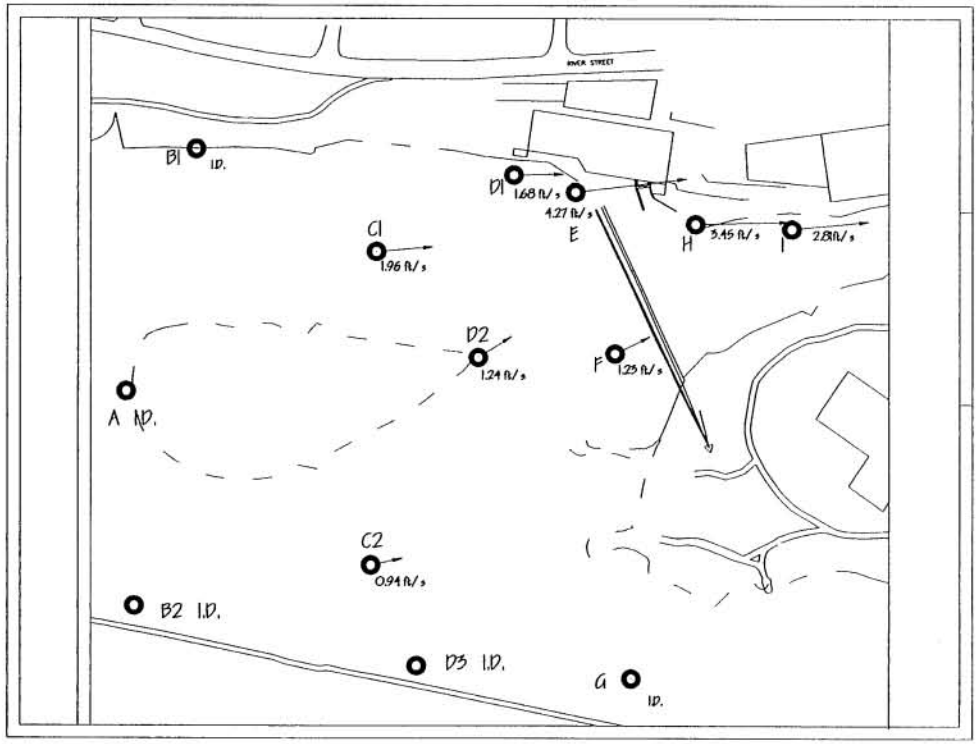

February 10, 1998

Scale: 1/10" = 1'

Figure 3.22. Existing condition - Point velocity measurments - 2 year flood (5700 cfs)

Batavia Dam
Model Study

University of Illinois
Hydrosystems
Laboratory:

Existing - Velocity
10 year flood

Velocity Key

→ = 5 ft/s

I.D. = Insufficient depth

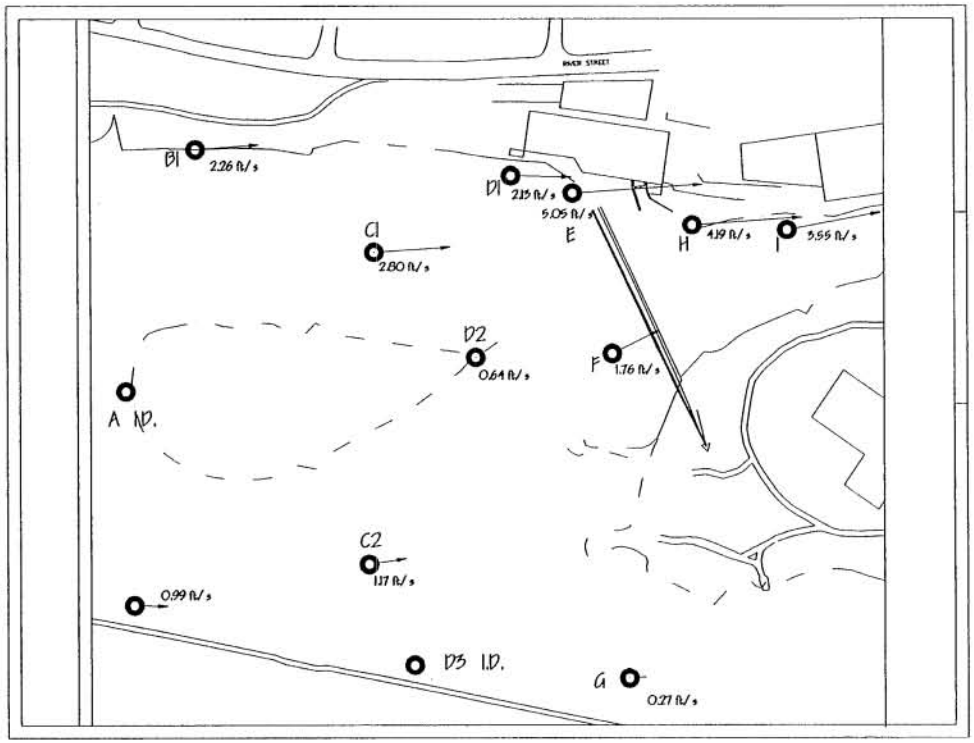

February 10, 1998

Scale: 1/10" = 1'

Figure 3.23. Existing condition - Point velocity measurments - 10 year flood (8500 cfs)

Batavia Dam Model Study

University of Illinois Hydrosystems Laboratory:

Existing - Velocity
50 year flood

Velocity Key

o ——→ = 5 ft/s

I.D. = Insufficient depth

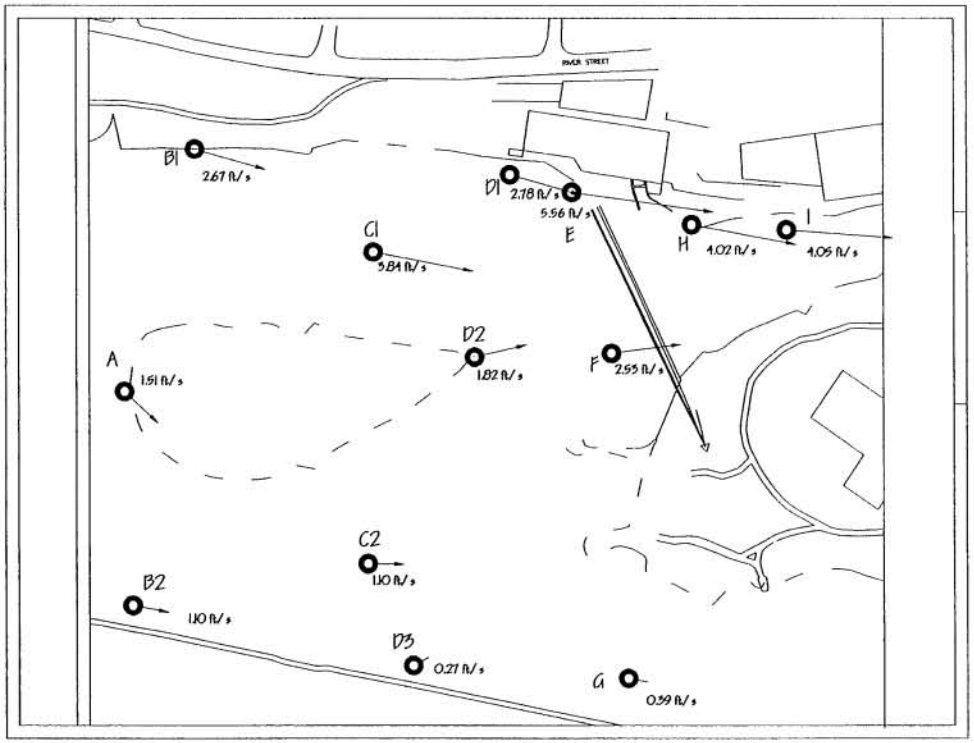

February 10, 1998

Scale: 1/10" = 1'

Figure 3.24. Existing condition - Point velocity measurments - 50 year flood (12500 cfs)

Batavia Dam Model Study

University of Illinois Hydrosystems Laboratory:

Existing - Velocity
100 year flood

Velocity Key

=5 ft/s

I.D. = Insufficient depth

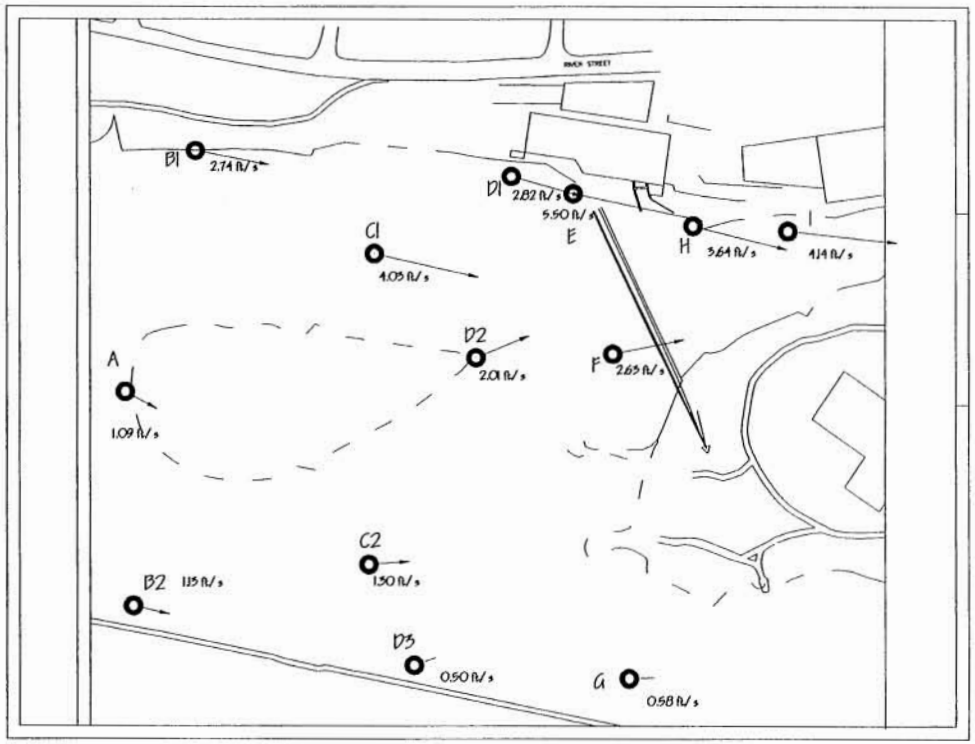

February 10, 1998

Scale: 1/10" = 1'

Figure 3.25. Existing condition - Point velocity measurments - 100 year flood (135500 cfs)

Batavia Dam
Model Study

University of Illinois
Hydrosystems
Laboratory:

Existing - Velocity
500 year flood

Velocity Key

=5 ft/s

I.D. = Insufficient depth

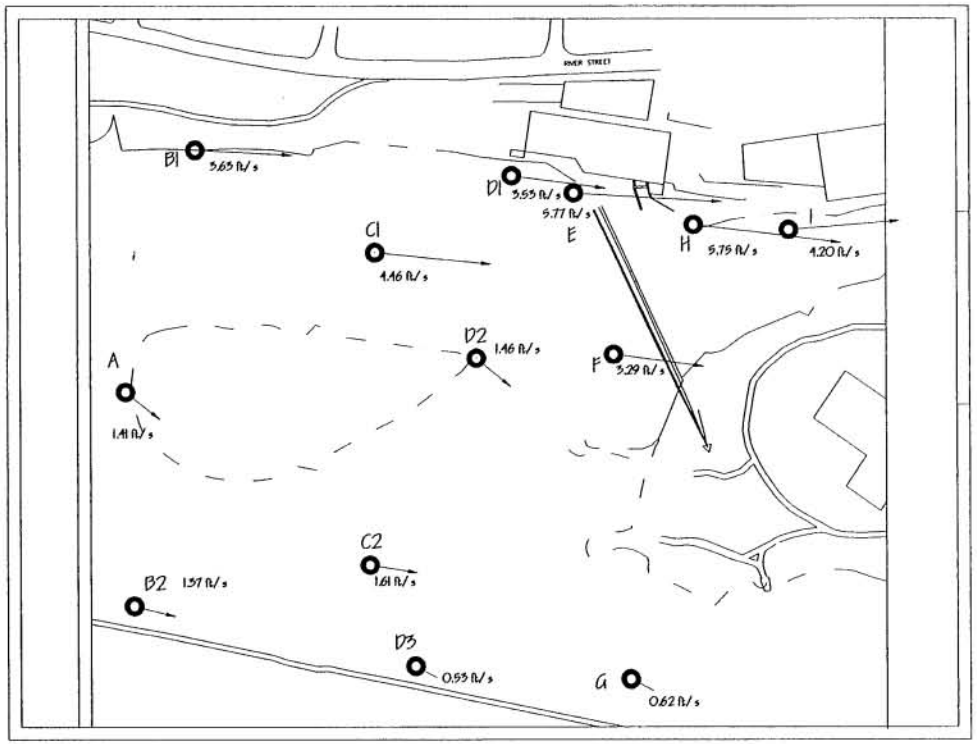

February 10, 1998

Scale: 1/10" = 1'

Figure 3.26. Existing condition - Point velocity measurments - 500 year flood (17630 cfs)

Batavia Dam
Model Study

University of Illinois
Hydrosystems
Laboratory:

Existing
Downstream discharge
2 year flood

Specific Discharge Key

×← = 20 cfs/ ft

I.D. = Insufficient depth

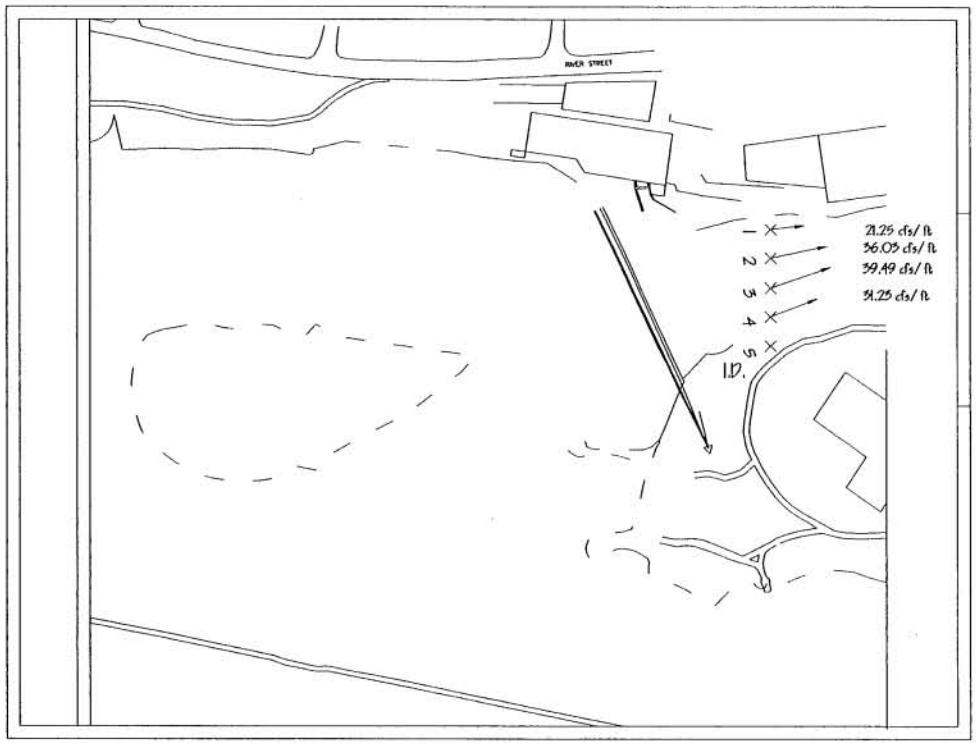

February 10, 1998

Scale: 1/10" = 1'

Figure 3.27. Existing condition - Specific discharge conditions downstream of stucture - 2 year flood (5700 cfs)

Batavia Dam
Model Study

University of Illinois
Hydrosystems
Laboratory:

Existing
Downstream discharge
10 year flood

Specific Discharge Key

×← = 20 cfs/ ft

I.D. = Insufficient depth

February 10, 1998

Scale: 1/10" = 1'

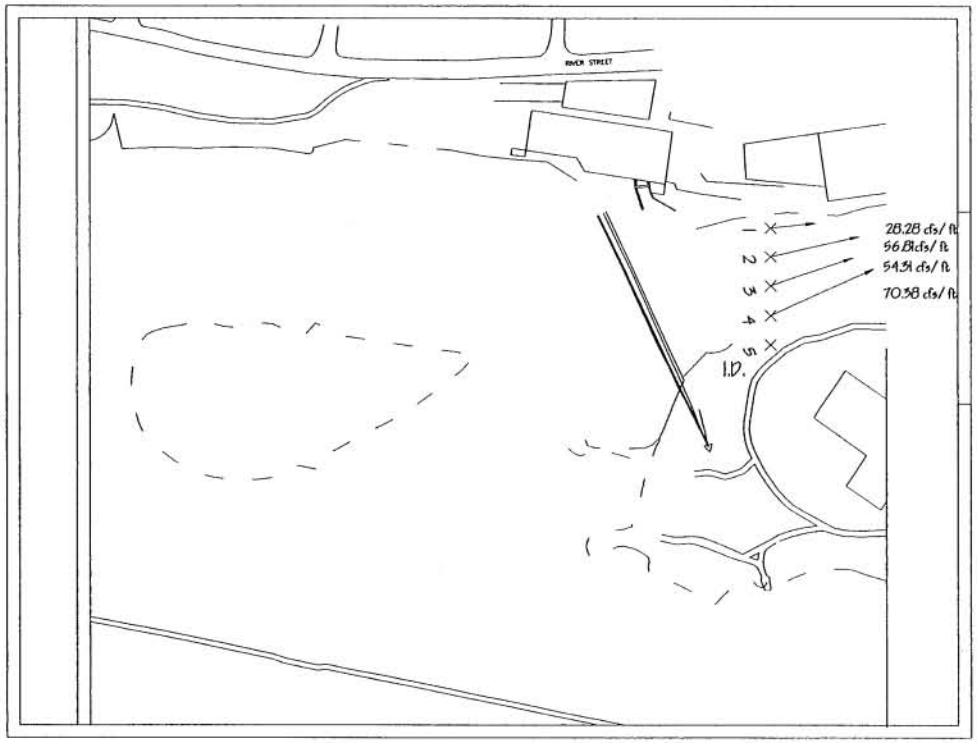

Figure 3.28. Existing condition - Specific discharge conditions downstream of stucture - 10 year flood (8500 cfs)

Batavia Dam
Model Study

University of Illinois
Hydrosystems
Laboratory:

Existing
Downstream discharge
50 year flood

Specific Discharge Key

×← = 20 cfs/ ft

I.D. = Insufficient depth

February 10, 1998

Scale: 1/10" = 1'

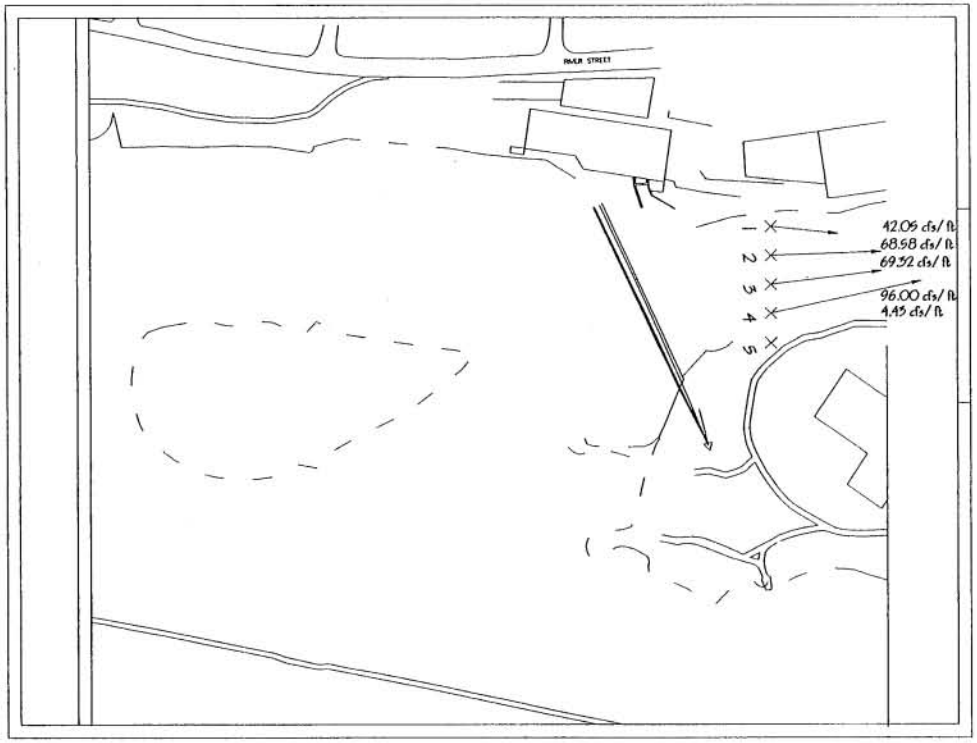

Figure 3.29. Existing condition - Specific discharge conditions downstream of stucture - 50 year flood (12500 cfs)

Batavia Dam
Model Study

University of Illinois
Hydrosystems
Laboratory:

Existing
Downstream discharge
100 year flood

Specific Discharge Key

×← = 20 cfs/ ft

I.D. = Insufficient depth

February 10, 1998

Scale: 1/10" = 1'

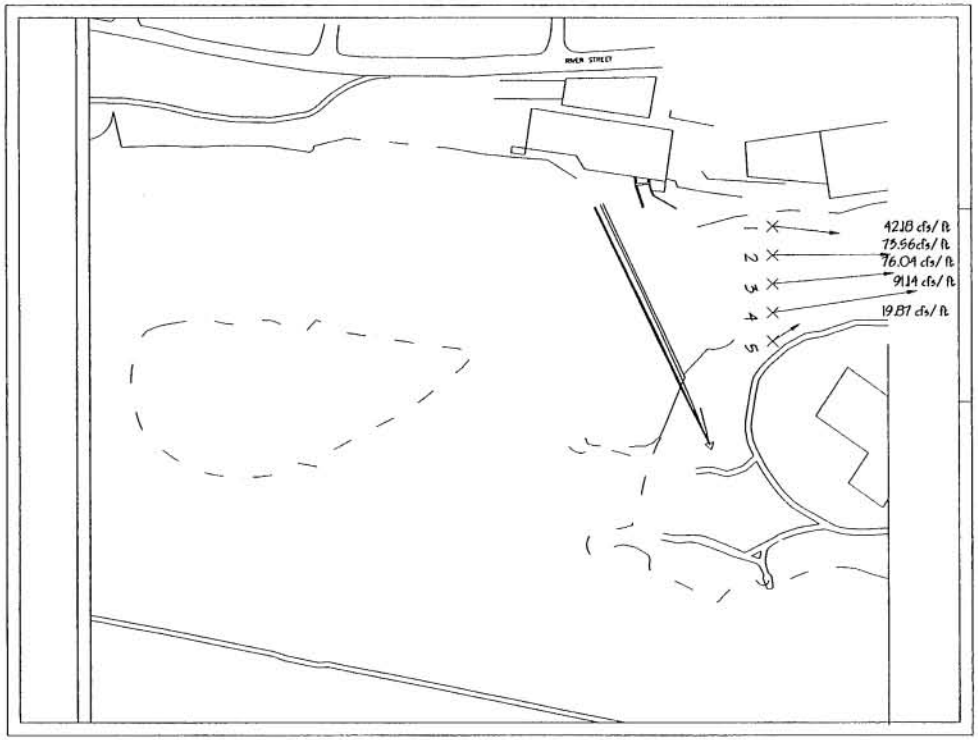

Figure 3.30. Existing condition - Specific discharge conditions downstream of stucture - 100 year flood (13500 cfs)

Batavia Dam
Model Study

University of Illinois
Hydrosystems
Laboratory:

Existing
Downstream discharge
500 year flood

Specific Discharge Key

×← = 20 cfs/ ft

I.D. = Insufficient depth

February 10, 1998

Scale: 1/10" = 1'

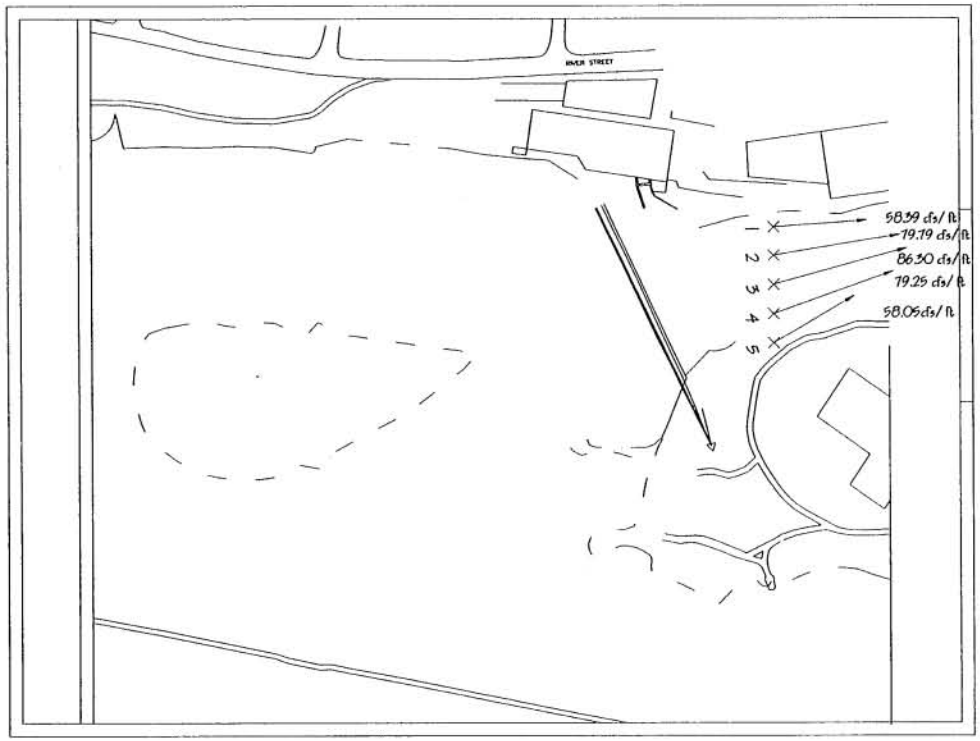

Figure 3.31. Existing condition - Specific discharge conditions downstream of stucture - 500 year flood (17630 cfs)

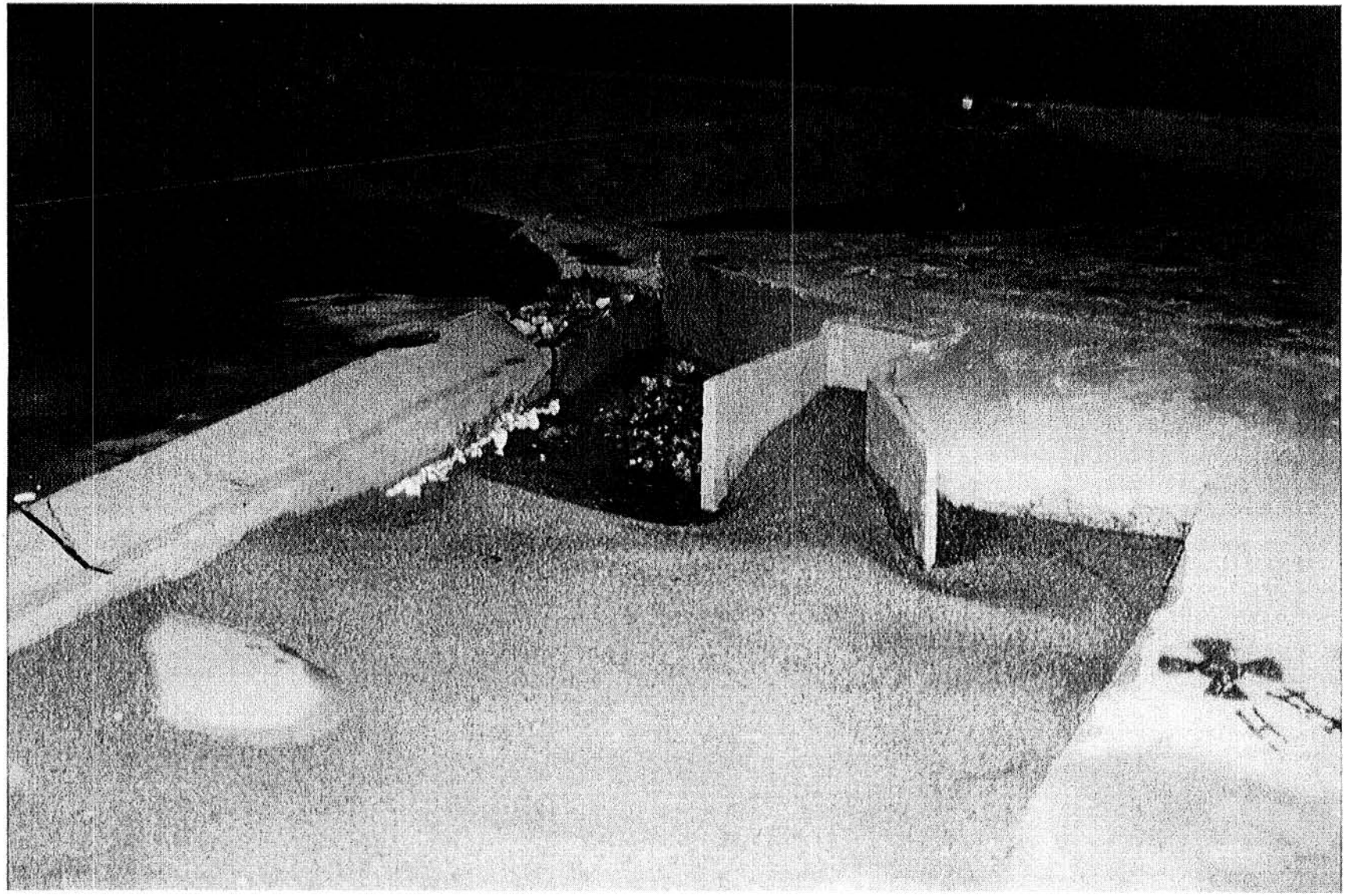

Figure 3.32. Scour hole developed downstream of dam breach

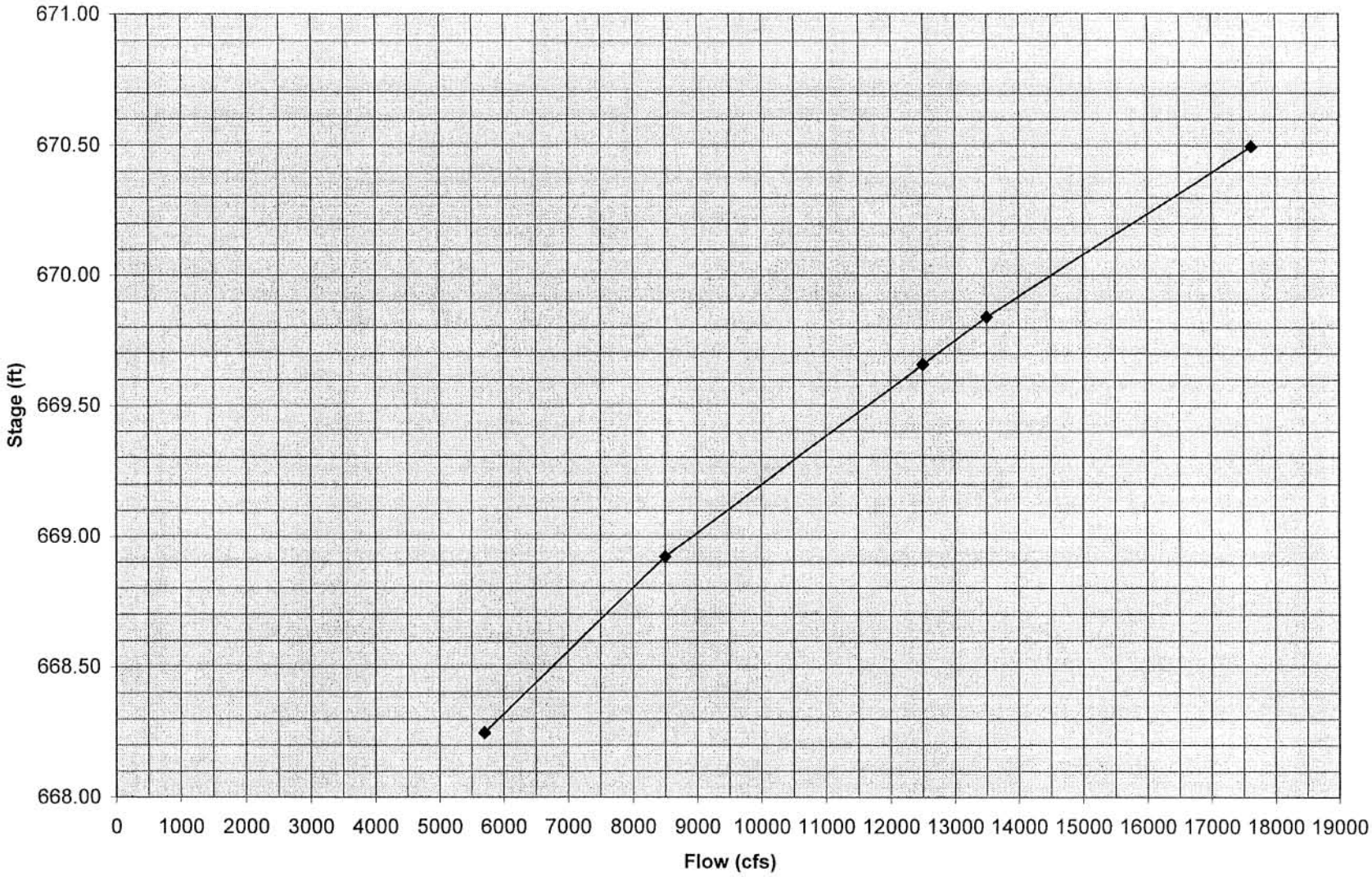

Figure 3.33. Averaged upstream pool stage response - Baseline condition

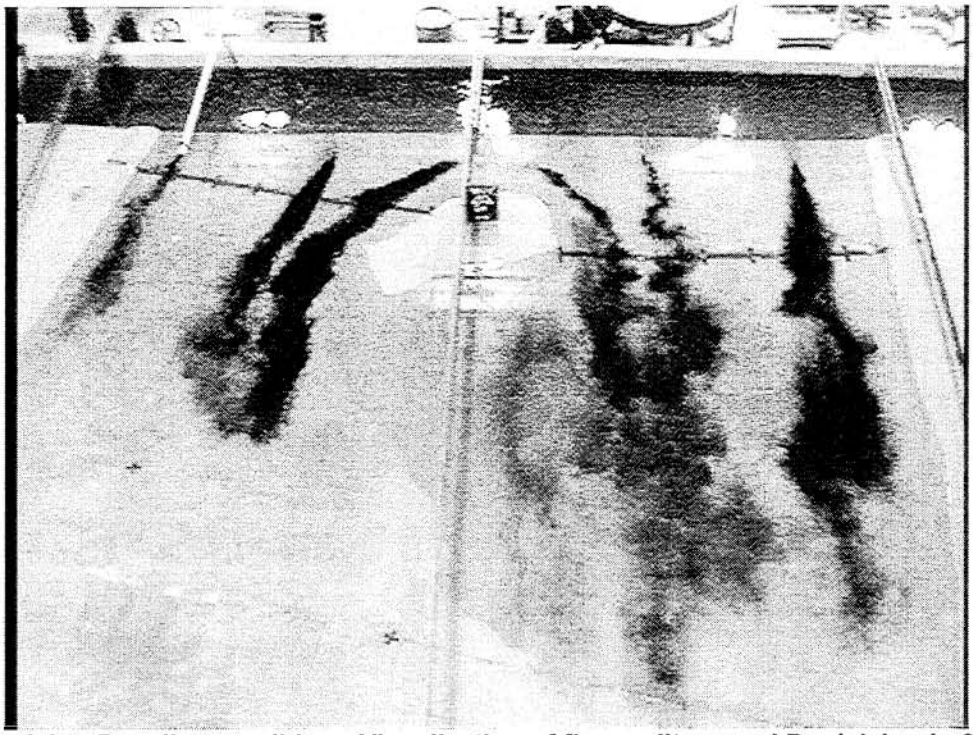

Figure 3.34. Baseline condition - Visualization of flow split around Duck Island - 2 year flood (5700 cfs)

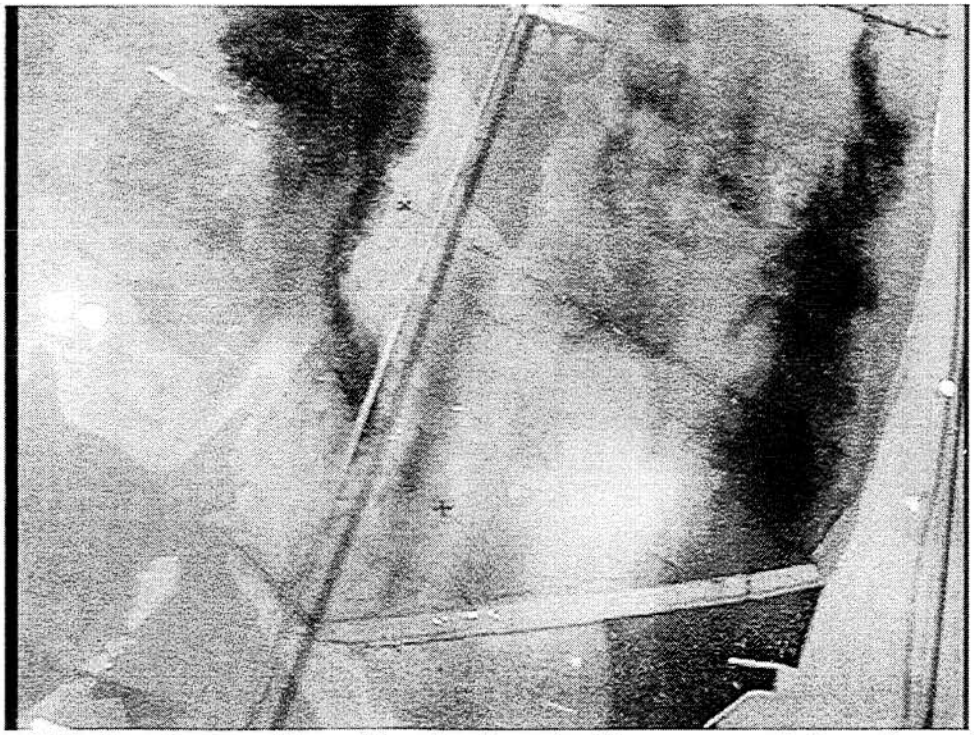

Figure 3.35. Baseline condition - Visualization of spillway approach flow - 2 year flood (5700 cfs)

Figure 3.36. Baseline condition - Visualization of flow split around Duck Island - 10 year flood (8500 cfs)

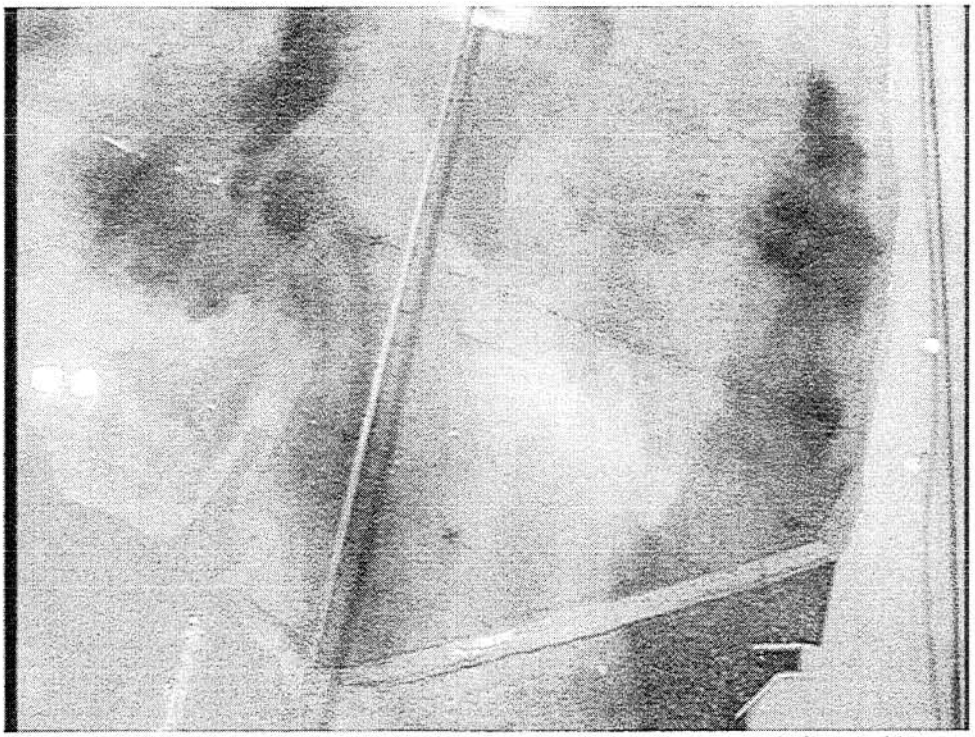

Figure 3.37. Baseline condition - Visualization of spillway approach flow - 10 year flood (8500 cfs)

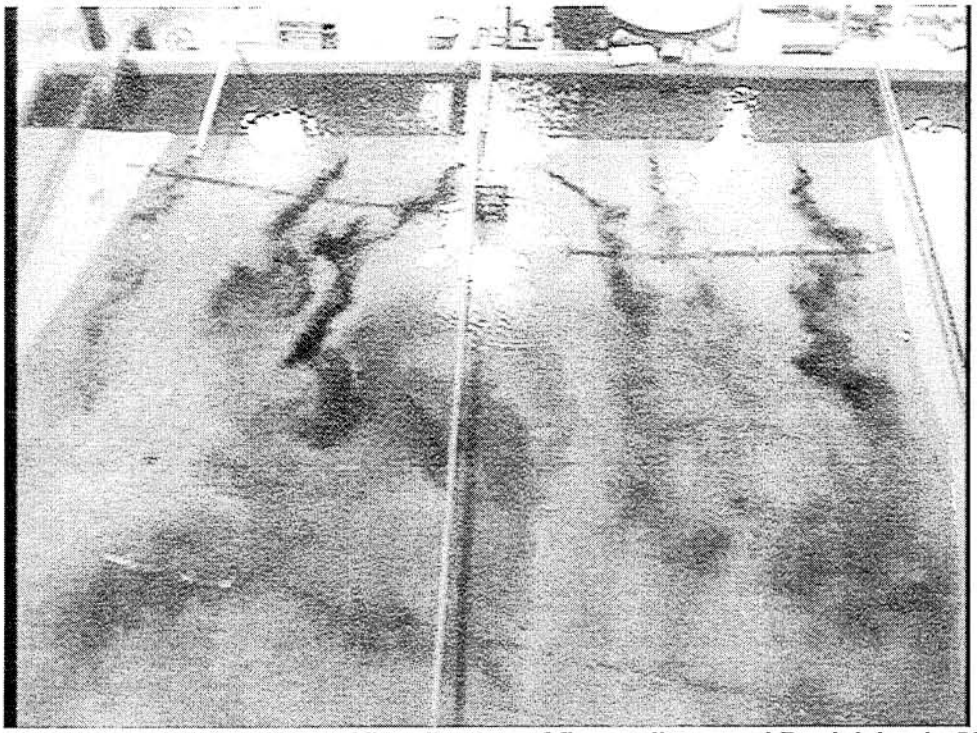

Figure 3.38. Baseline condition - Visualization of flow split around Duck Island - 50 year flood (12500 cfs)

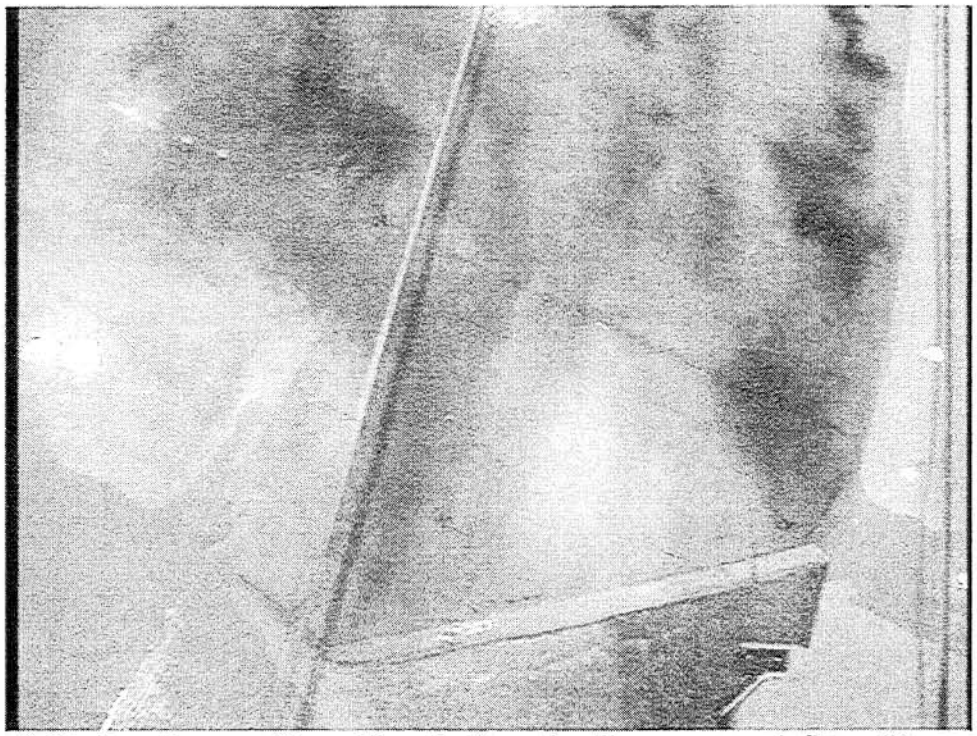

Figure 3.39. Baseline condition - Visualization of spillway approach flow - 50 year flood (12500 cfs)

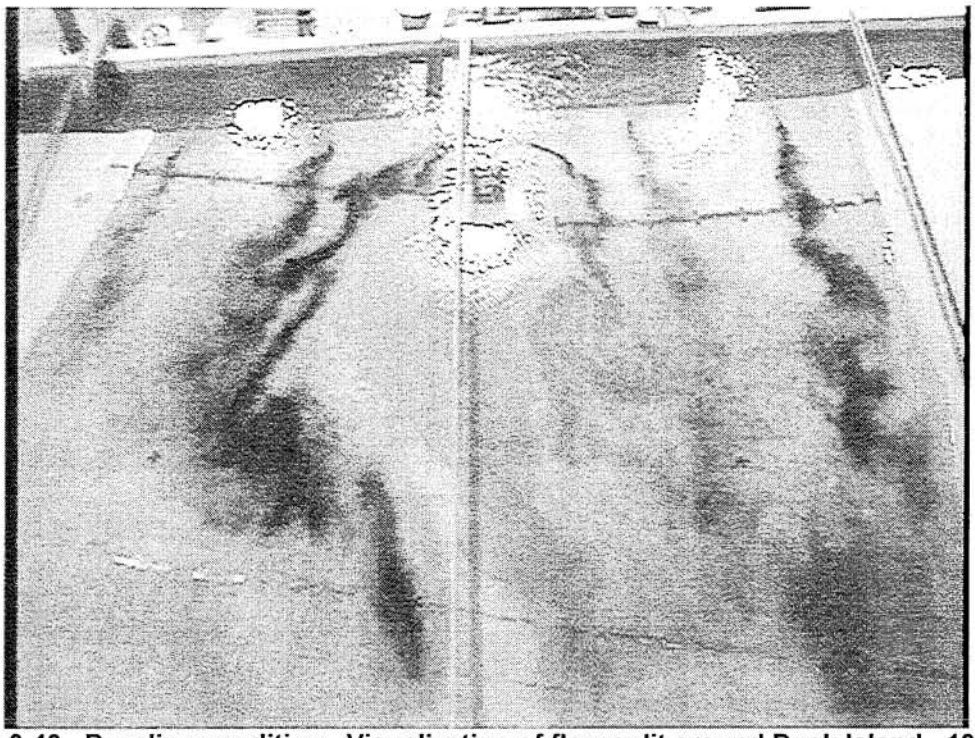

Figure 3.40. Baseline condition - Visualization of flow split around Duck Island - 100 year flood (13500 cfs)

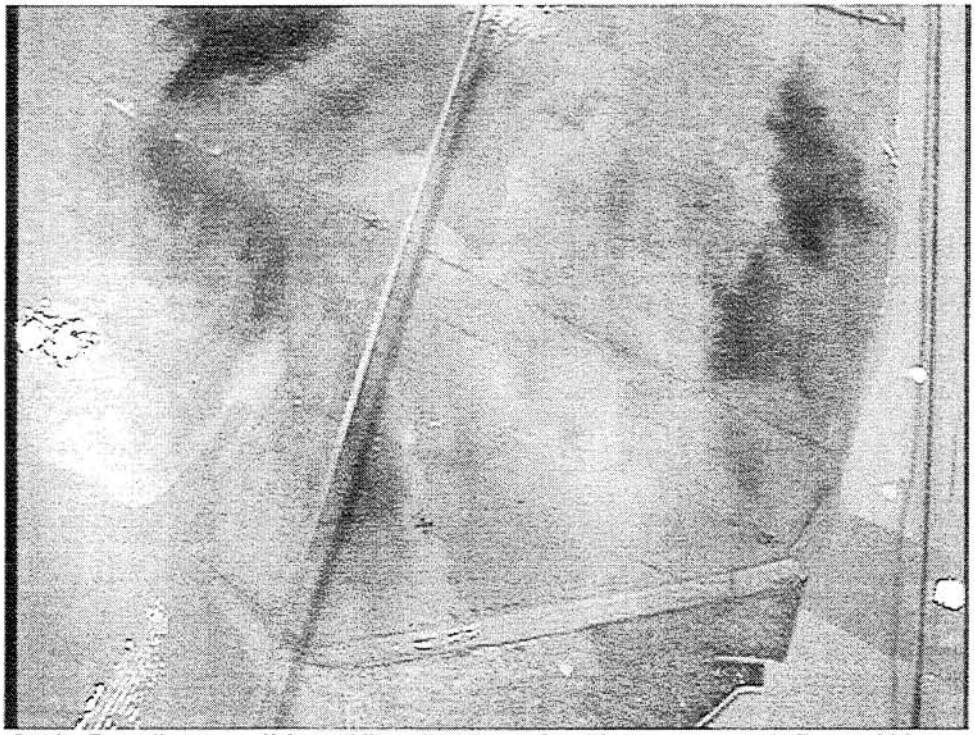

Figure 3.41. Baseline condition - Visualization of spillway approach flow - 100 year flood (13500 cfs)

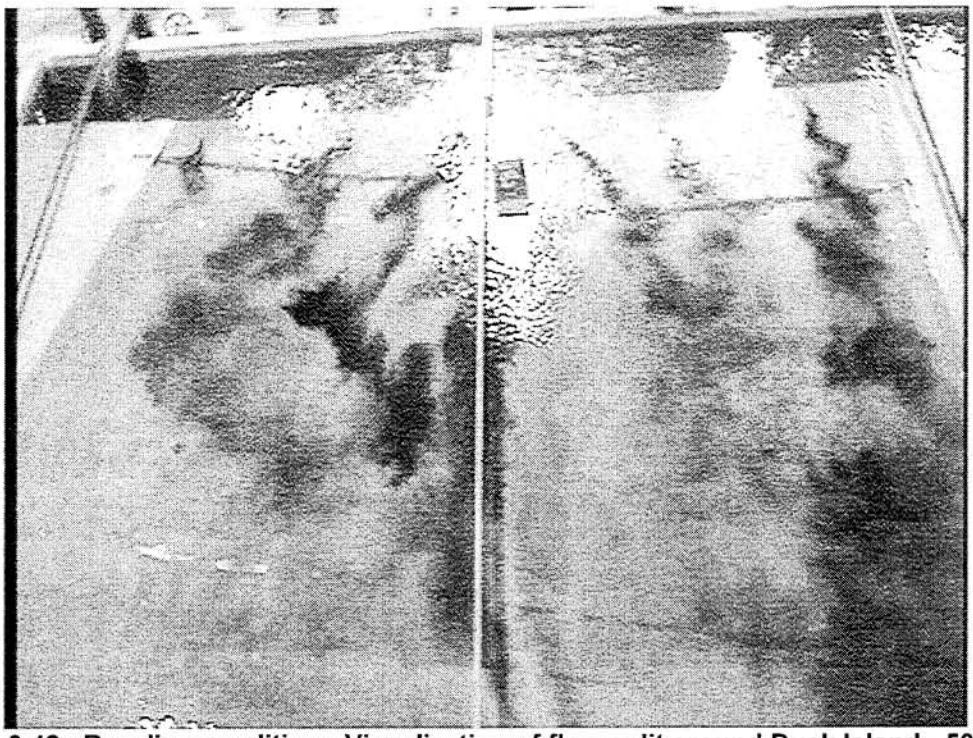

Figure 3.42. Baseline condition - Visualization of flow split around Duck Island - 500 year flood (17630 cfs)

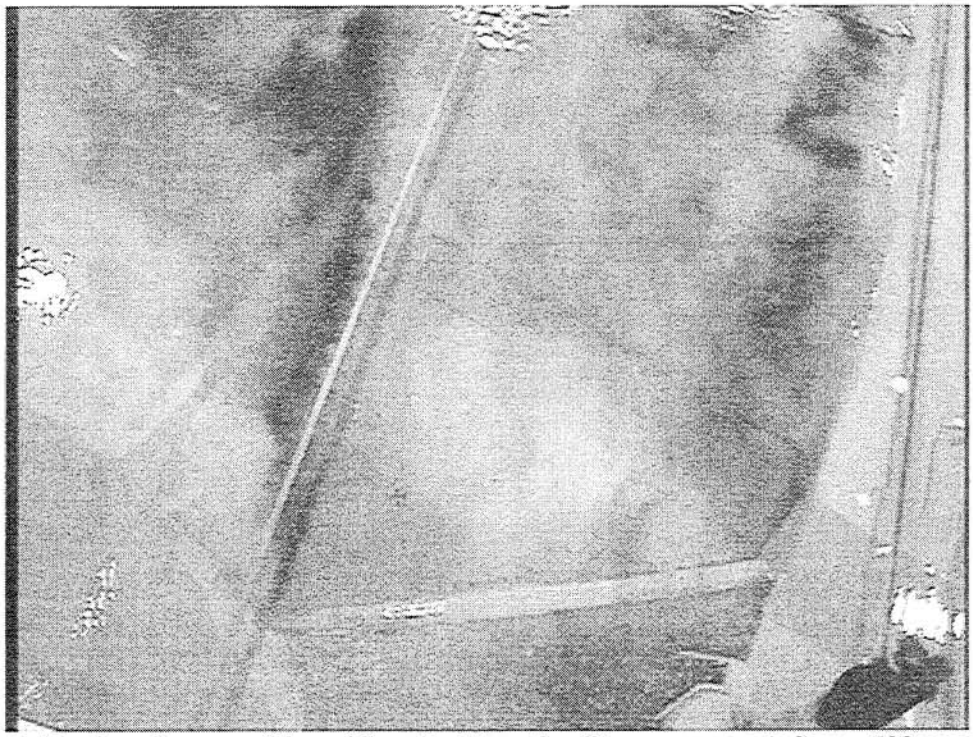

Figure 3.43. Baseline condition - Visualization of spillway approach flow - 500 year flood (17630 cfs)

Batavia Dam Model Study

University of Illinois Hydrosystems Laboratory:

Baseline - Flow Split

Specific Discharge Key

×⟶ = 10 cfs/ ft

63% = % total flow (cfs)

January 25, 1998

Scale: 1/ 10" = 1'

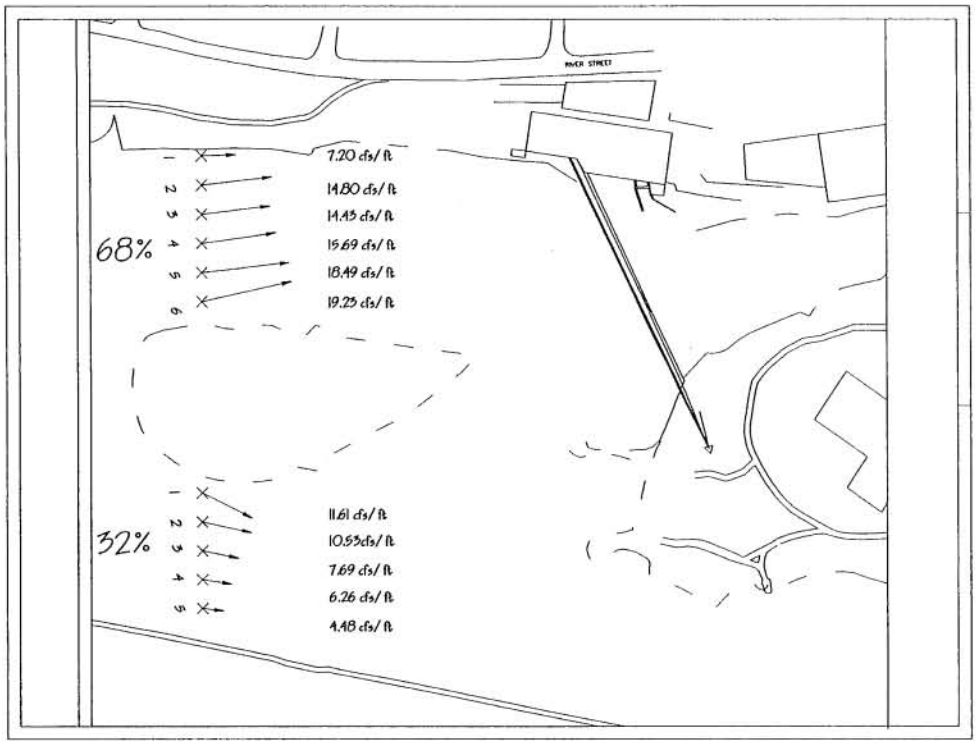

Figure 3.44. Baseline condition - Specific discharge flow split around Duck Island - Calibration flow (6062 cfs)

Batavia Dam Model Study

University of Illinois Hydrosystems Laboratory:

Baseline - Velocity
2 year flood

Velocity Key

=5 ft/s

I.D. = Insufficient depth

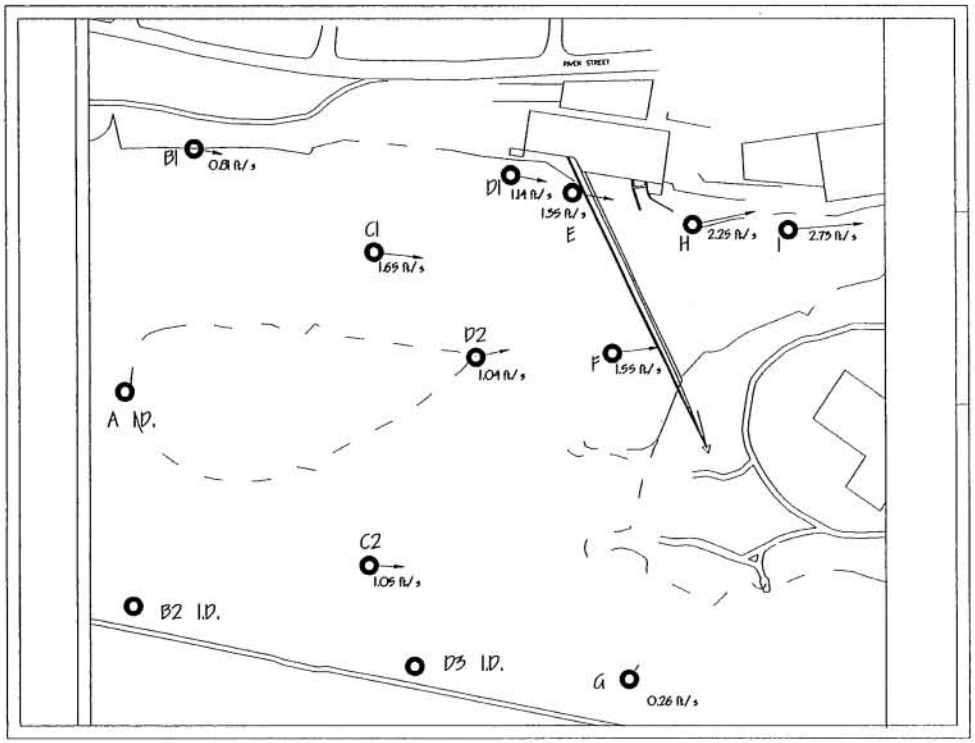

January 25, 1998

Scale: 1/10" = 1'

Figure 3.45. Baseline condition - Point velocity measurments - 2 year flood (5700 cfs)

Batavia Dam Model Study

University of Illinois Hydrosystems Laboratory:

Baseline - Velocity
10 year flood

Velocity Key

→ = 5 ft/s

I.D. = Insufficient depth

January 25, 1998

Scale: 1/10" = 1'

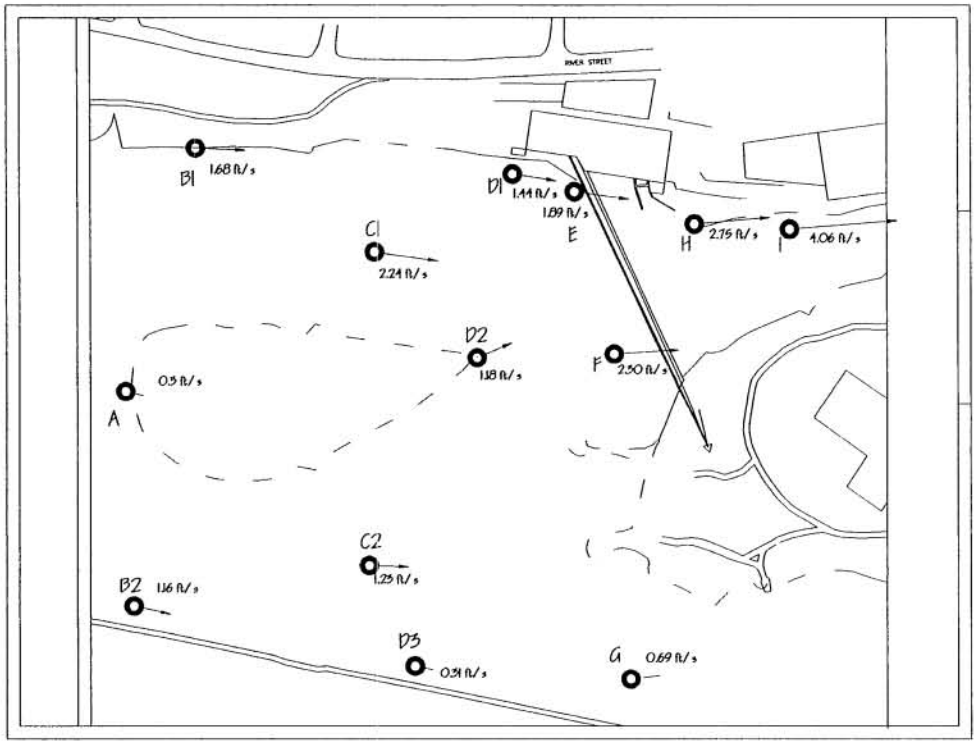

Figure 3.46. Baseline condition - Point velocity measurments - 10 year flood (8500 cfs)

Batavia Dam Model Study

University of Illinois Hydrosystems Laboratory:

Baseline - Velocity
50 year flood

Velocity Key

→ = 5 ft/s

I.D. = Insufficient depth

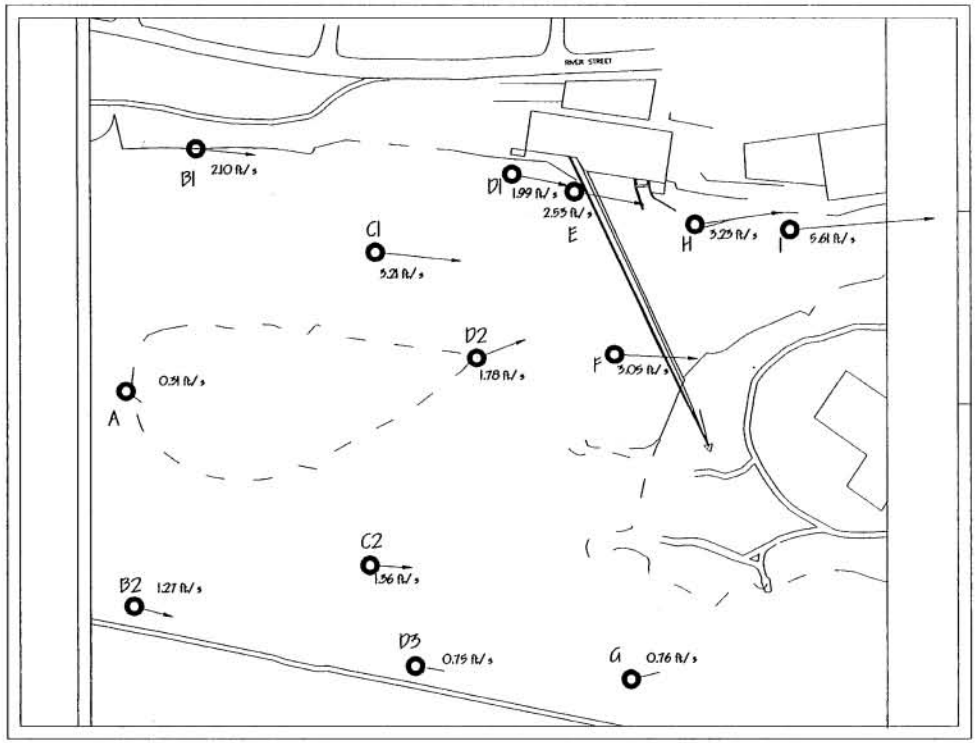

January 25, 1998

Scale: 1/10" = 1'

Figure 3.47. Baseline condition - Point velocity measurments - 50 year flood (12500 cfs)

Batavia Dam
Model Study

University of Illinois
Hydrosystems
Laboratory:

Baseline - Velocity
100 year flood

Velocity Key

=5 ft/s

I.D. = Insufficient depth

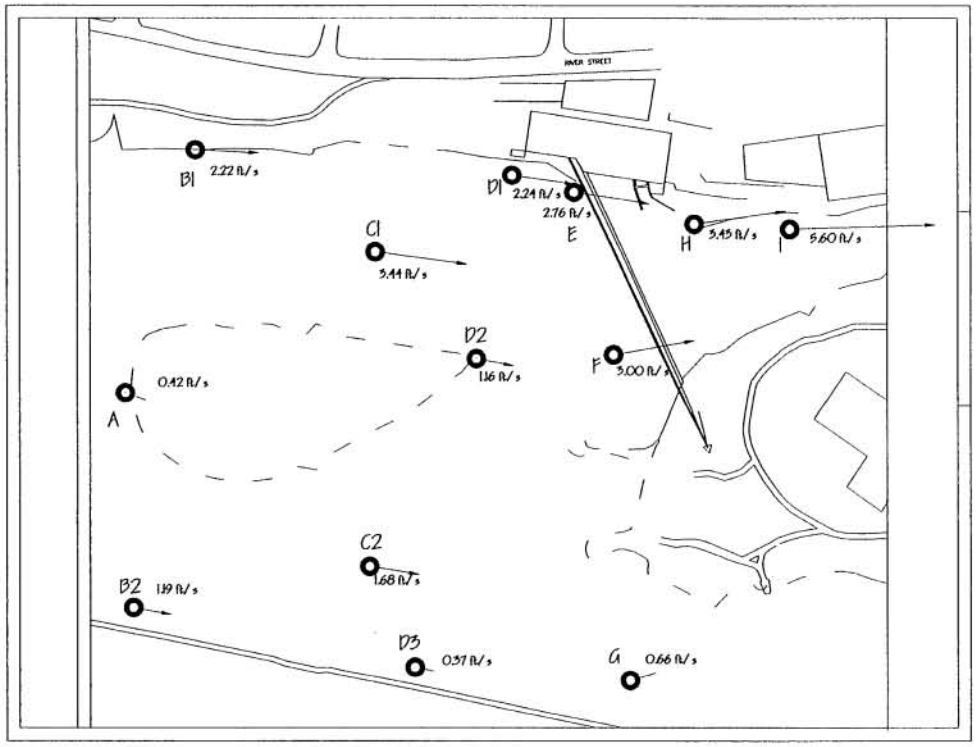

January 25, 1998

Scale: 1/10" = 1'

Figure 3.48. Baseline condition - Point velocity measurments - 100 year flood (13500 cfs)

Batavia Dam Model Study

University of Illinois Hydrosystems Laboratory:

Baseline - Velocity
500 year flood

Velocity Key

=5 ft/s

I.D. = Insufficient depth

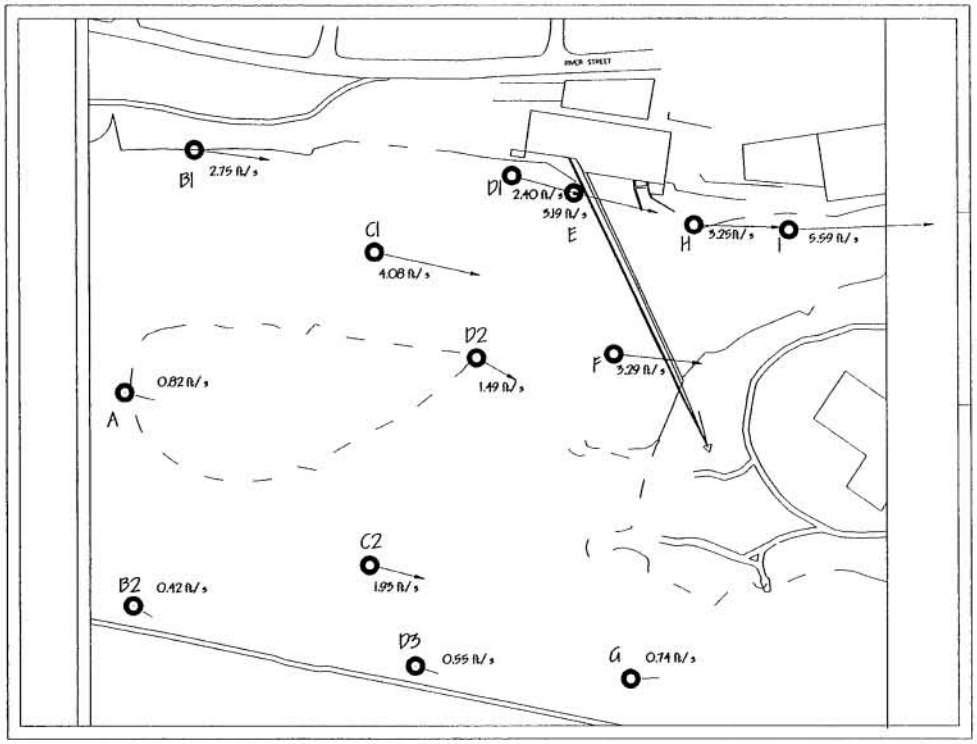

January 25, 1998

Scale: 1/10" = 1'

Figure 3.49. Baseline condition - Point velocity measurments - 500 year flood (17630 cfs)

Batavia Dam Model Study

University of Illinois Hydrosystems Laboratory:

Baseline
Downstream discharge
2 year flood

Specific Discharge Key

×⟵ = 20 cfs/ ft

I.D. = Insufficient depth

January 25, 1998

Scale: 1/10" = 1'

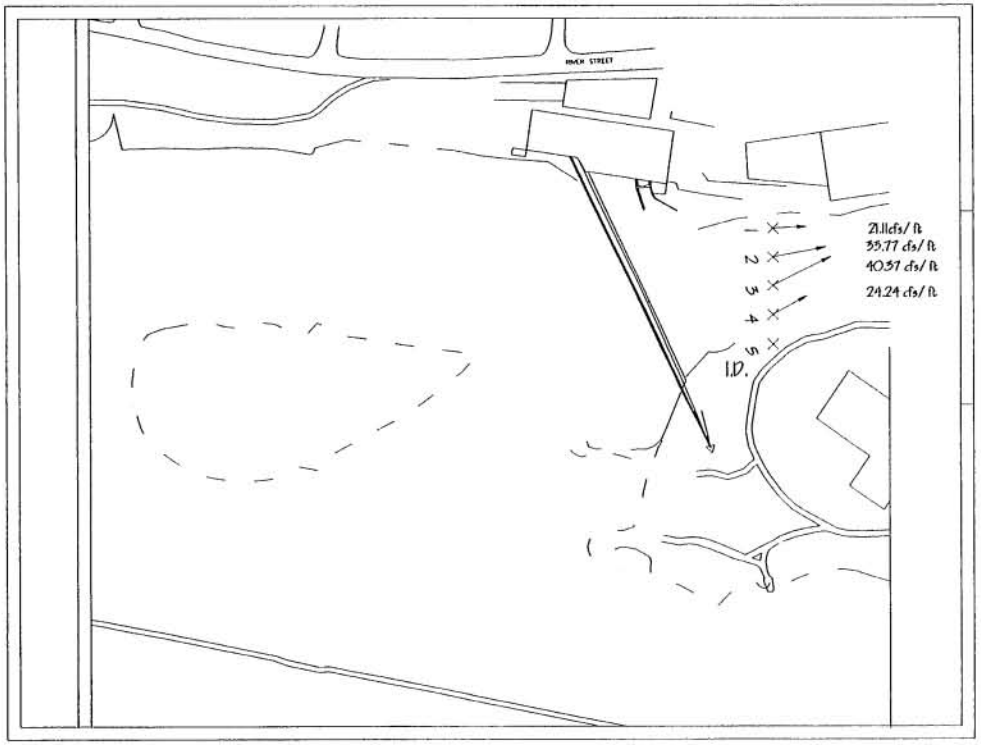

Figure 3.50. Baseline condition - Specific discharge conditions downstream of stucture - 2 year flood (5700 cfs)

Batavia Dam Model Study

University of Illinois Hydrosystems Laboratory:

Baseline
Downstream discharge
10 year flood

Specific Discharge Key

×← = 20 cfs/ ft

I.D. = Insufficient depth

January 25, 1998

Scale: 1/10" = 1'

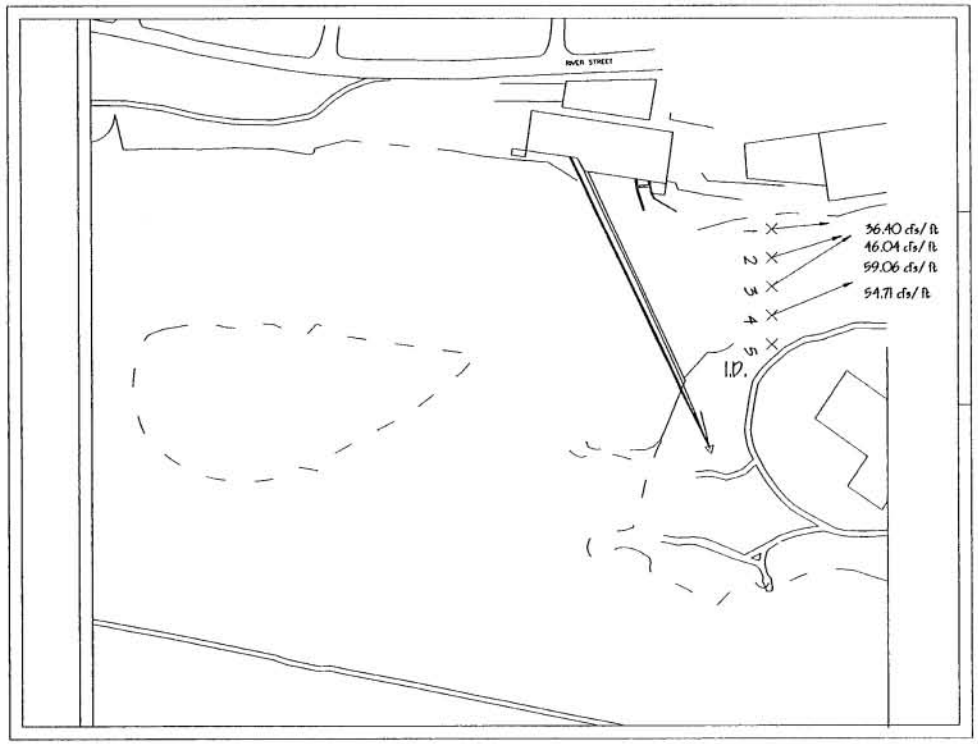

Figure 3.51. Basline condition - Specific discharge conditions downstream of stucture - 10 year flood (8500 cfs)

Batavia Dam Model Study

University of Illinois Hydrosystems Laboratory:

Baseline
Downstream discharge
50 year flood

Specific Discharge Key

×← = 20 cfs/ ft

I.D. = Insufficient depth

January 25, 1998

Scale: 1/10" = 1'

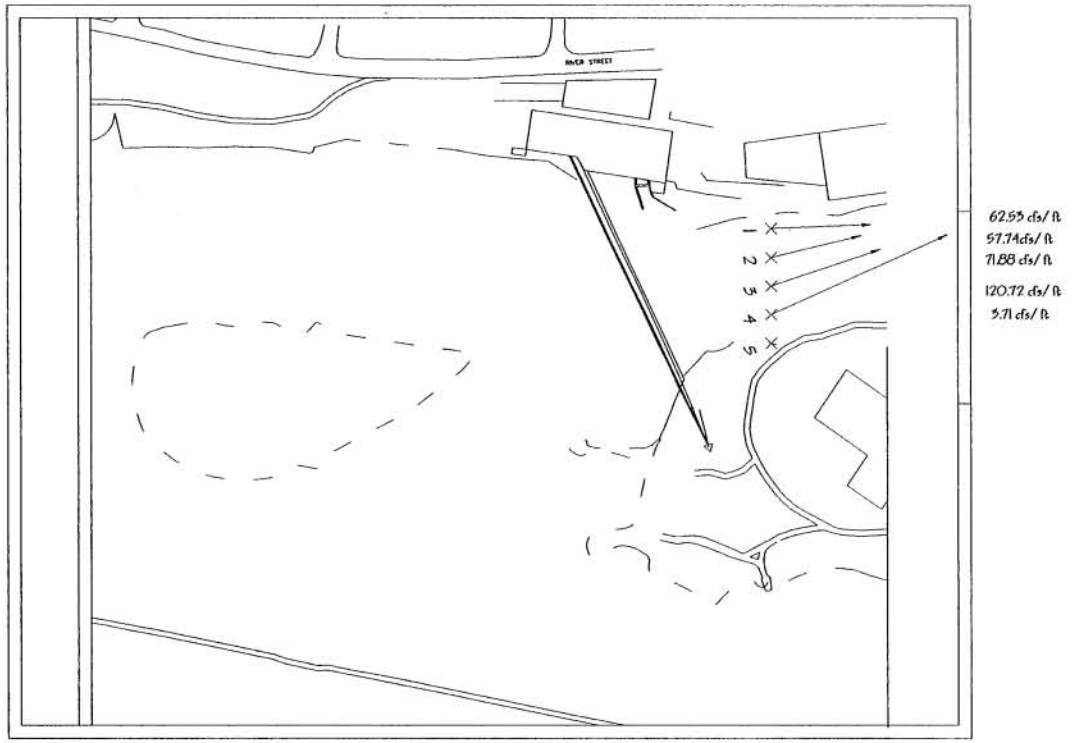

Figure 3.52. Basline condition - Specific discharge conditions downstream of stucture - 50 year flood (12500 cfs)

Batavia Dam Model Study

University of Illinois Hydrosystems Laboratory:

Baseline
Downstream discharge
100 year flood

Specific Discharge Key

×— = 20 cfs/ ft

I.D. = Insufficient depth

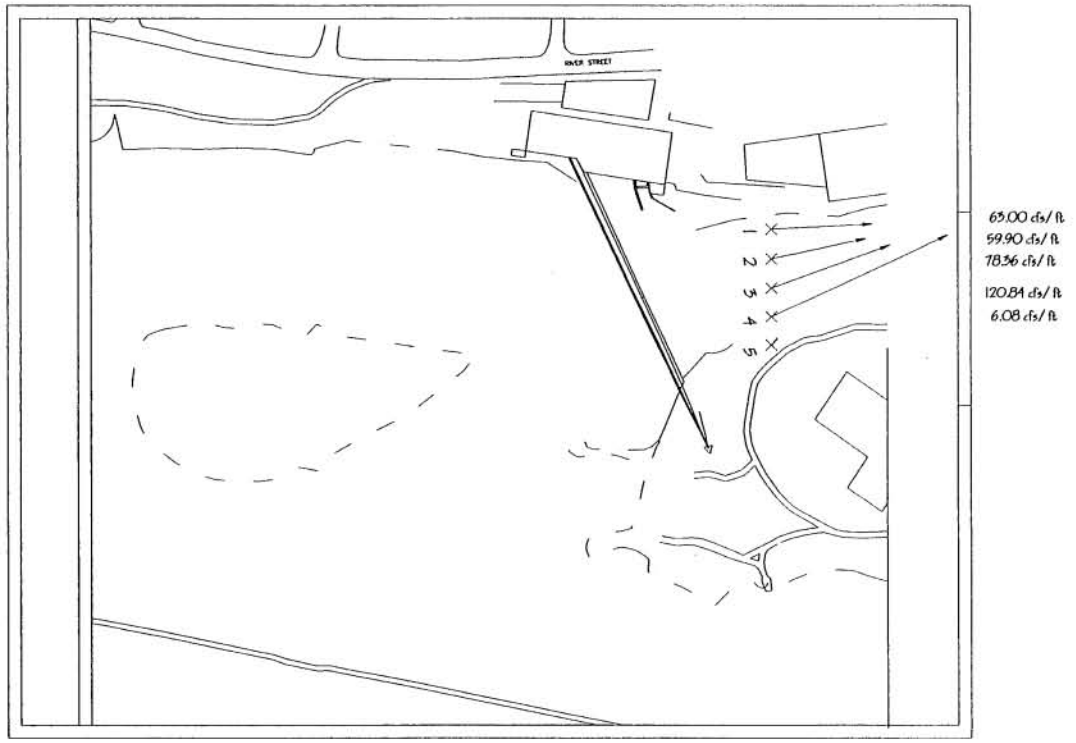

January 25, 1998

Scale: 1/10" = 1'

Figure 3.53. Basline condition - Specific discharge conditions downstream of stucture - 100 year flood (135000 cfs)

Batavia Dam Model Study

University of Illinois Hydrosystems Laboratory:

Baseline
Downstream discharge
500 year flood

Specific Discharge Key

×—→ = 20 cfs/ ft

I.D. = Insufficient depth

February 10, 1998

Scale: 1/10" = 1'

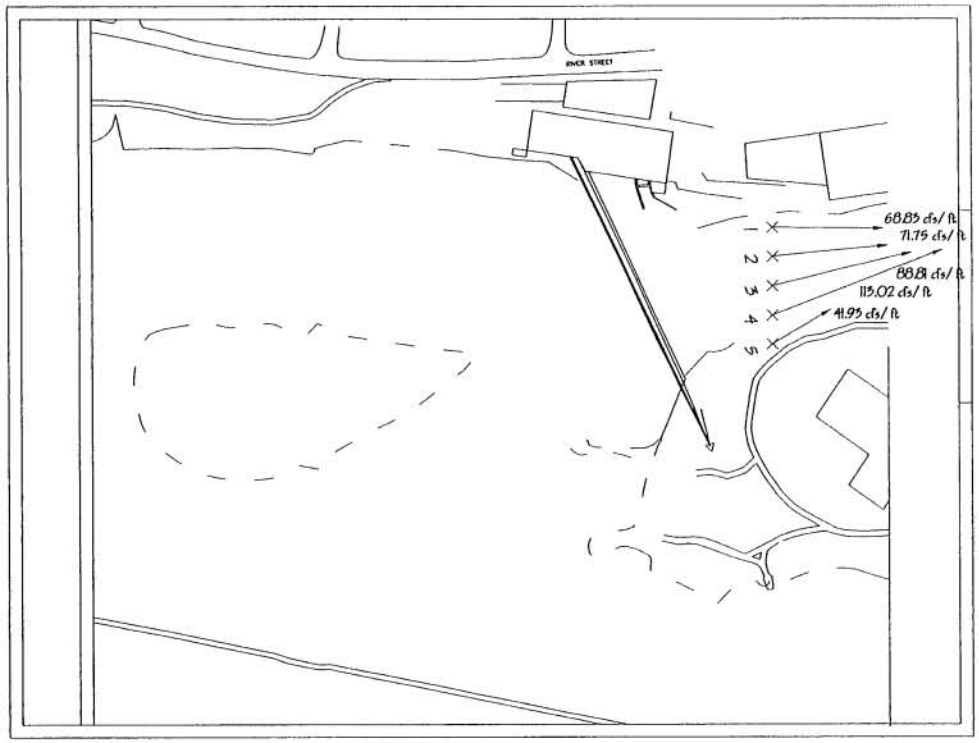

Figure 3.54. Baseline condition - Specific discharge conditions downstream of stucture - 500 year flood (17630 cfs)

4. Model-Tested Alternative Dam Configurations

4.1 Alternative I – The "bathtub" spillway

A bathtub spillway is a modified side channel spillway in which two control weirs are placed opposite each other and parallel to a spillway discharge channel. Flow over the two crests falls into the narrow trough between spillways, turns an approximate right angle, and continues through the discharge channel into the main body of the river or other control structure (chute, closed conduit, etc.). In general, the two parallel weir crests are connected at their upstream end by a semi-circular or straight length of spillway, giving the overall structure its characteristic bathtub shape. Structures of this type have, alternatively, been referred to as "U-spillways" or "duckbill spillways".

Discharge characteristics of bathtub spillway are similar to those of an ordinary overflow weir; they are dependent on the selected profile of the weir crest as well as the surcharge head along the weir. However, at high discharges, the flow in the trough may be restricted and may partly submerge the flow over the crest. In this case, flow characteristics will be controlled by a constriction in the channel at the downstream end of the trough. Generally, this constriction is the point of critical flow at the end of the discharge channel.

Although the bathtub spillway may not always be hydraulically efficient, it has advantages which make it useful for certain spillway layouts. Where a long overflow crest is desired to minimize surcharge head, or where the main body of flow must be concentrated into a relatively narrow discharge channel, a side channel bathtub spillway is often the best choice.

4.1.1 Motivation

Investigation of the existing conditions on the Batavia Dam site indicated the potential success of a bathtub spillway design Dye tracer studies (Section 3.3.2) showed that the central portion of the existing dam was relatively inactive due to the wake effects of Duck Island. Also, the breached left portion of the dam and the bedrock cascade on the right tended to concentrate the bulk of the flow on the extreme edges of the structure, threatening both banks.

Placing a bathtub spillway with its outlet channel centered on and at the toe of the existing structure provided several possible advantages. First, upstream of the dam, the bathtub spillway was expected to break into the wake effect from Duck Island, drawing flow from both the right and left channels into the center of the hydraulic structure. In order to facilitate this, it was necessary to repair the breached portion of the dam. Another advantage of the bathtub structure was derived from additional spillway crest length. Adding spillway crest length was expected to reduced head requirements and minimized threatening flood stages in the upstream pool. Downstream of the structure, the addition of the bathtub structure was expected to concentrate the bulk of the flow in the central portion of the relatively narrow downstream channel of the Fox River, protecting the banks from highly erosive forces during flooding events.

4.1.2 Generalized design procedure for bathtub spillways

The design of a bathtub spillway is accomplished by applying the procedures and approximations used in the design of a single crest side channel spillway. Of course, such a procedure ignores two basic physical differences between side channel and bathtub spillways. First, the interaction between flow from opposite crests can be expected to have some impact on energy and momentum dissipation. Second, the flow from the upstream end of the bathtub introduces additional downstream momentum which is not present in the conventional side channel spillway design. These two complications are difficult to incorporate within a theoretical design procedure. However, experience has proven that the side channel design procedure provides an adequate first approximation for the bathtub design. A physical model study can then be applied to verify and optimize the design.

The design procedures provided herein have been suggested by the US Department of the Interior, Bureau of Reclamation, in the third edition (1987) of the *Design of Small Dams* manual. Several other references on the topic are available. An ASCE paper (Hinds, 1926) provides the basic hydraulic theory for the design of side channel spillways. A second paper (Farney, 1962) provides a modification to the basic theory in order to account for momentum entering the discharge channel from the upstream end of an "L-shaped" side channel spillway crest. More recently a paper providing the basis for a computer algorithm to design and optimize a variety of side channel spillways was published (Knight, 1989).

The design of a side channel spillway is based on the principle of conservation of linear momentum. In order to easily apply this theory, one must assume that the only forces producing motion in the channel result from a fall in the water surface in the direction of the axis (water surface slope). This approximation requires that the entire energy of the flow over the crest be dissipated through its interaction with the discharge channel flow and is therefore of no assistance in moving water along the channel.

For a short reach of the discharge channel, the momentum at the beginning of the reach plus the increase in momentum due to external forces must equal the momentum at the end of the reach. A short reach, Δx in length, is considered, and the velocity and discharge at the upstream end of the section are v and Q, respectively. At the downstream end of the section, the velocity and discharge will be $v + \Delta v$ and $Q + q(\Delta x)$, where q is the inflow per foot of weir crest. The momenta at the two sections will be

$$\text{Upstream}.....M_u = \frac{Qv}{g} \qquad 4.1$$

$$\text{Downstream}.....M_d = \frac{[(Q + q\Delta x)]}{g}[v + \Delta v] \qquad 4..2$$

Subtracting 4.1 from 4.2 and dividing by Δx gives:

$$\frac{\Delta M}{\Delta x} = \frac{Q(\Delta v)}{g(\Delta x)} + \frac{q}{g}(v + \Delta v) \qquad 4.3$$

The rate of change of momentum with respect to time is *v* times the rate of change with respect to *x*, and considering the average velocity to be *[v + ½ (Δv)]*, equation 4.3 can be written as:

$$\frac{\Delta M}{\Delta t} = \frac{Q(\Delta v)}{g(\Delta x)}[v + \frac{1}{2}\Delta v] + \frac{q}{g}[v + \Delta v][v + \frac{1}{2}\Delta v] \qquad 4.4$$

ΔM/Δt is the accelerating force, which is equal to the slope of the water surface *Δy/Δx* times the average discharge. Equation 4.4 becomes:

$$\frac{\Delta y}{\Delta x}[Q + \frac{1}{2}(\Delta Q)] = \frac{Q(\Delta v)}{g(\Delta x)}[v + \frac{1}{2}\Delta v] + \frac{q}{g}[v + \Delta v][v + \frac{1}{2}\Delta v] \qquad 4.5$$

If Q_1 and v_1 are values at the beginning of the reach and Q_2 and v_2 are the values at the end of the reach, equation 4.5 can be solved for the change of water surface elevation:

$$\Delta y = \frac{Q_1}{g}\frac{[v_1 + v_2]}{[Q_1 + Q_2]}\left[(v_2 - v_1) + \frac{v_2(Q_2 - Q_1)}{Q_1}\right] \qquad 4.6$$

Using equation 4.6, it is possible to compute a water surface profile along the bathtub spillway discharge channel by assuming successive short reaches of channel once a starting point is found. The solution to equation 4.6 must be arrived at through trial and error computation. For a given reach length, *Δx*, the flows Q_1 and Q_2 will be known . Once the depth at one end of the reach is determined via a previous calculation step or the known downstream control point, the depth at the other end of the reach can be determined in order to satisfy equation 4.6.

As with any water surface profile calculation, the depth and hydraulic characteristics of the flow will be affected by backwater influence from some control point. In bathtub spillway design, this control point is usually the point of critical flow at the exit of the discharge channel. Within the discharge channel itself, it is preferred to maintain subcritical flow. Velocities at this stage will be less than critical and the greater depths will result in a smaller drop from reservoir crest to channel water surface. Minimizing this drop ensures that incoming flow will not develop high transverse velocity, thus effecting good mixing with the bulk of the water within the channel. Both the incoming velocity and discharge channel velocity will be relatively slow, and a fairly complete mixing of flow will produce a comparatively smooth flow within the discharge channel.

These goals can be achieved by creating a control section resulting in a critical condition at the downstream end of the discharge channel. A control point of this type is usually achieved by constricting the channel sides from trapezoidal to rectangular or elevating the channel bottom. For the design flow, the exiting conditions must be set to adequately match the downstream condition. This can be adjusted by modifying the width and elevation of the discharge channel toe. Once an appropriate critical control point is determined, the channel water surface profile can be calculated using equation 4.6. Then, the central channel bottom elevation, slope, and control dimensions must be adjusted to maximize the in-channel depth without submerging the crest beyond 2/3 of the design head. Design procedure of this type can become quite circular with numerous variables to be adjusted. However, pool and tailwater stage requirements combined with reasonable initial assumptions on

bathtub spillway dimension usually results in rapid design convergence. In general, however, the design resulting from the above procedure should be model tested to verify appropriate operation and optimize design dimensions.

4.1.3 Layout and design of the Batavia Dam bathtub spillway

The first requirement in the design of the bathtub spillway at the Batavia site was the selection of an alignment axis along which the spillway discharge channel would be centered. This axis was chosen through consideration of downstream channel conditions; the projection of the axis was aligned so that it traversed the center portion of the downstream channel. As a result, the bathtub spillway was not set perpendicular to the existing Batavia Dam alignment. Instead, it was cocked slightly toward the left bank of the river. The exit channel control point of the bathtub spillway was set at the toe of the existing structure.

The next design decision made was the selection of a design flow. In choosing a design flow, it was necessary to recognize that a portion of the total river flow would travel over the straight spillway section, having no impact on design of the bathtub portion of the structure. The interaction between these two types of structures could not be evaluated during design phase, and only analysis of model response resulted in overall characterization of the system. However, engineering judgement indicated that designing the bathtub portion of the spillway to pass the total flow for a 2 year flood event (5700 cfs) would result in a practical structure, providing a starting point for model investigation.

Once a design flow was chosen, it was possible to design the control reach of the bathtub spillway. The control reach was set as a contraction from a trapezoidal discharge channel to a rectangular channel cutting through the existing dam. The length of the control channel was set by geometric considerations at 20'. The width of the control channel was iterated until the water surface elevation of critical flow through the channel matched the water surface elevation for the 2 year flow (661.92 ft above sea level). Table AIII.1 in Appendix III outlines the numerical calculations and hydraulic conditions in the control channel for the design flow. A width of 54' was chosen in order to sufficiently match downstream river conditions. Knowing the water surface elevation and energy grade line of the flow exiting the spillway it was possible to compute the water surface elevation at the entrance of the control channel. This computation was completed iteratively using Bernoulli's equation and the assumption that all head losses incurred in the control reach (contraction, friction, and mixing losses) can be approximated as 0.2 times the velocity head difference between the control channel exit and entrance (Bureau of Reclamation, 1987). The water surface elevation at the entrance of the control channel was found to be 663.96 ft above sea level. The point serves as the first elevation used in the backwater calculation using equation 4.6.

Knowing the width of the spillway and the design flow, it was possible to compute the length of bathtub crest required. These calculations have been outlined in Table AIII.1. The crest elevation was chosen to match that of the existing structure (665'), and the surcharge head (~2.75') was calculated using the upstream pool elevation at location F for the 2 year flood event. The length of straight crest required was found to be 132' with a semicircular upstream spillway end having a radius of 39'.

Finally, the backwater computation (Table AIII.2 of Appendix II) was completed. The discharge channel slope, and thus floor elevations, were adjusted to provide for maximum allowable submergence of bathtub crest. The optimum slope was found to be approximately 0.002 ft/ft.

This design procedure incorporates considerable approximations and assumptions. For this reason, a detailed model of the structure was necessary. The results of the design effort were used in placing the bathtub spillway structure within the Batavia Dam model. Figure 4.1 and 4.2 provide a schematic representation of the modeled structure. Figures 4.3 and 4.4 are photographs of the structure as it was modeled in the laboratory environment.

4.1.4 Model stage response – Bathtub spillway

The data collected during investigation of the bathtub spillway stage-flow response are included In Appendix III (Table AIII.3). Stage data for the primary investigation flows at the measurement stations (Figure 3.1) have been converted to field scale and are summarized in Table 4.1. The final row of the table presents the average upstream pool stage response across all upstream measurement locations. This averaged rating curve is presented as Figure 4.5.

Table 4.1. Stage data results – Alternative I (bathtub spillway)

Flood Year	2	10	50	100	500
Flow (cfs)	5700	8500	12500	13500	17630
Gage Location	Stage (ft above sea level)				
A	667.63	668.17	669.19	669.31	670.09
B1	667.69	668.32	669.19	669.43	670.30
B2	667.64	668.27	668.93	669.26	669.89
C1	667.56	668.04	668.82	669.09	669.72
C2	667.31	668.06	668.72	668.99	669.65
D1	667.85	668.57	669.62	669.68	670.58
D2	667.67	668.48	669.11	669.23	670.10
D3	667.60	668.23	669.04	669.19	669.94
E	667.60	668.38	669.16	669.25	670.21
F	667.52	668.15	668.69	668.96	669.68
G	667.48	668.05	668.74	668.95	669.79
H	661.97	663.71	665.54	666.56	668.24
I	661.92	663.42	665.37	666.12	667.92
Average	667.60	668.25	669.02	669.21	670.00

4.1.5 Dye tracer flow visualization – Bathtub spillway

A dye tracer study was completed on the river model in order to examine effects of the newly installed bathtub spillway on approach flow patterns. This portion of the investigation was completed with the same apparatus and procedures followed during calibration (section 3.3.2). Several interesting observations were made; some general conclusions for the various flow magnitudes are discussed below.

2 year flood – 5700 cfs

The flow orientation and patterns developed by the 2 year flood (5700 cfs) are presented in Figures 4.6 and 4.7.

Closure of the breach on the right side (looking upstream) and addition of the bathtub had a pronounced effect on flow development. Dye from the rightmost plume traveled more slowly, taking a less direct path toward the structure. In the vicinity of the dam, this plume tended to curl inward toward the center of the structure, reaching the downstream pool over the central portion of the right side of the straight spillway. Some dye originating on the far right was also observed entering at the right, downstream end of the bathtub spillway. The next two plumes, moving from right to left, also showed a modified approach flow. The first plume traveled in a relatively direct path to the head and upstream right side of the bathtub spillway. The third plume showed continued vortex shedding as observed in the original conditions. However, the two plumes showed markedly less mixing than observed in the existing condition (see Figure 3.17). Instead, the plume closest to the island moved to the left, breaking into the central wake region of the island. This portion of the flow tended to attack the hydraulic structure on the left side of the bathtub spillway.

In the left channel, the dye plumes showed similar patterns to those observed for the existing condition. The two plumes closest to the island were observed to undergo mixing downstream of the island. Again, the leftmost plume showed flow in the region to be low in velocity and separated from the main body of flow.

10 year flood – 8500 cfs

Figures 4.8 and 4.9 show some results of the dye tracer study conducted for the 10 year flood. Patterns for this flood were similar to those observed for the 2 year event. Here, the shift to the left observed in the right channel island plume was more prominent. The dye from this plume clearly passes the structure on the left side.

50 year flood – 12500 cfs

Figure 4.10 and 4.11 provide representation of the flow observed for the 50 year flood event. Again, the two rightmost plumes passed the hydraulic structure on the right side, utilizing both the straight and bathtub portion of spillway. The clear water divide between right and left channel flows continued to shift left. The head of the bathtub spillway seemed to be relatively inactive in passing any of the dye laden flow.

100 year flood – 13500 cfs

Figures 4.12 and 4.13 show results of the dye tracer study for the 100 year flood event. For this flow, several new features were observed. Mixing between plumes in the right channel was more evident. The upstream head of the bathtub spillway played a more active role in passing flow from the right channel. The leftward push originating in the right channel was very distinct, causing the development of an sinuous clear water divided between left and right channel plumes. A similarly

circuitous approach flow was evident for the right side island plume with the curve terminating on the left side of the structure. Strong vortex shedding on both sides of the island was also observed.

500 year flood – 17630 cfs

Figures 4.14 and 4.15 characterize approach flows for the 500 year flood event. In this case, patterns similar to those for the 100 year event were observed. In general, the flow was more completely mixed. The clear water divide between left and right channel flow remained and continued to show a left channel orientation and approach to the structure. The bathtub spillway clearly played an role in passing dye laden flows from both right and left channels to the downstream end of the structure.

4.1.6 Flow split, velocity, and discharge characteristics – Bathtub spillway

The flow trends observed qualitatively through dye tracer visualization were confirmed and quantified with the use of the 2-D electromagnetic velocity probe.

An investigation of the flow split around Duck Island was conducted at the calibration flow (6026 cfs) in order to quantify magnitude and direction of flow in both the right and left channels. The product of the velocity and the depth provided a measure of the specific discharge (cfs/ft) which described flow strength at the given location. The data collected are included in Table AIII.4 in Appendix III. The results are summarized in Figure 4.16. In both the right and left channels, the maximum specific discharge was recorded nearest to the island shores. In general, all specific discharge measurements showed an orientation directed toward the banks with the attack angle sharpest near the island shores. Away from the island, the effect decreased, and the specific discharge vectors were nearly parallel to the banks. Multiplying the x component of the velocity by the lane flow area provided an estimate of flow across a lane; these estimates were used to determine the percentage of flow passing the left and right channels respectively. Comparing the flow split for the bathtub spillway to either the baseline or existing condition measurements generally revealed an increase in specific discharges in the right lane with a commensurate decrease in the left lane. As a result, the left lane was calculated to take 60% of the flow. The increased flow in the right lane may be attributed to the bathtub spillway's ability to pull flow from the right lane

Point measurements of velocities provided further understanding of the flow field in the river. The data collected in this effort are summarized Table AIII.4 in Appendix III. Figures 4-17 through 4-21 graphically present velocities measured for the 2, 10, 50, 100, and 500 year floods. Velocity vectors in the left channel (C1) showed flow to be traveling toward the bathtub spillway. The vectors in the right channel (C2) showed little variation in direction toward the bathtub spillway. Here, the flow continued to be dominated by the flow split around the island. Flow at the tail of the island (D2) was observed to rotate toward the head of the bathtub spillway with increased velocity magnitude. Point F, located between the crux of the bathtub and straight spillway, exhibited the greatest flow velocity and was directed over straight (original) portion of the structure for all flow magnitudes. This observation, in conjunction with those made during dye tracer visualization, indicated that the bulk of right channel flow and some cross-over left channel flow passed over this portion of the spillway. Downstream velocities

were, as expected, higher than those observed upstream. Point H, shielded slightly by the concrete wing-wall and out of the direct path of the bathtub discharge, exhibited velocities lower than those at point I. Not surprisingly, the maximum velocity was observed at the exit of the bathtub spillway. For the 2 year flow, this location yielded a velocity of 8.22 ft/s. The velocity increased for each flow thereafter until it reached a maximum for the 100 year flood of approximately 12 ft/s. The 500 year event resulted in a marked decrease in bathtub spillway velocity (9.4 ft/s). This corresponds well with the observation that, for this flood event, the bathtub was completely submerged, and there was no downstream hydraulic jump (see Section 4.1.7). In effect, this indicated that, for the extreme 500 year event, the bathtub spillway was operating at a low efficiency, passing less flow than observed for the 100 year event. It was, however, encouraging that this efficiency drop-off was not observed at a lower flow magnitude. Table 4.2 provides a summary of point velocity data in field scale.

A specific discharge analysis downstream of the dam helped provide insight into the flow patterns developed by the addition of the bathtub spillway. Figures 4.22 through 4.26 depict the specific discharge vectors for the five major flood events. The original data used to create these figures can be found in Table AIII.4 in Appendix III, and a field scale summary is provided in Table 4.3. For the 2 year flood, the bathtub spillway directed the bulk of the flow toward the center of the channel (measurement stations 2 and 3). However, flows greater than the 10 year flood produced sufficient upstream stage to allow significant flow to circumvent the dam around the right abutment and cascade down the existing bedrock formation. This flow contribution can be seen at measurement location 4 and 5 in the increased discharge and slightly skewed attack angle. The strength of the centralized flow from the bathtub spillway toe was observed to minimize the extent of this cross flow intrusion into the center of the channel. Also, for the high flows (50, 100, and 500 year events) generally less flow (than baseline condition) was measured along the right bank (locations 4 and 5). This was attributed to the fact that the bathtub spillway successfully decreased flow over the bedrock cascade.

4.1.7 General response characteristics – Bathtub spillway

The hydraulic jump characteristics for the bathtub spillway at the primary investigation flows were observed and photographed. These photographs are documented in Figures 4.27 through 4.36. Some general comments are provided below.

For the 2 year flow (Figures 4.27-28), the bathtub spillway was seen to work well in conjunction with the original Batavia structure. The depth of flow within the control channel was contained by the abutments. The exit condition exhibited a strong stable hydraulic jump located at the toe of the structure.

The 10 year flow (Figures 4.29-30) showed marked increase in control channel depth. Still, the hydraulic jump was strong and maintained a position at the exit of the structure.

At the 50 year flow (Figures 4.30-31), the depth of flow within the control channel surpassed the design depth of the control channel, causing some flow to skirt over the abutments. The observed jump remained strong and stable.

Table 4.2. Summary of field scale point velocity measurements – Alternative I (bathtub spillway)

Flow (cfs)	5700		8500		12500		13500		17630	
Gage	Current (ft/s)	Angle (deg)	Current (ft/s)	Angle (deg)	Current (ft/s)	Angle (deg)	Current (ft/s)	Angle (deg)	Current (ft/s)	Angle (deg)
A	Insufficient Depth		Insufficient Depth		0.36	26.57	0.31	-45.00	1.30	-33.69
B1	Insufficient Depth		1.74	-8.97	2.02	-1.53	2.73	1.14	2.57	3.63
B2	Insufficient Depth		1.28	-16.39	1.31	-11.93	1.28	-8.93	1.10	-17.24
C1	1.46	-8.53	2.14	-14.15	3.05	-6.45	3.18	-3.25	4.12	-3.26
C2	0.90	-2.29	1.25	-6.61	1.66	1.87	2.01	4.12	2.25	-5.07
D1	0.92	-11.31	1.31	-15.95	1.55	-8.04	2.12	-5.86	2.28	-5.44
D2	1.10	-9.46	1.18	-4.40	1.64	14.65	1.95	24.86	2.42	18.71
D3	Insufficient Depth		0.18	11.31	0.39	15.95	0.50	14.53	1.07	-3.88
E	0.93	-13.50	1.51	-14.53	2.19	-8.53	2.20	-6.13	2.91	-4.26
F	2.50	25.64	3.34	26.29	3.94	29.03	4.38	31.00	4.64	29.05
G	Insufficient Depth		0.28	-50.19	0.49	-17.10	0.55	9.46	1.01	21.99
H	1.09	30.80	1.80	1.15	2.68	8.13	2.73	12.20	2.97	8.38
I	3.25	2.86	2.89	-1.79	3.95	4.72	3.99	5.45	5.39	5.77
Tub	8.22	8.84	10.95	8.53	10.99	9.93	12.01	18.84	9.41	12.17

Table 4.3. Summary of field scale specific discharge downstream of structure – Alternative I (bathtub spillway)

Flow (cfs)	5700		8500		12500		13500		17630	
Station	Flow (cfs/ft)	Angle (deg)	Flow (cfs/ft)	Angle (deg)	Flow (cfs/ft)	Angle (deg)	Flow (cfs/ft)	Angle (deg)	Flow (cfs/ft)	Angle (deg)
5	Insufficient Depth		Insufficient Depth			51.84	30.94	40.40	38.04	35.01
4	16.33	12.34	69.09	15.07	101.37	25.77	67.44	22.50	75.30	19.93
3	37.07	9.16	50.23	5.04	75.00	12.72	78.67	12.01	92.80	14.41
2	51.76	6.17	74.06	2.54	97.73	12.34	86.11	12.44	91.47	14.41
1	19.22	4.09	18.82	-4.76	40.65	3.91	43.37	4.62	76.92	7.73

For the 100 year flow (Figures 4.32-33), both the straight and bathtub portions of the structure began to approach crest submergence. The downstream end of the control channel abutments were fully submerged, and the channel was flowing at maximum capacity. The jump at the tail of the structure, however, was observed to remain strong. This indicated that, for all flow up to and including the 100 year event, the flow in the channel experienced critical conditions. Critical flow conditions pass the maximum amount of flow, and therefore, they represent maximum efficiency for the bathtub structure.

For the 500 year flood, complete crest submergence was reached. No hydraulic jump was visible; however, surface perturbations indicated the presence of a submerged roller. At this flow magnitude, the desired critical condition within the control channel was not reached, and the efficiency of the bathtub spillway, as well a the straight Batavia spillway, declined. In fact, velocity measurements at the toe of the bathtub (compare Figures 4.20 and 4.21) indicated that the bathtub spillway carried less flow for the 500 year event than the 100 year event.

4.2 Alternative II – The rock dam

A rock dam is simply a number of boulders placed in such a way that they provide the flow resistance necessary to raise upstream stage to a desired level. In this way, the rocks act as a dam, and flow energy is dissipated through the cascade of water over the irregular rocky surface. A rock dam emulates natural rapids which are often found in rivers providing a means of head drop (Barr et al., 1991). The primary disadvantage of a rock spillway is that it is difficult for designers to predict stage and flow response over such a "natural" structure. This uncertainty can be mitigated through model study investigation of proposed rock dams. Rock dams do have advantages over the traditional concrete spillway in that they are often more economically feasible and aesthetically pleasing.

4.2.1 Motivation

The primary physical motivation for the installation of a rock dam at Batavia was the porous nature inherent to the structure. Such a structure provided the potential advantage of promoting more evenly distributed flow. Rather than place a solid obstruction in the path of the flow, a more natural structure of this sort provided numerous paths for flow to reach the downstream channel. Here, again, the goal was to bring more flow into the center of the structure while diverting some of the flow from the over-stressed abutments.

A rock dam was also motivated by economic consideration. The cost of a rock structure was expected to be considerably more affordable than that of a traditional concrete spillway.

Also, aesthetic and community issues entered into the selection of a rock dam. Conditions on-site presented designers with a dam having near natural conditions on the extreme right and left margins. On the left abutment, the breached area of the dam was filled with rip-rap, resulting in insufficiently controlled, yet breathtaking rapids. On the right abutment, a bedrock formation provided both energy dissipation and natural beauty. ". . .Batavia has been very active along the river in this

area, building a Riverwalk with many features designed to allow visitors vistas of the river and dam along with the natural limestone bedrock formations that typically see cascading water during the spring each year. . .The brick path and benches were located close to the water in these areas because it was the committee's desire to take advantage of the incredible beauty of the water falling over the rock surface while also allowing easy accessibility to the river for recreational type activities. . .the entire project has cost several million dollars. . .This Riverwalk project has become a major focus of the community and is used by thousands of people each year." (Correspondence: Gary Larson, Batavia Director of Public Works to Bill Rice , DNR Project Manager, December 3, 1997) The Town of Batavia obviously desired to maintain the natural features of the existing dam. A rock dam provided a means of installing a controlled structure while maintaining and enhancing the natural aesthetics of the dam.

4.2.2 Layout and design of the rock dam

The rock dam had a layout along the same alignment as the existing Batavia Dam. The upstream edge of the rock dam was placed to approximate the alignment of the crest and upstream batter of the existing structure. Then, rocks sloped from here to the natural downstream bed elevation approximately 39 feet away. The resulting slope of the rock face was 1:4. Figures 4.37 and 4.38 provide schematic illustrations of the rock dam as constructed in the model.

The rocks used in modeling were scaled down from boulders ranging in weight from two to three tons. This corresponds, roughly, to prototype boulders ranging in size from 6 to 7.5 feet in diameter. Scaling of these large features was accomplished using Froude similarity; the rocks used in modeling were 2 to 3 inch, smooth river stone.

These rocks were hand placed within the model. Of course, the rocks resulted in an irregular structure. After placement, ten elevation measurements were surveyed along the "crest" of the dam. The average resulting "crest" elevation was 665.9 ft above sea level. This represents a slight increase of crest elevation in comparison to the original structure (approximately 665.1 ft).

Figures 4.39 and 4.40 provide photographic documentation of the rock dam as it was modeled in the laboratory.

4.2.3 Model stage response – Rock dam

The data collected during investigation of the rock dam stage flow response are included in Appendix III (Table AIII.5). Stage data for the primary investigation flows at the 13 measurement locations (see Figure 3.1) have been converted to field scale and are summarized in Table 4.4. The final row in the table presents the average upstream pool stage response across all upstream measurement locations. This rating curve is provided in Figure 4.41.

Table 4.4. Stage data results – Alternative II (rock dam)

Flood Year	2	10	50	100	500
Flow (cfs)	5700	8500	12500	13500	17630
Gage Location	Stage (ft above sea level)				
A	667.84	668.74	669.73	669.97	670.81
B1	667.87	668.71	669.79	669.94	670.57
B2	667.70	668.75	669.65	669.89	670.64
C1	667.65	668.58	669.54	669.69	670.38
C2	667.55	668.42	669.44	669.65	670.31
D1	668.21	669.26	670.07	670.22	670.88
D2	667.76	668.78	669.65	669.86	670.49
D3	667.78	668.71	669.70	669.91	670.54
E	667.90	668.77	669.76	669.97	670.60
F	667.85	668.75	669.65	669.95	670.70
G	667.57	668.47	669.37	669.76	670.48
H	661.97	662.72	665.90	666.50	667.79
I	661.92	662.52	665.52	665.85	667.92
Average	667.79	668.72	669.67	669.89	670.58

4.2.4 Dye tracer flow visualization – Rock dam

A dye tracer investigation was completed on the model in order to examine the effect of installation of the rock dam. Several observations were made; the conclusions for the various flow magnitudes are discussed below.

2 year flood – 5700 cfs

The flow orientation and dye tracer development for the 2 year flood are presented in Figures 4.42 and 4.43.

In general, the dye tracer development for the rock dam at the 2 year flood level was similar to those observed for both the existing and baseline conditions. Vortex shedding was again observed along the right (looking upstream) side of the island. The rightmost plume continued to travel directly to the structure along the shore. A strong concentration of dye along the right and left margins of the rock dam continued to be the dominant features. The wake of the Island shielded the central portion of the dam from dye laden flow.

10 year flood – 8500 cfs

Figures 4.44 and 4.45 are photographs of the dye tracer investigation for the 10 year flood event.

Vortex shedding was observed to occur in both the right and left channels along the island shore. This phenomena, however, was noted to occur somewhat more downstream than previously recorded. In most aspects, the tracer patterns for the rock dam at the 10 year flood resembled those developed for the baseline condition at the same flow magnitude. This is to be expected because the two structures are very similar. The development of a bulb of dye in the lower left channel was evident.

As in the baseline condition, this dye tended to circulate within the still pool on the left of the peninsula before being drawn over the structure on the left extreme edge.

50 year flood – 12500 cfs

Figures 4.46 and 4.47 are still frame captures of the video taken during the dye study of the rock dam for the 50 year flood event.

In particular, Figure 4.46 shows the beginning of the development of the bulb of dye in the left channel. This feature grew over time, becoming trapped within the wake of the island. Cross-over flow from the right channel was observed to push this bulb toward the left where higher velocity flow in the center of the left channel tended to move dye from the circulation point toward the rock structure.

The approach upstream of the structure continued to exhibit the tendency of the flow to concentrate on the right and left extremes of the rock dam

100 year flood – 13500 cfs

Figures 4.48 and 4.49 show the results collected during the 100 year flood dye tracer test of the rock dam.

At this flow magnitude, increased mixing between left and right channels was noted. A highly concentrated bulb of dye was again observed to develop in the left channel. Cross channel mixing resulted in more dye traveling over the rock structure in the central portion; however, a clear water divide generated by the island wake, though somewhat blurred, was still evident.

500 year flood – 17630 cfs

The results for the dye tracer investigation for the 500 year flood event are provided in Figures 3.50. and 3.51.

Considerable mixing between dye from the right and left channels was observed. A strong right to left cross channel flow was noticed for this event. The flow intrusion form the right channel forced dye in the left channel to take a circuitous path to the rock structure. Figure 4.51 clearly shows that the right and left extremes of the rock dam took the brunt of the dye laden flow. However, as time progressed and mixing became more complete, the central portion of the structure did play a more active role in flow passage.

4.2.5 Flow split, velocity, and discharge characteristics – Rock dam

Figure 4.52 provides the result of the flow split analysis for the rock dam alternative. The original data collected in the laboratory are presented in Appendix III, Table AIII.6. The flow split showed the familiar characteristics previously seen in the investigation of initial and baseline conditions. Those measurements nearest the island shore showed attack angles directed away from the island; these locations exhibited the greatest specific discharges. The discharge in the left channel (looking downstream) was greater than those in the right. The procedure of multiplying the x-component of the velocity by the flow area across a lane was again used to calculated the percentage flow in the left and

right channels respectively. The results indicated that 67% of the total flow passed the left channel. This was in close agreement with data taken for the existing and baseline conditions, reflecting the similarity in the rock dam to the original Batavia Dam structure.

Point velocity data are also summarized in Table AIII.6 of Appendix III; these results, presented in field scale, are depicted in Figures 4.53 to 4.57. Several noteworthy velocity patterns were observed and are discussed below. First, location B1 generally showed an increase in velocity over that documented for the baseline condition. The velocities measured at B1 had magnitudes closer to those observed in for the existing (breached dam) condition. Magnitudes at C1, E, D, and F also showed an increase. This was attributed to the porous nature of the rock dam allowing for generation of slightly higher upstream velocities. Also, a more prominent left bank orientation was observed for these locations. Such a clear directional trend in this comparatively uncontrolled structure was taken as evidence of the flow's natural tendency to be directed towards the left extreme of the dam. Such conditions might have been responsible for the generation of a breach in the existing structure. In the right channel, a strong left orientation was observed for locations B2, C2, D3, and G. This was in keeping with dye tracer observation showing that dye did not tend to accumulate on the extreme right margins. In fact, the generation of a circulating bulb of dye between C2 and D2 may have been sustained by this cross channel flow orientation. Downstream velocities at locations H and I were slightly larger than observed for baseline and existing conditions. This was attributed to the previously discussed tendency for flow over the rock dam to be concentrated on the left shore. The rock dam continued the trend observed in the baseline condition, with greater magnitudes at I than at H. The velocity at H appeared to have an orientation directed perpendicular to the structure and more threatening to the banks. The field scale summary of the point velocity data for Alternative II is provided in Table 4.5 on the following page.

Downstream specific discharge conditions for the 2, 10, 50, 100, and 500 year floods are provided in Figures 4.58 through 5.62. The laboratory data used to compile these figures are included in Table AIII.6 in Appendix III. The trend of higher flow magnitude along the left bank was again observed with increased (over baseline) specific discharge measurements at locations 1 and 2 for nearly all flow events. At all flood magnitudes, flow was observed over the peninsula. The greater the flooding event, the more significant this contribution became. The cross-channel nature of the peninsula flow was documented in the measurement taken at location 5 for the 50 year event. This vector was nearly perpendicular to the downstream flow direction. The strength of the overland flow was observed to affect the orientation of discharge vectors at locations 3 and 4, resulting in a more left channel orientation of the flow. For the 500 year event, the increased flow over the rock dam itself helped to mitigate the cross channel intrusion, and the vectors had an orientation more directly downstream. Table 4.6 summarizes the field scale downstream discharge characteristics.

Table 4.5. Summary of field scale point velocity measurements – Alternative II (rock dam)

Flow (cfs)	5700		8500		12500		13500		17630	
Gage	Current (ft/s)	Angle (deg)	Current (ft/s)	Angle (deg)	Current (ft/s)	Angle (deg)	Current (ft/s)	Angle (deg)	Current (ft/s)	Angle (deg)
A	Insufficient Depth		Insufficient Depth		1.26	21.04	1.34	53.75	1.61	34.94
B1	Insufficient Depth		2.12	16.28	2.66	18.56	3.36	17.17	3.33	10.94
B2	Insufficient Depth		0.94	37.97	1.53	43.09	1.30	47.25	1.35	32.41
C1	1.52	13.05	2.68	16.00	3.30	16.85	3.58	14.60	3.23	5.77
C2	1.12	37.79	1.28	29.45	1.74	30.56	1.45	51.56	1.92	28.01
D1	1.04	13.07	1.71	30.34	1.99	26.33	2.38	21.32	2.57	4.43
D2	1.03	47.12	0.39	27.76	1.40	17.27	1.74	34.85	1.86	52.91
D3	Insufficient Depth		0.81	77.20	1.12	69.23	1.34	66.19	1.12	52.21
E	1.45	5.71	2.28	16.57	2.75	13.67	3.15	12.92	3.22	-2.57
F	1.64	35.61	2.06	21.61	2.31	25.00	2.64	19.55	2.45	5.92
G	Insufficient Depth		0.89	63.43	1.39	60.44	1.51	59.15	1.80	59.33
H	3.57	1.16	5.24	23.12	4.36	22.64	4.46	19.61	4.14	2.75
I	3.75	-4.42	6.05	9.97	6.13	9.32	5.82	12.36	5.11	-1.62

Table 4.6. Summary of field scale specific discharge downstream of structure – Alternative II (rock dam)

Flow (cfs)	5700		8500		12500		13500		17630	
Station	Flow (cfs/ft)	Angle (deg)	Flow (cfs/ft)	Angle (deg)	Flow (cfs/ft)	Angle (deg)	Flow (cfs/ft)	Angle (deg)	Flow (cfs/ft)	Angle (deg)
5	Insufficient Depth		Insufficient Depth		12.49	84.49	12.10	56.31	36.98	31.89
4	19.03	13.37	24.64	40.03	85.15	23.79	121.50	29.95	89.13	20.18
3	36.12	15.22	51.01	25.37	62.58	28.09	65.77	26.57	65.38	11.82
2	31.87	9.22	56.78	33.11	70.04	18.81	77.16	18.33	81.60	2.79
1	29.96	-1.02	49.17	10.45	62.21	9.89	54.98	16.46	59.90	-2.07

4.2.6 General response characteristics – Rock dam

The rock dam did not exhibit characteristic hydraulic jump conditions. Rather, the flow energy was dissipated by flow over and through the irregular rocky surface. These conditions resulted in a downstream flow in the vicinity of the structure being slightly more turbulent than a traditional concrete spillway. Figure 4.63 shows the rock dam flow conditions for the 2 year flood event. The head drop between upstream and downstream elevations was accomplished solely through energy dissipation encountered by flow through the rock field. For comparative purposes, the flow conditions of the 500 year flood event in shown in Figure 4.64. In this case, as for all alternative structures, the downstream stage resulted in near crest submergence. Still, flow over the rock field resulted in surface turbulence and continued energy dissipation.

Minimal scour was observed in the sediment bed on the left extreme and downstream end of the structure. Some sediment movement was noted, but this was negligible in comparison to the scour generated by the breach in the existing condition (see Figure 3.38).

4.3 Alternative III – The 2-Sided spillway

In the context of this report, the term 2-Sided spillway refers to a modified ogee spillway with two distinct lengths of crest joining at a vertex. Such a multiple crest structure is useful when flow patterns reveal separate paths of approach to the structure. Arranging crest lengths in patterns other than the conventional direct linear alignment allows for the accommodation of complicated approach flow patterns. Such a layout also generally results in a structure which spans the water body in such a way that provides greater crest lengths. This results in a decrease in required heads to pass a given flow, ultimately, reducing flood stages. Of course, the design of such a spillway is site dependent, and flow development for these structures can be unpredictable. Hydraulic modeling allows for verification and optimization of the structure-flow interaction.

4.3.1 Motivation

Observed flow patterns induced by the flow splitting around Duck Island was the primary motivation for the development of this final alternative. Investigation of Alternative I and II had proved the strength of the wake behind the island. The 2-Sided structure was a departure from the previously governing conceptual premise of "breaking" or weakening the wake effect of the Island. Here, it was decided to use the low flow zone just downstream of the island to the structure's advantage. The wake naturally divided the flow into two separate approach flows with only minimal mixing. This motivated the design of a structure which provided two distinct overflow structures.

A second advantage of such a structure was the increased crest length resulting from the layout. Flood stages were expected to be reduced. Also, overland flow crossing into the downstream channel over the peninsula was expected to be mitigated, resulting in more uniform and beneficial downstream discharge characteristics.

4.3.2 Layout and design of the 2-Sided spillway

The layout of the 2-Sided spillway was governed by the location and flow splitting characteristics observed to dominate the flow. Two lengths of crest were proposed in order to accommodate the two distinct approach flow from the left and right channels.

The vertex of the structure was anchored at the downstream point of the island. The angle and crest layout for the structure were determined through consideration of the predicted amount of flow passing the left and right legs respectively (60%, 40%). Flow over the right side of the structure was expected to be directed cross-channel toward the left bank. In order to shield the left bank, flow over the left side of the structure was required to redirect the flow down the channel. This balance was achieved by angling the left spillway slightly toward the peninsula. The higher flow over this crest was expected to realign the right spillway flow . The desired net effect was the canceling of cross-channel flow components within the region between the two lengths of spillway, providing uniform downstream discharge characteristics. Under these considerations, the left and right abutments for the structure were chosen. The left abutment was placed just upstream of the old mill building. The right abutment was placed at the extreme right end of the low retaining wall spur off the existing structure. Figure 4.65 provides a plan view of the 2-Sided spillway as it was modeled in the laboratory environment.

The cross section of the spillway was selected to be similar to that of the existing condition. In general, the selected spillway was a modified ogee shape. The crest elevation was chosen at 665.5 feet above sea level. This was a slight increase in elevation over the existing crest. The crest elevation was raised in order to partially compensate for the additional crest length which may have excessively decreased hydraulic head within the river. The toe elevation was located at elevation 657.00. Figure 4.66 is a schematic representation of the spillway cross section.

The region between the toe of the structure and the existing dam alignment was modeled as a moveable bed, and sediment was sized using the procedure outlined in Appendix I (Calculation AI.2). The sediment provided an indication of how the flow would modify the river bed under the influence of scour from the proposed structure. Figures 4.67 and 4.68 are photographs of the modeled 2-Sided spillway.

4.3.3 Model stage response – 2-Sided spillway

The data collected during investigation of 2-Sided spillway stage-flow response are included in Appendix III (Table AIII.7). Stage data for the primary investigation flows at 11 measurement locations (see Figure 3.1) have been converted to field scale and are summarized in Table 4.7. Measurements at locations F and E were not taken as these locations were situated within the moveable bed portion of the model and no longer contributed to the upstream pool average. The final row in the table presents the average upstream pool stage response across all upstream measurement locations. This rating curve is provided in Figure 4.69.

Table 4.7. Stage data results – Alternative III (2-Sided spillway)

Flood Year	2	10	50	100	500
Flow (cfs)	5700	8500	12500	13500	17630
Gage Location	Stage (ft above sea level)				
A	667.51	668.05	668.77	668.95	670.06
B1	667.63	667.90	669.04	669.19	669.94
B2	667.40	668.03	668.57	668.84	669.92
C1	667.32	667.89	668.55	668.82	669.90
C2	667.22	667.85	668.60	668.87	669.68
D1	667.40	667.94	668.51	669.05	669.92
D2	667.52	668.06	668.36	668.72	669.53
D3	667.30	667.84	668.77	668.92	670.03
G	667.12	667.87	668.50	668.65	669.85
H	662.33	663.83	665.78	666.32	668.21
I	661.92	663.42	665.52	666.12	667.92
Average	667.38	667.94	668.63	668.89	669.87

4.3.4 Dye tracer flow visualization – 2-Sided spillway

A dye tracer investigation was conducted following the installation of the 2-Sided spillway model. This study helped to more thoroughly characterize the general flow characteristics developed by the structure. Some conclusions and observation for the five primary investigation flows are discussed below.

2 year flood – 5700 cfs

Figure 4.70 and 4.71 provide still frame captures of the video collected during the 2 year flood investigation of Alternative III.

Approach flows for the 2-Sided spillway showed considerable variation from those observed for the existing condition. The plume of dye on the far right (looking upstream) continued to flow along the bank. The central plume traveled toward the new structure along a generally direct path. There was less mixing between this plume and the plume originating at the head (and right) of the island. The island plume tended to travel across the silted region downstream of the island and cross the dam on the upper portion of the left (looking upstream) leg. In the left channel, the island plume split around the island as previously observed. However, after passing the head of the island, the plume trace showed curvature toward the right spillway side. The central left plume also demonstrated more pronounced curvature toward the center of the river. The far left plume was observed to travel with higher velocity along the shore. In the vicinity of the still pool on the left of the peninsula, the plume showed bending toward the structure.

Figure 4.71 shows conditions immediately upstream and downstream of the 2-Sided spillway. The two plumes originating at the island head were observed to cross the spillway on the left side of the structure in the vicinity of the center abutment. This dye tract was observed to interact with the flow over the right crest. The dye indicated that the resulting flow was well aligned in the center of the

downstream channel. The plume on the far right traveled over the crest on the right side margin of the structure. This flow appeared to travel uninterrupted along the bank of the downstream channel. The remaining wing-wall played a minimal role in directing the flow. No flow traveled over the bedrock cascade at the left lower abutment.

10 year flood – 8500 cfs

Figures 4.72 and 4.73 show the dye tracer results for the 10 year flood magnitude.

In general, the dye patterns developed were similar to those discussed for the 2 year flood. The right island plume tended to become more dispersed in the silt region downstream of the island with more mixing with the left island plume. The strength of the right to left cross flow was noted in the development of a more sinuous approach on the left leg of the structure. Downstream conditions were very similar to those observed for 2 year flow.

50 year flood – 12500 cfs

Figure 4.74 and 4.75 are photographs of the dye tracer test conducted on Alternative III for the 50 year flow event.

The approach flow in the left channel showed an increase in vortex shedding downstream of the head of the island. This resulted in more mixing between the center and island plumes. The right plumes showed similar approach patterns as observed in previous flows. The downstream dye tracts showed paths with little variation in position. At this flow, a small quantity of water did reach the tailwater by passing over the bedrock cascade at the lower left abutment.

100 year flood – 13500 cfs

Figure 4.76 and 4.77 are representative of the results collected during the 100 year flood dye tracer investigation.

Vortex shedding downstream of the island was observed in the right island plume. This feature induced increased mixing between left and right channel flows. In the left channel, the two right plumes underwent considerable mixing. As a result, the majority of the dye traveled to the left side of the structure. Figure 4.77 shows the center region of the structure became more active in passing dye laden flow. The center right channel plume passed the crest in the center of the right leg. A bulb of dye was observed to develop on the left edge of the structure, intruding into the still pool. Flow over the bedrock increased. Downstream flow indicated increased mixing as a majority of the crest was active in passing dye. In general, the downstream discharge characteristics appeared to follow the same orientation as described above.

500 year flood – 17630 cfs

Figure 4.78 and 4.79 show the dye tracer results observed for the 500 year flood event.

In general, flow patterns for this flow magnitude were similar to those described for the 100 year event. More mixing in the upstream approach was observed. Vortex shedding on the right and

left of the island was prominent. The bulb of dye in the lower left channel increased in size, and as a result , the lower portion of the left side of the structure became more active in passing dye. Standing waves in the area between the spillway legs tended to aid in mixing of dye. The downstream discharge characteristics as indicated by the dye tracts continued to be favorable. However, at this high flow, the wing-wall played an increasing role in directing flow away from the right bank.

4.3.5 Flow split, velocity, and discharge characteristics – 2-Sided spillway

Figure 4.80 provides the result of the transect flow split analysis conducted on Alternative III. The data taken during this phase of the study can be found in Appendix III (Table AIII.8). The introduction of a 2-Sided spillway resulted in changed conditions, particularly in the left channel (looking downstream). Near the left shore of the island, specific discharge vectors were not angled as sharply away form the island as previously observed. Instead, these measurements indicated flow directly downstream. Those vectors closer to the shore of the left channel were directed toward the center of the river. In the right channel, the flow direction was similar to those observed for the baseline and existing condition. However, the magnitudes in the right channel were slightly increased with a balancing decrease in the left channel. Following procedures previously described (Section 3.4.4), it was estimated that 61% of the flow passed the left channel. Therefore, the 2-Sided spillway did show success in more evenly balancing the quantity of flow between the left and right channels.

Figures 4.81 through 4.85 are graphical representations of the point velocity measurements taken. These data can also be found in Table AIII.8 of Appendix III. Data collected reflected some changes in flow orientation and magnitude under the influence of the 2-Side spillway. First, velocities at locations B1 and B2 showed an increase. This was an expected result of moving the control structure upstream and closer to these locations. Point B2, in particular, was observed to have increased velocity with direction rotated toward the newly installed spillway. Velocity at C1 decreased slightly and was directed over the spillway crest. Location C2 showed a marked increase in velocity; these vectors were clearly rotated toward the right side spillway. Measurements at D1, at the very base of the upstream side of the left spillway, indicated a slight decrease in velocity for most flow magnitudes. Measurement location D2 showed an increase in velocity and was directed over the right side of the spillway. Velocity data along the right shore (D3 and G) showed magnitudes comparable to those previously observed. However, these measurement locations exhibited a rotation of vector orientation toward the spillway. Downstream measurements along the left shore (H and I) showed an alignment similar to those observed for the baseline condition. The magnitudes, however, were slightly increased. A summary of this data is presented in Table 4.8.

The downstream specific discharge characteristics for this alternative were favorable. These data are presented in Figures 4.86 through 4.90 and are summarized in Table 4.9 in field scale. The data collected from the model can be found in Table AIII.8 in Appendix III. Several distinct changes in downstream characteristics were noticeable. First, there was generally an increase in specific discharge along the left shore. The discharge vectors showed that flow was uniformly distributed across the downstream channel from locations 1 through 4 for nearly all flow magnitudes. Location 5

Table 4.8. Summary of field scale point velocity measurements – Alternative III (2-Sided spillway)

Flow (cfs)	5700		8500		12500		13500		17630	
Gage	Current (ft/s)	Angle (deg)	Current (ft/s)	Angle (deg)	Current (ft/s)	Angle (deg)	Current (ft/s)	Angle (deg)	Current (ft/s)	Angle (deg)
A	Insufficient Depth		Insufficient Depth		1.16	10.78	1.24	8.37	1.30	-2.39
B1	Insufficient Depth		1.54	6.04	2.49	-7.07	3.01	6.53	3.52	-2.94
B2	Insufficient Depth		1.47	17.10	1.50	-5.51	1.55	8.04	1.79	1.16
C1	1.30	8.81	1.91	1.08	2.71	-4.19	3.24	3.84	3.35	-3.71
C2	1.41	16.35	2.62	11.54	1.91	5.98	2.22	10.30	2.55	4.06
D1	0.95	21.19	1.34	14.78	1.75	-3.54	2.27	13.82	2.69	0.77
D2	1.56	20.32	2.11	19.52	2.26	8.26	2.43	15.07	2.74	9.46
D3	Insufficient Depth		0.65	56.31	0.26	56.31	0.64	68.50	1.25	5.79
G	0.39	21.80	0.61	63.43	0.68	39.61	0.84	43.26	1.40	27.55
H	2.81	10.73	3.82	5.15	4.09	3.54	4.76	8.50	4.09	3.80
I	3.99	2.85	4.88	3.60	5.05	-0.61	5.38	-0.77	6.12	4.74

Table 4.9. Summary of field scale specific discharge downstream of structure – Alternative III (2-Sided spillway)

Flow (cfs)	5700		8500		12500		13500		17630	
Station	Flow (cfs/ft)	Angle (deg)	Flow (cfs/ft)	Angle (deg)	Flow (cfs/ft)	Angle (deg)	Flow (cfs/ft)	Angle (deg)	Flow (cfs/ft)	Angle (deg)
5	Insufficient Depth		Insufficient Depth		27.20	-0.86	31.43	2.63	53.00	17.35
4	22.55	11.52	38.77	10.25	57.90	5.47	67.58	6.15	83.87	13.89
3	27.22	12.72	43.10	10.25	58.25	7.63	67.40	3.88	95.29	10.92
2	36.81	7.04	51.35	8.45	60.44	4.76	69.36	3.24	88.53	8.13
1	30.36	2.89	41.73	4.36	50.12	-1.17	65.51	2.20	77.50	5.69

showed a decreased in discharge when compared to other location across the transect. However, the orientation (directly downstream) at location 5 did agree well. Alternative III eliminated overland flow for the 2 and 10 year flood magnitude, and overland flow for all other floods was greatly reduced. As a result, the influence of the cross channel intrusion previously observed to dominate the downstream discharge characteristics was not observed. This alternative provided a uniform distribution of flow across the downstream channel.

4.3.6 General response characteristics – 2-Sided spillway

The 2-Sided spillway performed reasonably well for all tested flow magnitudes. Flows from the left and right overflow crests tended to interact and efficiently cancel cross-channel flow components within the regions between the structure's two sides. This resulted in quiescent flow conditions and uniform distribution of flow within the downstream channel.

Figures 4.91 and 4.92 are photographs of the 2-Sided spillway during a 2 year flooding event. For comparative purposes, Figures 4.93 and 4.94 show the spillway operation during a 500 year flooding event. Addition of sediment at the toe of the spillway resulted in development of a scour hole. The extent of scour can be observed in Figures 4.95 and 4.96. As a result , a strong hydraulic jump was not observed to develop at any flow magnitude. The scour hole promoted the development of a submerged roller for the 2 (see Figure 4.92) through 100 year flooding events.

This condition is not desirable because it is neither efficient for energy dissipation nor safe for recreation in the vicinity of the dam's toe. Whether this condition would develop on-site is not certain. The site is situated in a region where bedrock is quite shallow. There may not be sufficient sediment available to result in such extensive scour. This is the case with the existing dam. The current Batavia structure is situated on a bedrock ridge and is known to experience a strong hydraulic jump. Still, if this alternative is implemented, conditions may warrant investigation of spillway shapes which has been proven to suppress the development of a submerged roller (Freeman and Garcia, 1996).

The crest was observed to approach submergence for the 100 year event. The 500 year event resulted in complete submergence and the development of standing surface waves (See Figure 4.92). The waves from the two sides of the structure tended to interfere with each other, resulting in an irregular water surface between the spillway sides. However, this phenomena was observed to dissipate away from the structure, and water surface in the downstream channel was generally uniform.

Batavia Dam
Model Study

University of Illinois
Hydrosystems
Laboratory:

Alternative I
Bathtub Spillway
Plan View

Notes:

N

October 23, 1997

Scale:
Model: 1/10" = 1'
Site: 1/10" = 30'

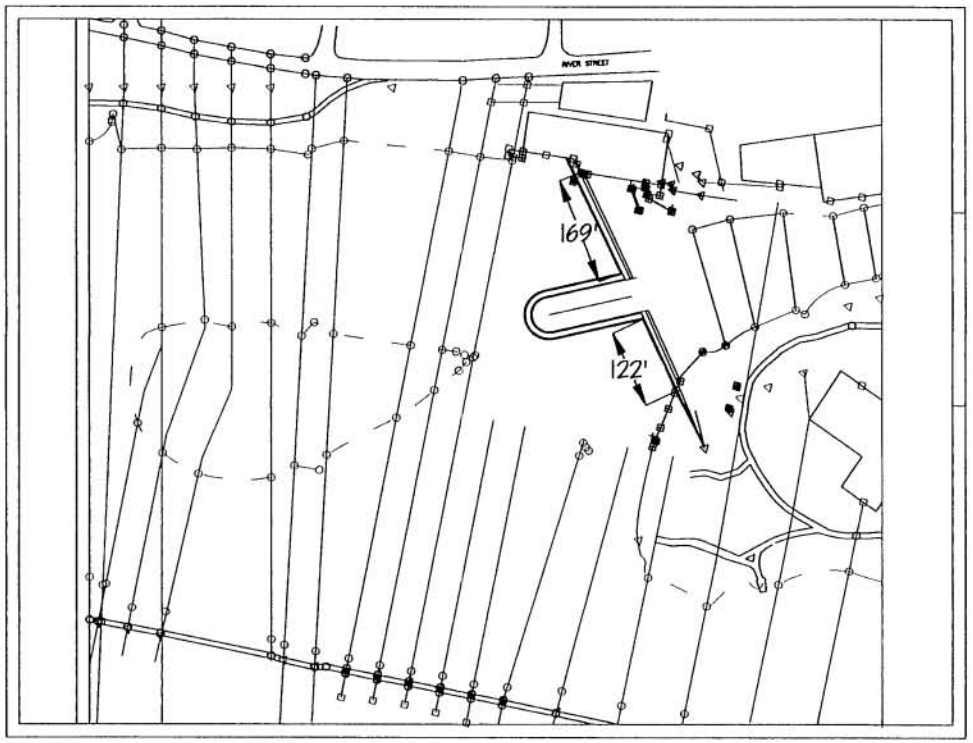

Figure 4.1. Schematic representation of bathtub spillway orientation - Plan view

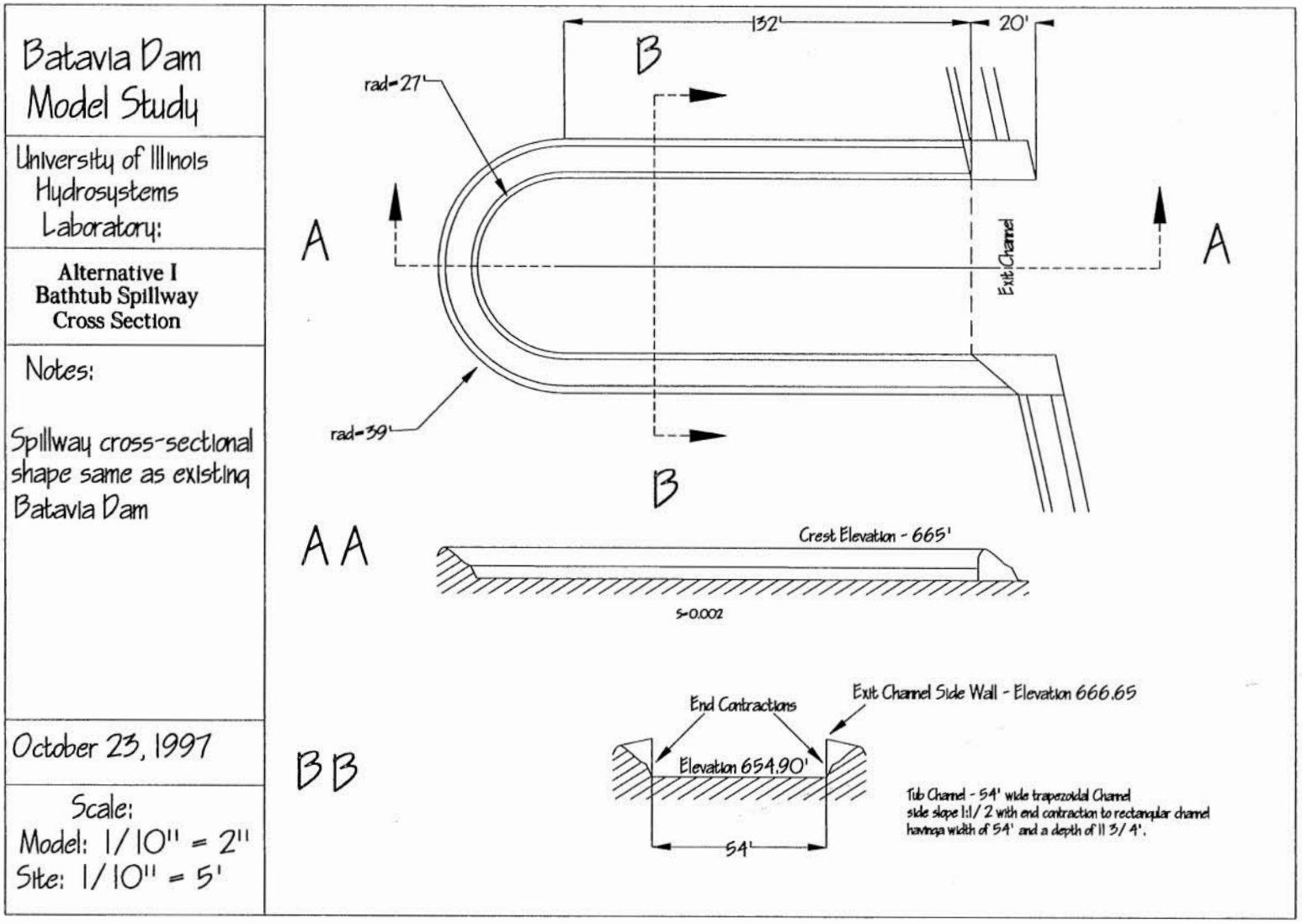

Figure 4.2. Schematic representation of bathtub spillway design - Cross section

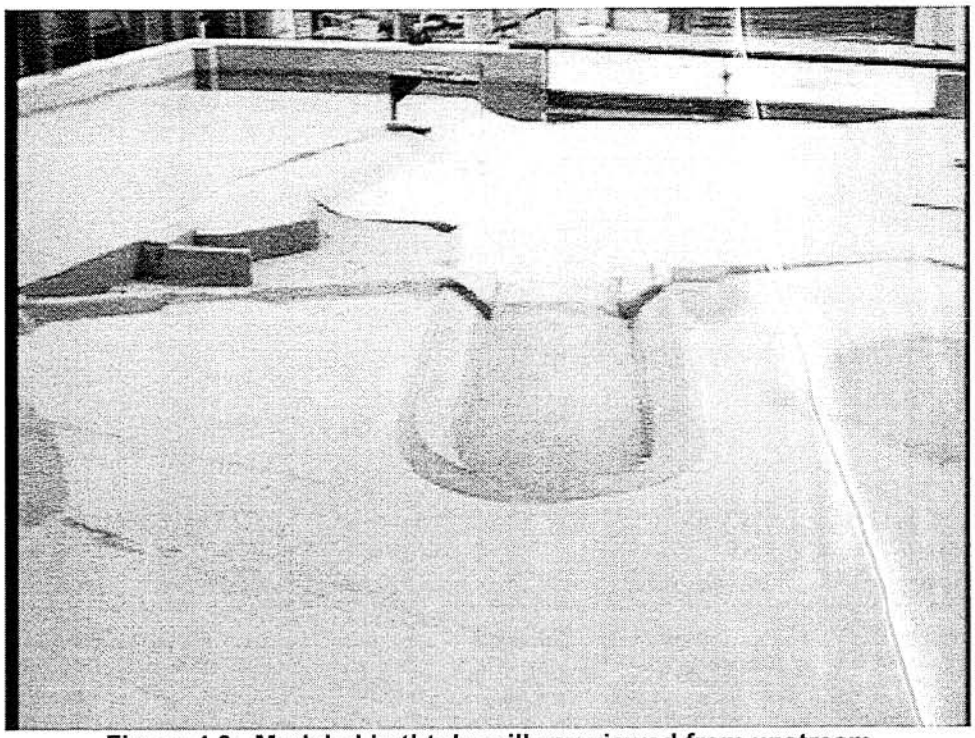

Figure 4.3. Modeled bathtub spillway viewed from upstream

Figure 4.4. Modeled bathtub spillway viewed from side

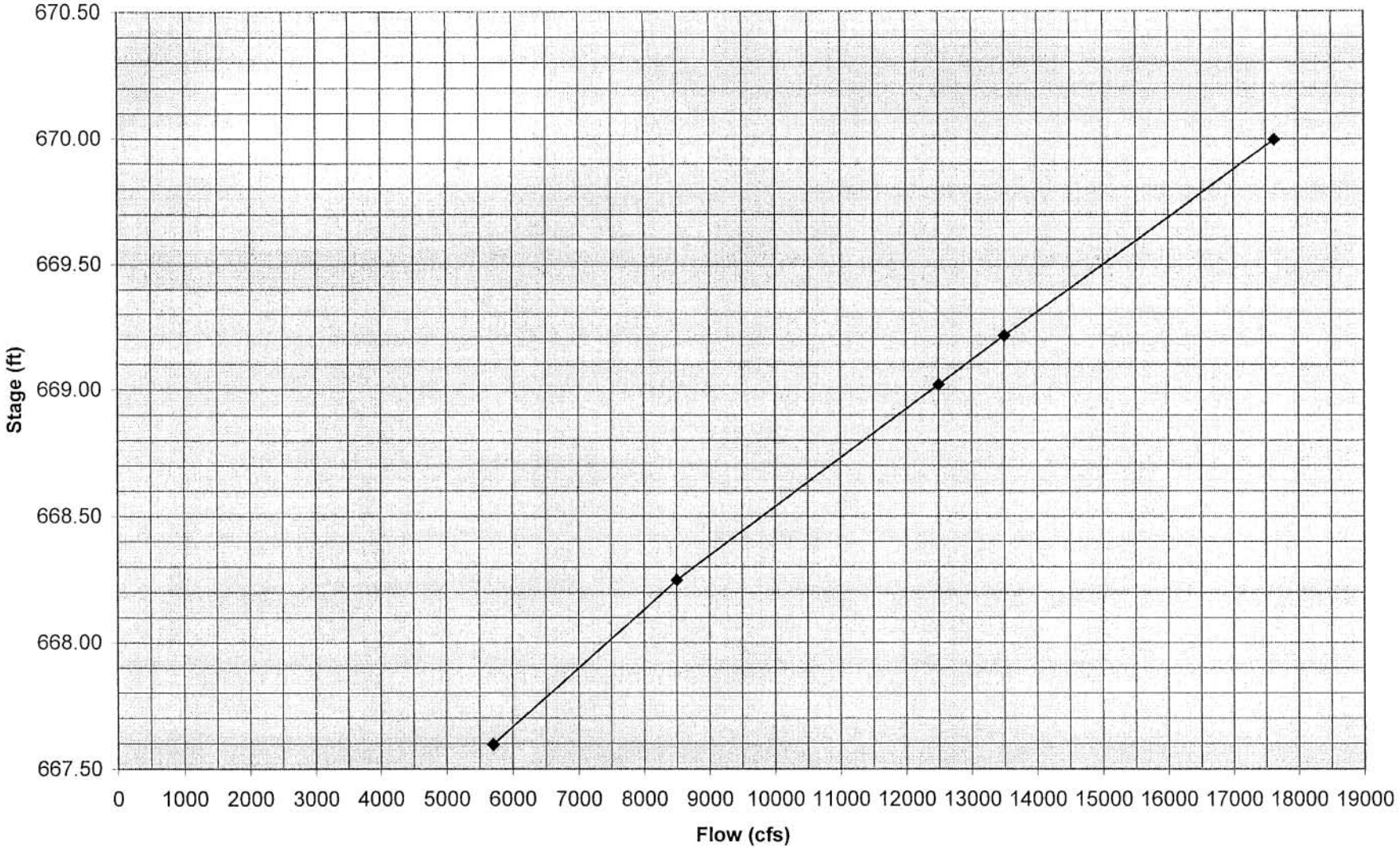

Figure 4.5. Averaged upstream pool stage response - Alternative I

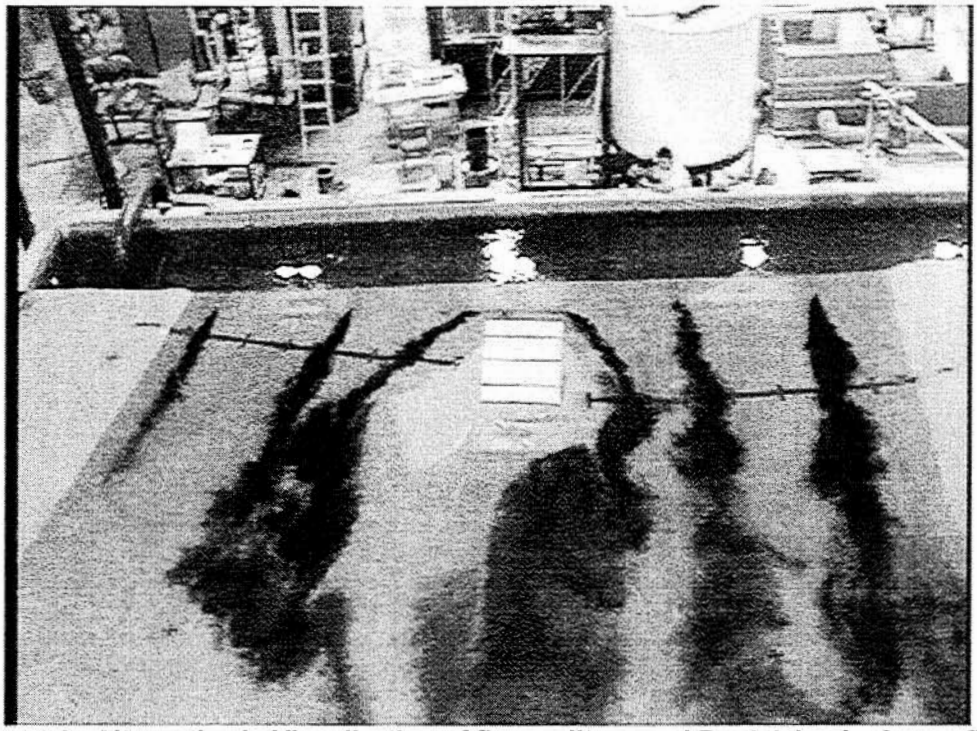

Figure 4.6. Alternative I - Visualization of flow split around Duck Island – 2 year flood (5700 cfs)

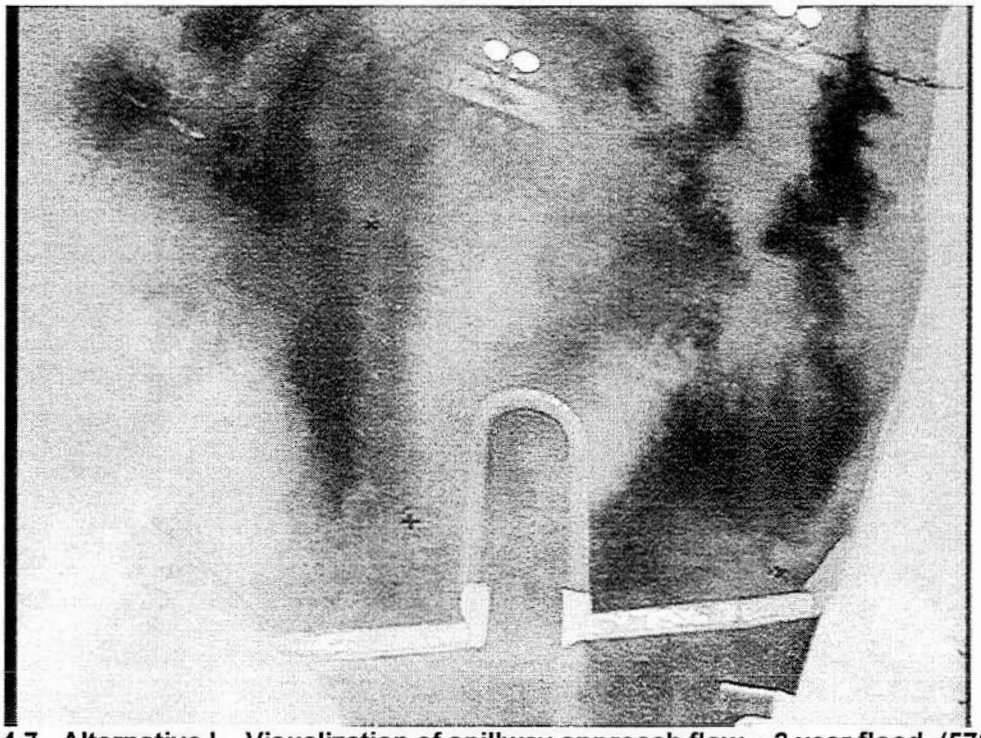

Figure 4.7. Alternative I – Visualization of spillway approach flow – 2 year flood (5700 cfs)

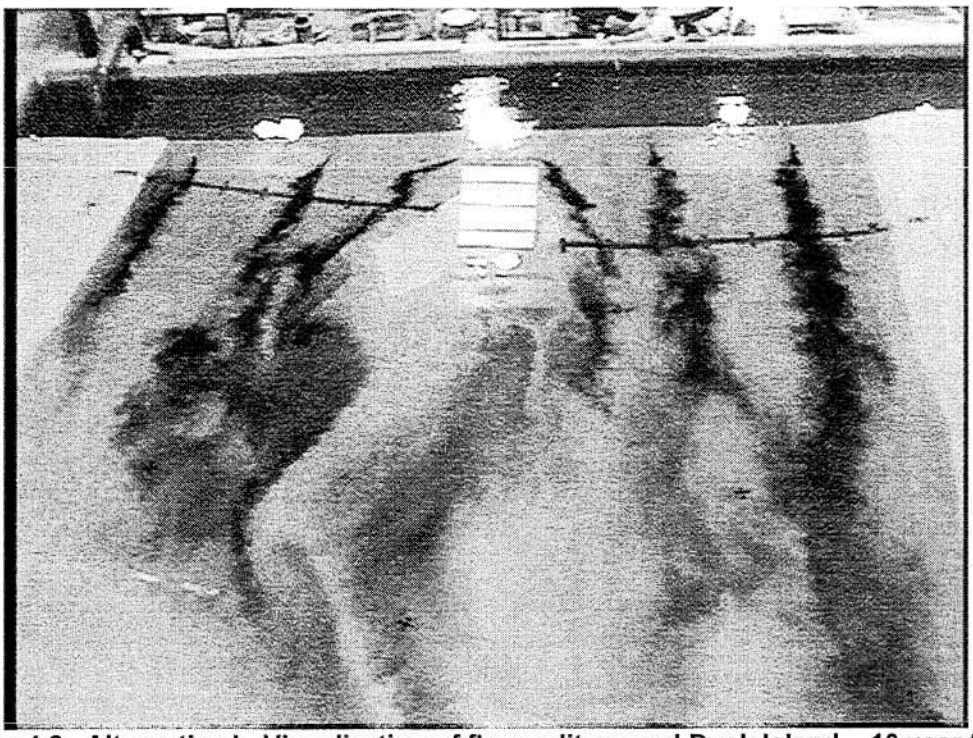

Figure 4.8. Alternative I - Visualization of flow split around Duck Island – 10 year flood (8500 cfs)

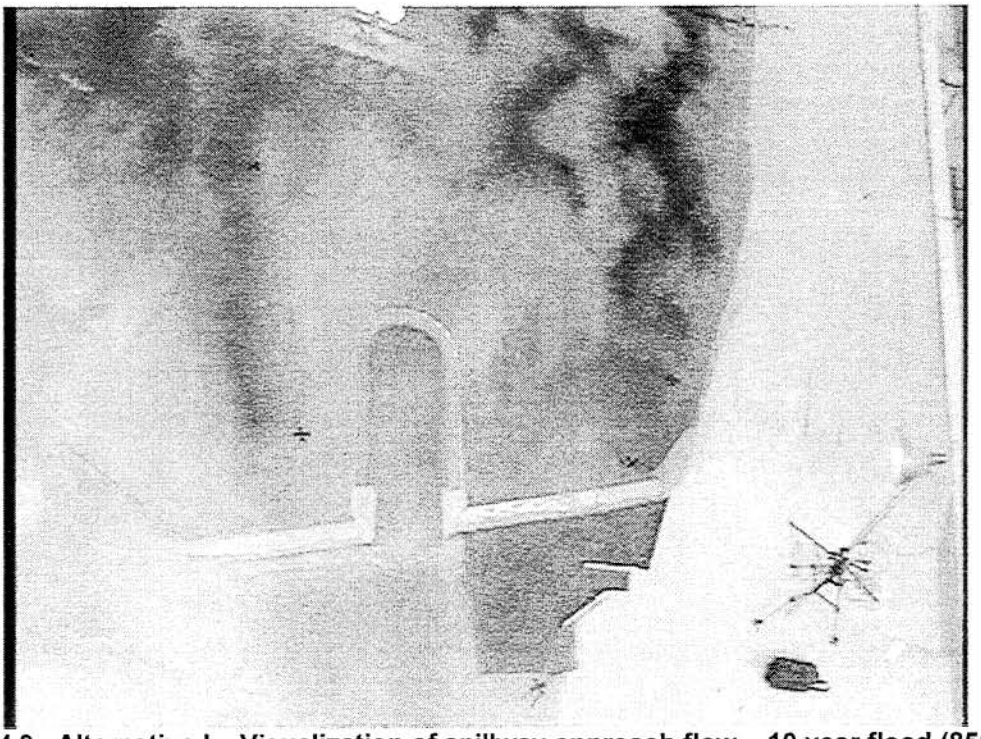

Figure 4.9. Alternative I – Visualization of spillway approach flow – 10 year flood (8500 cfs)

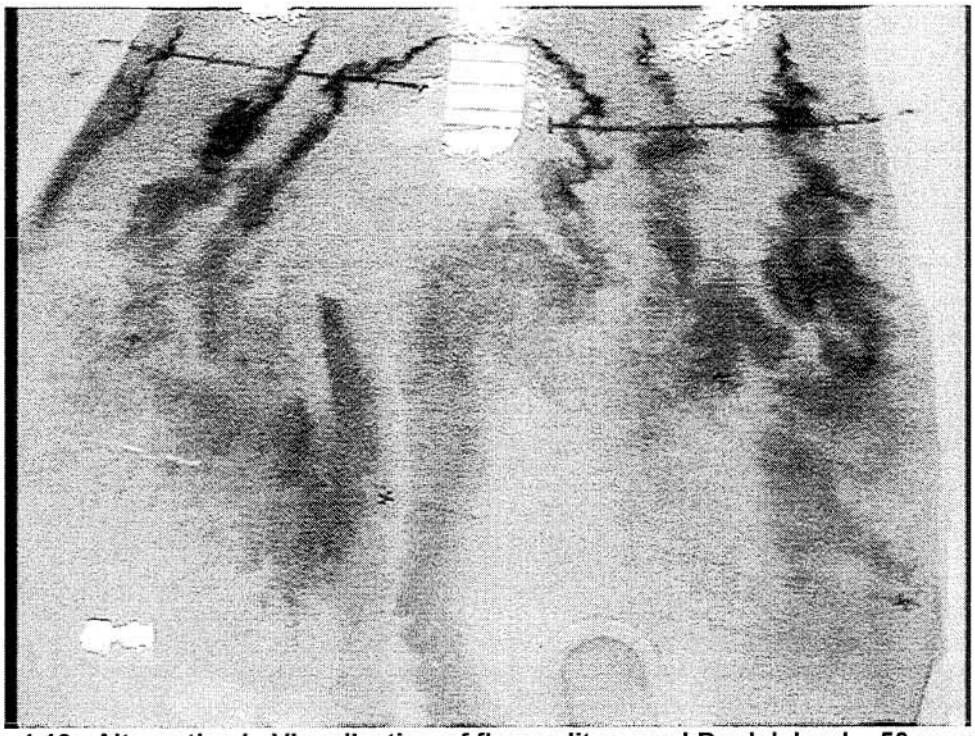

Figure 4.10. Alternative I - Visualization of flow split around Duck Island – 50 year flood (12500 cfs)

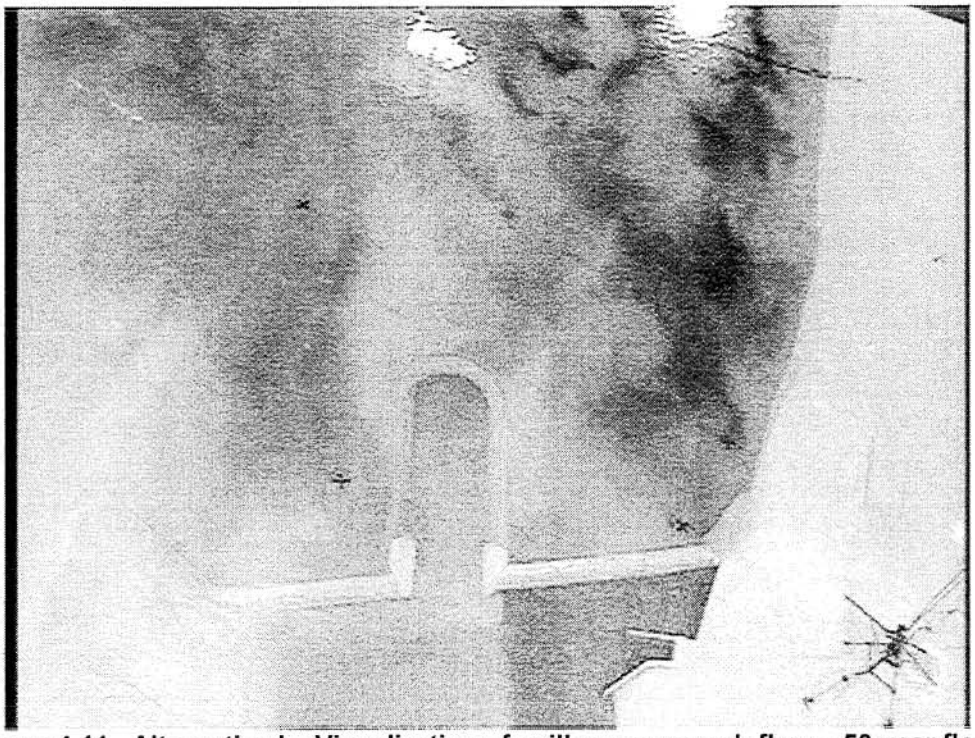

Figure 4.11. Alternative I – Visualization of spillway approach flow – 50 year flood (12500 cfs)

Figure 4.12. Alternative I - Visualization of flow split around Duck Island – 100 year flood (13500 cfs)

Figure 4.13. Alternative I – Visualization of spillway approach flow – 100 year flood (13500 cfs)

Figure 4.14. Alternative I - Visualization of flow split around Duck Island – 500 year flood (17630 cfs)

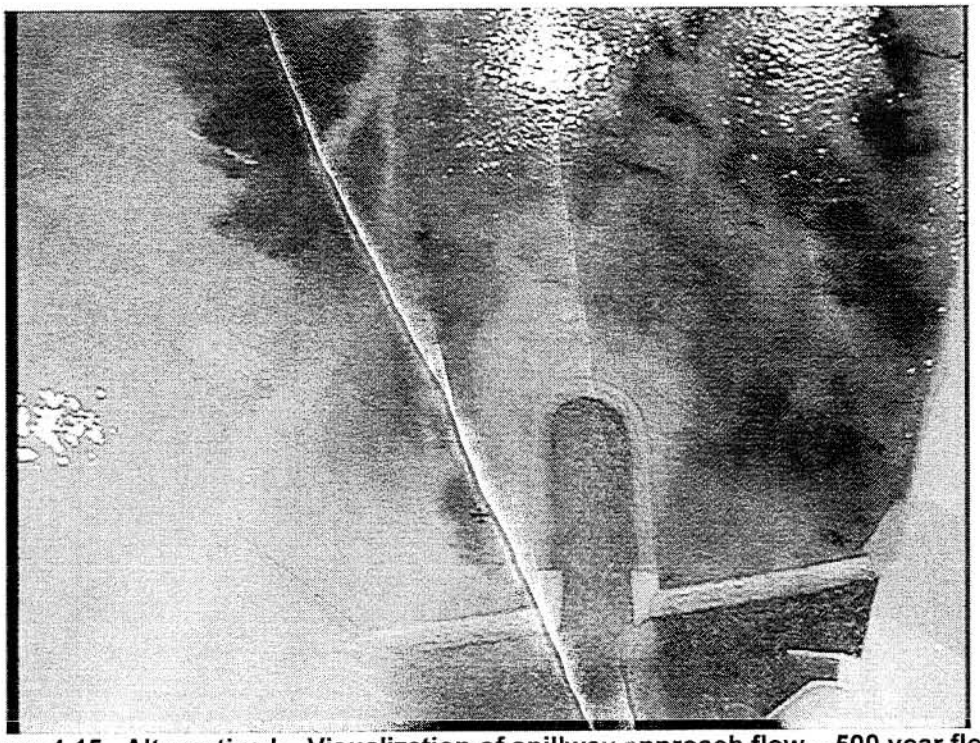

Figure 4.15. Alternative I – Visualization of spillway approach flow – 500 year flood (17630 cfs)

Batavia Dam Model Study

University of Illinois Hydrosystems Laboratory:

Alternative I - Flow Split

Specific Discharge Key

× ⟶ = 10 cfs/ ft

63% = % total flow (cfs)

January 25, 1998

Scale: 1/10" = 1'

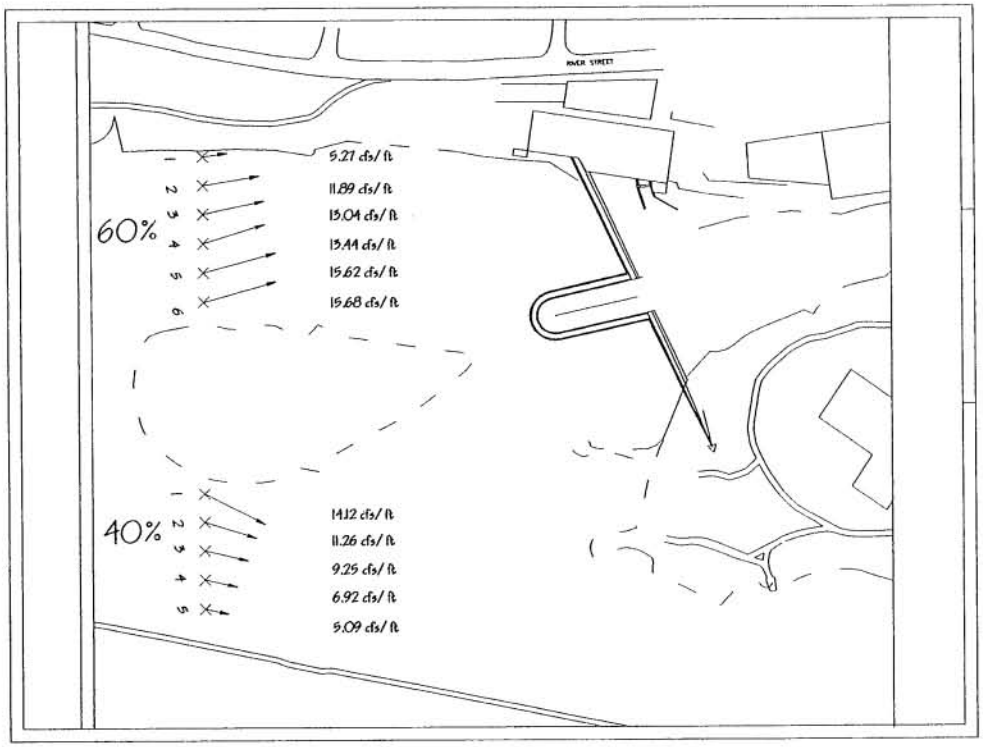

Figure 4.16. Alternative I - Specific discharge flow split around Duck Island - Calibration flow (6062 cfs)

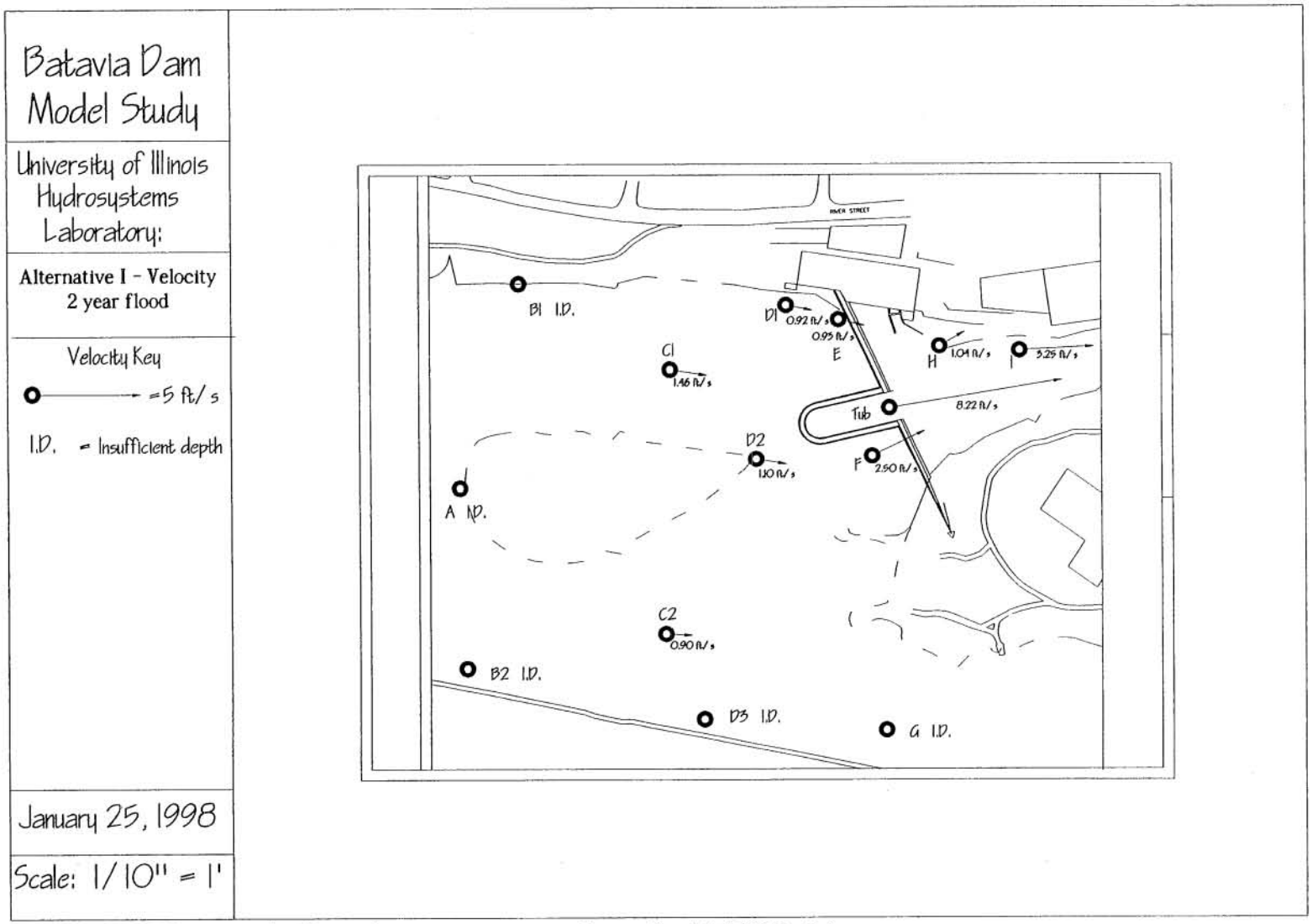

Figure 4.17. Alternative I - Point velocity measurments - 2 year flood (5700 cfs)

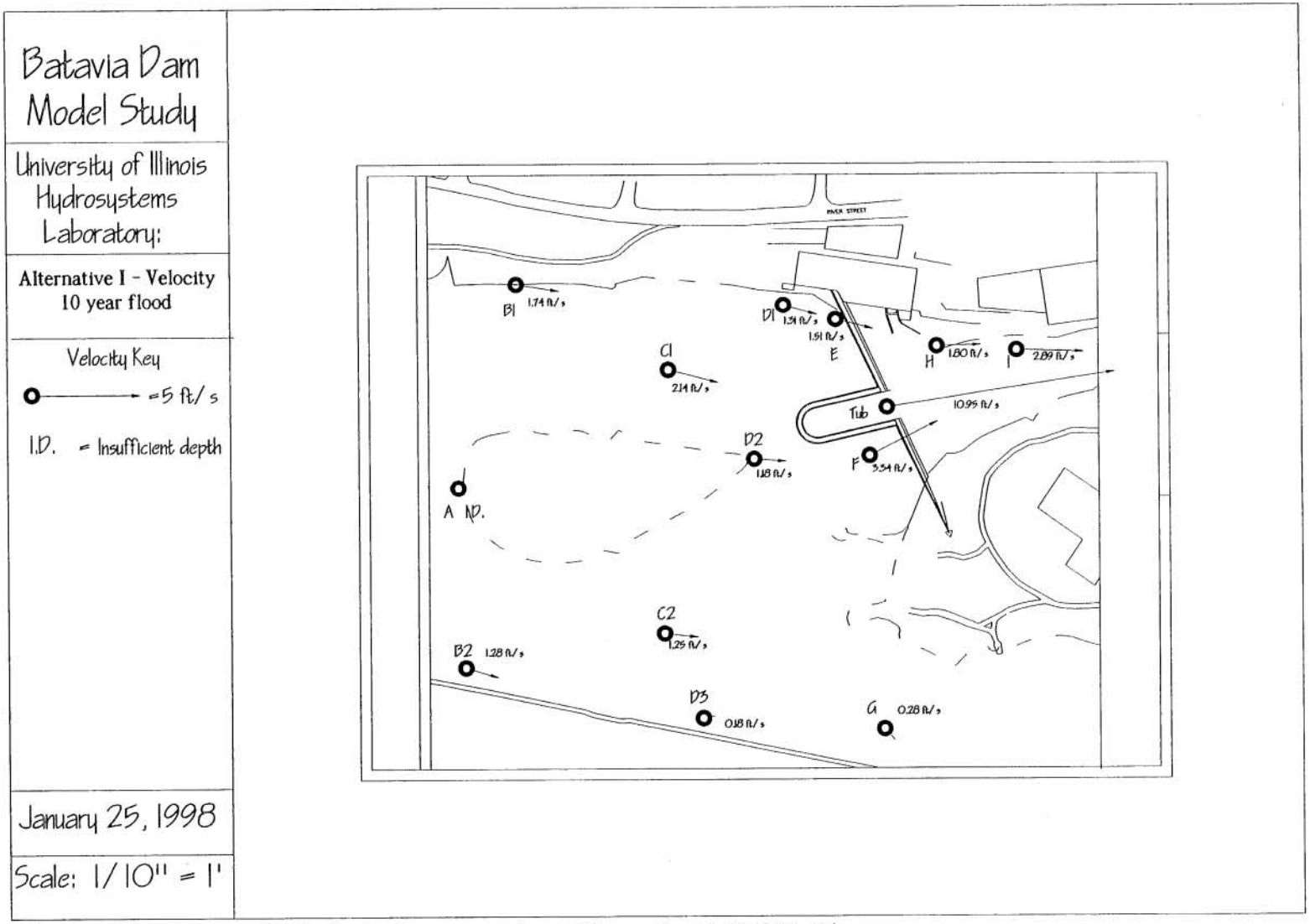

Figure 4.18. Alternative I - Point velocity measurments - 10 year flood (8500 cfs)

Batavia Dam Model Study

University of Illinois Hydrosystems Laboratory:

Alternative I - Velocity 50 year flood

Velocity Key

→ = 5 ft/s

I.D. = Insufficient depth

January 25, 1998

Scale: 1/10" = 1'

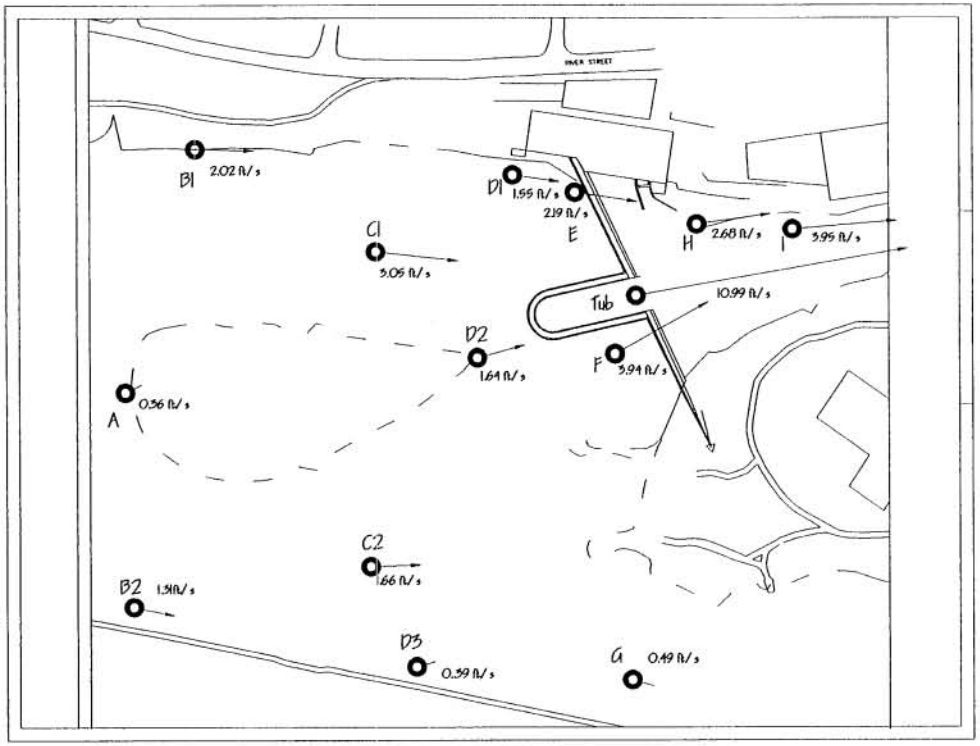

Figure 4.19. Alternative I - Point velocity measurments - 50 year flood (12500 cfs)

Batavia Dam Model Study

University of Illinois Hydrosystems Laboratory:

Alternative I - Velocity 100 year flood

Velocity Key

→ = 5 ft/s

I.D. = Insufficient depth

January 25, 1998

Scale: 1/10" = 1'

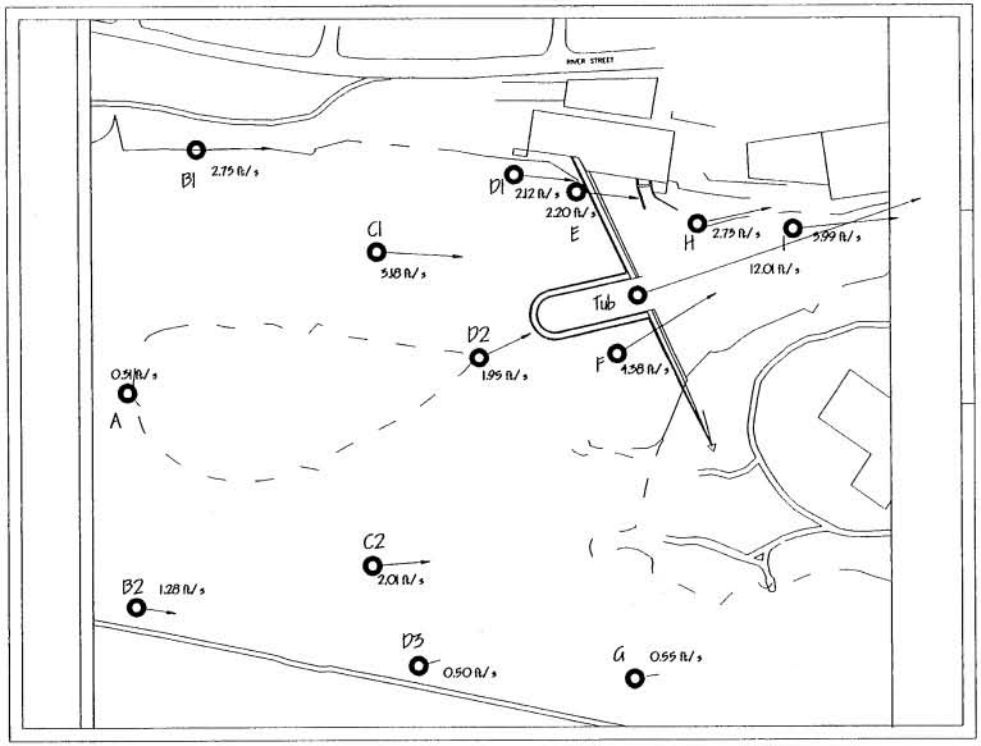

Figure 4.20. Alternative I - Point velocity measurments - 100 year flood (135500 cfs)

Batavia Dam Model Study

University of Illinois Hydrosystems Laboratory:

Alternative I - Velocity 500 year flood

Velocity Key

→ = 5 ft/s

I.D. = Insufficient depth

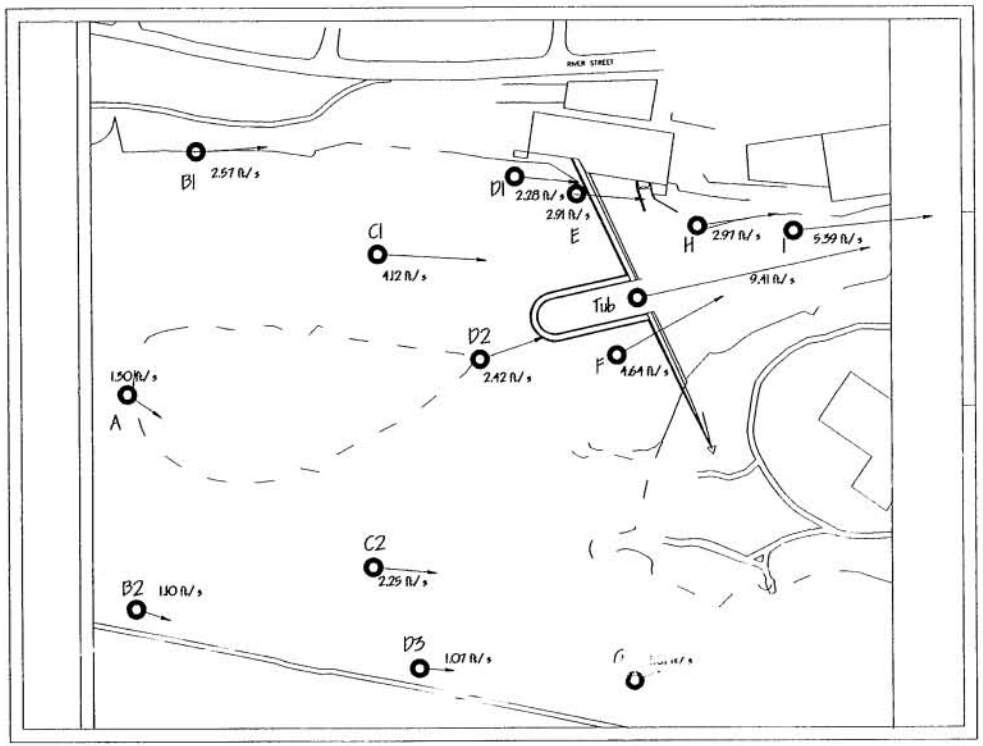

January 25, 1998

Scale: 1/10" = 1'

Figure 4.21. Alternative I - Point velocity measurments - 500 year flood (17630 cfs)

Batavia Dam Model Study

University of Illinois Hydrosystems Laboratory:

Alternative I - Downstream discharge 2 year flood

Specific Discharge Key

×← = 20 cfs/ ft

I.D. = Insufficient depth

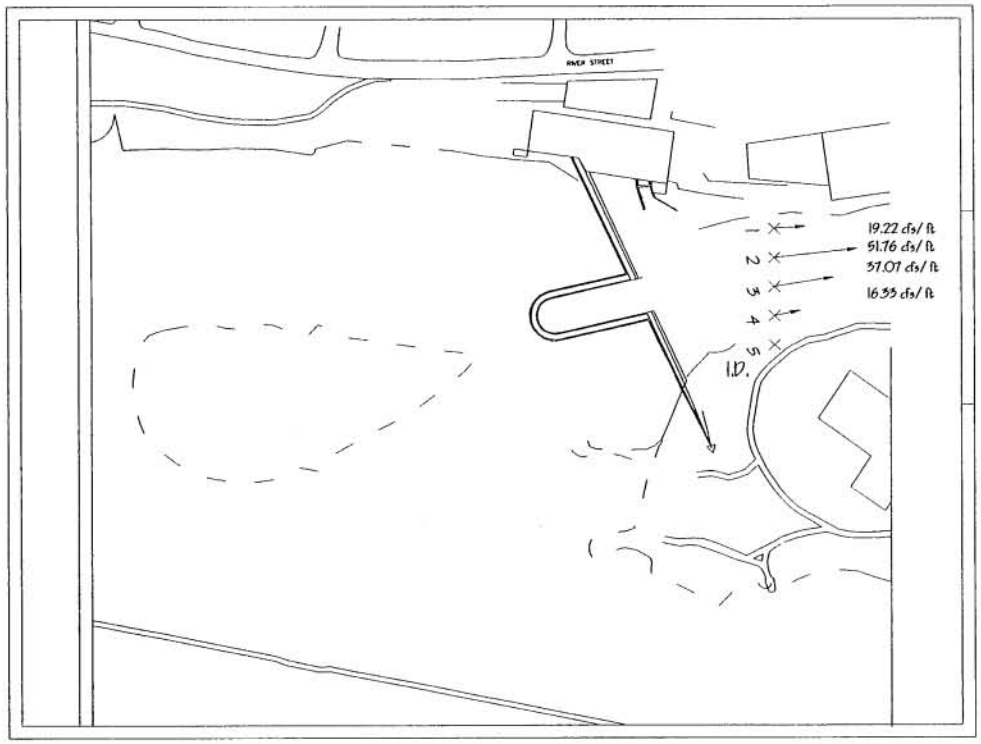

January 25, 1998

Scale: 1/10" = 1'

Figure 4.22. Alternative I - Specific discharge conditions downstream of stucture - 2 year flood (5700 cfs)

Batavia Dam Model Study

University of Illinois Hydrosystems Laboratory:

Alternative I - Downstream discharge 10 year flood

Specific Discharge Key

×← = 20 cfs/ ft

I.D. = Insufficient depth

January 25, 1998

Scale: 1/10" = 1'

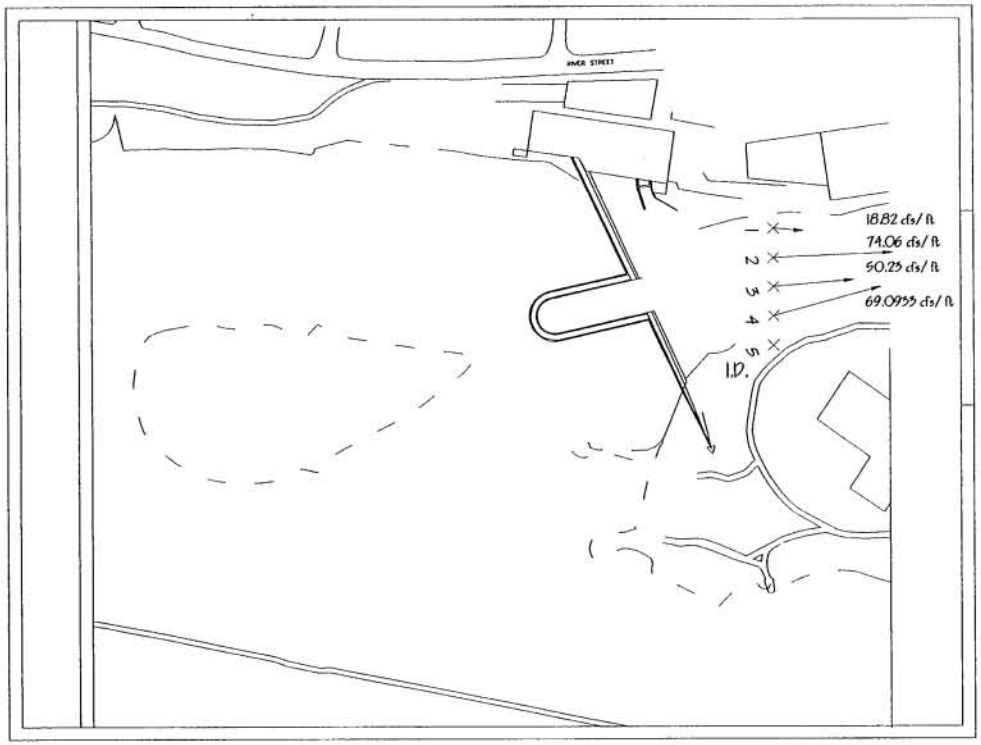

Figure 4.23. Alternative I - Specific discharge conditions downstream of stucture - 10 year flood (8500 cfs)

Batavia Dam Model Study

University of Illinois Hydrosystems Laboratory:

Alternative I - Downstream discharge 50 year flood

Specific Discharge Key

×← = 20 cfs/ ft

I.D. = Insufficient depth

January 25, 1998

Scale: 1/10" = 1'

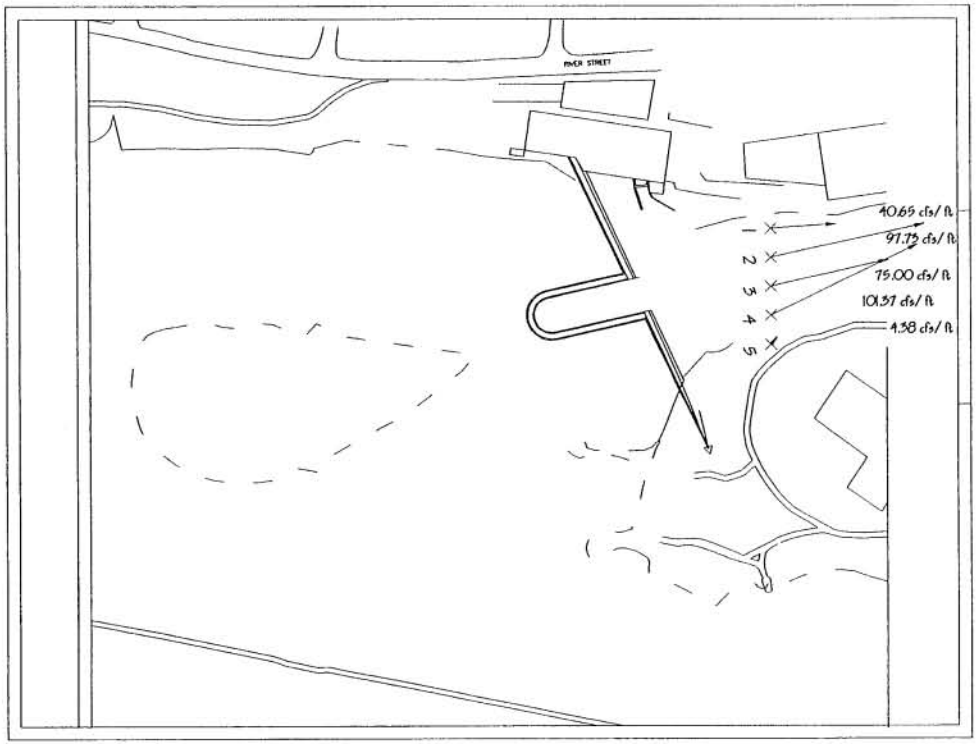

Figure 4.24. Alternative I - Specific discharge conditions downstream of stucture - 50 year flood (12500 cfs)

Batavia Dam Model Study

University of Illinois Hydrosystems Laboratory:

Alternative I - Downstream discharge 100 year flood

Specific Discharge Key

×⟵ = 20 cfs/ ft

I.D.= Insufficient depth

January 25, 1998

Scale: 1/10" = 1'

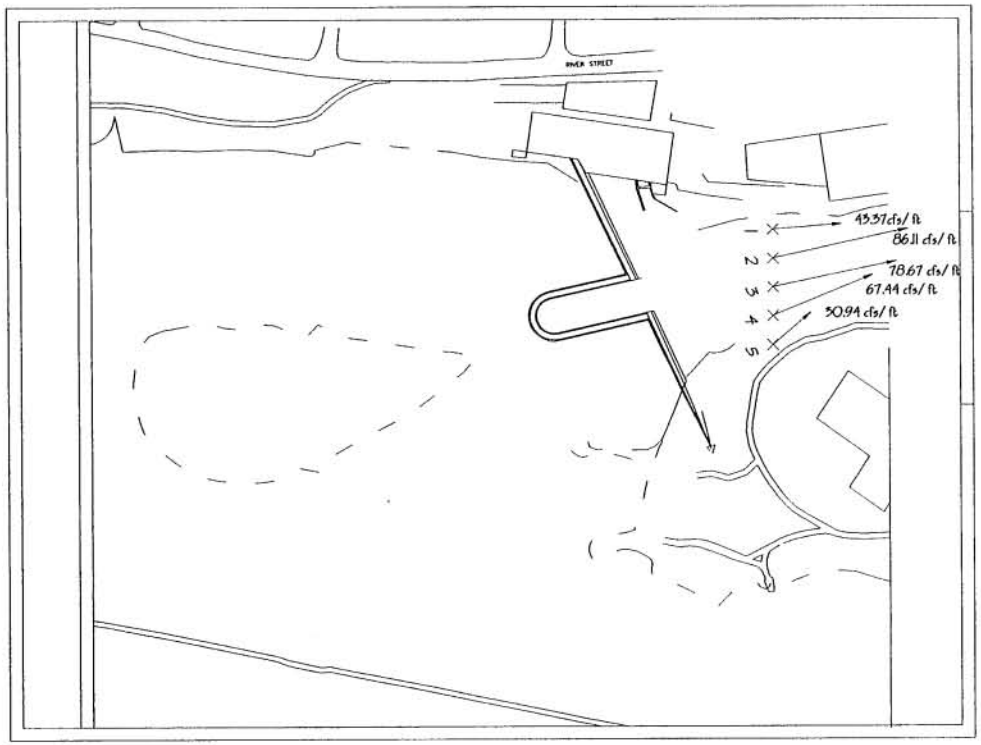

Figure 4.25. Alternative I - Specific discharge conditions downstream of stucture - 100 year flood (135000 cfs)

Batavia Dam Model Study

University of Illinois Hydrosystems Laboratory:

Alternative I - Downstream discharge 500 year flood

Specific Discharge Key

×← = 20 cfs/ ft

I.D. = Insufficient depth

January 25, 1998

Scale: 1/10" = 1'

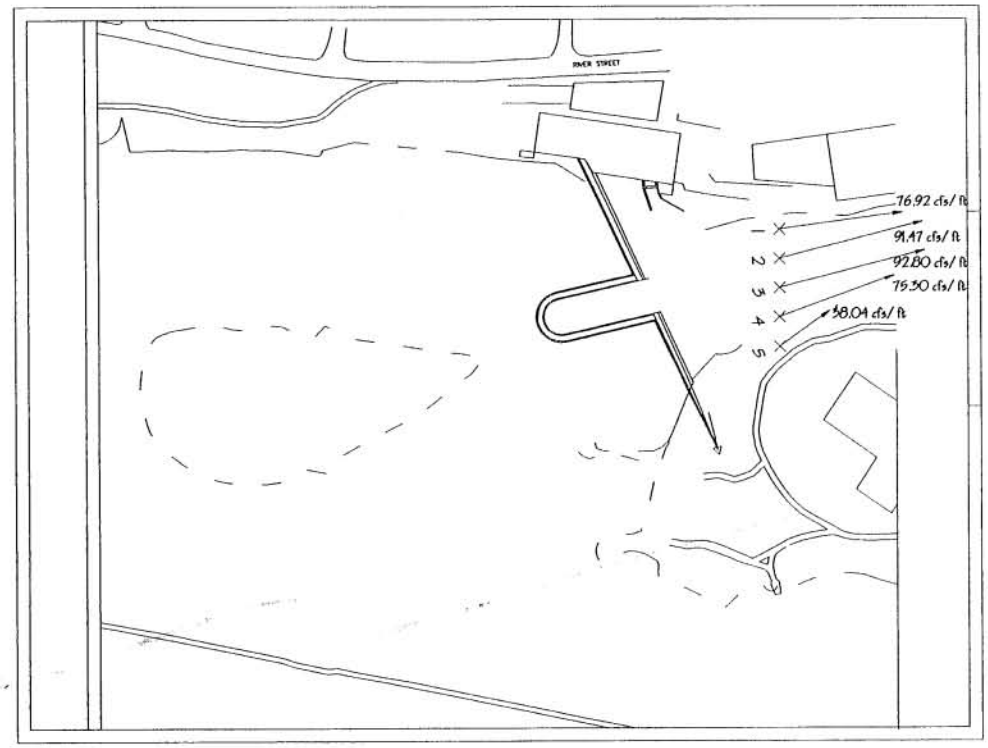

Figure 4.26. Alternative I - Specific discharge conditions downstream of stucture - 500 year flood (17630 cfs)

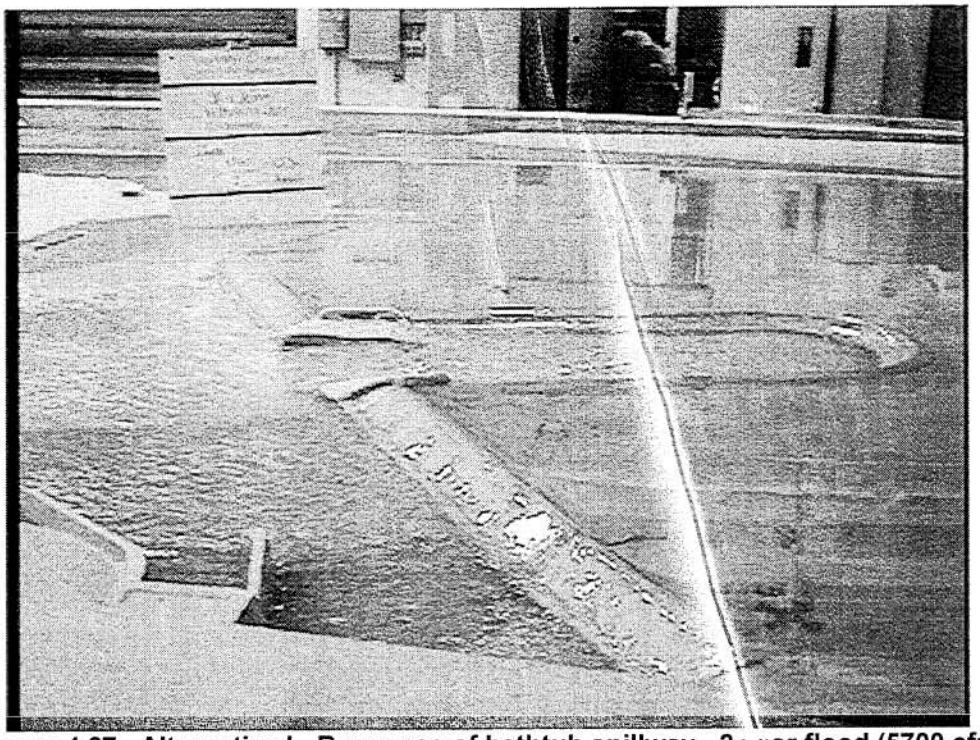

Figure 4.27. Alternative I - Response of bathtub spillway - 2 year flood (5700 cfs)

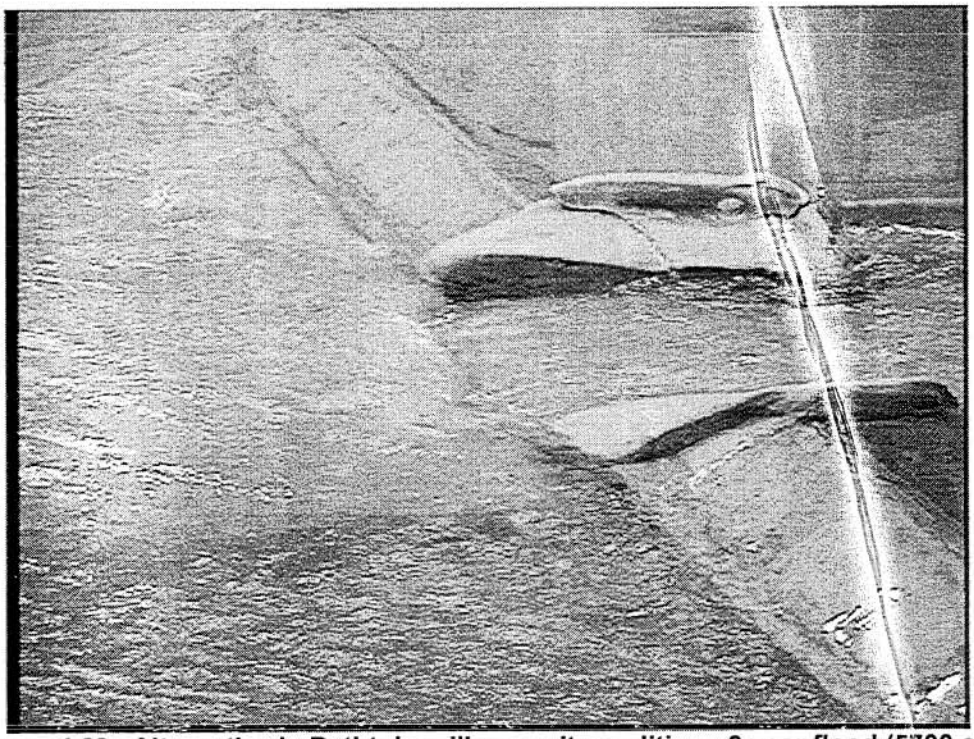

Figure 4.28. Alternative I - Bathtub spillway exit condition - 2 year flood (5700 cfs)

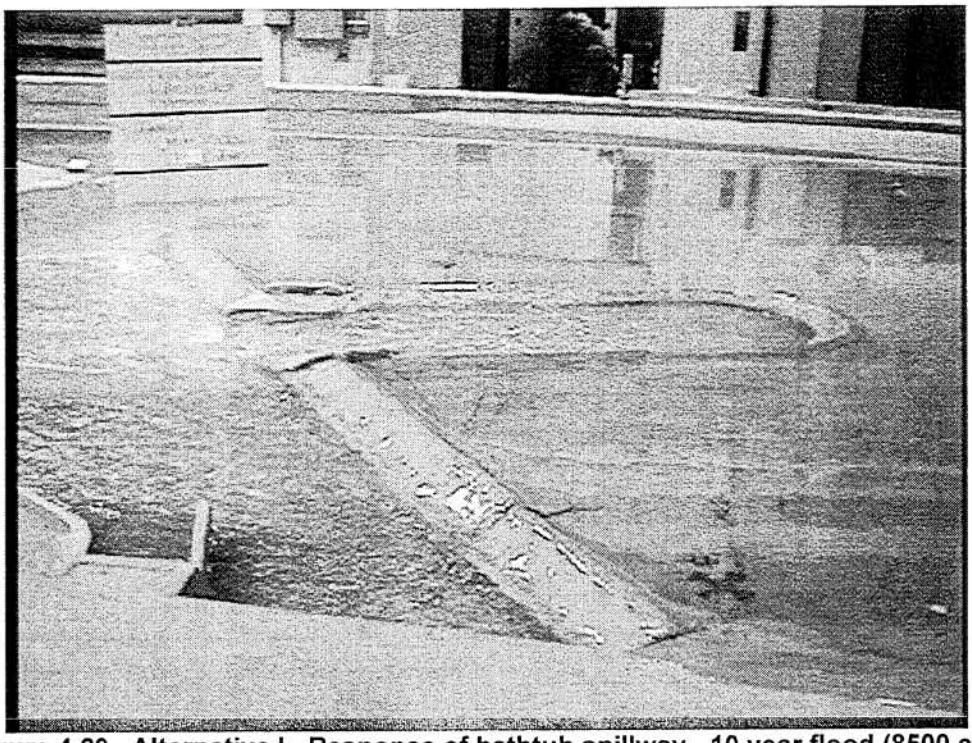

Figure 4.29. Alternative I - Response of bathtub spillway - 10 year flood (8500 cfs)

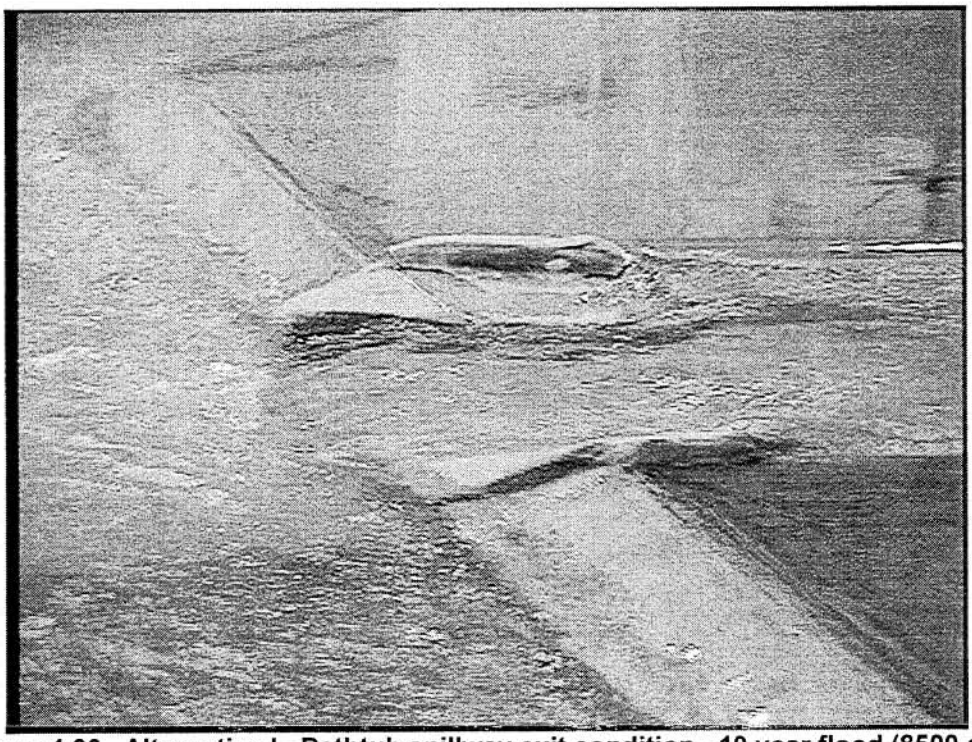

Figure 4.30. Alternative I - Bathtub spillway exit condition - 10 year flood (8500 cfs)

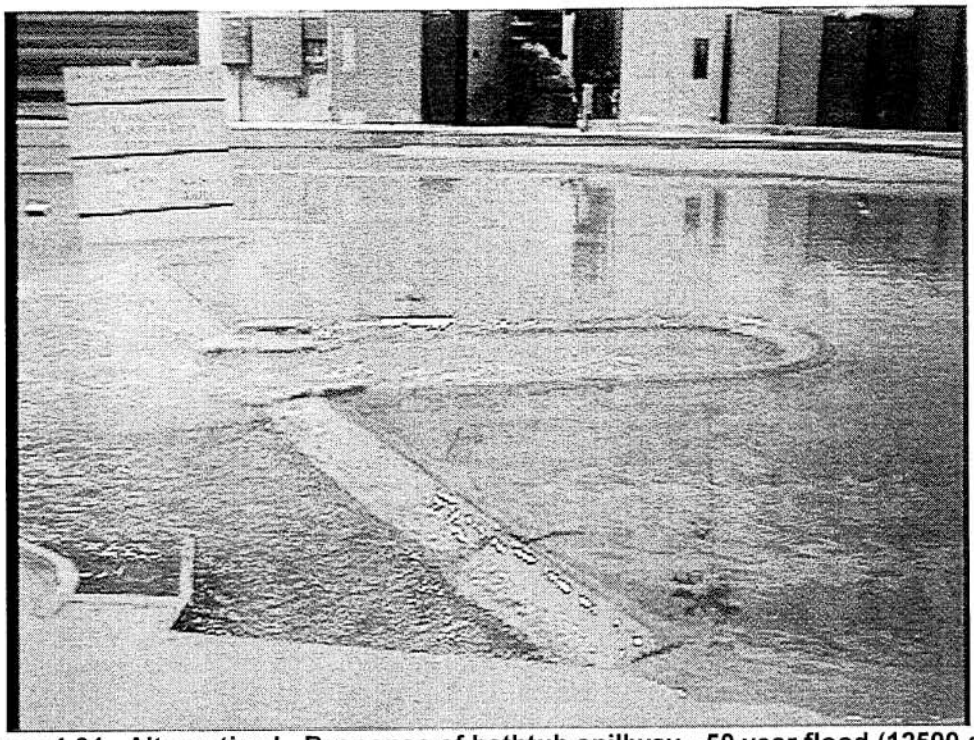

Figure 4.31. Alternative I - Response of bathtub spillway - 50 year flood (12500 cfs)

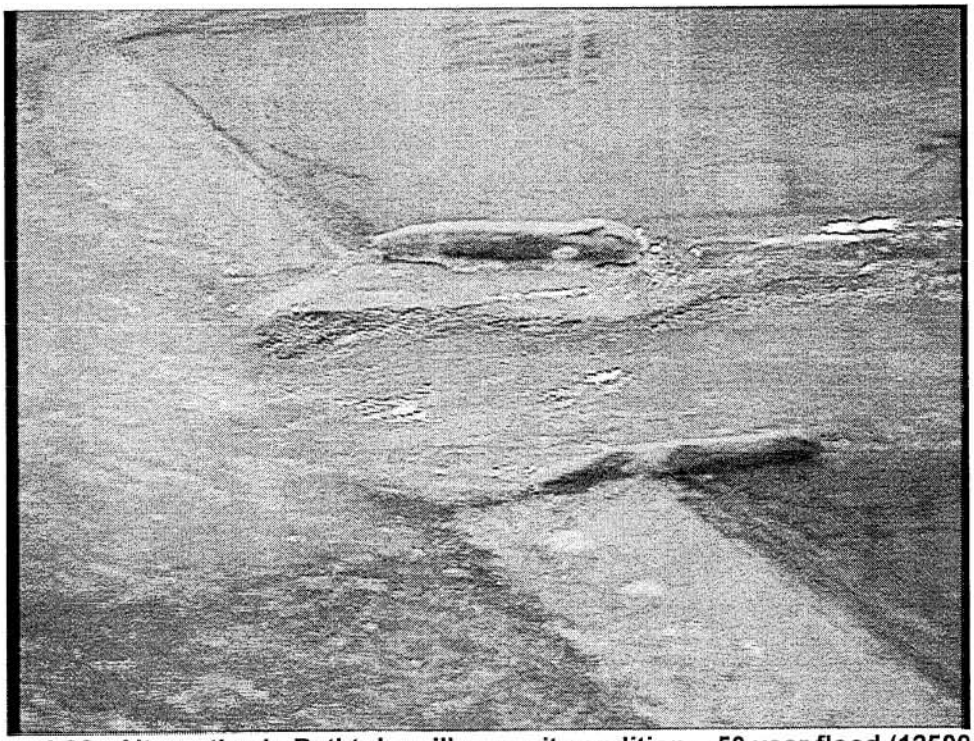

Figure 4.32. Alternative I - Bathtub spillway exit condition – 50 year flood (12500 cfs)

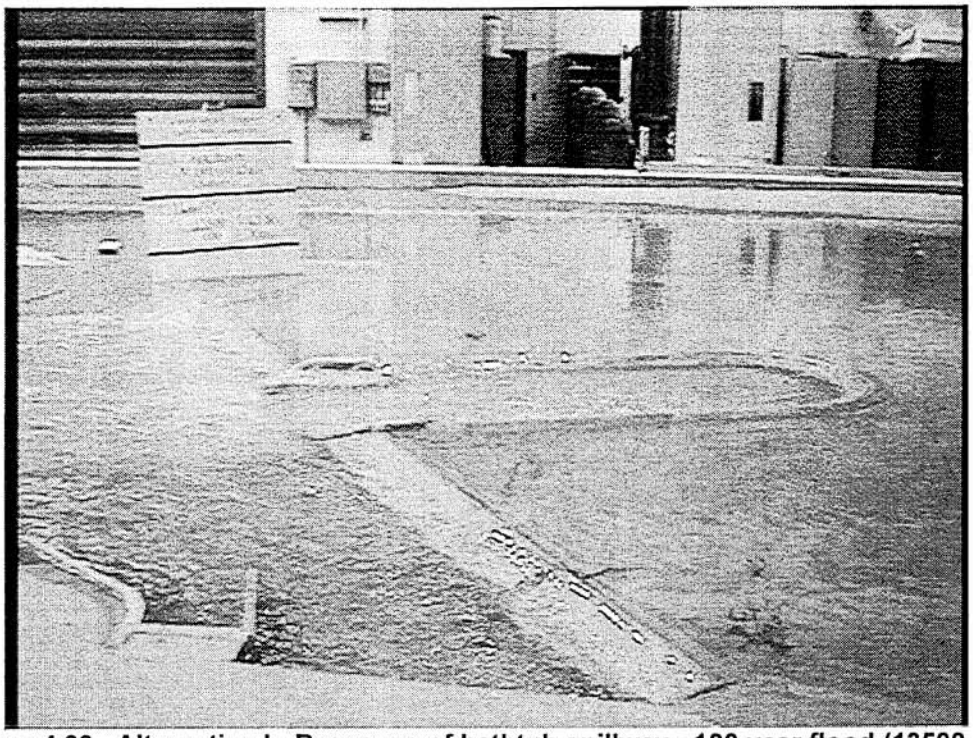

Figure 4.33. Alternative I - Response of bathtub spillway - 100 year flood (13500 cfs)

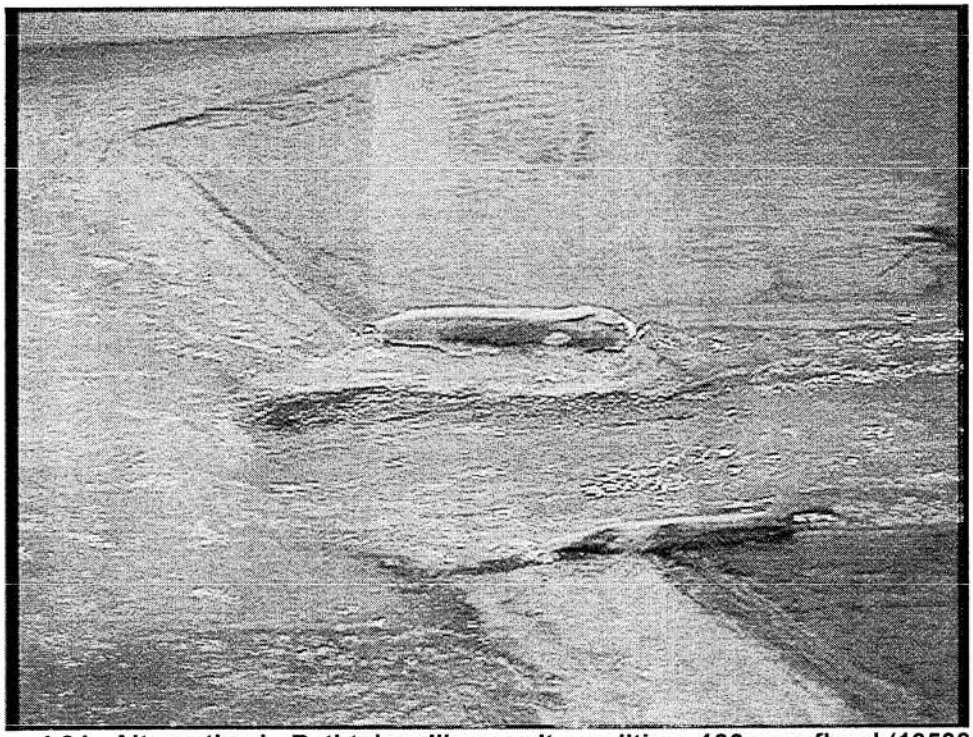

Figure 4.34. Alternative I - Bathtub spillway exit condition -100 year flood (13500 cfs)

Figure 4.35. Alternative I - Response of bathtub spillway - 500 year flood (17630 cfs)

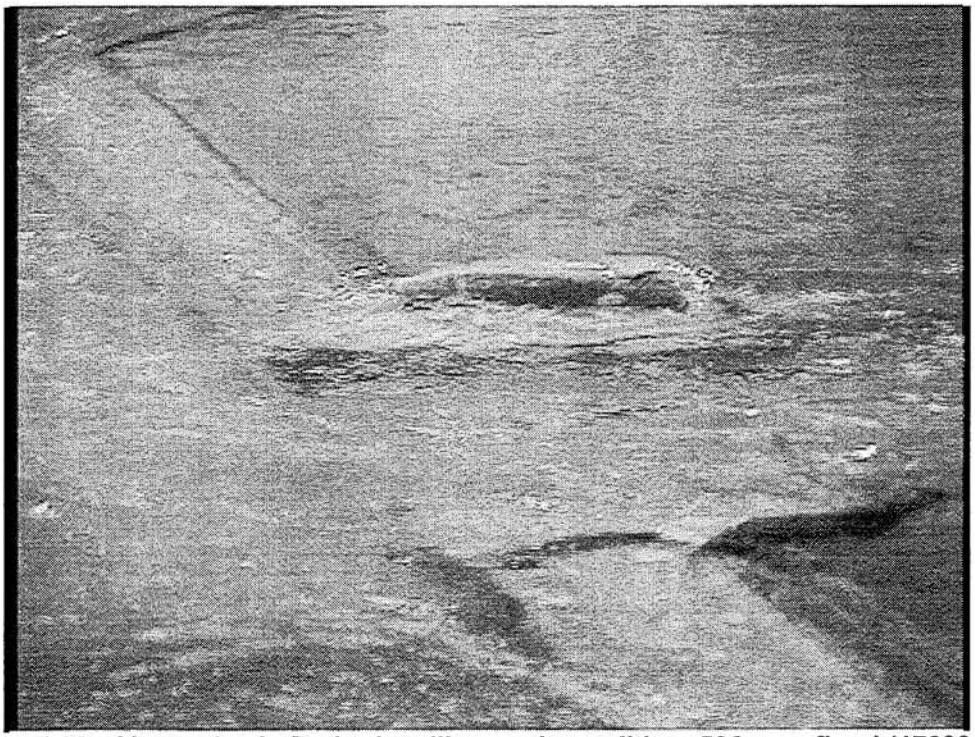

Figure 4.36. Alternative I - Bathtub spillway exit condition -500 year flood (17630 cfs)

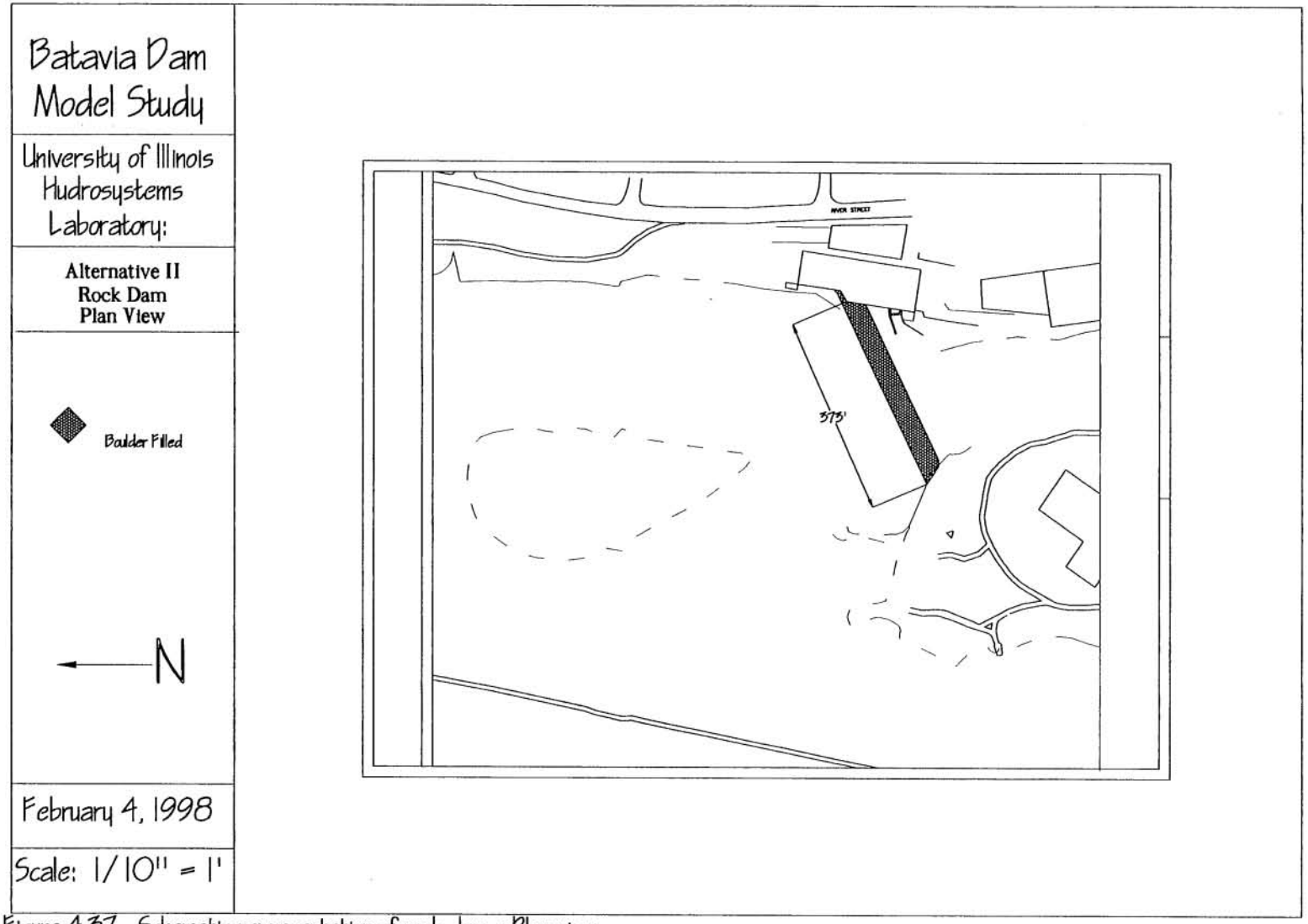

Figure 4.37. Schematic representation of rock dam - Plan view

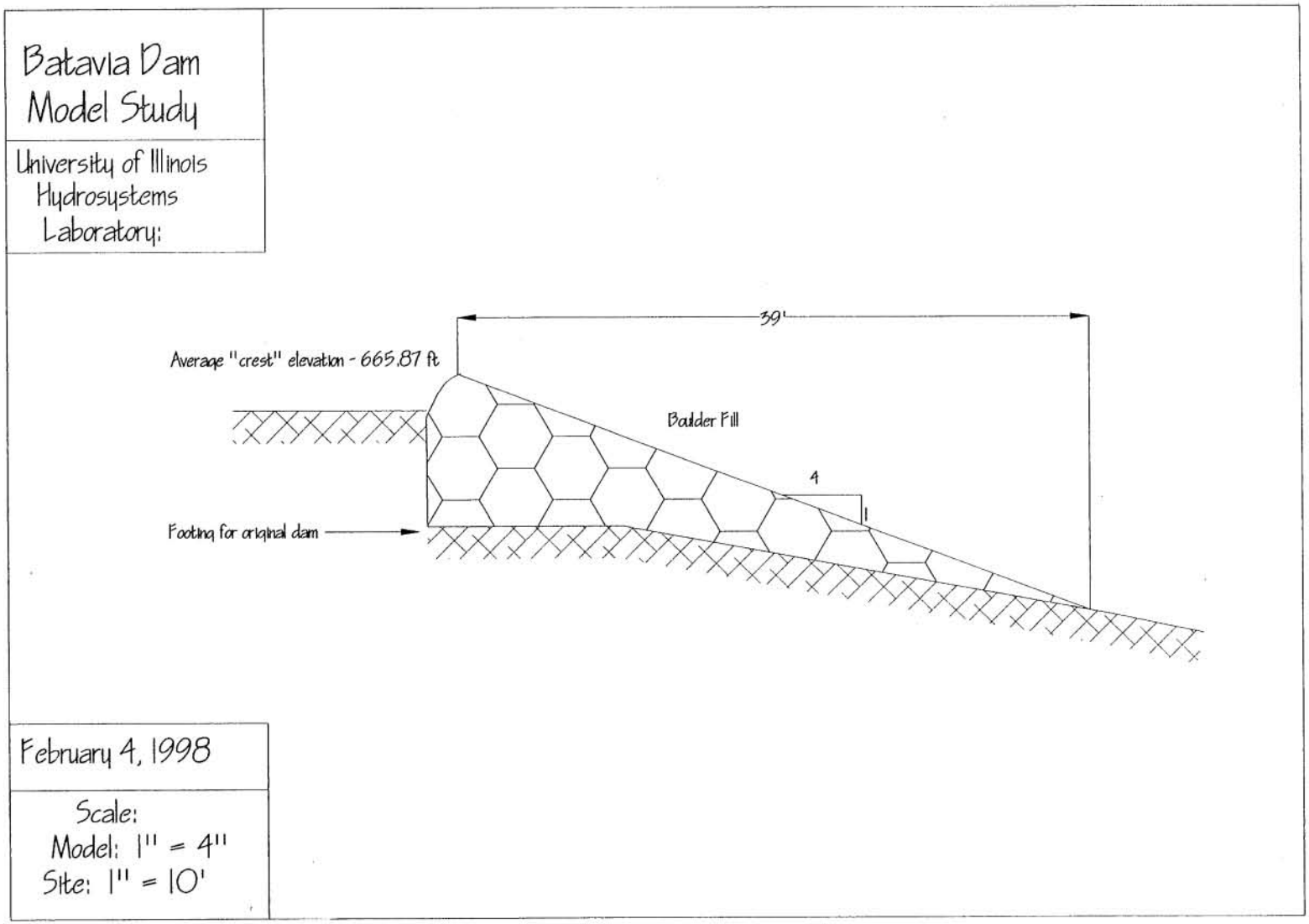

Figure 4.38. Schematic representation of rock dam - Cross section

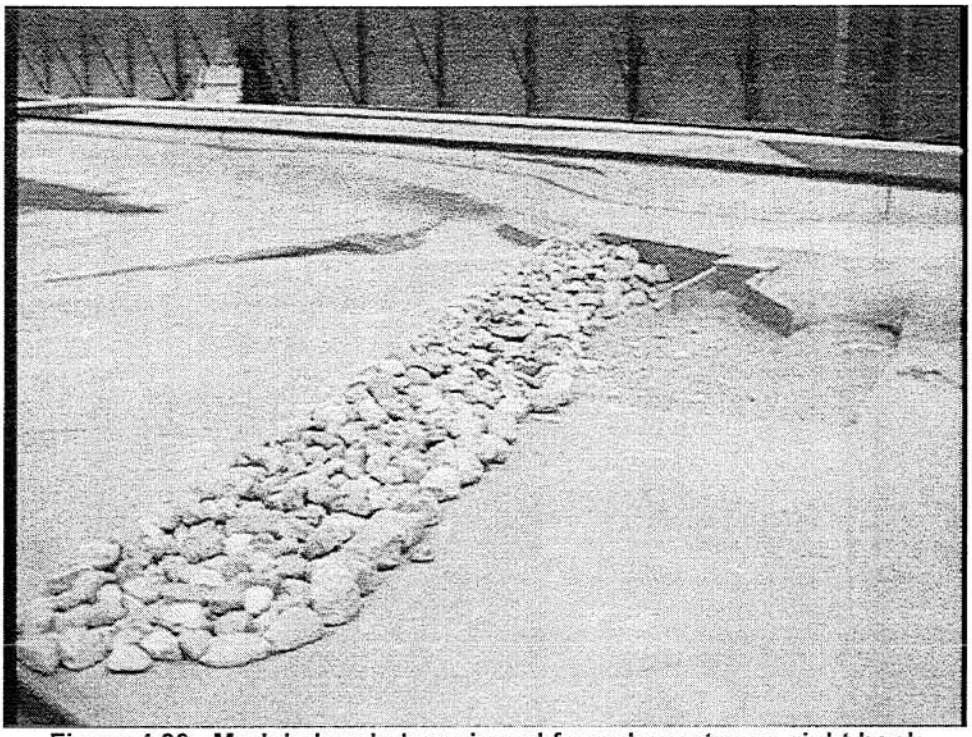

Figure 4.39. Modeled rock dam viewed from downstream, right bank

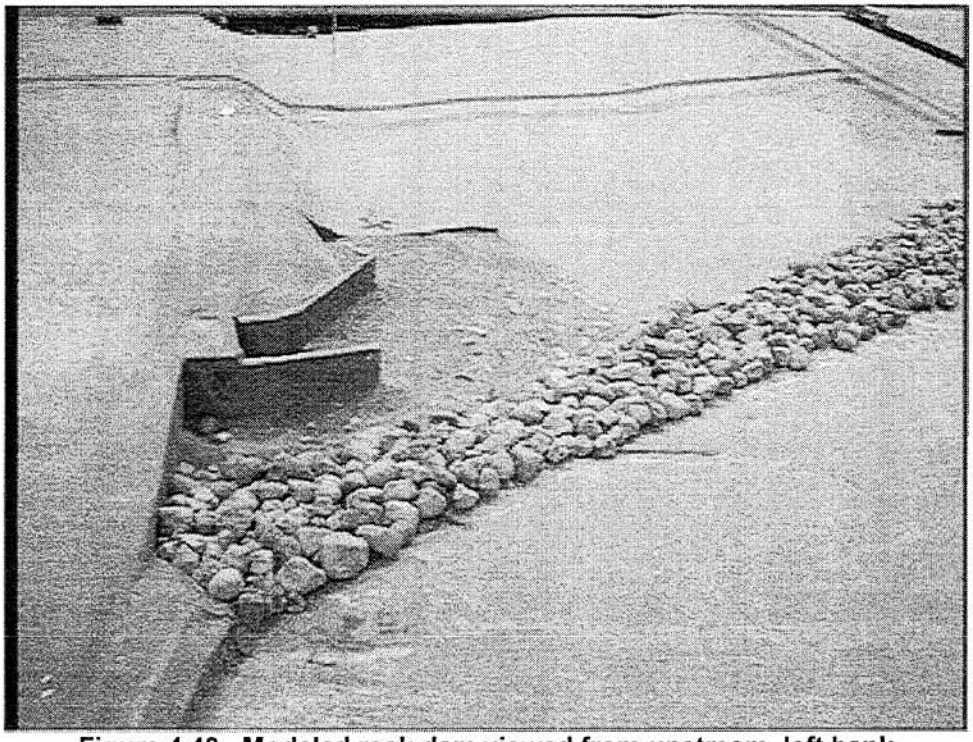

Figure 4.40. Modeled rock dam viewed from upstream, left bank

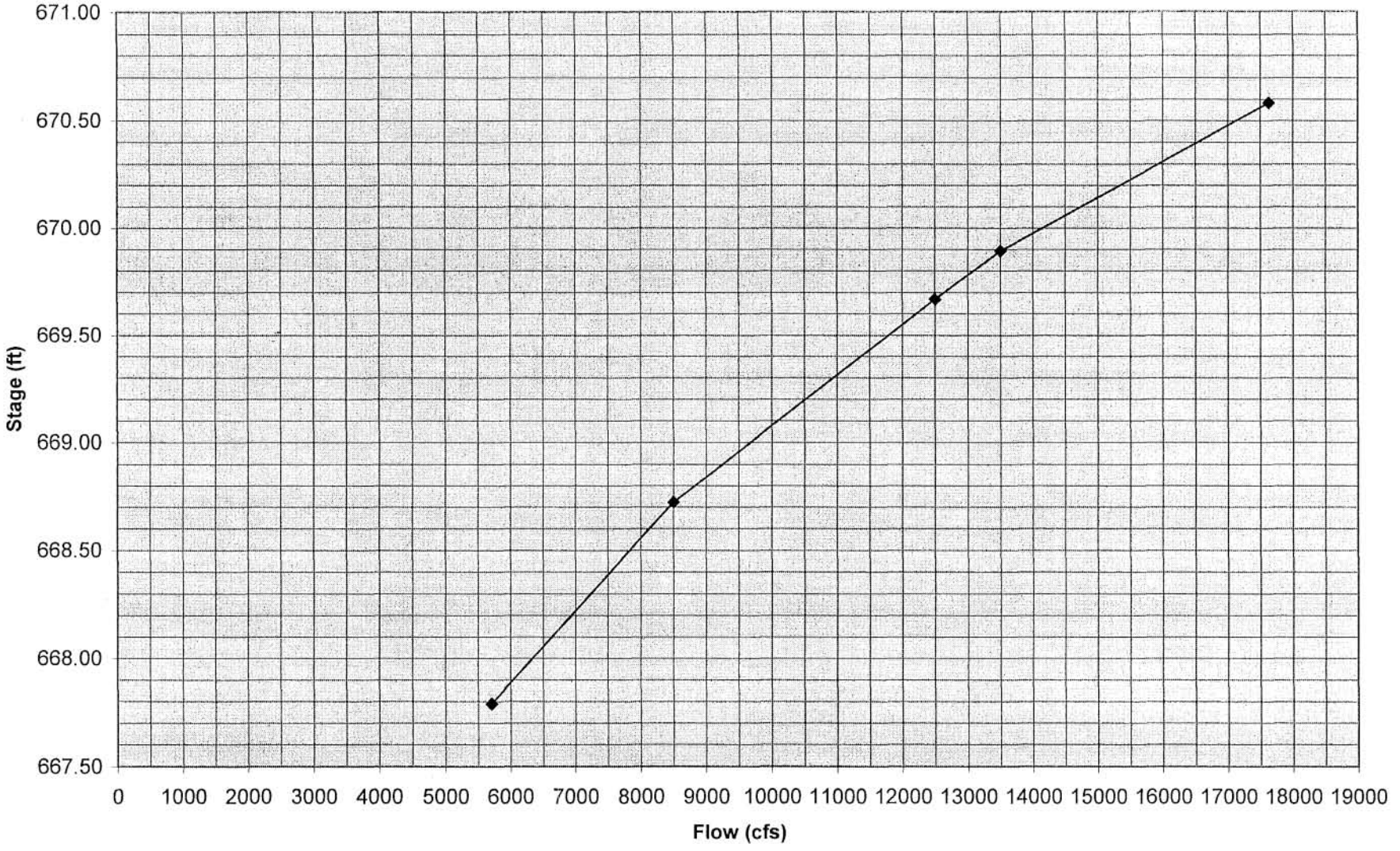

Figure 4.41. Averaged upstream pool stage response - Alternative II

Figure 4.42. Alternative II - Visualization of flow split around Duck Island – 2 year flood (5700 cfs)

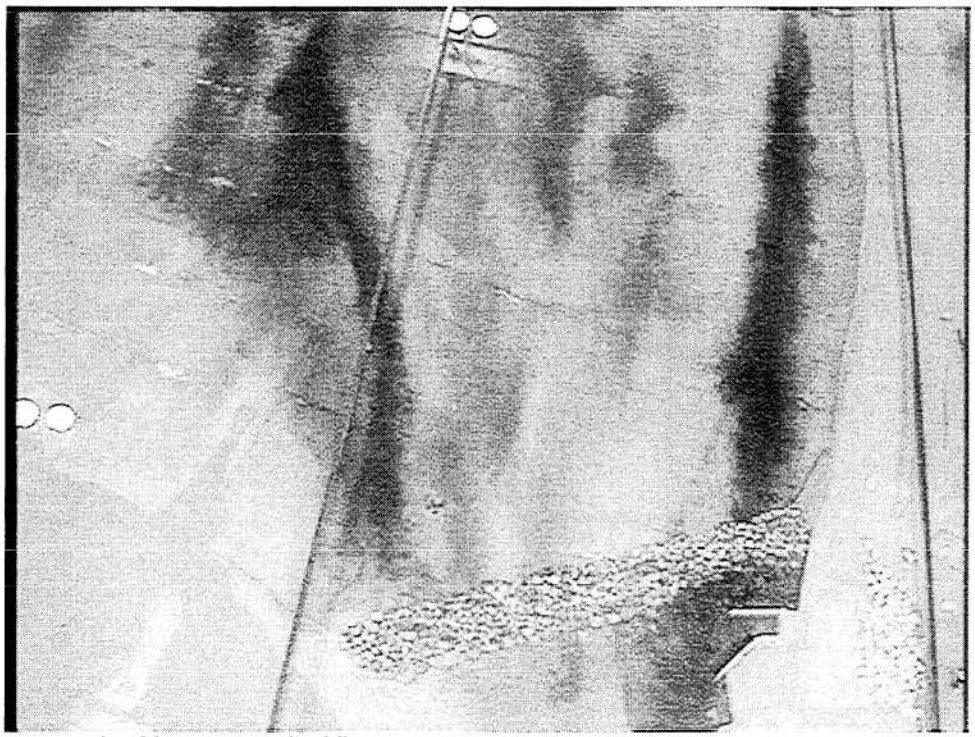

Figure 4.43. Alternative II – Visualization of spillway approach flow – 2 year flood (5700 cfs)

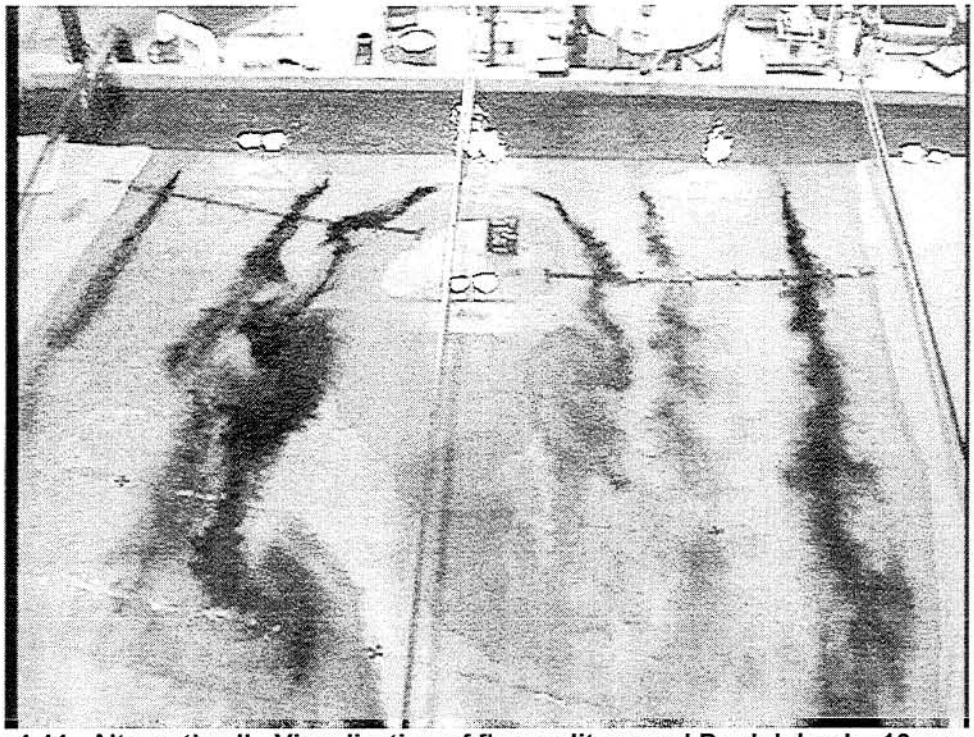

Figure 4.44. Alternative II - Visualization of flow split around Duck Island – 10 year flood (8500 cfs)

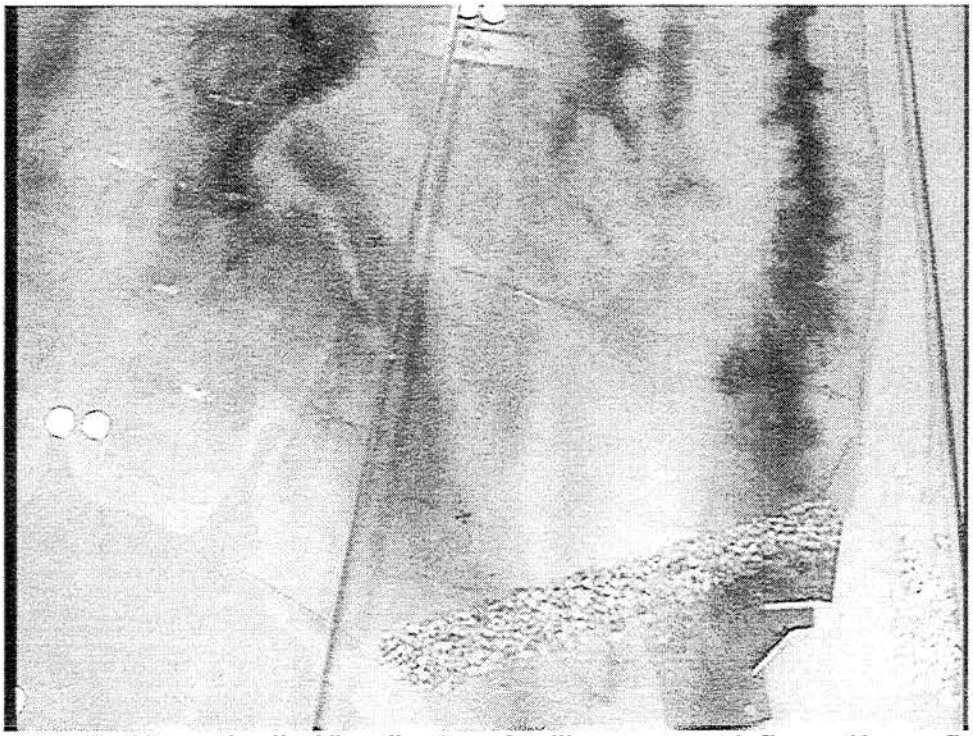

Figure 4.45. Alternative II – Visualization of spillway approach flow – 10 year flood (8500 cfs)

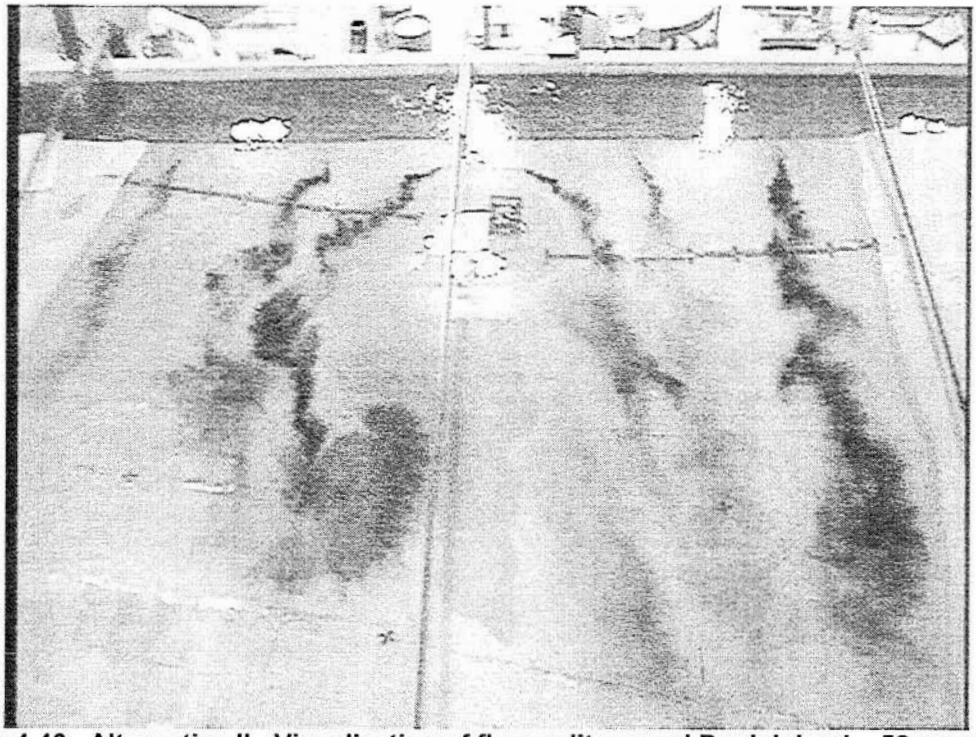

Figure 4.46. Alternative II - Visualization of flow split around Duck Island – 50 year flood (12500 cfs)

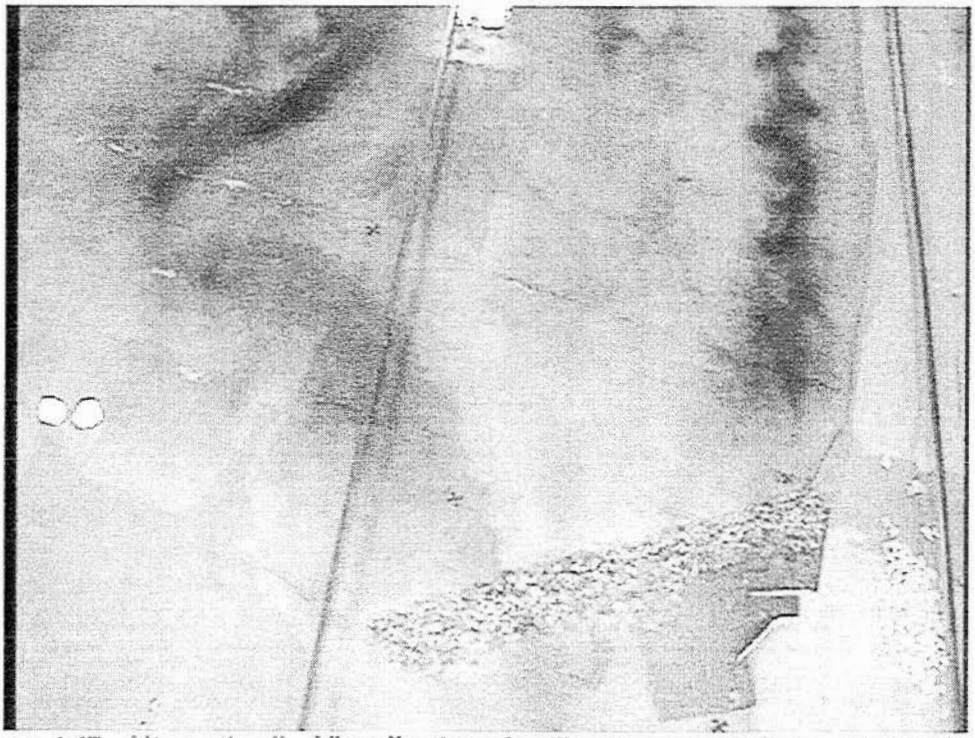

Figure 4.47. Alternative II – Visualization of spillway approach flow – 50 year flood (12500 cfs)

Figure 4.48. Alternative II - Visualization of flow split around Duck Island – 100 year flood (13500 cfs)

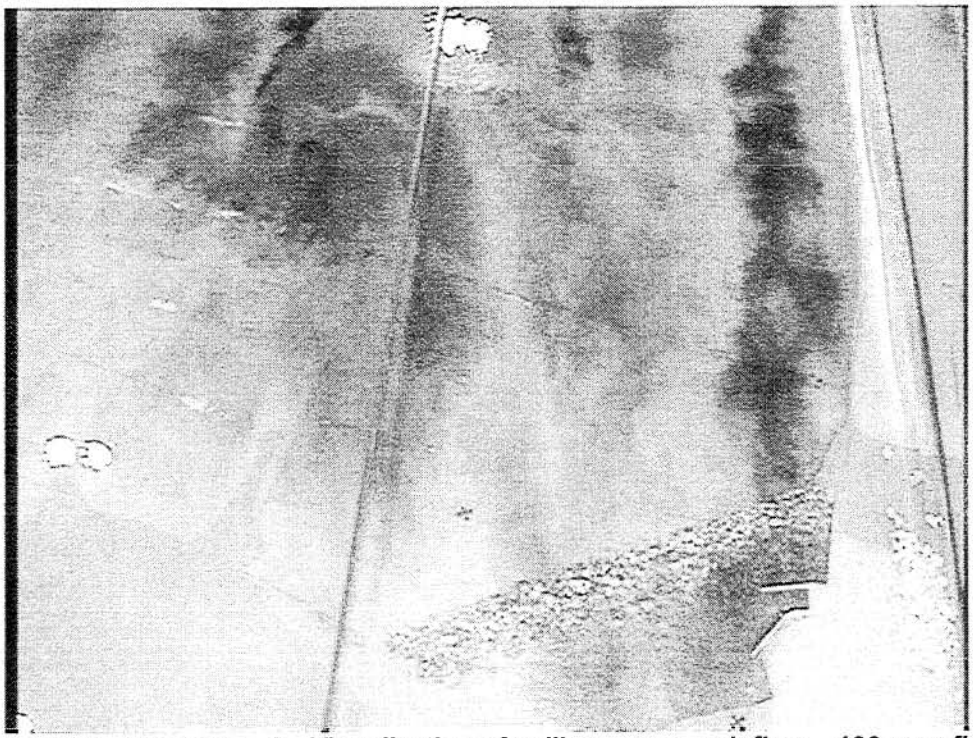

Figure 4.49. Alternative II – Visualization of spillway approach flow – 100 year flood (13500 cfs)

Figure 4.50. Alternative II - Visualization of flow split around Duck Island – 500 year flood (17630 cfs)

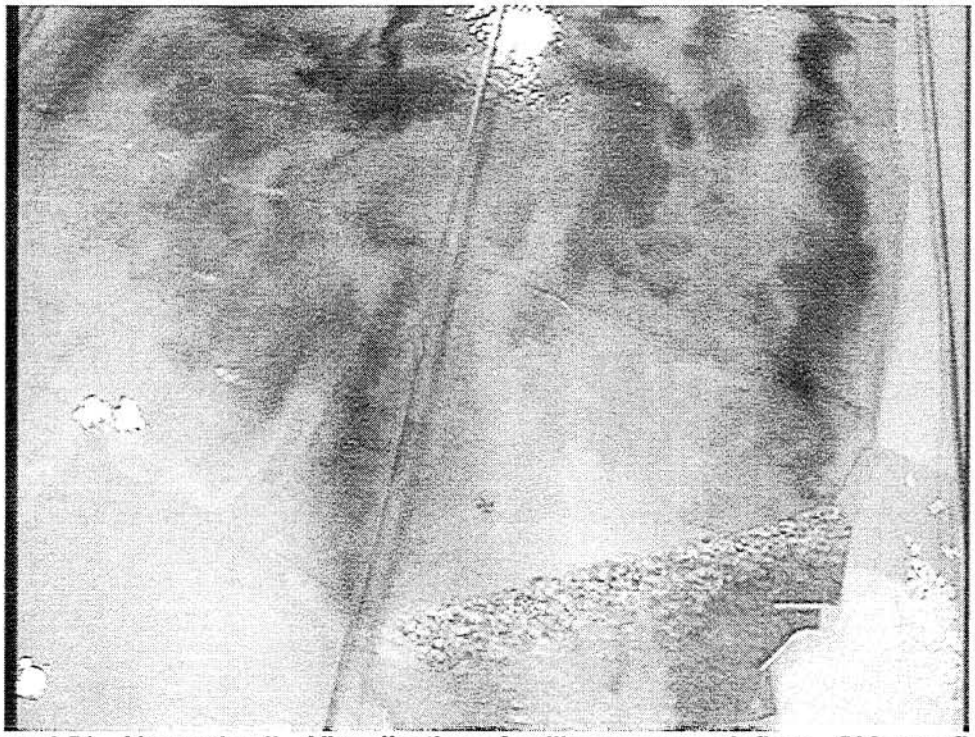

Figure 4.51. Alternative II – Visualization of spillway approach flow – 500 year flood (17630 cfs)

Batavia Dam Model Study

University of Illinois Hydrosystems Laboratory:

Alternative II- Flow Split

Specific Discharge Key

- 10 cfs/ ft

63% - % total flow (cfs)

February 25, 1998

Scale: 1/10" = 1'

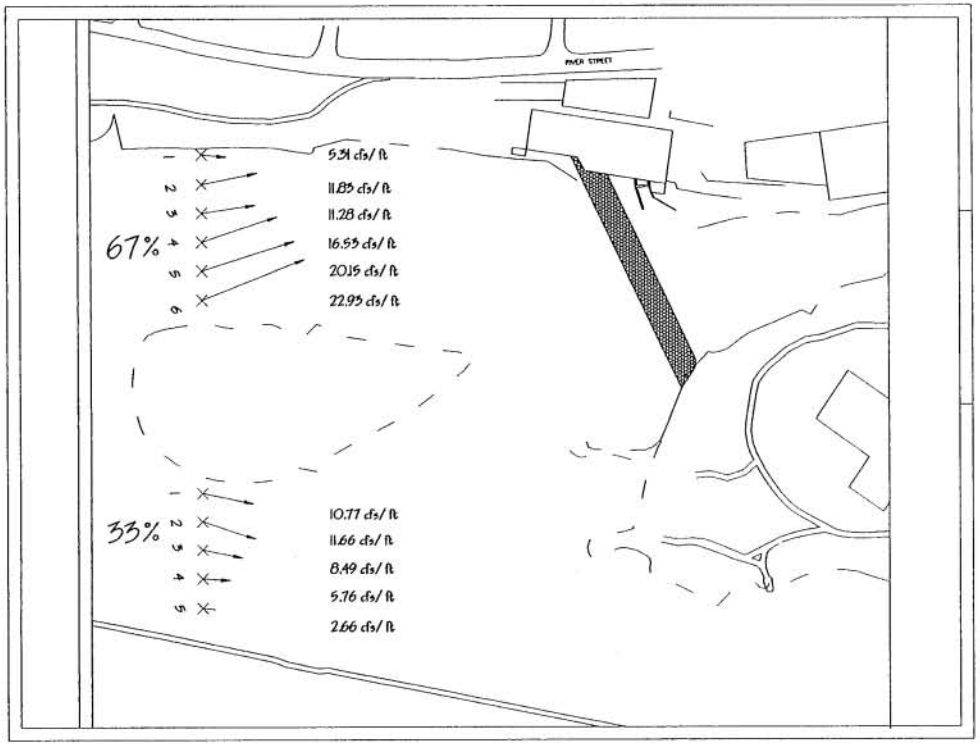

Figure 4.52. Alternative II - Specific discharge flow split around Duck Island - Calibration flow (6062 cfs)

Batavia Dam Model Study

University of Illinois Hydrosystems Laboratory:

Alternative II - Velocity 2 year flood

Velocity Key

→ = 5 ft/s

I.D. = Insufficient depth

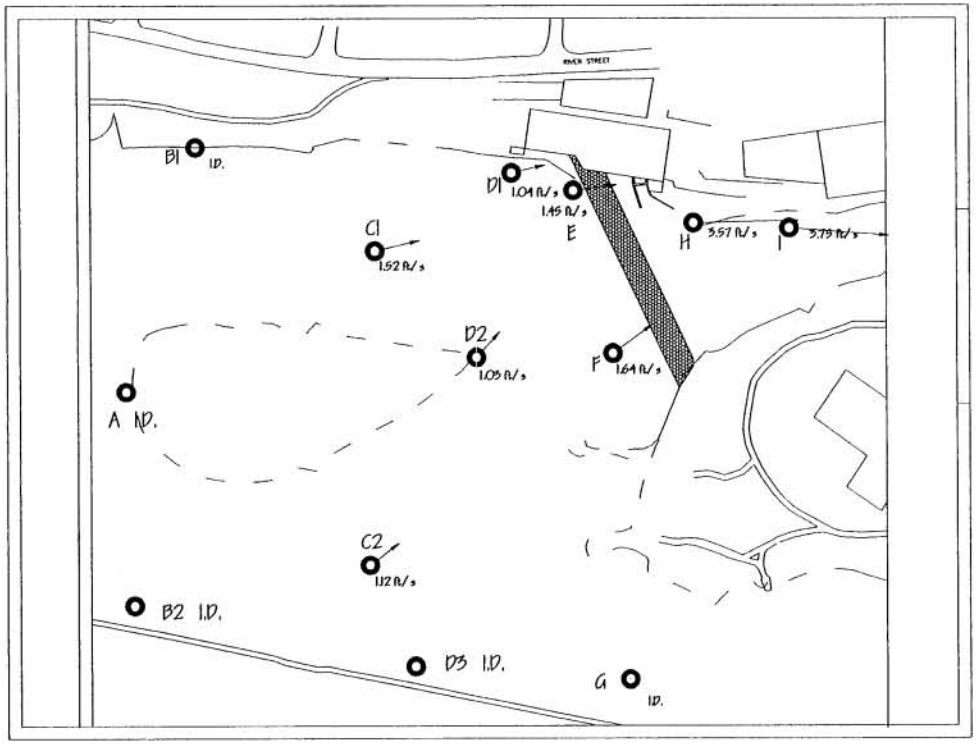

February 20, 1998

Scale: 1/10" = 1'

Figure 4.53. Alternative II - Point velocity measurments - 2 year flood (5700 cfs)

Batavia Dam Model Study

University of Illinois Hydrosystems Laboratory:

Alternative II - Velocity 10 year flood

Velocity Key

→ = 5 ft/s

I.D. = Insufficient depth

February 20, 1998

Scale: 1/10" = 1'

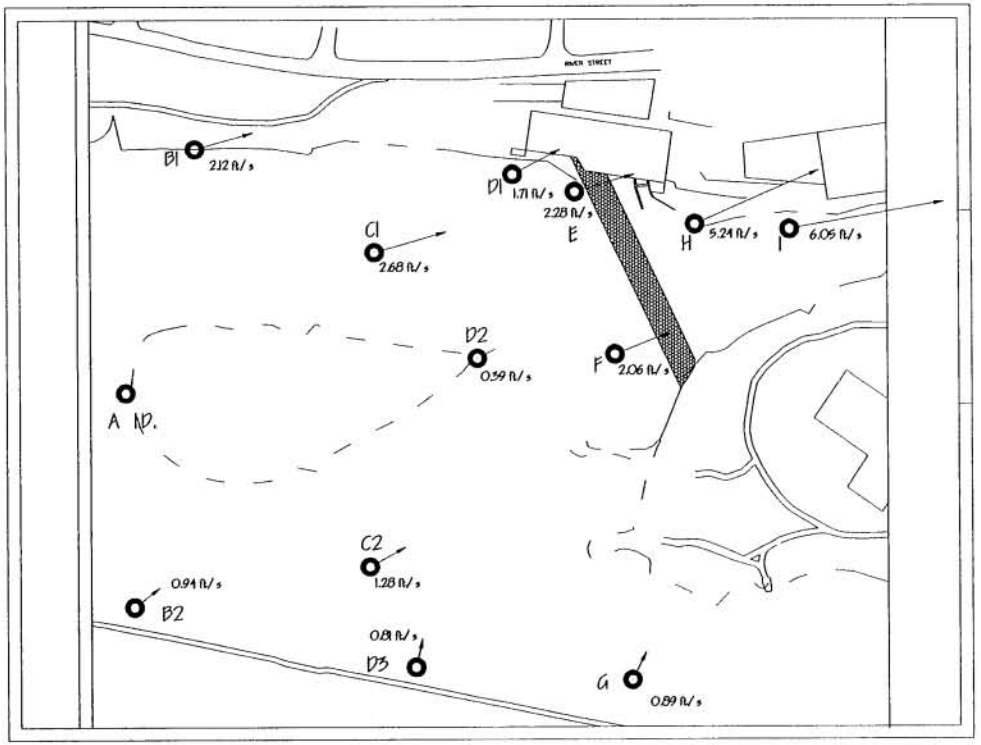

Figure 4.54. Alternative II - Point velocity measurments - 10 year flood (8500 cfs)

Batavia Dam Model Study

University of Illinois Hydrosystems Laboratory:

Alternative II - Velocity 50 year flood

Velocity Key

→ = 5 ft/s

I.D. = Insufficient depth

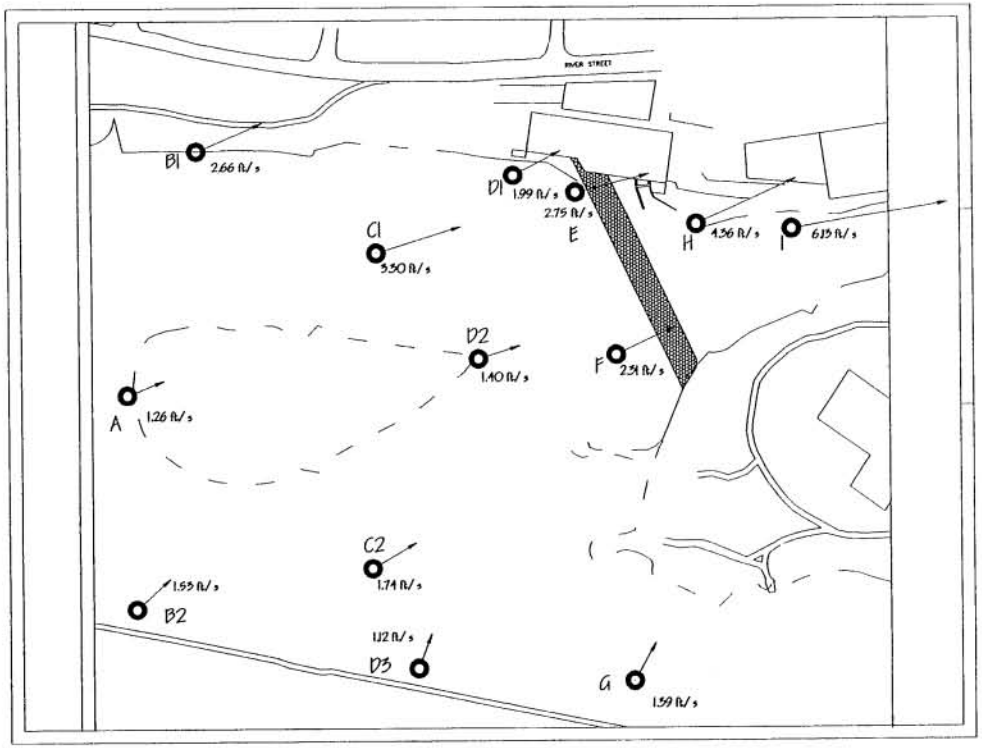

February 20, 1998

Scale: 1/10" = 1'

Figure 4.55. Alternative II - Point velocity measurments - 50 year flood (12500 cfs)

Batavia Dam Model Study

University of Illinois Hydrosystems Laboratory:

Alternative II - Velocity 100 year flood

Velocity Key

→ = 5 ft/s

I.D. = Insufficient depth

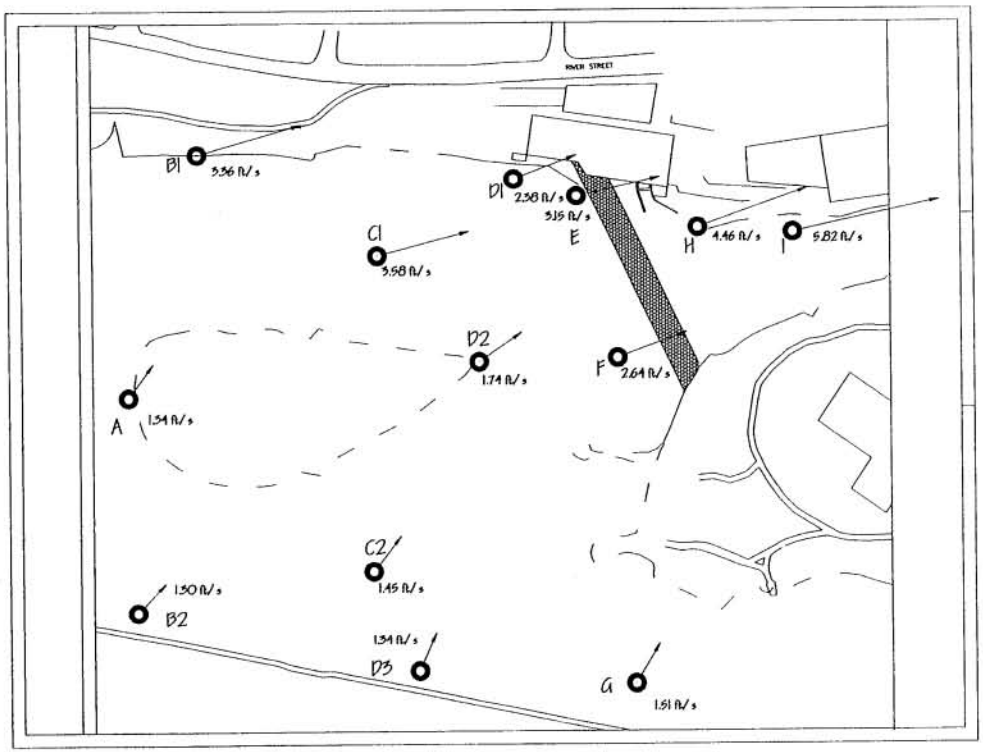

February 20, 1998

Scale: 1/10" = 1'

Figure 4.56. Alternative II - Point velocity measurments - 100 year flood (13500 cfs)

Batavia Dam Model Study

University of Illinois Hydrosystems Laboratory:

Alternative II - Velocity 500 year flood

Velocity Key

=5 ft/s

I.D. = Insufficient depth

February 20, 1998

Scale: 1/10" = 1'

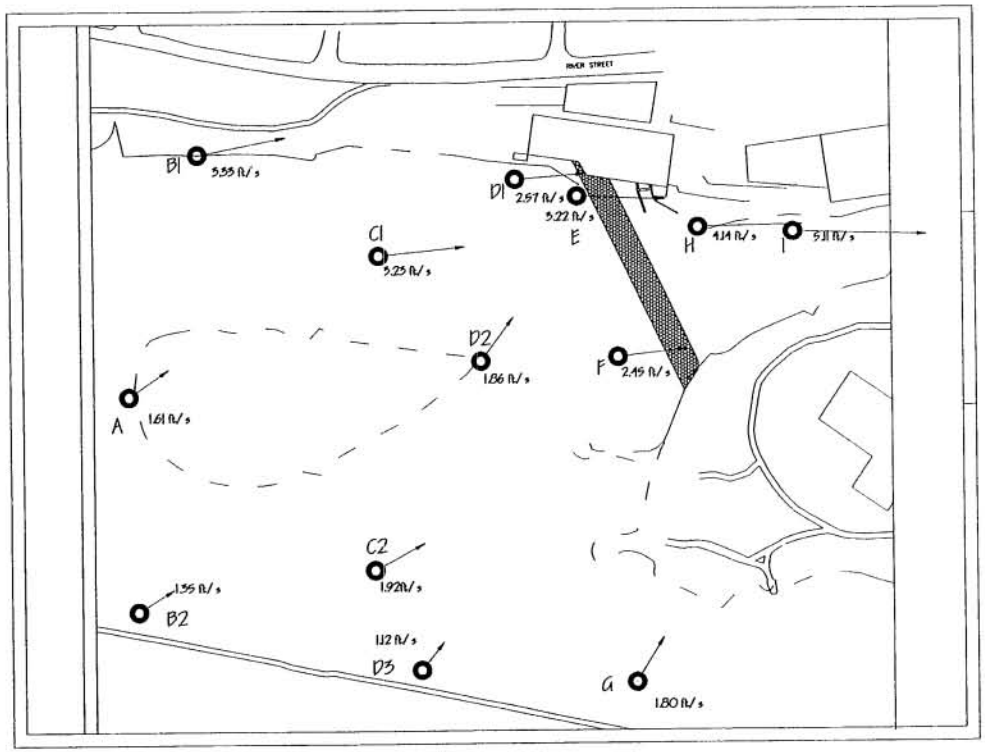

Figure 4.57. Alternative II - Point velocity measurments - 500 year flood (17630 cfs)

Batavia Dam
Model Study

University of Illinois
Hydrosystems
Laboratory:

Alternative II
Downstream discharge
2 year flood

Specific Discharge Key

×← = 20 cfs/ ft

I.D. = Insufficient depth

February 20, 1998

Scale: 1/10" = 1'

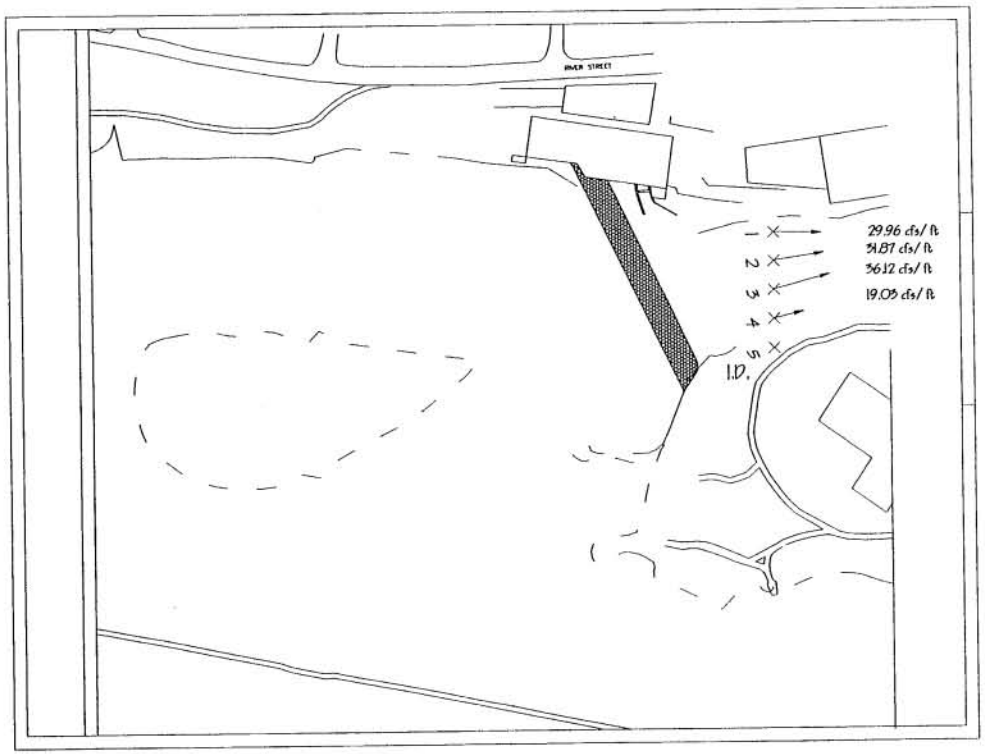

Figure 4.58. Alternative II - Specific discharge conditions downstream of stucture - 2 year flood (5700 cfs)

Batavia Dam
Model Study

University of Illinois
Hydrosystems
Laboratory:

Alternative II
Downstream discharge
10 year flood

Specific Discharge Key

×← = 20 cfs/ ft

I.D. = Insufficient depth

February 20, 1998

Scale: 1/10" = 1'

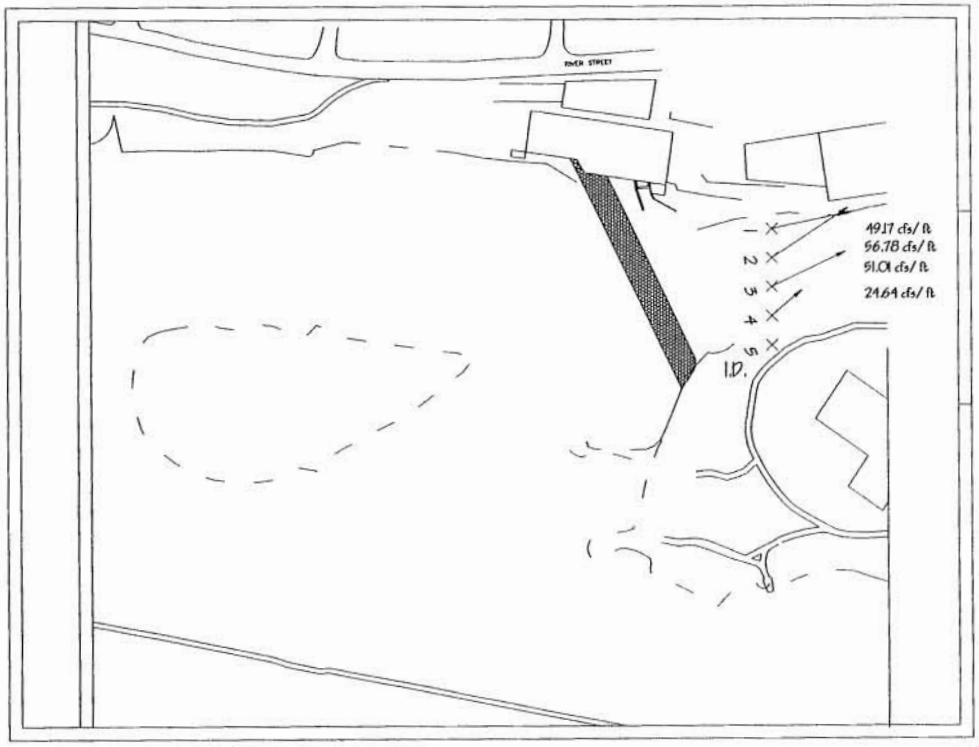

Figure 4.59. Alternative II - Specific discharge conditions downstream of stucture - 10 year flood (8500 cfs)

Batavia Dam Model Study

University of Illinois Hydrosystems Laboratory:

Alternative II
Downstream discharge
50 year flood

Specific Discharge Key

×← = 20 cfs/ ft

I.D. = Insufficient depth

February 20, 1998

Scale: 1/10" = 1'

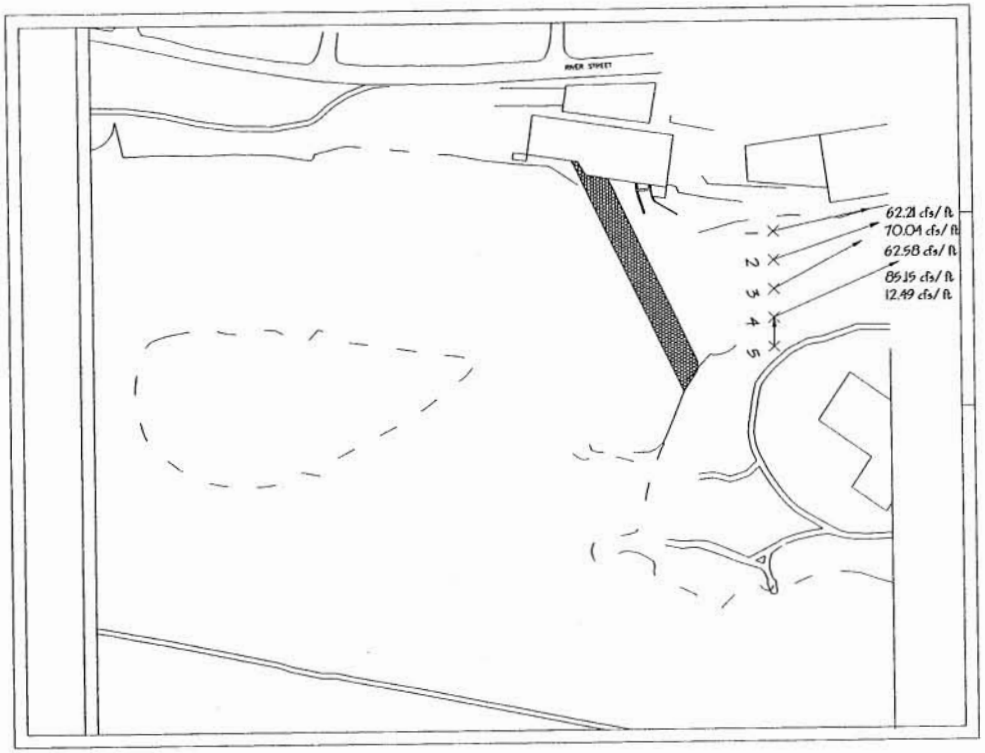

Figure 4.60. Alternative II - Specific discharge conditions downstream of stucture - 50 year flood (12500 cfs)

Batavia Dam Model Study

University of Illinois Hydrosystems Laboratory:

Alternative II
Downstream discharge
100 year flood

Specific Discharge Key

×← = 20 cfs/ ft

I.D. = Insufficient depth

February 20, 1998

Scale: 1/10" = 1'

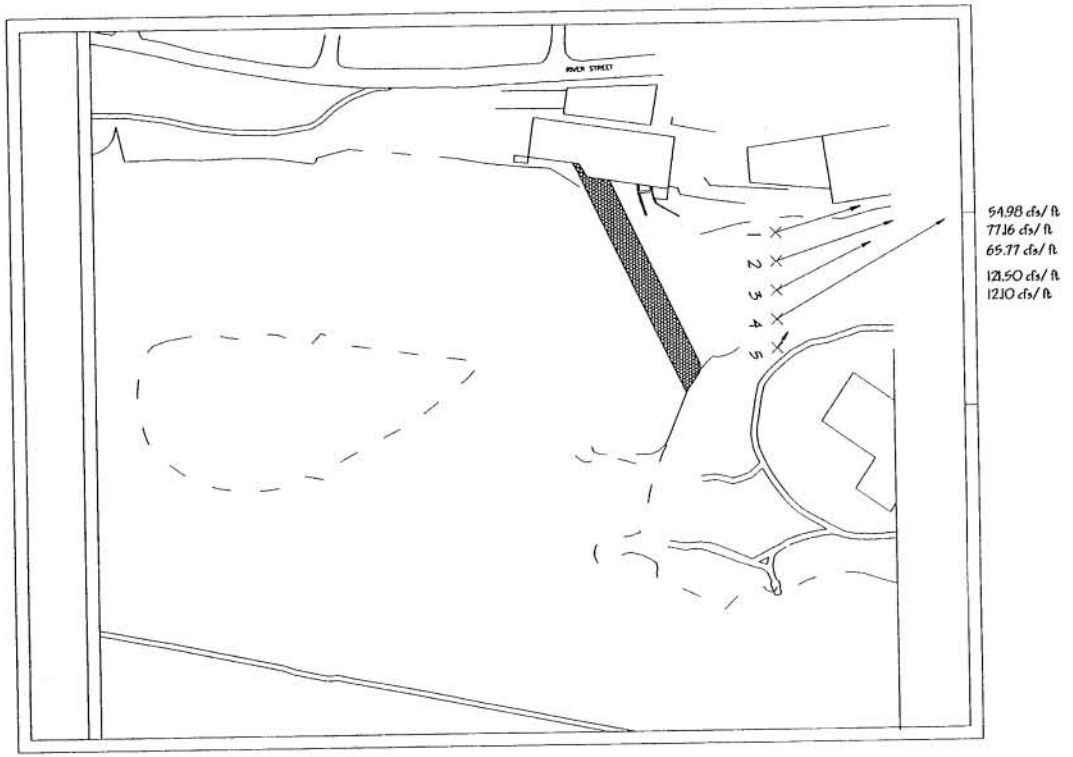

Figure 4.61. Alternative II - Specific discharge conditions downstream of stucture - 100 year flood (135000 cfs)

Batavia Dam Model Study

University of Illinois Hydrosystems Laboratory:

Alternative II
Downstream discharge
500 year flood

Specific Discharge Key

×⟵ = 20 cfs/ ft

I.D. = Insufficient depth

February 20, 1998

Scale: 1/10" = 1'

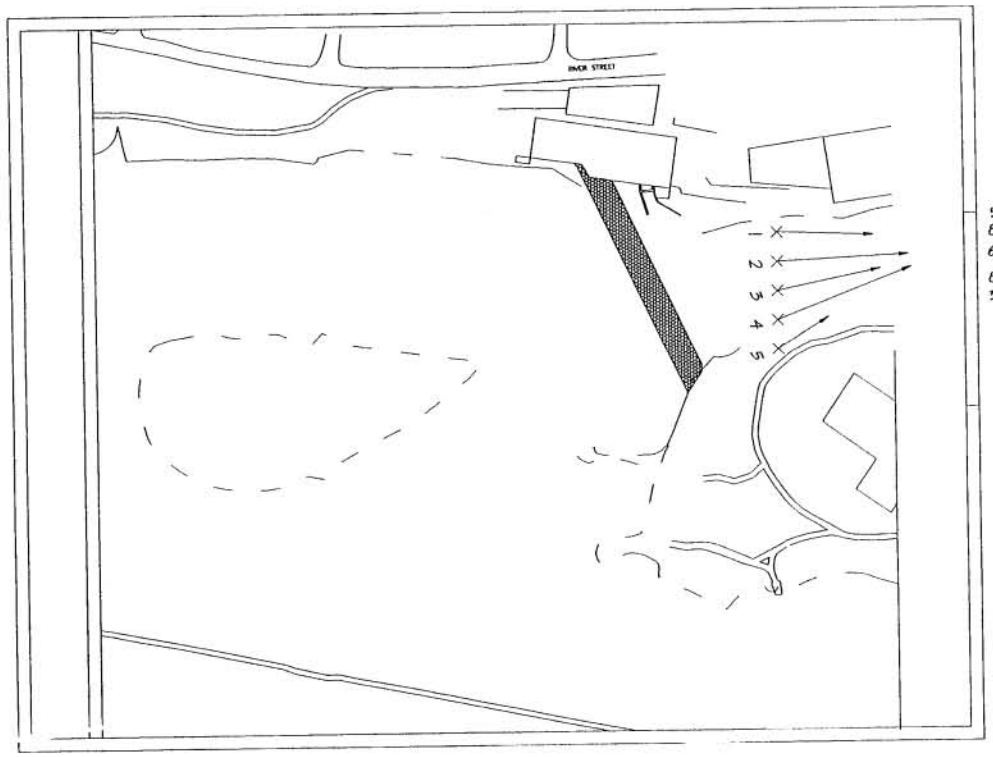

Figure 4.62. Alternative II - Specific discharge conditions downstream of stucture - 500 year flood (17630 cfs)

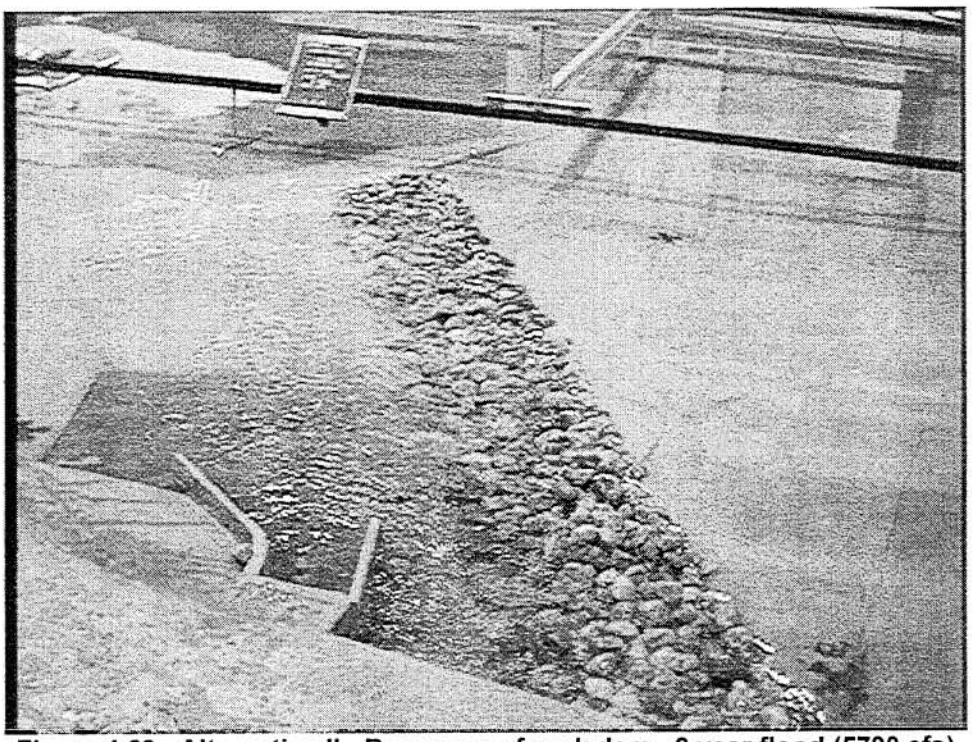

Figure 4.63. Alternative II - Response of rock dam - 2 year flood (5700 cfs)

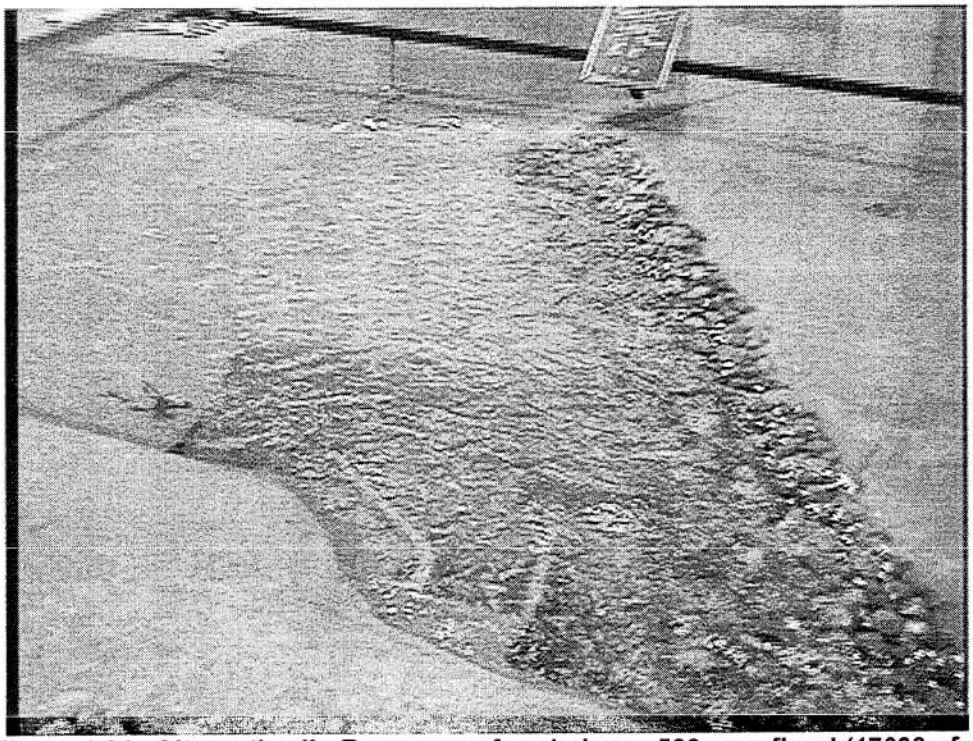

Figure 4.64. Alternative II - Response of rock dam – 500 year flood (17630 cfs)

Batavia Dam
Model Study

University of Illinois
Hydrosystems
Laboratory:

Alternative III
2-Sided Spillway
Plan View

Notes:

N

February 25, 1998

Scale:
Model: 1/10" = 1'
Site: 1/10" = 30'

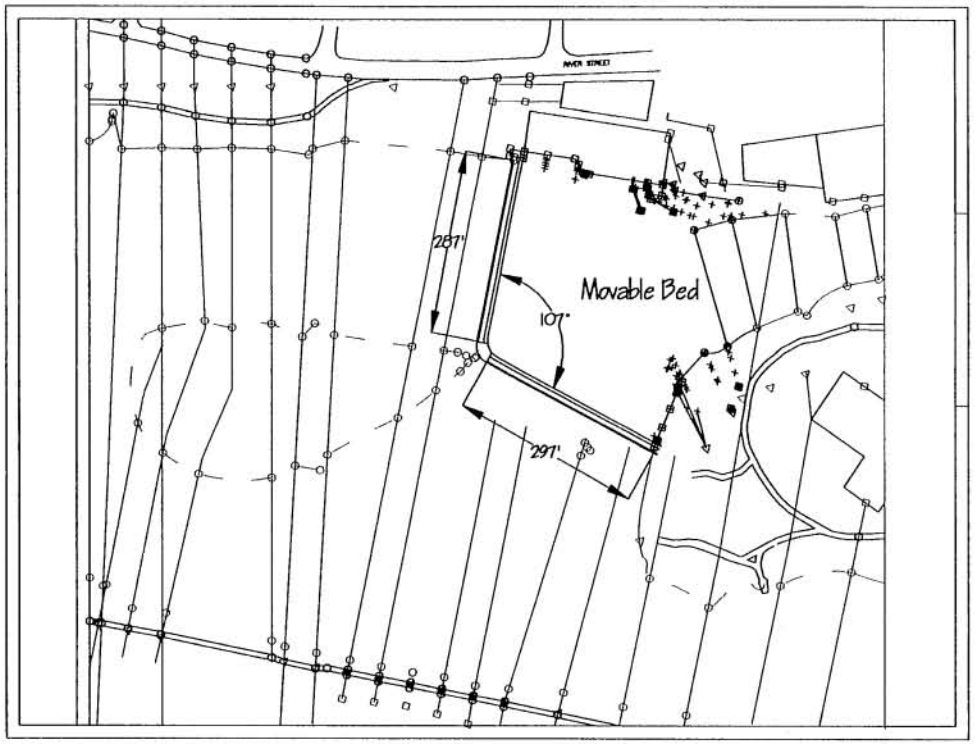

Figure 4.65. Schematic representation of 2-sided spillway - Plan view

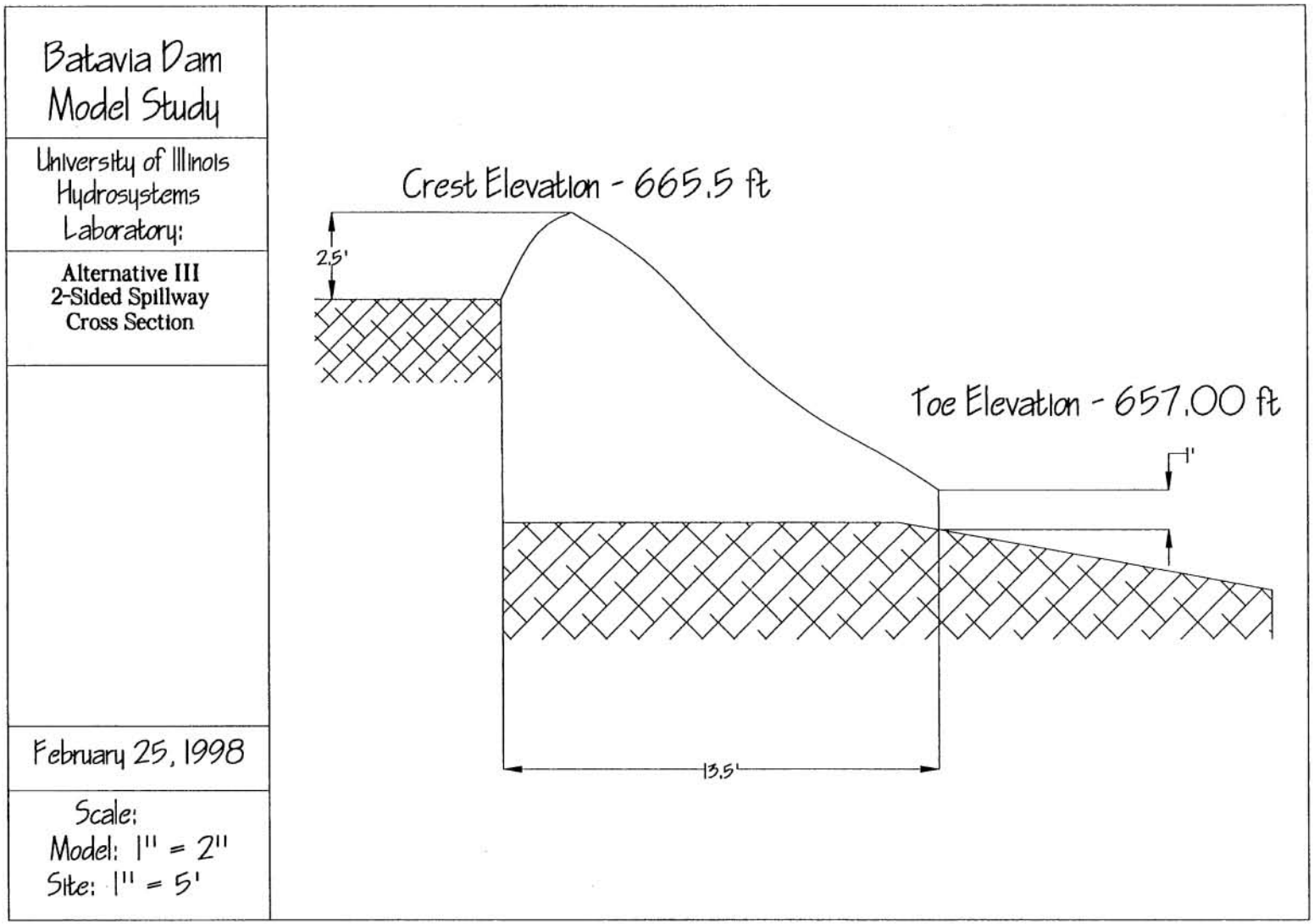

Figure 4.66. Schematic representation of 2-sided spillway - Cross section

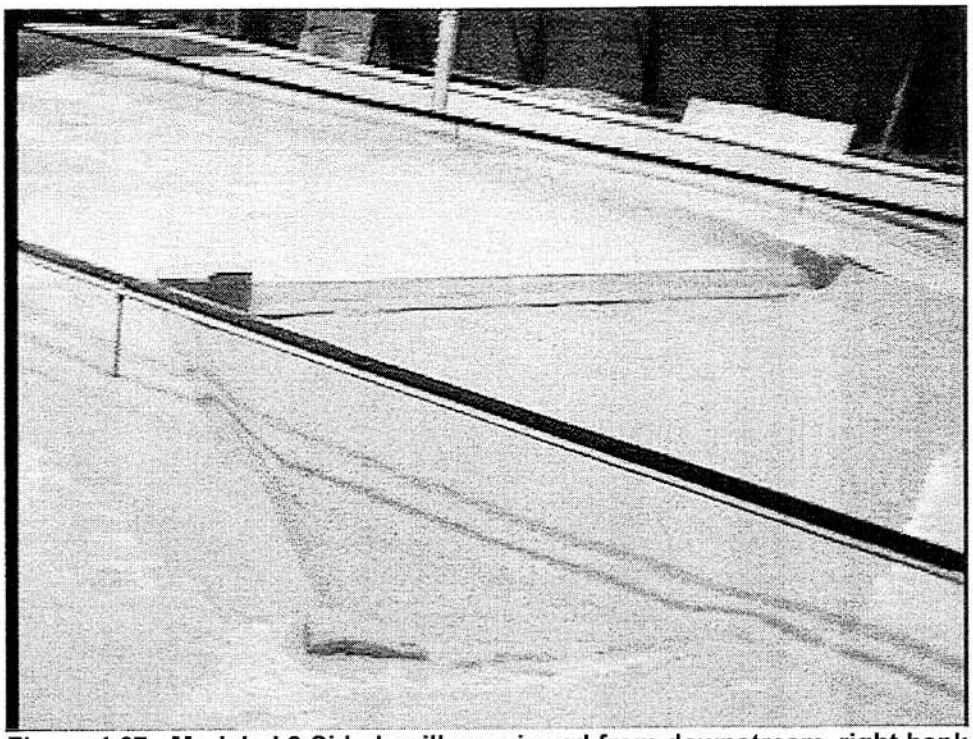

Figure 4.67. Modeled 2-Sided spillway viewed from downstream, right bank

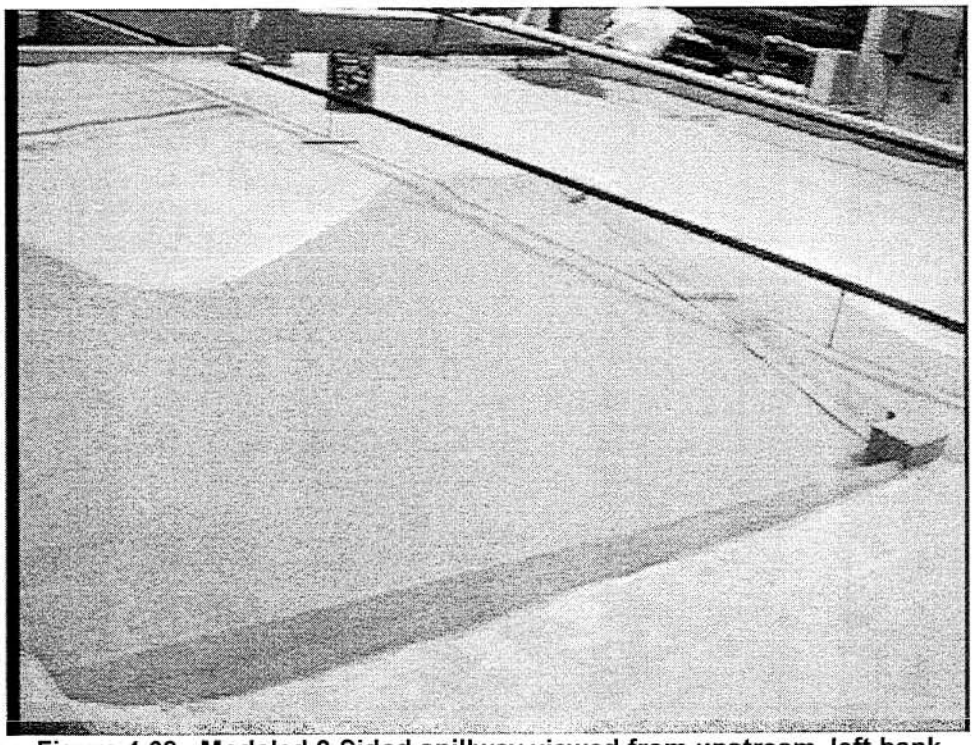

Figure 4.68. Modeled 2-Sided spillway viewed from upstream, left bank

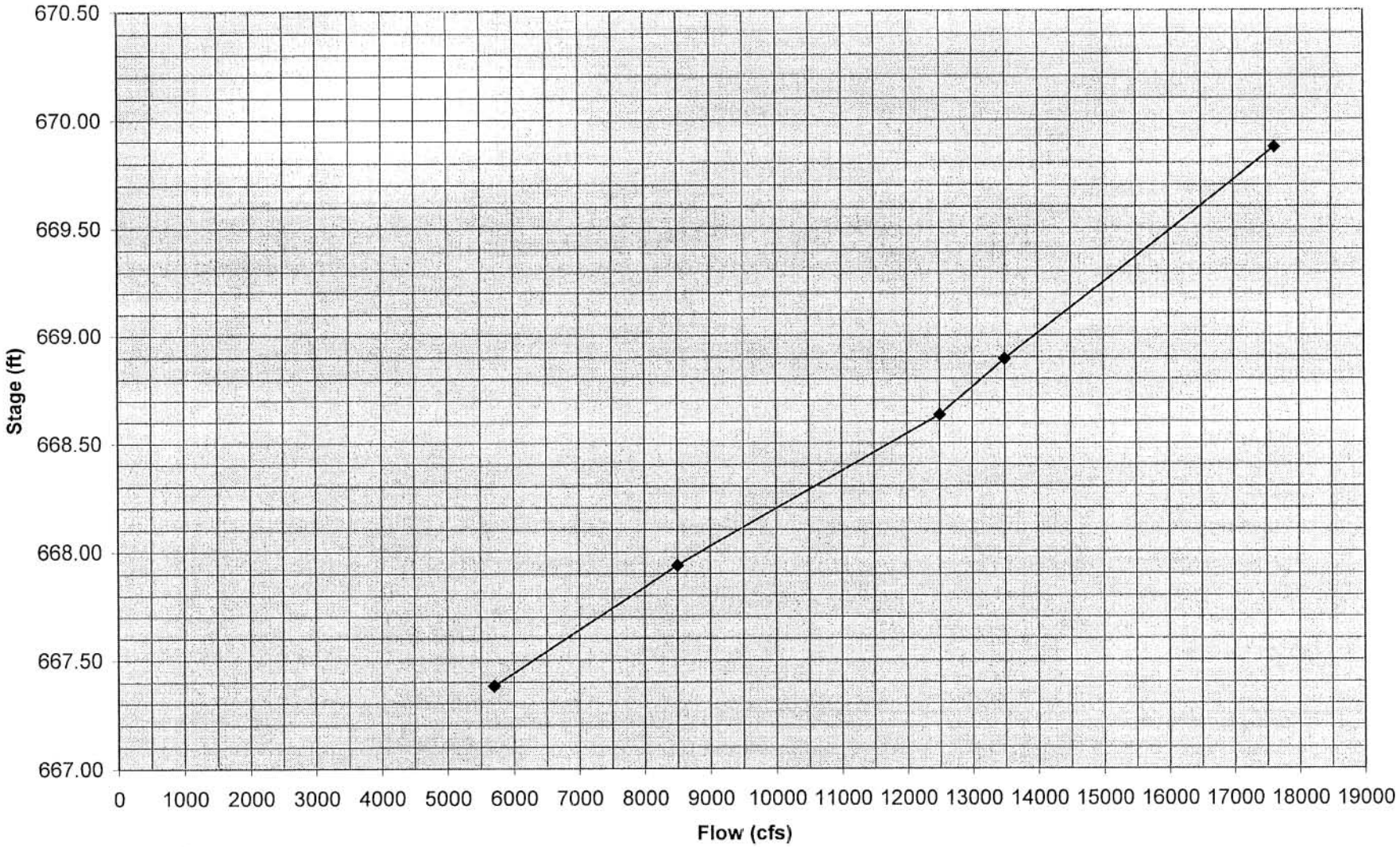

Figure 4.69. Averaged upstream pool stage response - Alternative III

Figure 4.70. Alternative III - Visualization of flow split around Duck Island – 2 year flood (5700 cfs)

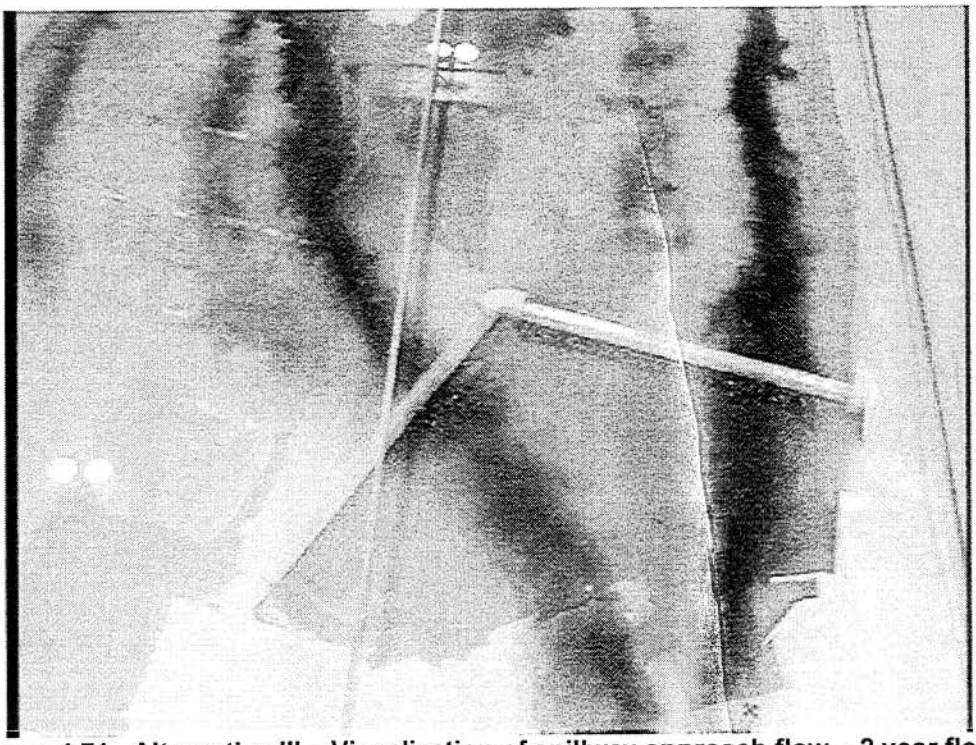

Figure 4.71. Alternative III – Visualization of spillway approach flow – 2 year flood (5700 cfs)

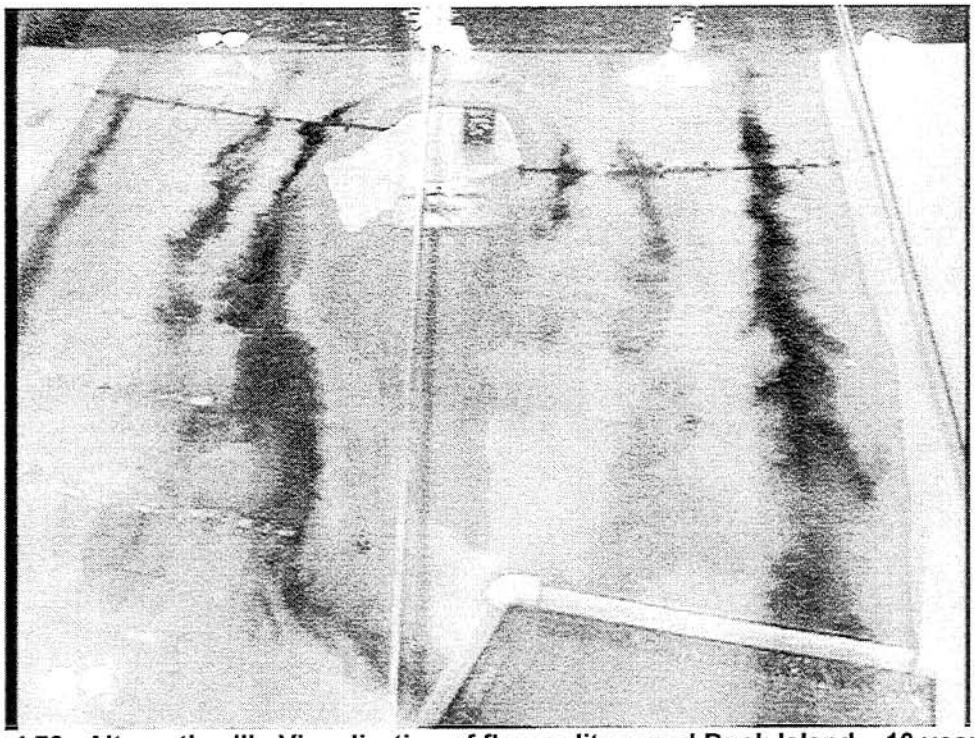

Figure 4.72. Alternative III - Visualization of flow split around Duck Island – 10 year flood (8500 cfs)

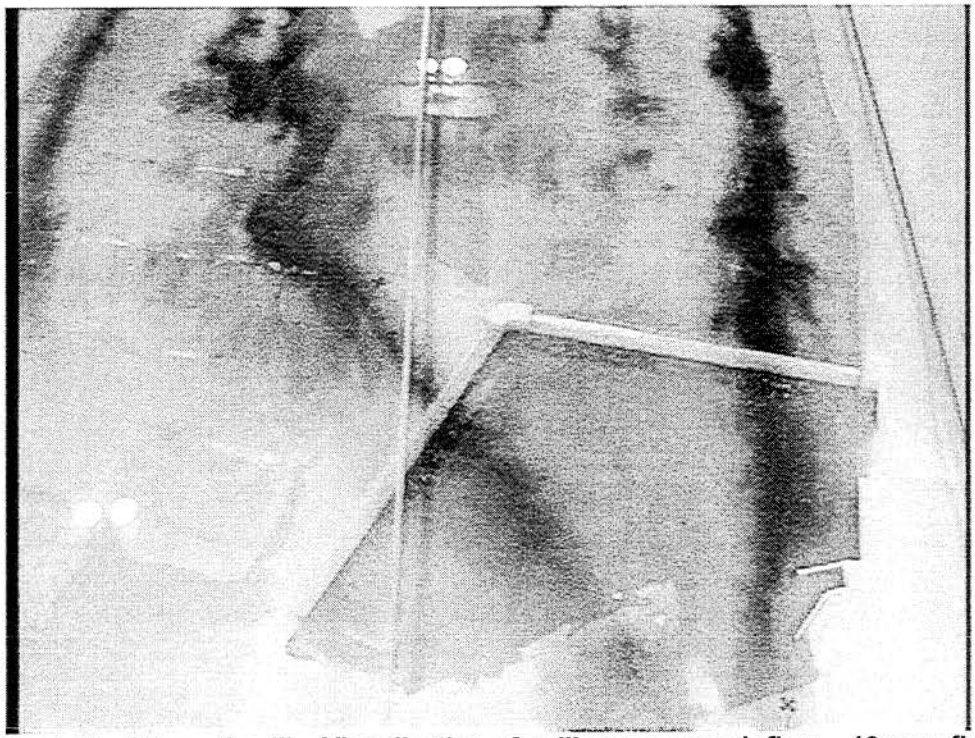

Figure 4.73. Alternative III – Visualization of spillway approach flow – 10 year flood (8500 cfs)

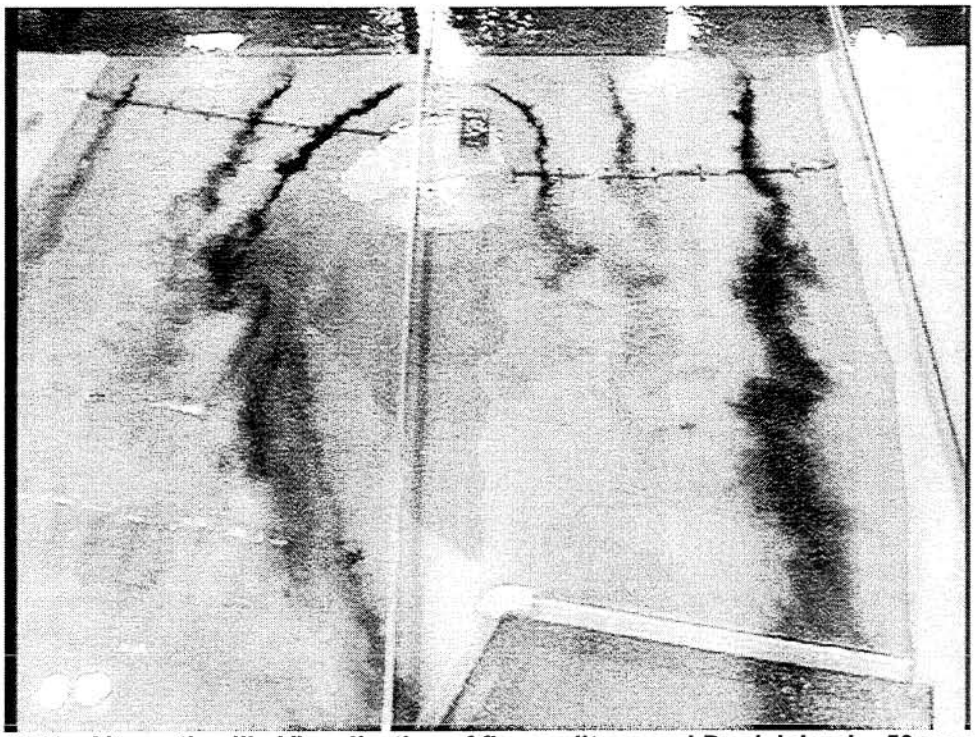

Figure 4.74. Alternative III - Visualization of flow split around Duck Island – 50 year flood (12500 cfs)

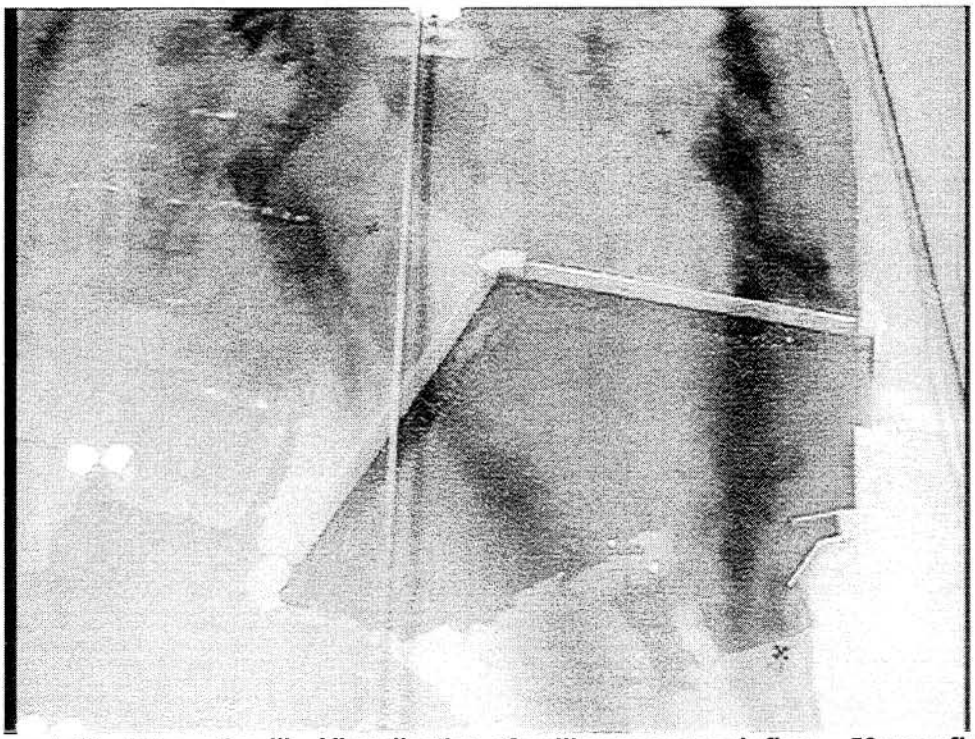

Figure 4.75. Alternative III – Visualization of spillway approach flow – 50 year flood (12500 cfs)

Figure 4.76. Alternative III - Visualization of flow split around Duck Island – 100 year flood (13500 cfs)

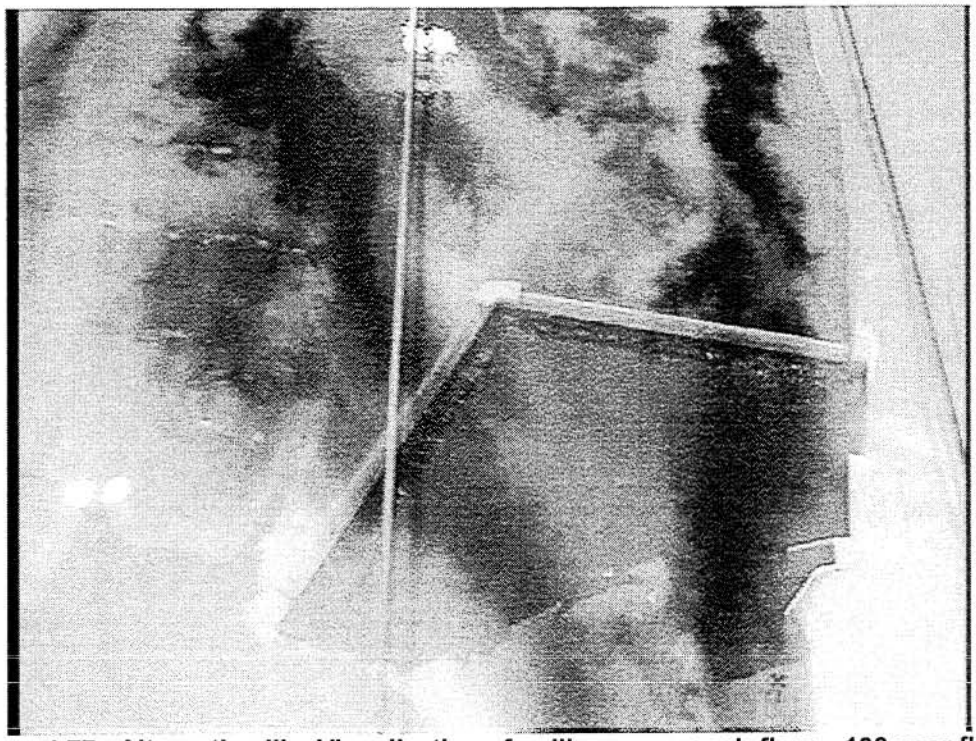

Figure 4.77. Alternative III – Visualization of spillway approach flow – 100 year flood (13500 cfs)

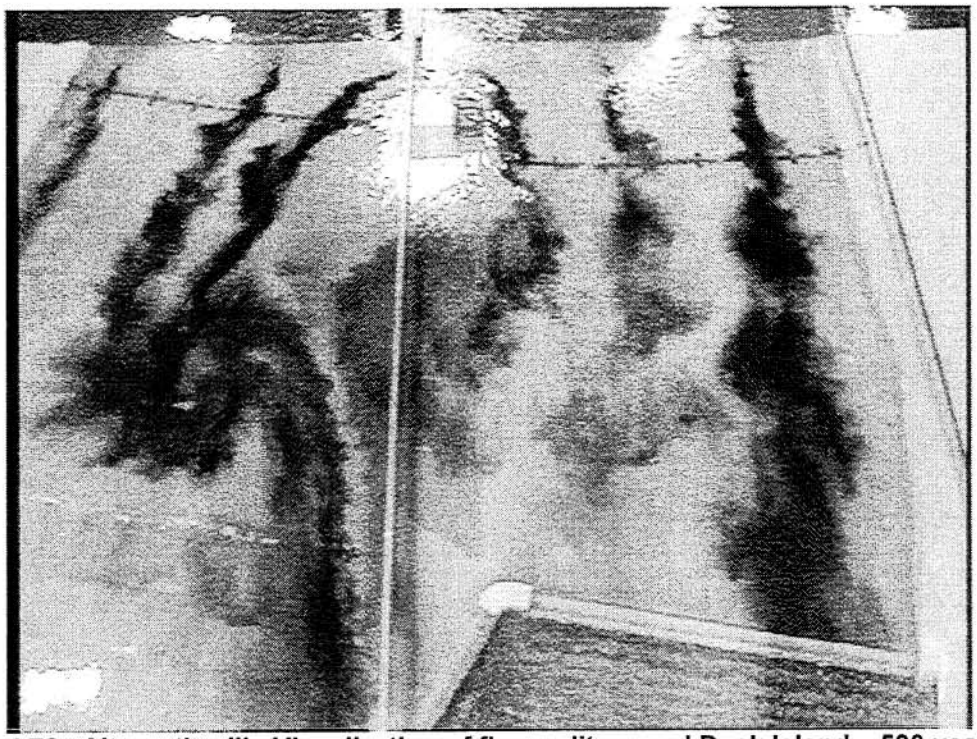

Figure 4.78. Alternative III - Visualization of flow split around Duck Island – 500 year flood (17630 cfs)

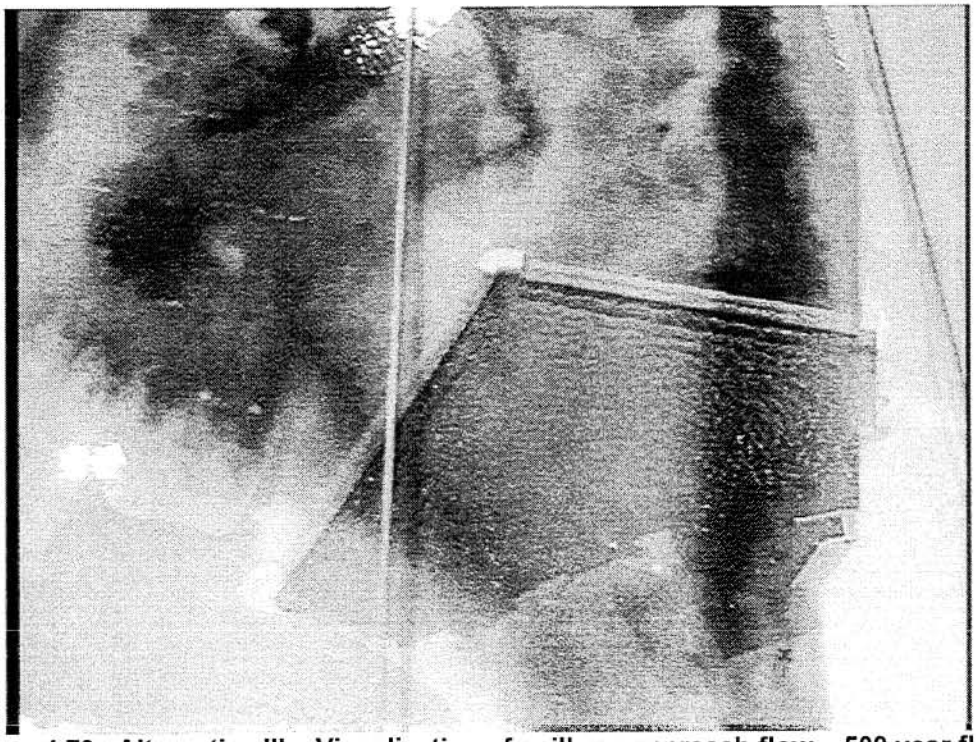

Figure 4.79. Alternative III – Visualization of spillway approach flow – 500 year flood (17630 cfs)

Batavia Dam Model Study

University of Illinois Hydrosystems Laboratory:

Alternative III- Flow Split

Specific Discharge Key

→ = 10 cfs/ ft

63% = % total flow (cfs)

March 10, 1998

Scale: 1/10" = 1'

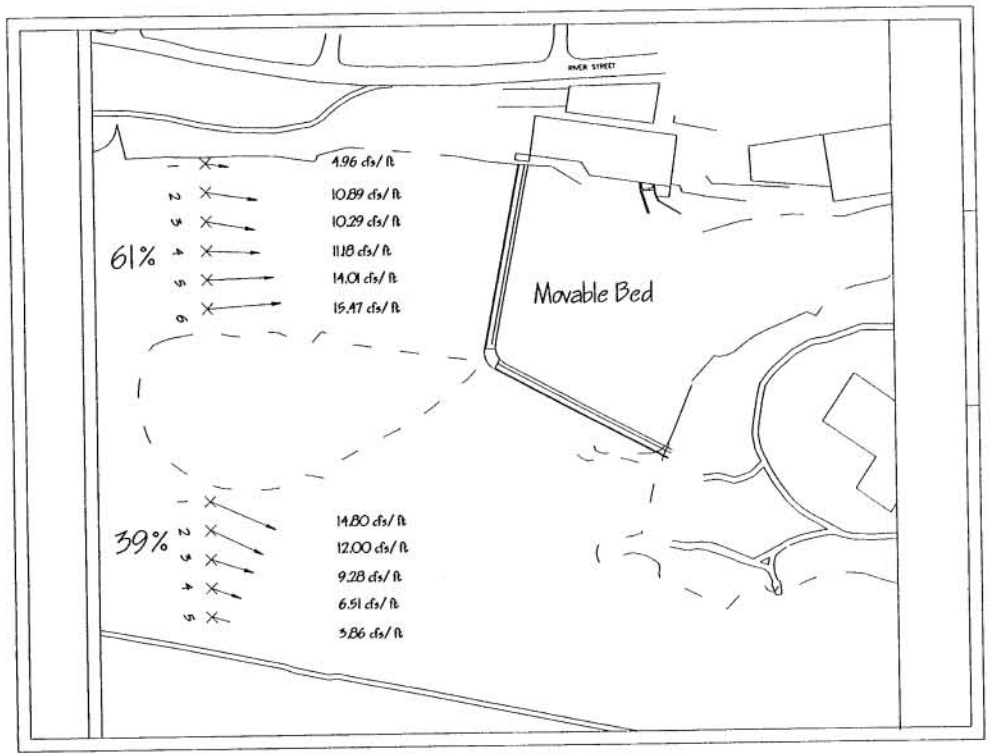

Figure 4.80. Alternative III - Specific discharge flow split around Duck Island - Calibration flow (6062 cfs)

Batavia Dam Model Study

University of Illinois Hydrosystems Laboratory:

Alternative III - Velocity 2 year flood

Velocity Key

→ = 5 ft/s

I.D. = Insufficient depth

March 10, 1998

Scale: 1/10" = 1'

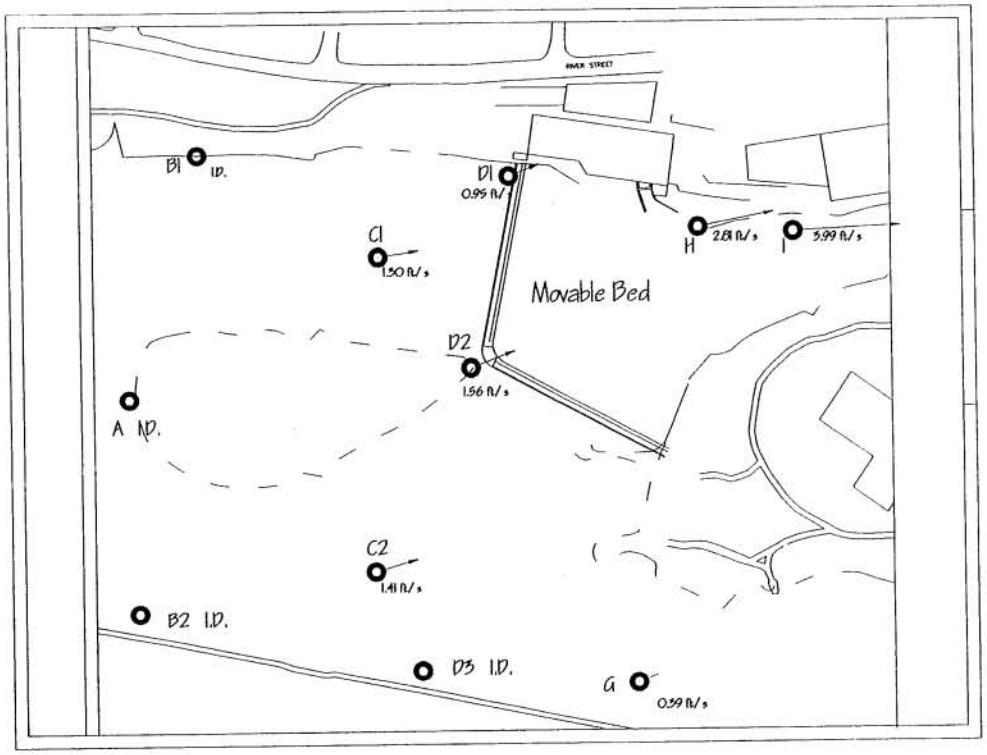

Figure 4.81. Alternative III - Point velocity measurments - 2 year flood (5700 cfs)

Batavia Dam Model Study

University of Illinois Hydrosystems Laboratory:

Alternative III - Velocity 10 year flood

Velocity Key

=5 ft/s

I.D. = Insufficient depth

March 10, 1998

Scale: 1/10" = 1'

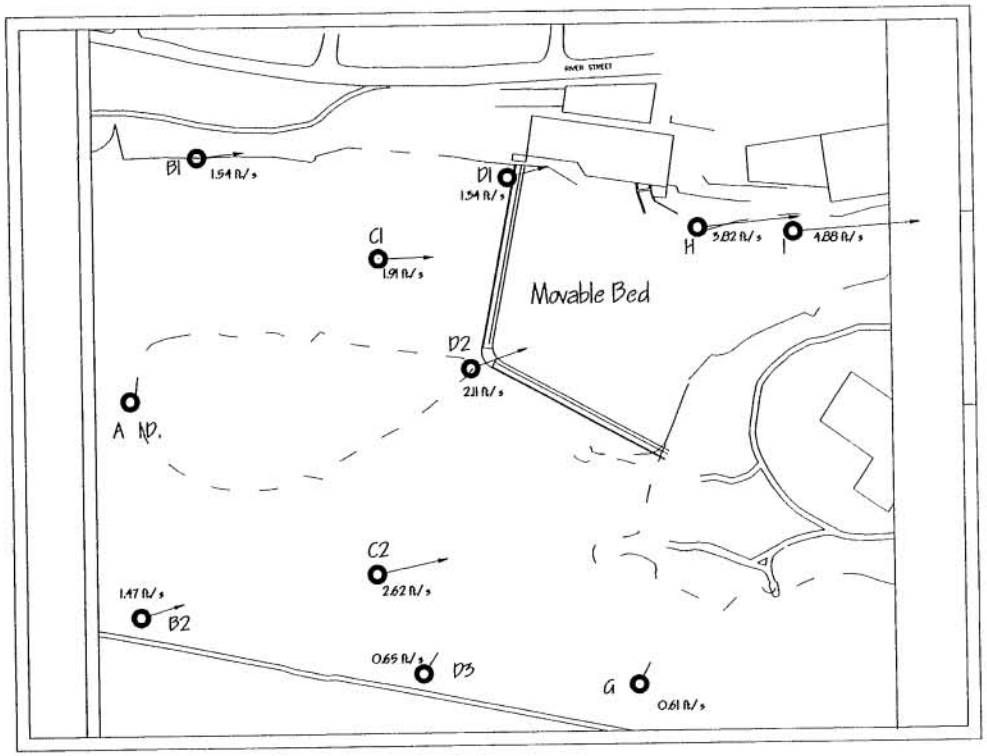

Figure 4.82. Alternative III - Point velocity measurments - 10 year flood (8500 cfs)

Batavia Dam Model Study

University of Illinois Hydrosystems Laboratory:

Alternative III - Velocity
50 year flood

Velocity Key

=5 ft/s

I.D. = Insufficient depth

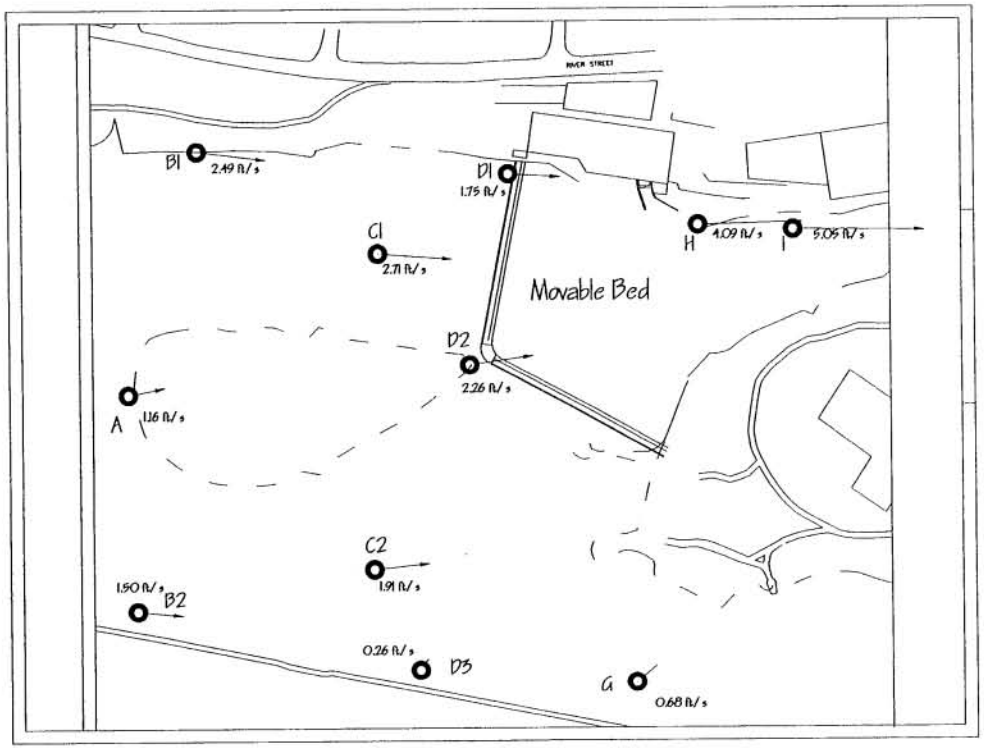

March 10, 1998

Scale: 1/10" = 1'

Figure 4.83. Alternative III - Point velocity measurments - 50 year flood (12500 cfs)

Batavia Dam Model Study

University of Illinois Hydrosystems Laboratory:

Alternative III - Velocity
100 year flood

Velocity Key

=5 ft/s

I.D. = Insufficient depth

March 10, 1998

Scale: 1/10" = 1'

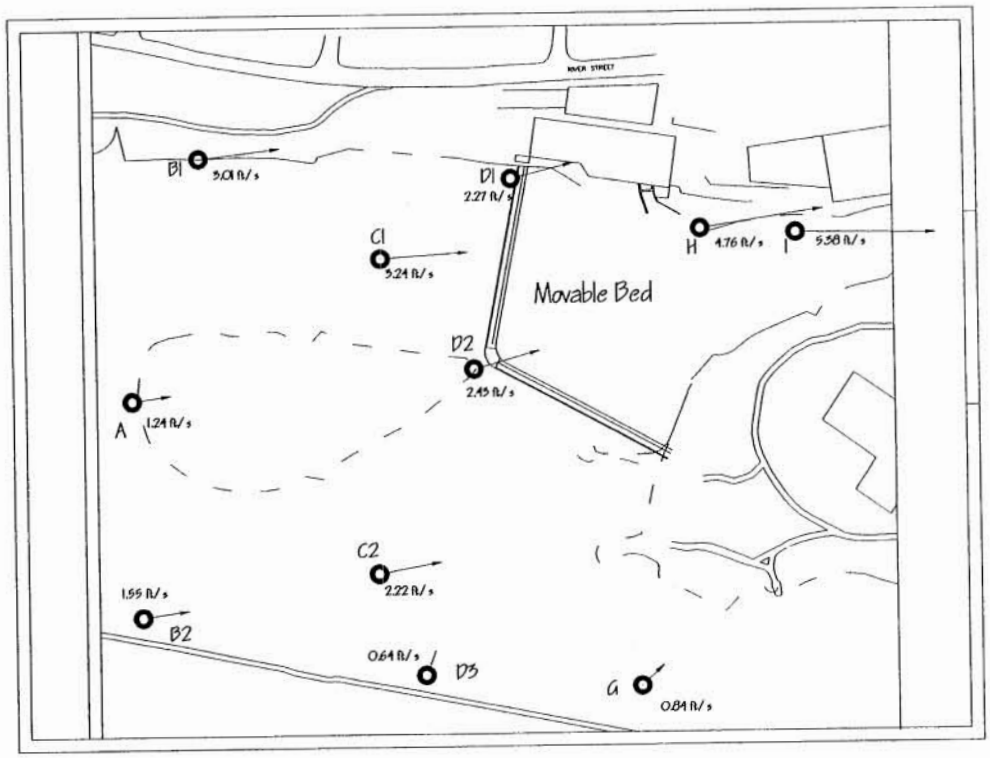

Figure 4.84. Alternative III - Point velocity measurments - 100 year flood (135000 cfs)

Batavia Dam Model Study

University of Illinois Hydrosystems Laboratory:

Alternative III - Velocity 500 year flood

Velocity Key

=5 ft/s

I.D. = Insufficient depth

March 10, 1998

Scale: 1/10" = 1'

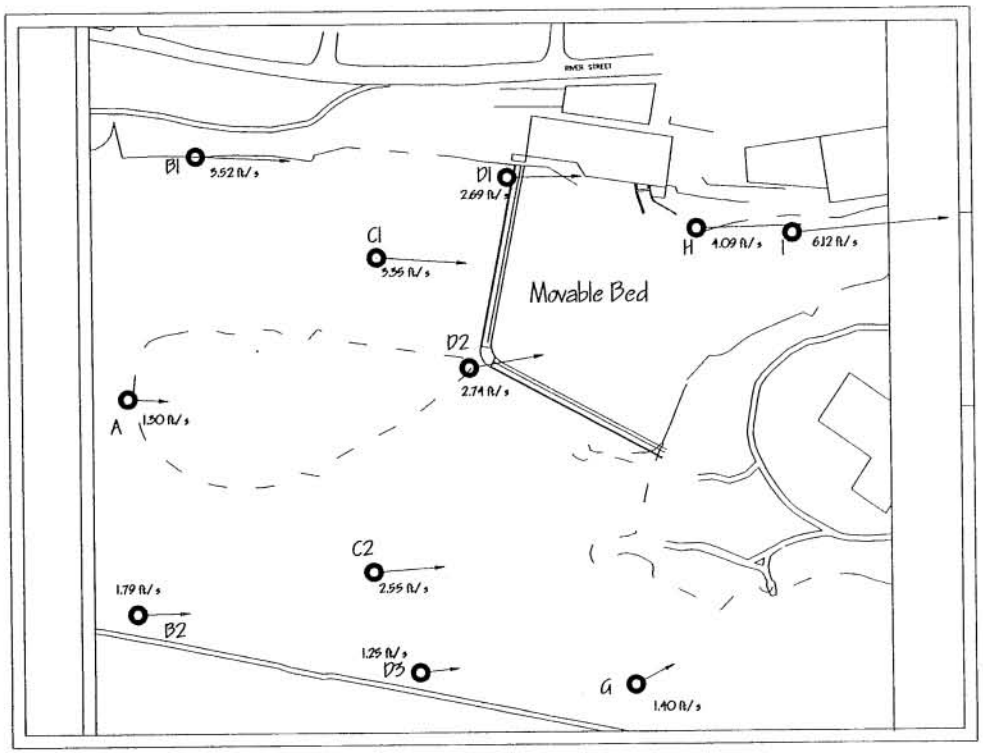

Figure 4.85. Alternative III - Point velocity measurments - 500 year flood (17630 cfs)

Batavia Dam Model Study

University of Illinois Hydrosystems Laboratory:

Alternative III
Downstream discharge
2 year flood

Specific Discharge Key

×← = 20 cfs/ ft

I.D. = Insufficient depth

March 10, 1998

Scale: 1/10" = 1'

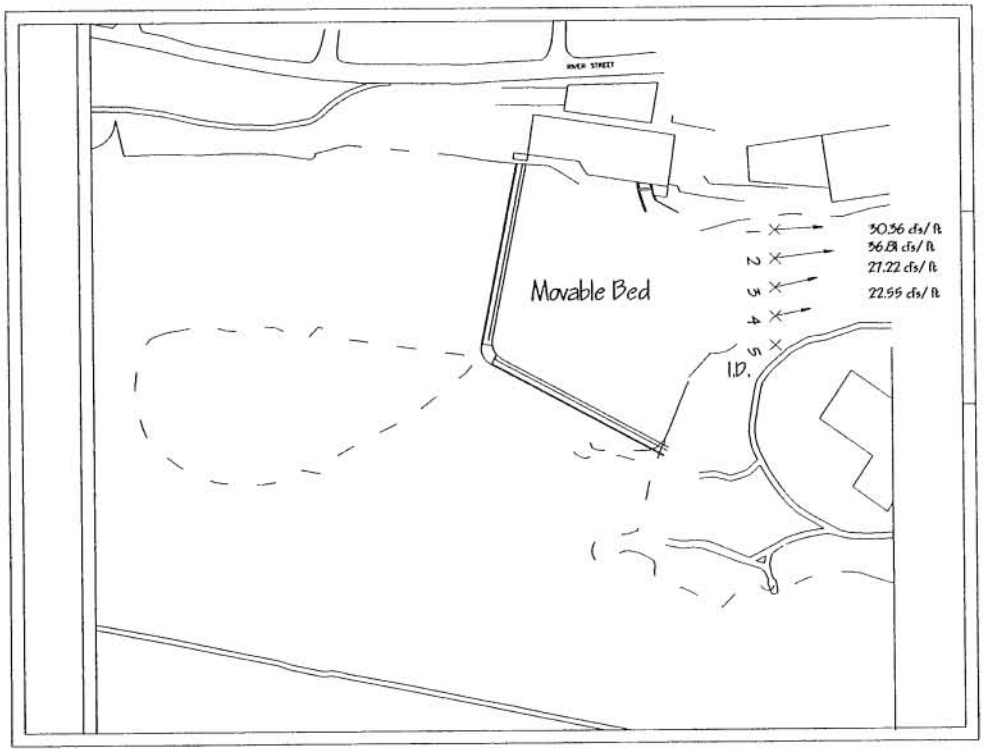

Figure 4.86. Alternative III - Specific discharge conditions downstream of stucture - 2 year flood (5700 cfs)

Batavia Dam Model Study

University of Illinois Hydrosystems Laboratory:

Alternative III
Downstream discharge
10 year flood

Specific Discharge Key

×← = 20 cfs/ ft

I.D. = Insufficient depth

March 10, 1998

Scale: 1/10" = 1'

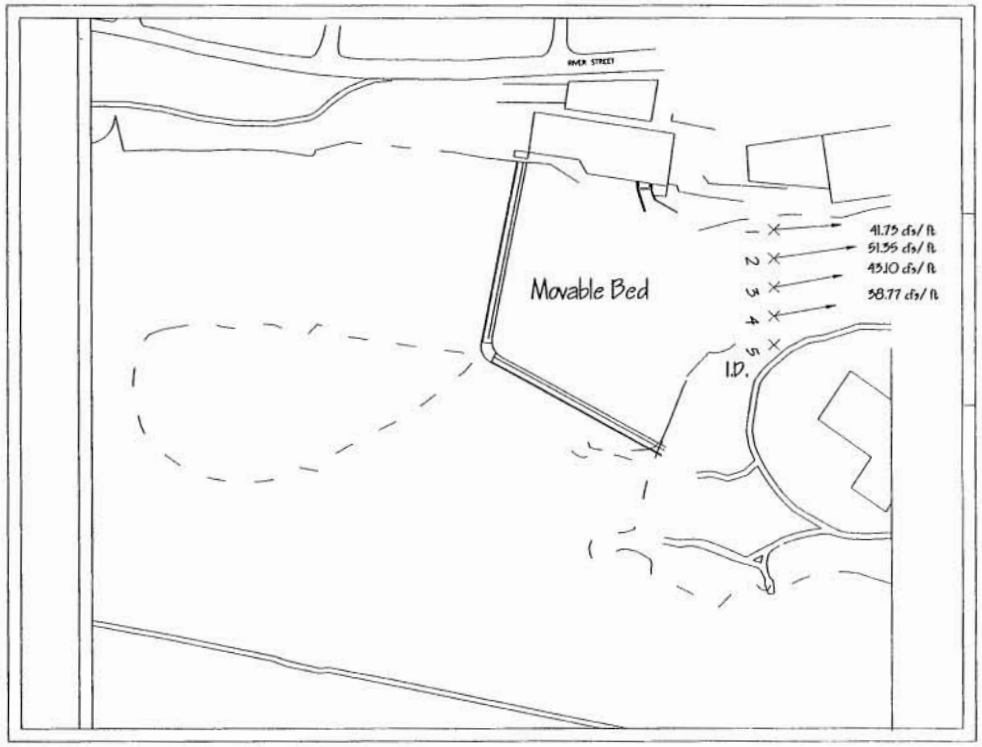

Figure 4.87. Alternative III - Specific discharge conditions downstream of stucture - 10 year flood (8500 cfs)

Batavia Dam Model Study

University of Illinois Hydrosystems Laboratory:

Alternative III
Downstream discharge
50 year flood

Specific Discharge Key

×← = 20 cfs/ ft

I.D. = Insufficient depth

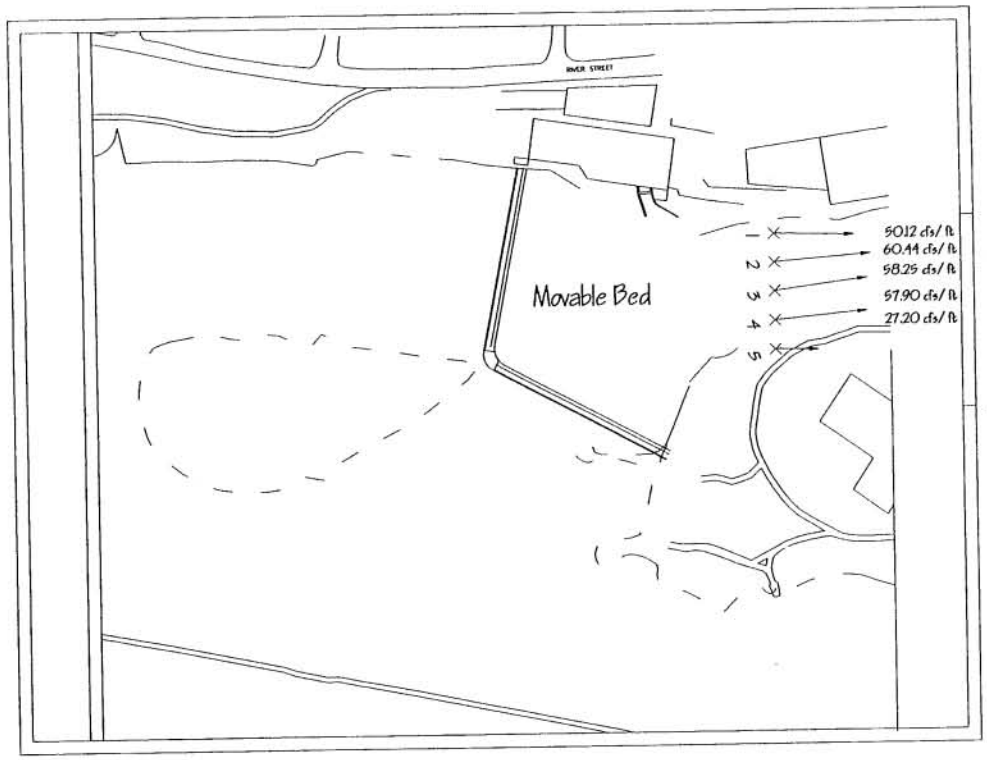

March 10, 1998

Scale: 1/ 10" = 1'

Figure 4.88. Alternative III - Specific discharge conditions downstream of stucture - 50 year flood (12500 cfs)

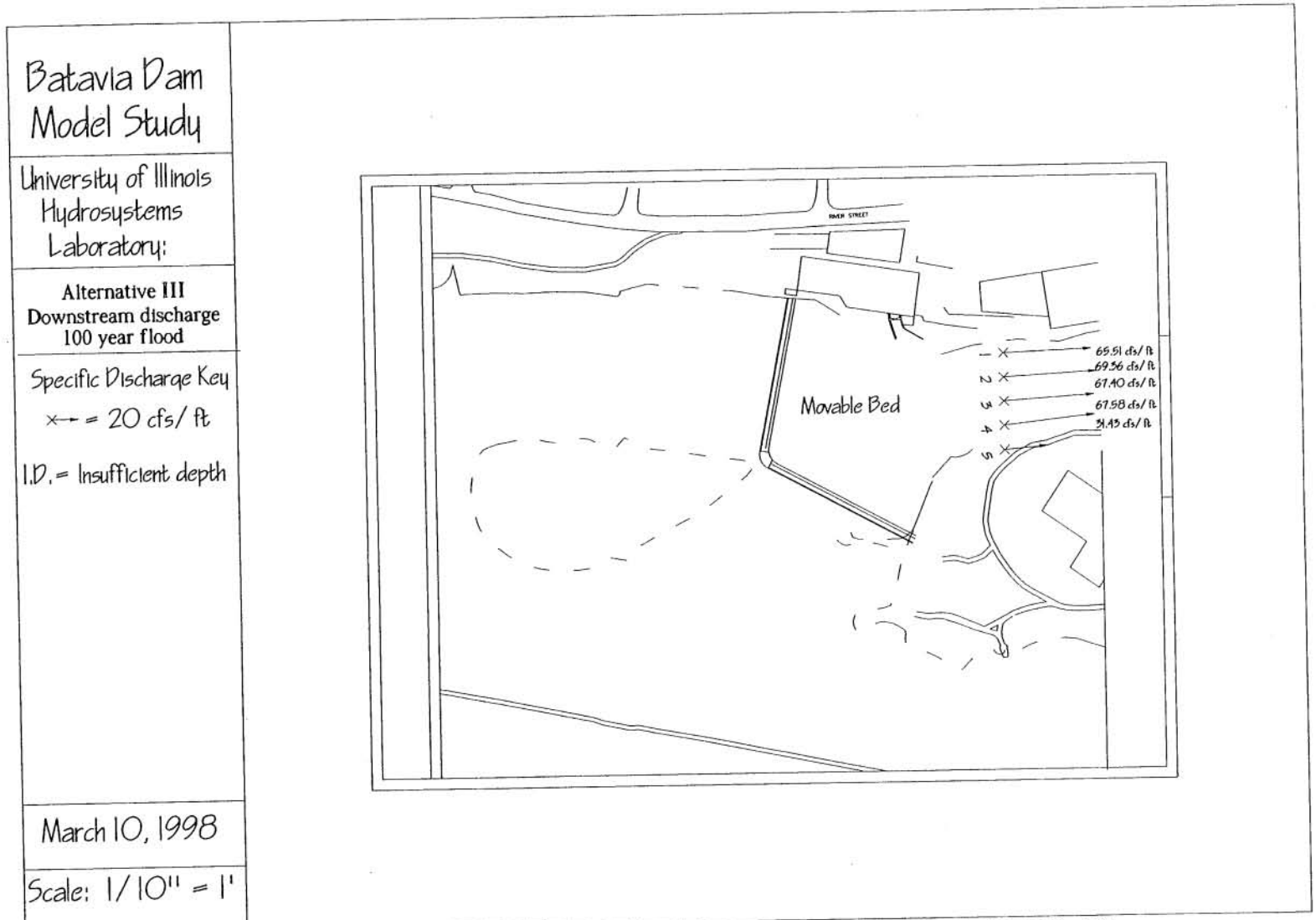

Figure 4.89. Alternative III - Specific discharge conditions downstream of stucture - 100 year flood (135000 cfs)

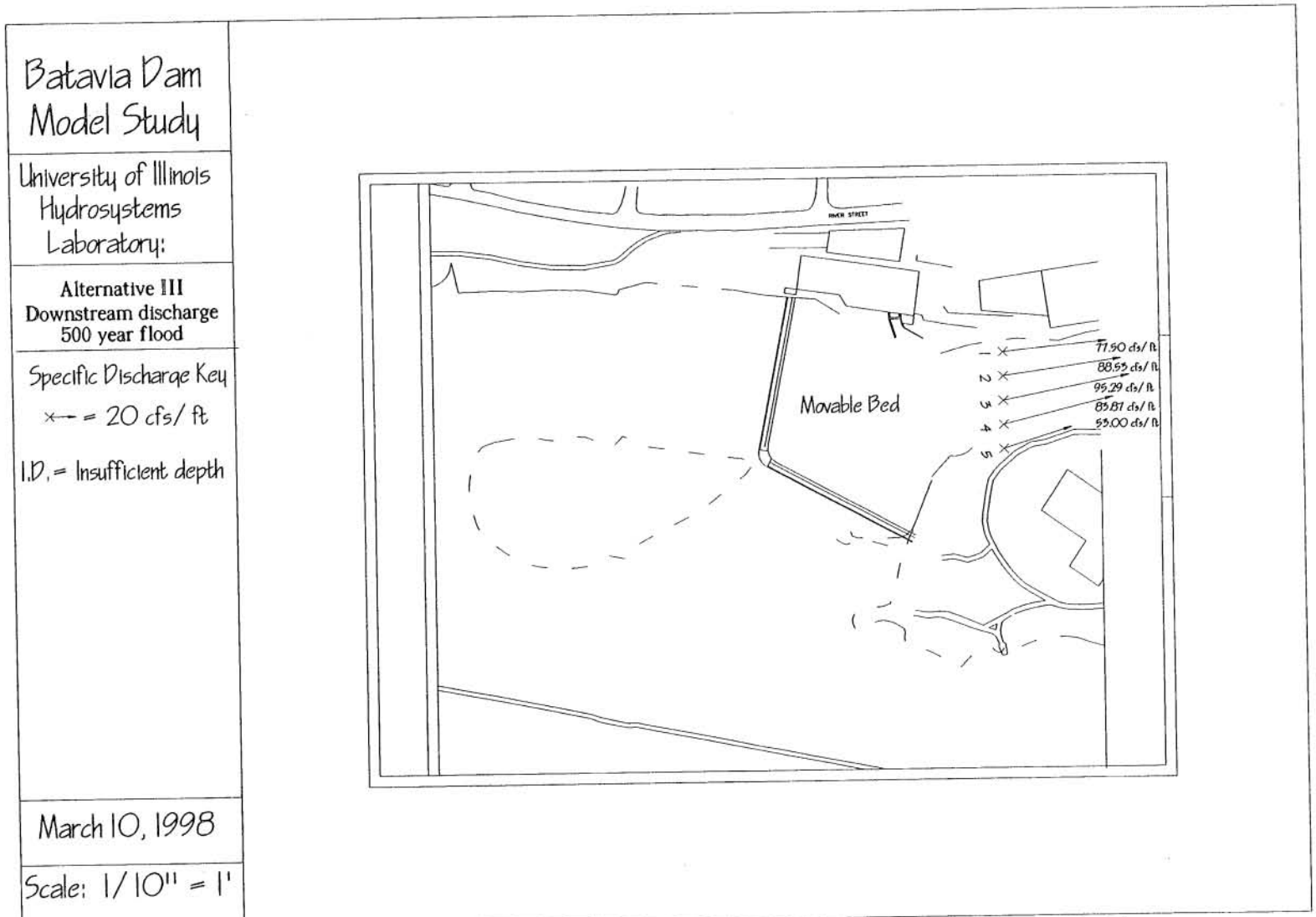

Figure 4.90. Alternative III - Specific discharge conditions downstream of stucture - 500 year flood (17630 cfs)

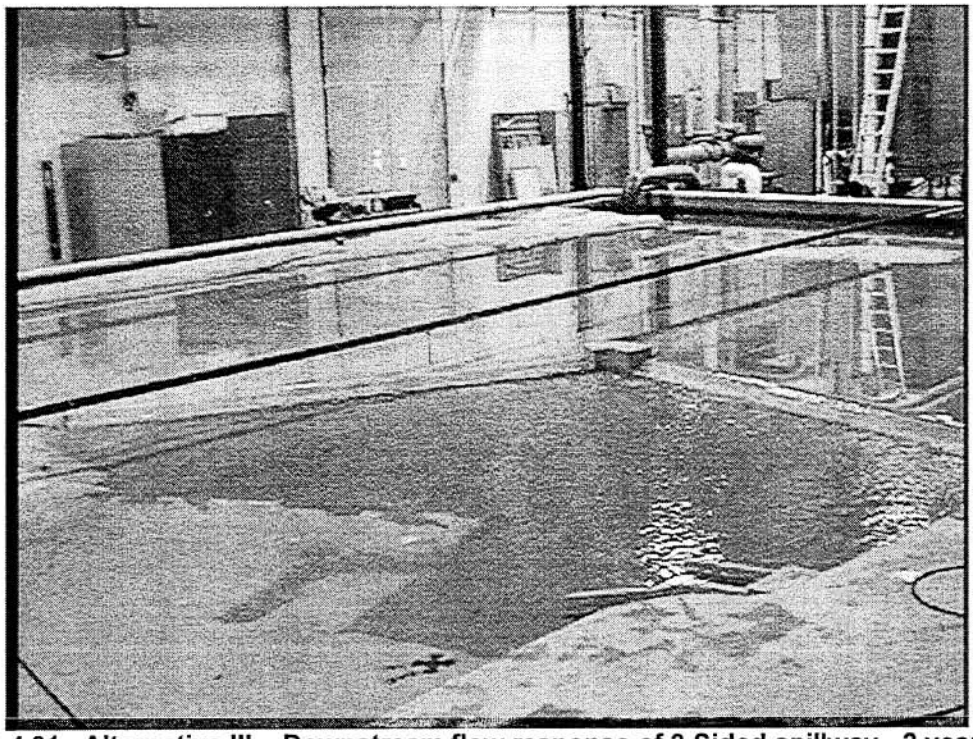

Figure 4.91. Alternative III – Downstream flow response of 2-Sided spillway - 2 year flood (5700 cfs)

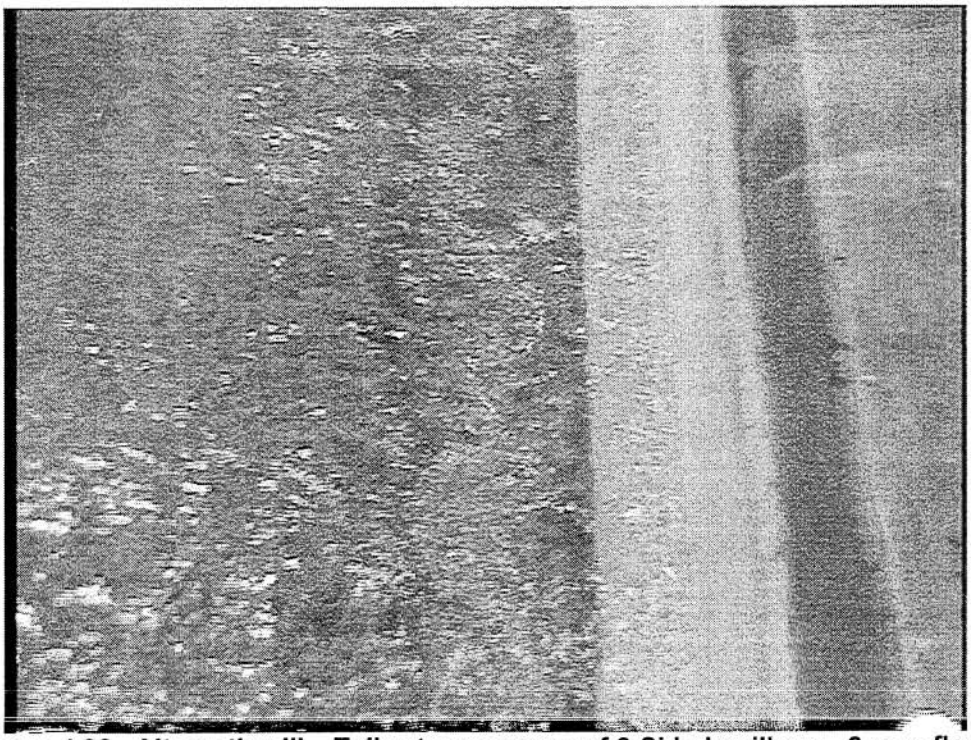

Figure 4.92. Alternative III – Tailwater response of 2-Sided spillway - 2 year flood (5700 cfs)

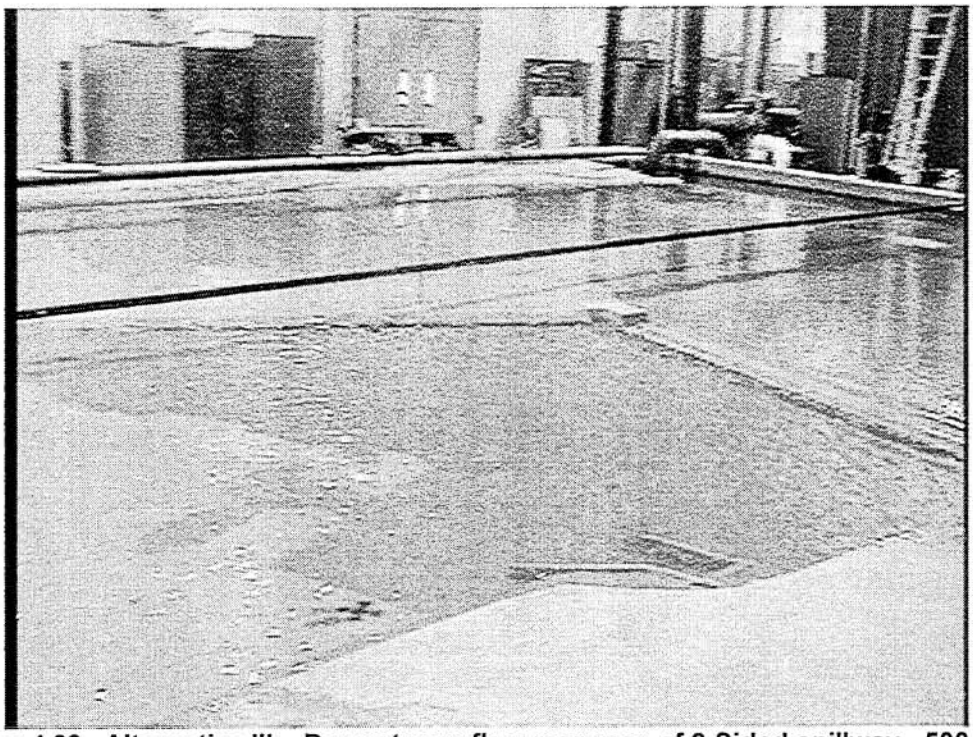

Figure 4.93. Alternative III – Downstream flow response of 2-Sided spillway - 500 year flood (17630 cfs)

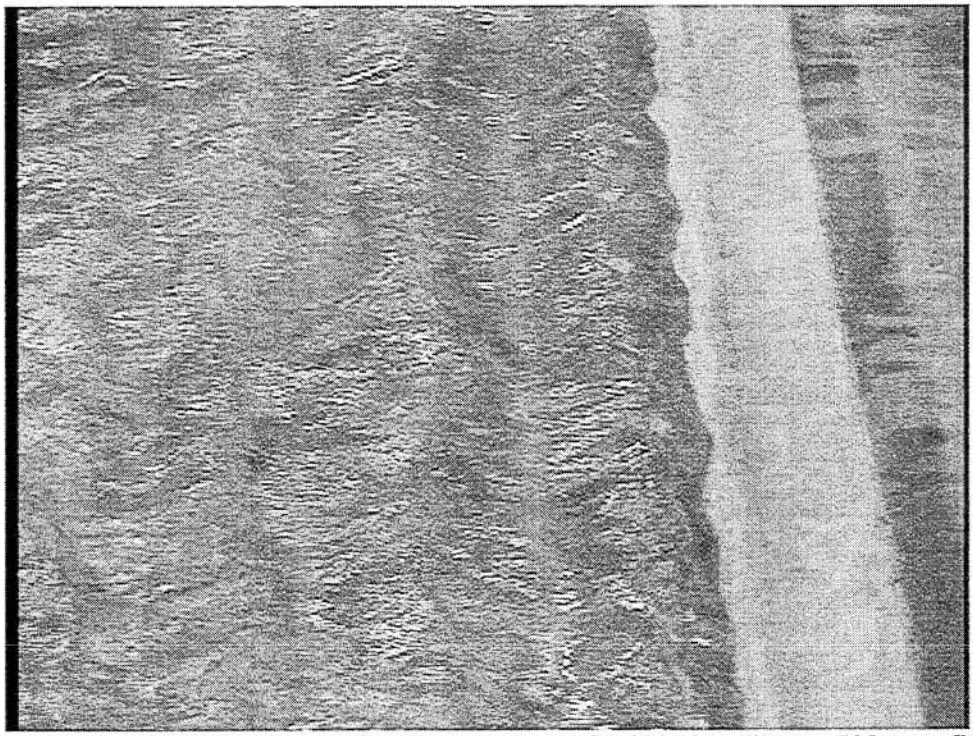

Figure 4.94. Alternative III – Tailwater response of 2-Sided spillway - 500 year flood (17630 cfs)

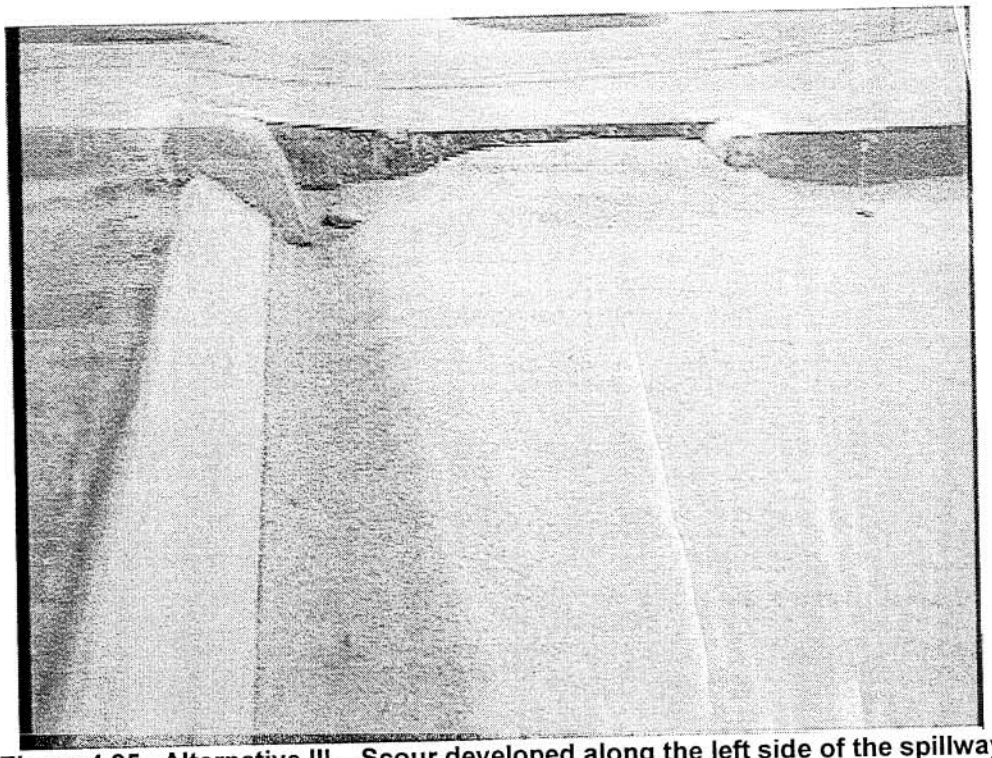

Figure 4.95. Alternative III – Scour developed along the left side of the spillway

Figure 4.96. Alternative III – Scour developed along the right side of the spillway

5. Comparison and Evaluation of Alternative Dam Configurations

5.1 Comparison and evaluation of stage response

The most crucial and telling means of comparing the three different alternative dam configurations was through investigation of the average upstream pool stage response. Here, the existing and baseline conditions provided a benchmark against which to compare the three alternatives. Figure 5.1 is a plot of all five rating curves. Alternative I, the bathtub spillway, produced stages closest to the existing condition rating. For low flows (between 2 and 10 year events), the curve fell slightly above the existing rating. For events greater than the 10 year, the bathtub rating was slightly below that of the existing condition. The rock dam, Alternative II, resulted in a rating which was, at all flows, greater than the existing condition. For flows between the 2 and 50 year flood, the rock dam stages were between the existing and baseline condition rating curves. Above the 50 year flood, the rock dam developed stages slightly above the baseline condition. Alternative III, the 2-Sided spillway, exhibited the lowest flood stages for all flows. This was attributed to the increased spillway crest length for the structure. At low flows (2 year) the stage was only slightly below that of the existing condition. For greater flows, flood stages were decreased on the order of 0.5 feet below the existing condition. The 2-Sided spillway actually had a crest elevation higher than the existing dam. Therefore, for low flow events (< 2 year) the rating for Alternative III can be expected to cross above the existing condition rating curve.

Design considerations often require an estimate of hydraulic head above spillway crest. These data have been compiled and plotted in Figure 5.2. The spillway crest elevation for each of the five investigated conditions can be found in the graph key. Head was calculated by subtracting the spillway crest elevation from the average upstream pool elevation. The head above the existing condition crest was found to vary from approximately 2.5 to 5.25 feet for events between the 2 year to 500 year magnitude. The crest elevation of the baseline and bathtub spillways were the same as the existing condition. As a result, the curves depicting head above the crest exhibited the same trends as described in the above paragraph. However, Alternative II, the rock dam, had an average crest elevation of 665.9; this increase resulted in lower overall head above crest than the first three cases. Alternative III, the 2-Sided spillway, generated the lowest hydraulic heads. This was a function of the increased spillway length and crest elevation. Head on the 2-Sided spillway varied from 1.9 to 4.4 feet for flows between the 2 and 500 year event.

A third relation of interest was the water surface drop between upstream pool and downstream tailwater. These data were collected by subtracting the tailwater rating at location I from the average upstream pool rating for each investigated case. The resulting plot is provided as Figure 5.3. Not surprisingly, the difference between upstream and tailwater elevation decreased as flow increased and the structure approached submergence. The 2-Sided spillway produced the lowest water surface drop, ranging from 5.5 feet for the 2 year flow and 2 feet for 500 year event. Alternative II, the rock dam, resulted in water surface drops similar to the baseline condition while Alternative I more closely matched the existing condition.

5.2 Comparison and evaluation of upstream approach flow conditions

The three alternatives produced different approach flow patterns as observed through dye tracer, flow split, and point velocity measurements. Several generalizations were made as to the merit of each alternative in terms of maintaining or improving the existing condition approach flow characteristics.

Alternative I, the bathtub spillway, proved to be somewhat successful at breaking into the strong wake developed downstream of the island. Flow split investigation showed 60% of the flow passing the left channel. This was slightly more balanced than measured for the existing condition (67%,33%). More mixing was observed to occur in the silted region immediately downstream of the island. In fact, a strong left to right cross-channel current was observed to develop as flow from the left channel traveled to the head and right side of the bathtub portion of the spillway. The bathtub spillway was successful at concentrating more flow through the center of the structure. At the same time, the effect of the upstream island still had apparent impact on approach flow to the structure.

The rock dam, Alternative II, exhibited approach flow conditions similar to those noted for the baseline condition. The measured flow split was the same as that of the existing condition (left-67%, right-33%). In this case, the wake downstream of the island tended to force flow to attack the structure at right and left margins. Some left to right flow near the lower tip of the silt region of the island forced circulating flow in the still pool left of the peninsula and structure. Alternative II did not produce any significant advantages in terms of approach flow conditions.

Alternative III, the 2-Sided spillway produced the most significant variation from existing condition in approach flow patterns. First, similar to the bathtub spillway, flow split was measured to be more evenly balanced with 61% of the flow passing the left channel. Also, flow split data showed a weakening of the island's ability to direct flow against the left bank. In the right channel, measurements indicated an approach flow successfully directed toward the right side of the spillway with a beneficial increase in velocity and vector orientation. The island and wake again served to partition flow into two separate paths. The 2-Sided spillway accommodated this situation well. Strong left to right cross-flow mixing was observed. Spillway orientation was successful at drawing this mixed flow over the spillway in the central region of the river. In general, Alternative III produced the most beneficial approach flow conditions of those alternatives investigated.

5.3 Comparison and evaluation of downstream discharge characteristics

Alternative I provided acceptable downstream discharge characteristics. The bathtub spillway was observed to successfully concentrate high flow velocities in the center of the downstream channel. Stages developed by the bathtub spillway were sufficient to sustain flow over the bedrock cascade for all investigated flow magnitudes. As a result, downstream discharge characteristics were observed to be skewed toward the left bank, and this cross-channel intrusion increased with flow magnitude. Still, the overland discharge was reduced from that observed from existing condition, and this resulted in a minor improvement in alignment. Closing the breach for implementation of the bathtub design removed the strong current generated by the wing-wall on the left shore. In short, the downstream conditions

generated by implementation of the bathtub spillway design, while not ideal, did exhibit improvement over the existing condition.

The rock dam tested as Alternative II tended to generate downstream discharge characteristics similar to the baseline condition. However, increased upstream stage resulted in a stronger flow contribution over the bedrock on the right abutment. Therefore, discharge vectors reflected a stronger alignment toward the left shore. The porous rock structure also resulted in increased downstream turbulence with slightly more erratic discharge conditions. In general the downstream conditions exhibited by the rock dam were not as favorable as Alternatives I and III.

Downstream discharge results collected for Alternative III, the 2-Sided spillway, showed highly uniform conditions for all flow magnitudes. The opposing cross-channel flow components generated by the angled spillway crests were cancelled within the region between the crests. The wing-wall played a diminishing role in aligning downstream flow, especially for low flows. Decreased upstream stage eliminated or greatly decreased (depending on flow magnitude) flow over the bedrock cascade. As a result, cross-channel intrusion was diminished and discharge vectors were found to be aligned more directly downstream. Velocities along the left shore were observed to increase slightly above those recorded for existing condition. In summary, the 2-Sided spillway produced highly uniform and desirable downstream discharge characteristics.

5.4 Comparison and evaluation of general response characteristics

The bathtub spillway tested for Alternative I produced a strong hydraulic jump response for flows from the 2 to the 100 year events. The exit point of the bathtub portion of the structure operated at highest possible efficiency for all tested flows through the 100 year event. For the 500 year event, the crest of the structure was submerged. In general, Alternative I was observed to provide good energy dissipation and flow conveyance characteristics. Velocities at the exit of the tub were observed to reach a maximum of 12 ft/s. At these conditions, scour may be a concern; however, bedrock on-site may protect against this problem.

The rock dam did not generate a hydraulic jump. Energy dissipation was accomplished by flow over and through the irregular rock surface. The flow over the structure, while aesthetically pleasing, was slightly more turbulent and less controlled than those observed for other alternatives. The rock field did provide strong energy dissipation characteristics.

Testing of the 2-Sided spillway with a moveable bed downstream of the structure resulted in the development of a considerable scour hole at the tailwater. As a result, a submerged roller was noted for all flow magnitudes. This condition may not develop on-site if bedrock is encountered at a sufficiently high elevation to preclude extensive scour. Regardless, if Alternative III is implemented, precautions should be taken to assure that the unsafe and inefficient submerged roller does not develop. For the 500 year flow event, crest submergence generated standing surface waves in the area between spillway crests.

Each alternative resulted in different flow lengths over the bedrock. The flow contribution along the bedrock as well as a summary of spillway dimensions for all alternatives is provided in Table AIV.1.

5.5 Recommendation for replacement Batavia Dam

Alternative II, the rock dam, was not deemed an appropriate alternative for replacement of the existing Batavia Dam structure for several reasons. First, investigation indicated that the rock structure tended to increase flood stages above the existing condition for all flows. Upstream approach characteristics for the rock dam were very similar to those observed for the baseline condition, and flow tended to concentrate on the extreme edges of the structure. Increased stages resulted in an commensurate increase in flow over the bedrock. The strength of this flow tended to skew the downstream discharge toward the left bank. Also, there was some fear that a porous structure of this nature might result in dewatering of the upstream pool during severe drought or prime recreation, summer low flow periods.

Alternatives I and III were both deemed candidates for replacement structures. Stage response of the bathtub spillway match excellently to the rating for the existing condition. The bathtub spillway was successful at breaking the wake of the island and drawing the flow into the center of the structure. Flow over the bedrock was decreased but not eliminated. High velocity flow was centralized in the downstream channel by the bathtub outlet, and in general, downstream discharge characteristics were acceptable. Hydraulic jump characteristics of the structure were strong for nearly all flows.

Alternative III decreased flood stage for all tested flows. The upstream approach flow was most improved by this structure. The 2-Sided spillway accommodated the two distinct approach flows from the right and left channels while drawing high velocity flows into the center of the river. Lower flood stages eliminated or greatly decreased flow over the bedrock feature. This, combined with the structures response, generated quite uniform downstream discharge characteristics. Model testing of this spillway revealed the possibility of the development of a submerged roller.

Choosing the most appropriate structure between Alternatives I and III requires consideration of many competing factors. Hydraulically they both present acceptable and beneficial conditions. The stage response, upstream approach, and downstream discharge characteristics of Alternative III are quite ideal. However, this choice results in the elimination of flow over the bedrock feature on the right margin of the structure. This feature is known to be of considerable importance to the Batavia community. At the same time, this Alternative provides the most reasonable possibility for incorporation of a canoe chute within the dam structure. This may be viewed as a balancing community concern. Also, selection of Alternative III produces the potential for development of a submerged roller on-site. This feature is avoidable, but further study will be required. Another possible disadvantage of the 2-Sided spillway may be encountered in the required increase of crest elevation (665.5) in order to compensate for extra spillway length. This change effectively raises the "permanent pool" elevation associated with the structure, and difficulties in permitting and land acquisition may be encountered.

Selection of Alternative I does not provide upstream and downstream flow characteristics that are as ideal as observed for Alternative III. However, stage response for this alternative is excellent, and the crest is maintained at the same elevation as that of the existing condition. Also, placing the structure along the same alignment assures that existing bedrock and a preserved head to tailwater difference (see Figure 5.3) will prevent the development of a submerged roller. This alternative reduces,

but does not eliminated, flow over the bedrock feature at the right abutment. At the same time, incorporation of a canoe chute in the bathtub spillway design would be more difficult and less safe because the risk of canoes being drawn over the dam is increased.

Alternatives I and III both provide viable alternatives for the replacement of the Batavia Dam. The two structures produce beneficial hydraulic conditions. These two spillways are quite distinct, each having their own advantages and disadvantages. The final decision for implementation will require a balancing of economic, community, and technical considerations.

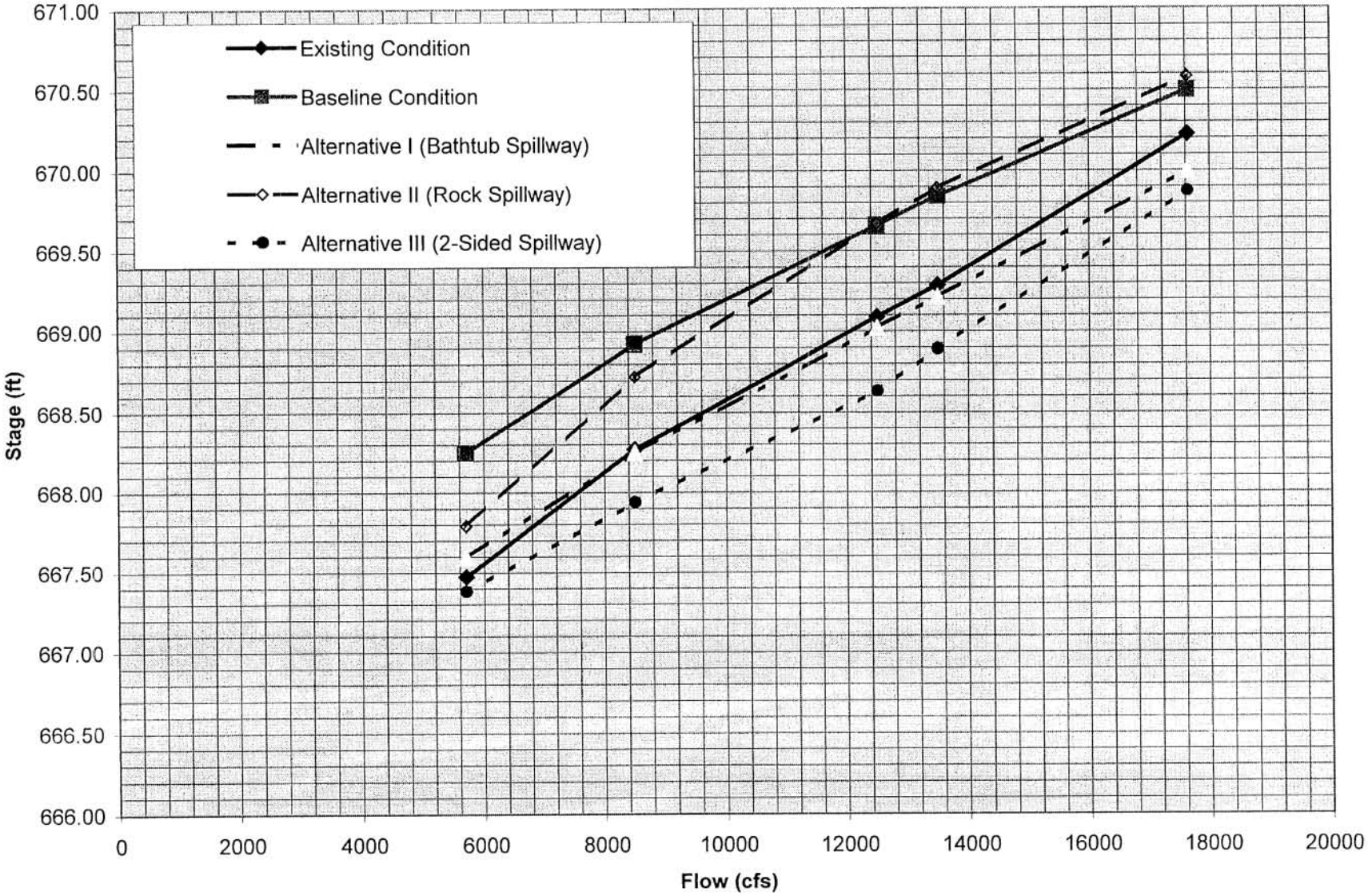

Figure 5.1. Comparison of averaged upstream pool stage response

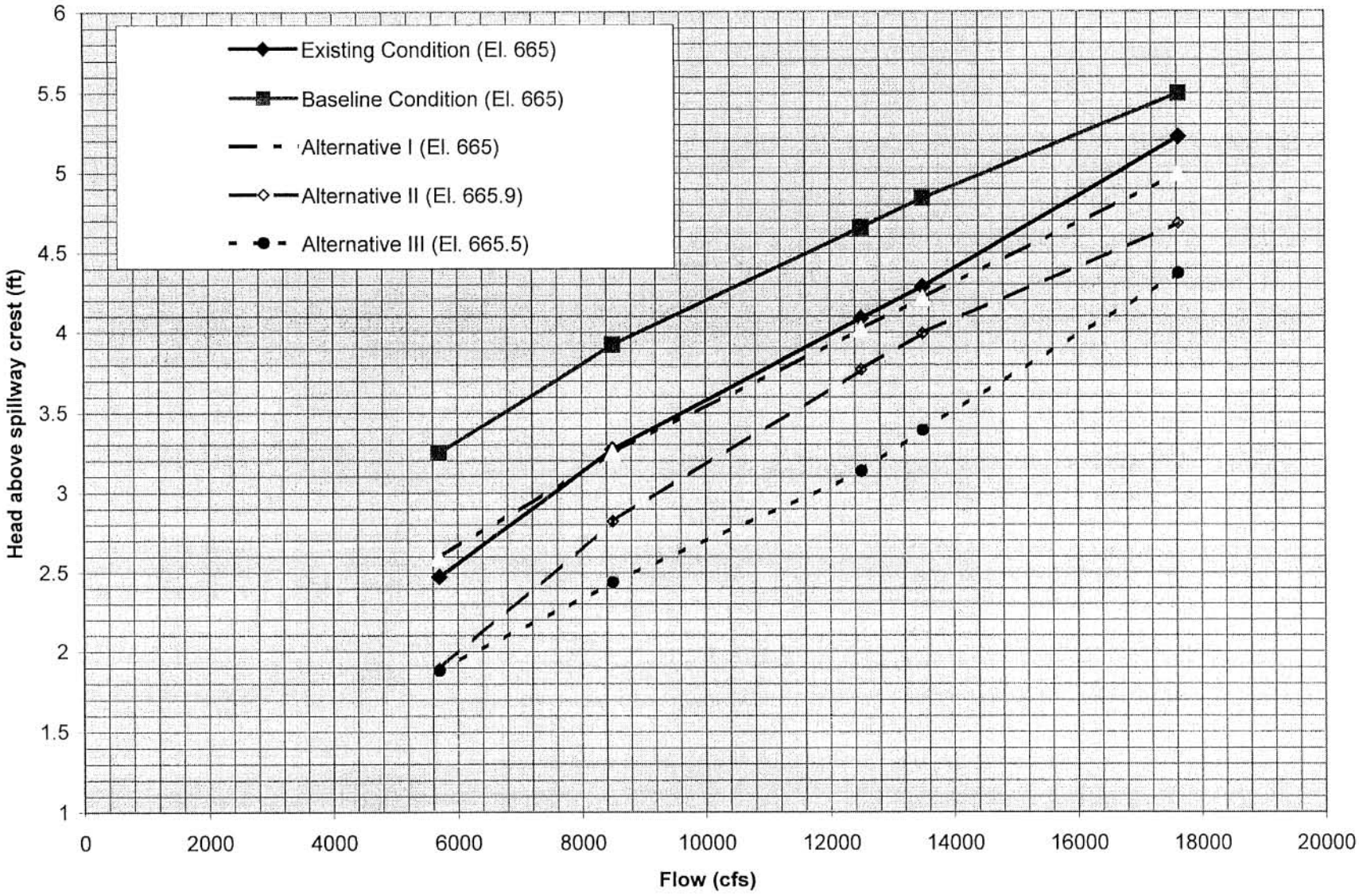

Figure 5.2. Comparison of averaged upstream head above spillway crest

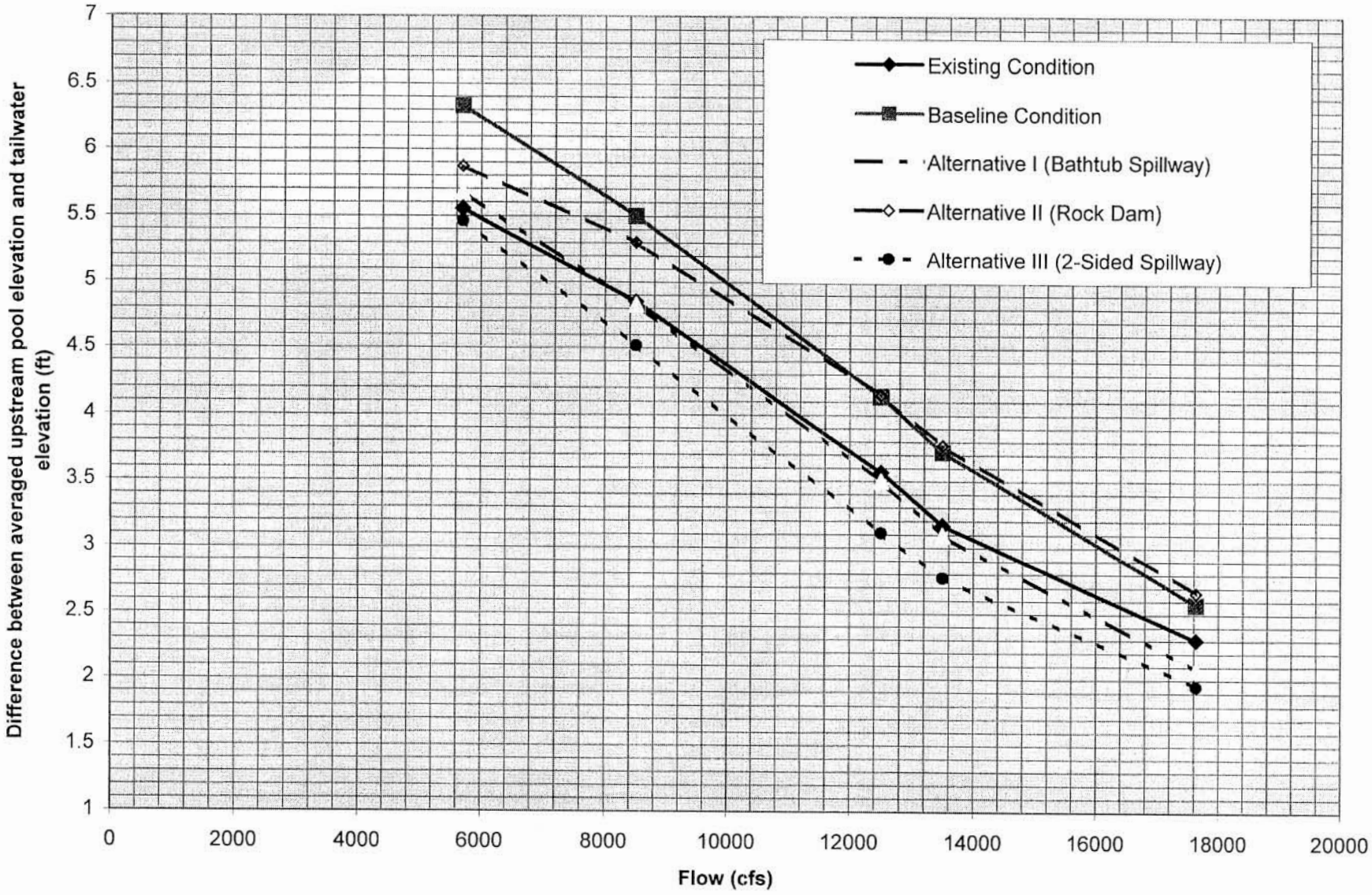

Figure 5.3. Comparison of averaged water surface drop from upstream pool to tailwater

6. Summary and Conclusions

A 30:1 scale model of the Fox River in the vicinity of the Batavia Dam was constructed in Hydrosystems Laboratory of the University of Illinois. The model was calibrated under the influence of the existing Batavia Dam structure for five distinct flooding conditions (2,10,50,100,500 year events). Calibration data were collected to compare laboratory generated stage-discharge relations to HEC-RAS generated ratings. The model tended to over-predict stages in comparison to computer produced rating curves. However, with the caveat that no field data were available to calibrate the computer model, the physical model was accepted to produce accurate stage-discharge rating relations. Three techniques were then applied to measure percentage approach flow split around the upstream island. These results were compared to data collected in the field which indicated that 61% of the flow passed the left channel with 38.5% of the flow in the right channel. All three laboratory analyses matched the field results within 6% accuracy. Flow conditions were further characterized through confetti and dye tracer flow visualization. This investigation indicated the strength of the flow split and wake effects generated by the upstream island. A majority of the flow was observed to be concentrated at the extreme right and left margins of the structure with significant flow through the breached left abutment and over the bedrock cascade on the right margin. Flow velocity and specific discharge data were collected using an electromagnetic velocity meter. Specific discharge measurements along a downstream transect showed the ability of the bedrock overland flow to skew downstream discharge alignment toward the left bank. At the same time, flow through the breach was deflected by the downstream protective wing-wall which resulted in a competing left to right current. A qualitative investigation of moveable bed displacement downstream of the breach showed this feature's ability to produce scour.

Next, as a benchmark comparison, the baseline condition was investigated. This condition represented the Batavia Dam structure before development of a breach on the left side. Stages for this condition were observed to increase considerably (on the order of 0.5 feet). Upstream flow visualization showed little change in approach flow conditions. Downstream discharge characteristics showed an increase in bedrock overland flow due to increased upstream stage. Simultaneously, breach closure decreased the influence of the downstream wing-wall current which had previously helped balance downstream alignment. As a result, downstream discharge direction was observed to be more threatening to the left bank.

In the second phase of this research, three proposed designs were tested in the laboratory. Alternative I consisted of an ogee spillway along the same alignment of the existing structure. In the center of the spillway, an additional bathtub spillway with its outlet channel at the toe of the structure was added. This design was motivated by the desire to break into the wake of the island and draw upstream flow toward the center of the structure. Flow through the outlet of the bathtub was expected to improve downstream alignment and centralize maximum velocities in the channel. At the same time, increased crest length gained in the bathtub design would lower or maintain flood stages and compensate for breach closure. This proved to be the case, and Alternative I emulated the existing condition stage rating very well. Flow visualization showed the bathtub structure was successful at shifting flow concentration toward the center of the structure. However, the island wake effect was still

quite strong. Measurements indicated that the bathtub spillway affected flow split conditions with only 60% of the flow in the left channel. Downstream discharge characteristics reflected the strong flow contribution centralized by the bathtub spillway. Still, overland bedrock flow did continue to play a role in downstream alignment. The hydraulic jump response characteristics were observed to be excellent for all flows through the 100 year event.

Alternative II was a rock dam along the same alignment as the existing structure. These features were modeled with Froude scaled boulders of prototype size ranging from two to three tons. This alternative was motivated by its economic and aesthetic merit; the community had expressed a desire to investigate the possibility of such a natural structure. Also, it was proposed that a porous structure of this type might produce more favorable upstream approach conditions. Stage-discharge relations for this alternative showed an increase in stage to levels between existing and baseline condition measurements. The flow split and approach flow conditions showed very little beneficial change, and the flow tended to attack the structure on its right and left margins as previously observed. Downstream discharge conditions were rather erratic, and bedrock overland flow tended to dominate alignment toward the left bank.

Alternative III was a modified ogee spillway structure providing two separate overflow structures to accommodate separate approach flow from the left and right channels. This alternative was motivated by the observed strength of the island wake and its ability to divide the flow into two distinct approaches. The spillway crest for this alternative was raised (0.5 ft) in order to compensated for increased spillway length. The resulting stage data still indicated a considerable decrease in flood stages for all investigated flows. Approach conditions for this alternative were excellent with dye tracer studies indicating good response in both the left and right channels. Flow split was more balanced than for the existing condition (61% left channel). Cross-channel currents generated by the angled legs of the structure were successfully cancelled in the region between spillway crests. Overland bedrock flow was eliminated or greatly decreased for all flow magnitudes. As a result, downstream discharge characteristics were well aligned and highly uniform. Moveable bed response at the toe of this alternative indicated the potential for development of a submerged roller. It was recommended that precautions be taken to assure this dangerous condition does not develop on-site.

In conclusion, Alternatives I and III are recommended for further consideration as replacement Batavia Dam structures. These configurations both produced acceptable and beneficial hydraulic conditions. Both alternatives are unique in nature, and as result, each comes with its own differing intrinsic set of advantages and disadvantages (See section 5.5). Final selection of a replacement structure will require balancing economic, community, and technical concerns. The information contained in this report provides the basis on which these decision are to be made. Regardless of which alternative is implemented, further study is recommended in order to optimize structure safety and performance.

References

Barr, Douglas W., and J.K. Bogart, (1991), "Rebuilding an Illusion," *Civil Engineering*, January 1991, pp 55-57.

Chow, V.T., (1959), Open Channel Hydraulics, McGraw Hill, Inc., New York.

Farney, H.S., and A. Markus, (1962), "Side Channel Spillway Design," *Journal of the Hydraulics Division*, ASCE, Vol. 88, No. HY3, pp 131-154.

FEMA, (1981), "Flood Insurance Study, City of Batavia Illinois, Kane and Du Page Counties," March 1981.

Freeman, J.W. Hydraulic Model Study for the Drown Proofing of Yorkville Dam, Illinois, Master's Thesis, University of Illinois at Urbana-Champaign.

Hinds, J., (1926), "Side Channel Spillways: Hydraulic Theory, Economic Factors, and Experimental Determination of Losses," ASCE Trans. Vol. 89, p 894.

Hwang, N.H.C., and C.E. Hita, (1987), Fundamentals of Hydraulic Engineering Systems, Second Edition, Prentice Hall, Inc., Englewood Cliffs, New Jersey, 318 p.

Illinois Department of Transportation, Division of Water Resources, (1974), "Fox River Dams Study Report"

Knight, A.C.E. (1989), "Design of Efficient Side-Channel Spillway," *Journal of Hydraulic Engineering*, ASCE, Vol. 115, No. 9, pp 1275-1289.

Novak, P., C. Nalluri, and R. Narayanan, (1990), Hydraulic Structures, Unwin Hyman, London.

Parker, G., M. Garcia, H. Johannesson, and K. Okabe, (1988), Model Study of the Minnesota River Near Wilmarth Power Plant, Minnesota, St. Anthony Falls Hydraulic Laboratory, University of Minnesota, Project Report No. 284.

Raymond International, Inc. (1978), "Test Boring Report: Batavia Dam Project, Batavia Illinois."

Subcommittee on Small Water Storage Projects, (1939), Low Dams, United States Government Printing Office, Washington.

United States Department of Interior, Bureau of Reclamation, (1987), Design of Small Dams, Third Edition, United States Government Printing Office, Washington, 377-383 pp.

U.S. Army Corps of Engineers, Chicago District, (1978), "Fox River and Tributaries, Illinois and Wisconsin; Flood Control Report."

Appendix I

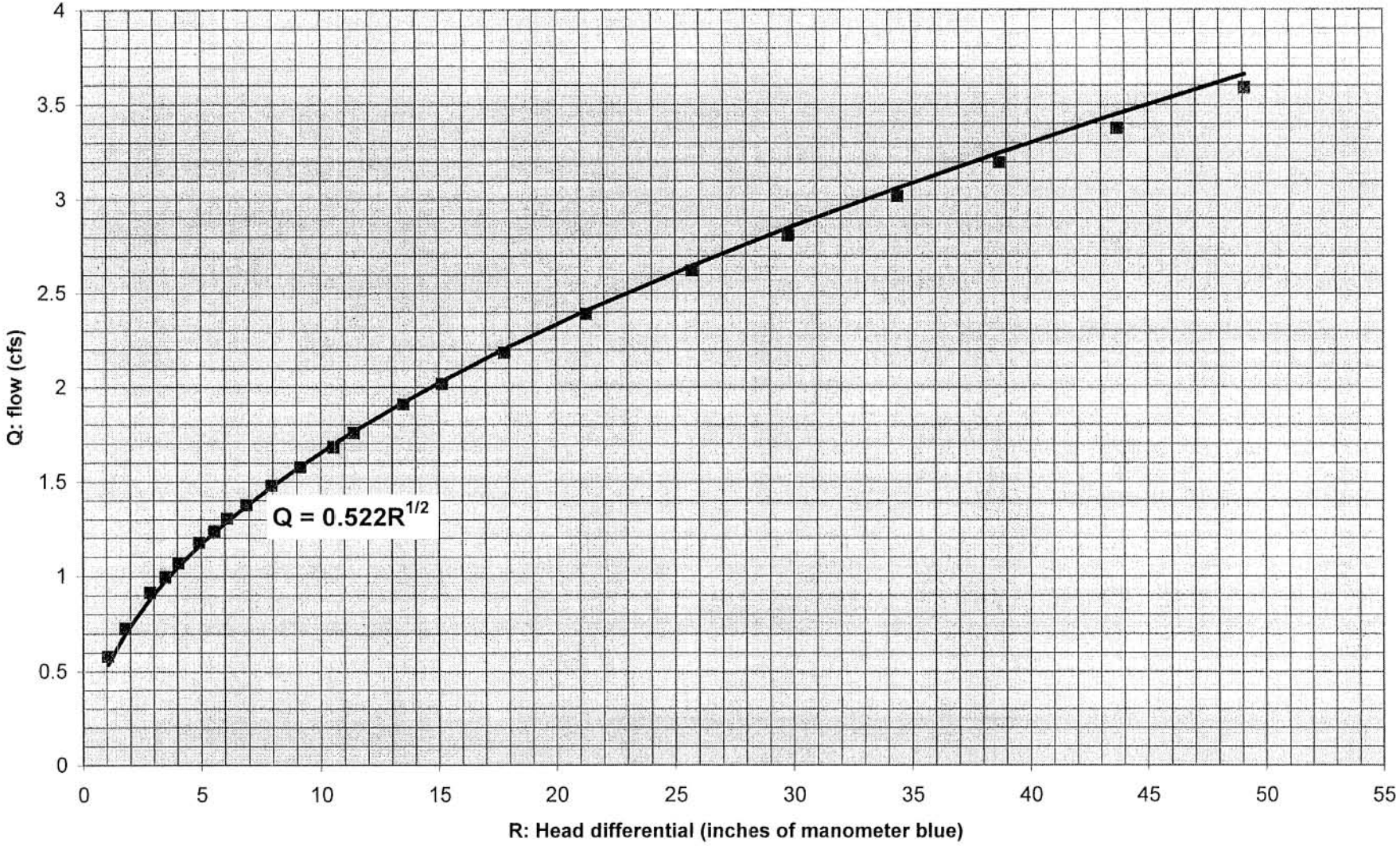

Figure AI.1. Model basin line - 14" Dall Flow Tube calibration (8/97)

Calculation A1.1 Dam breach elevation

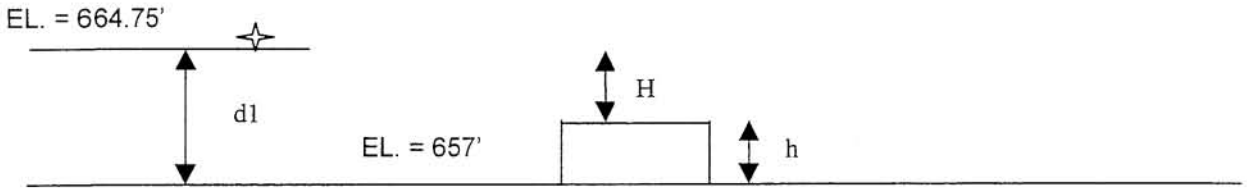

From survey:

L=58'
W=15'

Geometry

d1 = 664.75-657 = 7.75'
h = d1-H

From Geneva gaging station (3rd week of July 1997)

Q=800 cfs

Broad Crested Weir Theory (Hwang and Hita, 1987)

$$Q = 0.433\sqrt{2g}\left(\frac{d1}{d1+h}\right)^{1/2} LH^{3/2}$$

$$Q = 3.475\left(\frac{d1}{2d1-H}\right)^{1/2} \times 58 \times H^{3/2}$$

$$800 = 201.5\left(\frac{7.75}{15.5-H}\right)^{1/2} H^{3/2}$$

$$3.97 = \left(\frac{7.75}{15.5-H}\right)^{1/2} H^{3/2}$$

$H = 2.944$ ft (By Iteration)

$$h = d1 - H$$
$$h = 7.75 - 2.944 = 4.806'$$

Breach Elevation

657+4.81 = 661.81'

Calculation A1.2 Moveable bed sediment sizing

Prototype Data (HEC-RAS – River Mile 56.279)

W = 119 m
H = 4.35 m
S = 0.0007
D = 13.43 mm (Freeman and Garcia, 1996)
R = 1.65 (quartz)

$$U_{*p} = \sqrt{gHS} = \sqrt{9.81 \times 4.35 \times 0.0007} = 0.1728 \text{ m/s}$$

$$V_s = 0.22D^{1/2}$$

$$V_{sp} = 0.806 \text{ m/s}$$

Model Data

W = 3.967
H = 0.145
S = 0.0007
R = 1.65
D = ??

$$U_{*m} = \sqrt{gHS} = \sqrt{9.81 \times 0.145 \times 0.0007} = 0.0316 \text{ m/s}$$

$$\left(\frac{u_*}{V_s}\right)_m = \left(\frac{u_*}{V_s}\right)_p \quad \therefore$$

$$V_{sm} = 0.147 \text{ m/s}$$

Iterative Calculation of Diameter (final trial D=0.0009)

$$R_p = \frac{VD}{\nu} = \frac{0.147 * 0.0009}{1x10^{-6}} = 132$$

$$C_d = \frac{24}{R_p}(1 + 0.152R_p^{1/2} + 0.0151R_p) = 0.86$$

$$D = V_s^2 \frac{3}{4} \frac{C_d}{gR} = 0.0009 \text{ m}$$

Use 1 mm quartz sediment

Appendix II

Table All.1. Stage data - Existing condition

Gaging Data - "Calibration Flow"

Date		9/10/97		
Flow	Field	6062	Model	1.23
Manometer Displacement		5.55		
Gage F	Elevation	662.1	Depth	0.29

Gage Designation	Point Gage Depth (model, ft)	Water Depth (prototype, ft)	Bed Elevation (prototype, ft)	Water Surface (prototype, ft)
A	0.1	3	664.69	667.69
B1	0.123	3.69	664.06	667.75
B2	0.127	3.81	663.83	667.64
C1	0.31	9.3	663.83	673.13
C2	0.242	7.26	663.83	671.09
D1	0.397	11.91	655.94	667.85
D2	0.153	4.59	655.94	660.53
D3	0.12	3.6	664.06	667.66
E	0.247	7.41	659.77	667.18
F	0.184	5.52	659.77	665.29
G	0.13	3.9	659.77	663.67
H	0.146	4.38	657.74	662.12
I	0.289	8.67	653.52	662.19

Gaging Data - 2 Year Flood

Date		9/10/97		
Flow	Field	5700	Model	1.16
Manometer Displacement		4.91		
Gage F	Elevation	661.8	Depth	0.28

Gage Designation	Point Gage Depth (model, ft)	Water Depth (prototype, ft)	Bed Elevation (prototype, ft)	Water Surface (prototype, ft)
A	0.093	2.79	664.69	667.48
B1	0.119	3.57	664.06	667.63
B2	0.119	3.57	663.83	667.40
C1	0.311	9.33	658.20	667.53
C2	0.234	7.02	660.23	667.25
D1	0.379	11.37	655.94	667.31
D2	0.146	4.38	663.20	667.58
D3	0.116	3.48	664.06	667.54
E	0.251	7.53	659.77	667.30
F	0.177	5.31	662.42	667.73
G	0.131	3.93	663.52	667.45
H	0.142	4.26	657.74	662.00
I	0.28	8.4	653.52	661.92

Table AII.1. (Continued)

Gaging Data - 10 Year Flood

Date		9/10/97		
Flow	Field	8500	Model	1.72
Manometer Displacement		10.91		
Gage F	Elevation	663.5	Depth	0.33

Gage Designation	Point Gage Depth (model, ft)	Water Depth (prototype, ft)	Bed Elevation (prototype, ft)	Water Surface (prototype, ft)
A	0.123	3.69	664.69	668.38
B1	0.144	4.32	664.06	668.38
B2	0.147	4.41	663.83	668.24
C1	0.339	10.17	658.20	668.37
C2	0.263	7.89	660.23	668.12
D1	0.413	12.39	655.94	668.33
D2	0.181	5.43	663.20	668.63
D3	0.139	4.17	664.06	668.23
E	0.267	8.01	659.77	667.78
F	0.198	5.94	662.42	668.36
G	0.154	4.62	663.52	668.14
H	0.202	6.06	657.74	663.80
I	0.33	9.9	653.52	663.42

Gaging Data - 50 Year Flood

Date		9/10/97		
Flow	Field	12500	Model	2.54
Manometer Displacement		23.60		
Gage F	Elevation	665.6	Depth	0.40

Gage Designation	Point Gage Depth (model, ft)	Water Depth (prototype, ft)	Bed Elevation (prototype, ft)	Water Surface (prototype, ft)
A	0.15	4.5	664.69	669.19
B1	0.173	5.19	664.06	669.25
B2	0.17	5.1	663.83	668.93
C1	0.363	10.89	658.20	669.09
C2	0.29	8.7	660.23	668.93
D1	0.458	13.74	655.94	669.68
D2	0.201	6.03	663.20	669.23
D3	0.165	4.95	664.06	669.01
E	0.294	8.82	659.77	668.59
F	0.225	6.75	662.42	669.17
G	0.179	5.37	663.52	668.89
H	0.255	7.65	657.74	665.39
I	0.396	11.88	653.52	665.40

Table AII.1. (Continued)

Gaging Data - 100 Year Flood

Date		9/10/97		
Flow	Field	13500	Model	2.74
Manometer Displacement		27.52		
Gage F	Elevation	666	Depth	0.42

Gage Designation	Point Gage Depth (model, ft)	Water Depth (prototype, ft)	Bed Elevation (prototype, ft)	Water Surface (prototype, ft)
A	0.156	4.68	664.69	669.37
B1	0.183	5.49	664.06	669.55
B2	0.179	5.37	663.83	669.20
C1	0.369	11.07	658.20	669.27
C2	0.295	8.85	660.23	669.08
D1	0.46	13.8	655.94	669.74
D2	0.21	6.3	663.20	669.50
D3	0.174	5.22	664.06	669.28
E	0.299	8.97	659.77	668.74
F	0.228	6.84	662.42	669.26
G	0.188	5.64	663.52	669.16
H	0.276	8.28	657.74	666.02
I	0.42	12.6	653.52	666.12

Gaging Data - 500 Year Flood

Date		9/10/97		
Flow	Field	17630	Model	3.58
Manometer Displacement		46.94		
Gage F	Elevation	667.8	Depth	0.48

Gage Designation	Point Gage Depth (model, ft)	Water Depth (prototype, ft)	Bed Elevation (prototype, ft)	Water Surface (prototype, ft)
A	0.186	5.58	664.69	670.27
B1	0.22	6.6	664.06	670.66
B2	0.211	6.33	663.83	670.16
C1	0.4	12	658.20	670.20
C2	0.323	9.69	660.23	669.92
D1	0.486	14.58	655.94	670.52
D2	0.234	7.02	663.20	670.22
D3	0.211	6.33	664.06	670.39
E	0.337	10.11	659.77	669.88
F	0.259	7.77	662.42	670.19
G	0.217	6.51	663.52	670.03
H	0.344	10.32	657.74	668.06
I	0.48	14.4	653.52	667.92

Table AII.2. Flow velocity as determined by confetti image velocimetry - Right Channel: Lanes 1-7

Lane 1						
Point #	**start x**	**start y**	**end x**	**end y**	**Distance** (pixels)	**Velocity** (fps)
1	265	45	164	181	169.40	0.2614
2	224	61	113	221	194.73	0.3005
3	167	97	69	281	208.47	0.3217
4	218	156	137	339	200.12	0.3088
5	192	205	111	407	217.64	0.3359
Pixels/inch	27					
Time start	9:45:07					
Time end	9:47:07				**Avg Vel =**	0.3057
Time (sec)	2.00				**Std Dev.=**	0.0281

Lane 2						
Point #	**start x**	**start y**	**end x**	**end y**	**Distance** (pixels)	**Velocity** (fps)
1	261	84	169	241	181.97	0.2927
2	303	57	217	237	199.49	0.3209
3	332	67	238	239	196.01	0.3153
4	427	103	336	293	210.67	0.3389
5	505	139	413	324	206.61	0.3324
Pixels/inch	25.9					
Time start	9:31:21					
Time end	9:33:21				**Avg Vel =**	0.3201
Time (sec)	2.00				**Std Dev.=**	0.0179

Lane 3						
Point #	**start x**	**start y**	**end x**	**end y**	**Distance** (pixels)	**Velocity** (fps)
1	177	175	145	309	137.77	0.2278
2	240	131	188	272	150.28	0.2485
3	242	209	200	355	151.92	0.2512
4	419	124	401	281	158.03	0.2613
5	488	165	451	356	194.55	0.3217
Pixels/inch	25.2					
Time start	9:01:23					
Time end	9:03:23				**Avg Vel =**	0.2621
Time (sec)	2.00				**Std Dev.=**	0.0355

Lane 4						
Point #	**start x**	**start y**	**end x**	**end y**	**Distance** (pixels)	**Velocity** (fps)
1	151	216	94	362	156.73	0.2521
2	264	193	190	335	160.12	0.2576
3	331	185	265	333	162.05	0.2607
4	377	237	342	384	151.11	0.2431
5	488	233	448	420	191.23	0.3076
Pixels/inch	25.9					
Time start	8:44:28					
Time end	8:46:28				**Avg Vel =**	0.2642
Time (sec)	2.00				**Std Dev.=**	0.0252

Table AII.2. (Continued)

Lane 5						
Point #	**start x**	**start y**	**end x**	**end y**	**Distance** (pixels)	**Velocity** (fps)
1	126	170	86	257	95.75	0.1552
2	204	146	159	246	109.66	0.1778
3	276	181	244	282	105.95	0.1718
4	291	232	258	324	97.74	0.1585
5	365	169	349	261	93.38	0.1514
Pixels/inch	25.7					
Time start	8:30:05					
Time end	8:32:05				**Avg Vel =**	0.1629
Time (sec)	2.00				**Std Dev.=**	0.0113

Lane 6						
Point #	**start x**	**start y**	**end x**	**end y**	**Distance** (pixels)	**Velocity** (fps)
1	217	54	183	149	100.90	0.1744
2	305	136	286	240	105.72	0.1828
3	367	141	336	251	114.28	0.1976
4	423	109	393	223	117.88	0.2038
5	516	171	492	282	113.56	0.1963
Pixels/inch	24.1					
Time start	8:06:10					
Time end	8:08:10				**Avg Vel =**	0.1910
Time (sec)	2.00				**Std Dev.=**	0.0120

Lane 7						
Point #	**start x**	**start y**	**end x**	**end y**	**Distance** (pixels)	**Velocity** (fps)
1	218	142	174	242	109.25	0.1843
2	306	53	270	150	103.46	0.1745
3	341	204	306	298	100.30	0.1692
4	421	182	384	277	101.95	0.1720
5	475	244	437	337	100.46	0.1695
Pixels/inch	24.7					
Time start	7:40:20					
Time end	7:42:20				**Avg Vel =**	0.1739
Time (sec)	2.00				**Std Dev.=**	0.0062

Table AII.3. Flow velocity as determined by confetti image velocimetry - Left Channel: Lanes 1-6

Lane 1						
Point #	**start x**	**start y**	**end x**	**end y**	**Distance** (pixels)	**Velocity** (fps)
1	177	55	196	249	194.93	0.2874
2	200	95	230	273	180.51	0.2661
3	292	115	290	321	206.01	0.3037
4	346	85	345	288	203.00	0.2993
5	393	47	388	245	198.06	0.2920
Pixels/inch	27.8					
Time start	1:37:28					
Time end	1:39:29				**Avg Vel =**	0.2897
Time (sec)	2.03				**Std Dev.=**	0.0146

Lane 2						
Point #	**start x**	**start y**	**end x**	**end y**	**Distance** (pixels)	**Velocity** (fps)
1	148	45	130	248	203.80	0.3066
2	236	164	267	368	206.34	0.3104
3	333	59	381	263	209.57	0.3152
4	428	71	475	290	223.99	0.3369
5	528	83	554	306	224.51	0.3377
Pixels/inch	27.7					
Time start	2:29:06					
Time end	2:31:06				**Avg Vel =**	0.3214
Time (sec)	2.00				**Std Dev.=**	0.0149

Lane 3						
Point #	**start x**	**start y**	**end x**	**end y**	**Distance** (pixels)	**Velocity** (fps)
1	155	71	193	301	233.12	0.3536
2	265	53	302	285	234.93	0.3563
3	324	33	354	257	226.00	0.3428
4	460	97	496	317	222.93	0.3381
5	264	151	305	395	247.42	0.3753
Pixels/inch	27.02					
Time start	2:55:00					
Time end	2:57:01				**Avg Vel =**	0.3532
Time (sec)	2.03				**Std Dev.=**	0.0144

Lane 4						
Point #	**start x**	**start y**	**end x**	**end y**	**Distance** (pixels)	**Velocity** (fps)
1	66	59	163	261	224.08	0.3253
2	141	21	212	241	231.17	0.3356
3	270	49	299	332	284.48	0.4130
4	295	79	328	338	261.09	0.3791
5	423	148	465	430	285.11	0.4139
Pixels/inch	28.7					
Time start	3:14:10					
Time end	3:16:10				**Avg Vel =**	0.3734
Time (sec)	2.00				**Std Dev.=**	0.0418

Table AII.3. (Continued)

Lane 5						
Point #	**start x**	**start y**	**end x**	**end y**	**Distance** (pixels)	**Velocity** (fps)
1	63	69	101	329	262.76	0.4288
2	119	31	161	289	261.40	0.4266
3	156	13	208	272	264.17	0.4311
4	197	47	245	315	272.26	0.4443
5	328	55	377	293	242.99	0.3965
Pixels/inch	25.533333					
Time start	3:45:14					
Time end	3:47:14				**Avg Vel =**	0.4255
Time (sec)	2.00				**Std Dev.=**	0.0176

Lane 6						
Point #	**start x**	**start y**	**end x**	**end y**	**Distance** (pixels)	**Velocity** (fps)
1	207	26	135	282	265.93	0.4216
2	260	59	180	321	273.94	0.4343
3	313	83	267	339	260.10	0.4123
4	450	87	409	320	236.58	0.3750
5	517	46	489	270	225.74	0.3579
Pixels/inch	26.283333					
Time start	4:06:04					
Time end	4:08:04				**Avg Vel =**	0.4002
Time (sec)	2.00				**Std Dev.=**	0.0324

Table AII.4. Model velocity data - Existing condition

Velocity and Flow Spit Data - Calibration Flow

Location	Measurement Depth (ft)	X vel (cm/s)	Y vel (cm/s)	Angle with X-Axis (deg)	X vel (ft/s)	Y vel (ft/s)	Current Velocity (ft/s)	q (cfs/ft)	Q (cfs)
LLane1	0.077	9.5	0.9	5.4	0.31	0.03	0.31	0.05	0.08
LLane2	0.159	8.6	0.9	6.0	0.28	0.03	0.28	0.09	0.13
LLane3	0.150	8.9	1.3	8.3	0.29	0.04	0.30	0.09	0.14
LLane4	0.149	10.0	2.0	11.3	0.33	0.07	0.33	0.10	0.16
LLane5	0.181	10.1	1.5	8.4	0.33	0.05	0.33	0.12	0.19
LLane6	0.180	9.8	3.0	17.0	0.32	0.10	0.34	0.12	0.17
RLane1	0.153	8.0	-3.0	-20.6	0.26	-0.10	0.28	0.09	0.18
RLane2	0.163	6.0	-1.0	-9.5	0.20	-0.03	0.20	0.07	0.10
RLane3	0.132	6.0	-0.1	-1.0	0.20	0.00	0.20	0.05	0.08
RLane4	0.096	5.9	0.1	1.0	0.19	0.00	0.19	0.04	0.06
RLane5	0.072	5.0	0.1	1.1	0.16	0.00	0.16	0.02	0.03
A	Insufficient Depth								
B1	Insufficient Depth								
B2	Insufficient Depth								
C1	0.155	11.1	0.8	4.1	0.36	0.03	0.37		
C2	0.121	5.0	0.9	10.2	0.16	0.03	0.17		
D1	0.199	9.4	0.1	0.6	0.31	0.00	0.31		
D2	0.077	5.8	3.1	28.1	0.19	0.10	0.22		
D3	Insufficient Depth								
E	0.124	23.9	2.0	4.8	0.78	0.07	0.79		
F	0.092	6.9	2.1	16.9	0.23	0.07	0.24		
G	Insufficient Depth								
H	0.073	4.1	4.5	47.7	0.13	0.15	0.20		
I	0.145	24.9	2.5	5.7	0.82	0.08	0.82		
Down5	Insufficient Depth								
Down4	0.095	24.6	12.9	27.7	0.81	0.42	0.91	0.17	0.52
Down3	0.114	31.0	13.1	22.9	1.02	0.43	1.10	0.25	0.38
Down2	0.132	23.9	6.6	15.4	0.78	0.22	0.81	0.21	0.32
Down1	0.131	21.4	2.8	7.5	0.70	0.09	0.71	0.18	0.28

Table AII.4. (Continued)

Velocity Data - 2 Year Flood

Location	Measurement Depth (ft)	X vel (cm/s)	Y vel (cm/s)	Angle with X-Axis (deg)	X vel (ft/s)	Y vel (ft/s)	Current Velocity (ft/s)	q (cfs/ft)	Q (cfs)
A	Insufficient Depth								
B1	Insufficient Depth								
B2	Insufficient Depth								
C1	0.156	10.8	0.9	4.8	0.35	0.03	0.36		
C2	0.117	5.1	1.1	12.2	0.17	0.04	0.17		
D1	0.195	9.3	0.2	1.2	0.31	0.01	0.31		
D2	0.073	5.8	3.7	32.5	0.19	0.12	0.23		
D3	Insufficient Depth								
E	0.126	23.5	2.9	7.0	0.77	0.10	0.78		
F	0.089	6.1	3.0	26.2	0.20	0.10	0.22		
G	0.066	0.8	1.2	56.3	0.03	0.04	0.05		
H	0.071	19.1	0.5	1.5	0.63	0.02	0.63		
I	0.140	15.5	1.6	5.9	0.51	0.05	0.51		
Down5	Insufficient Depth								
Down4	0.096	28.1	11.0	21.4	0.92	0.36	0.99	0.19	0.57
Down3	0.116	30.1	10.0	18.4	0.99	0.33	1.04	0.24	0.36
Down2	0.131	25.1	5.1	11.5	0.82	0.17	0.84	0.22	0.33
Down1	0.131	15.0	1.8	6.8	0.49	0.06	0.50	0.13	0.19

Table AII.4. (Continued)

Velocity Data - 10 Year Flood

Location	Measurement Depth (ft)	X vel (cm/s)	Y vel (cm/s)	Angle with X-Axis (deg)	X vel (ft/s)	Y vel (ft/s)	Current Velocity (ft/s)	q (cfs/ft)	Q (cfs)
A	0.062	1.6	-0.4	-14.0					0.00
B1	0.072	12.5	0.9	4.1	0.41	0.03	0.41		0.00
B2	0.074	5.5	-0.1	-1.0	0.18	0.00	0.18		0.00
C1	0.170	15.5	1.1	4.1	0.51	0.04	0.51		0.00
C2	0.132	6.4	1.0	8.9	0.21	0.03	0.21		0.00
D1	0.216	11.8	-0.2	-1.0	0.39	-0.01	0.39		0.00
D2	0.091	2.9	2.0	34.6	0.10	0.07	0.12		0.06
D3	Insufficient Depth								0.00
E	0.134	27.9	1.9	3.9	0.92	0.06	0.92		0.36
F	0.099	9.2	3.2	19.2	0.30	0.10	0.32		0.09
G	0.077	1.5	0.1	3.8	0.05	0.00	0.05		0.01
H	0.101	23.2	0.1	0.2	0.76	0.00	0.76		
I	0.165	19.5	2.4	7.0	0.64	0.08	0.64		
Down5	Insufficient Depth								
Down4	0.120	50.0	22.0	23.7	1.64	0.72	1.79	0.43	0.86
Down3	0.137	35.0	11.7	18.5	1.15	0.38	1.21	0.33	0.50
Down2	0.160	32.2	7.4	12.9	1.06	0.24	1.08	0.35	0.52
Down1	0.149	17.5	1.9	6.2	0.57	0.06	0.58	0.17	0.26

Table AII.4. (Continued)

Velocity Data - 50 Year Flood

Location	Measurement Depth (ft)	X vel (cm/s)	Y vel (cm/s)	Angle with X-Axis (deg)	X vel (ft/s)	Y vel (ft/s)	Current Velocity (ft/s)	q (cfs/ft)	Q (cfs)
A	0.075	6.0	-5.8	-44.0	0.20	-0.19	0.27		0.00E+00
B1	0.086	14.2	-4.1	-16.1	0.47	-0.13	0.48		0.00E+00
B2	0.085	6.0	-1.1	-10.4	0.20	-0.04	0.20		0.00E+00
C1	0.182	20.9	-4.0	-10.8	0.69	-0.13	0.70		0.00E+00
C2	0.145	6.1	-0.1	-0.9	0.20	0.00	0.20		0.00E+00
D1	0.229	14.9	-4.0	-15.0	0.49	-0.13	0.51		0.00E+00
D2	0.097	9.8	2.3	13.2	0.32	0.08	0.33		2.15E-01
D3	0.083	1.3	0.7	28.3	0.04	0.02	0.05		2.09E-02
E	0.147	30.5	-4.2	-7.8	1.00	-0.14	1.01		3.90E-01
F	0.113	13.9	1.8	7.4	0.46	0.06	0.46		1.32E-01
G	0.089	2.1	-0.4	-10.8	0.07	-0.01	0.07		1.24E-02
H	0.128	21.9	-4.1	-10.6	0.72	-0.13	0.73		
I	0.198	22.3	-2.3	-5.9	0.73	-0.08	0.74		
Down5	0.079	4.1	3.2	38.0	0.13	0.10	0.17	0.03	0.04
Down4	0.148	59.0	12.8	12.2	1.94	0.42	1.98	0.58	0.88
Down3	0.168	38.1	4.7	7.0	1.25	0.15	1.26	0.42	0.63
Down2	0.187	34.0	1.1	1.9	1.12	0.04	1.12	0.42	0.63
Down1	0.187	20.8	-2.2	-6.0	0.68	-0.07	0.69	0.26	0.38

Table AII.4. (Continued)

Velocity Data - 100 Year Flood

Location	Measurement Depth (ft)	X vel (cm/s)	Y vel (cm/s)	Angle with X-Axis (deg)	X vel (ft/s)	Y vel (ft/s)	Current Velocity (ft/s)	q (cfs/ft)	Q (cfs)
A	0.078	5.3	-2.9	-28.7	0.17	-0.10	0.20		0.00E+00
B1	0.092	14.9	-2.9	-11.0	0.49	-0.10	0.50		0.00E+00
B2	0.089	6.1	-1.4	-12.9	0.20	-0.05	0.21		0.00E+00
C1	0.185	21.8	-4.9	-12.7	0.72	-0.16	0.73		0.00E+00
C2	0.148	7.2	0.5	4.0	0.24	0.02	0.24		0.00E+00
D1	0.227	15.1	-4.1	-15.2	0.50	-0.13	0.51		0.00E+00
D2	0.105	10.3	4.3	22.7	0.34	0.14	0.37		2.26E-01
D3	0.087	2.6	0.9	19.1	0.09	0.03	0.09		4.18E-02
E	0.150	29.9	-5.8	-11.0	0.98	-0.19	1.00		3.83E-01
F	0.114	14.3	2.9	11.5	0.47	0.10	0.48		1.36E-01
G	0.094	3.2	0.1	1.8	0.10	0.00	0.11		1.89E-02
H	0.138	19.6	-4.8	-13.8	0.64	-0.16	0.66		
I	0.210	22.8	-2.4	-6.0	0.75	-0.08	0.75		
Down5	0.091	17.2	10.9	32.4	0.56	0.36	0.67	0.12	0.18
Down4	0.164	51.0	7.5	8.4	1.67	0.25	1.69	0.55	0.83
Down3	0.183	38.5	3.4	5.0	1.26	0.11	1.27	0.46	0.69
Down2	0.200	34.2	0.1	0.2	1.12	0.00	1.12	0.45	0.67
Down1	0.197	19.8	-2.1	-6.1	0.65	-0.07	0.65	0.26	0.39

Table AII.4. (Continued)

Velocity Data - 500 Year Flood

Location	Measurement Depth (ft)	X vel (cm/s)	Y vel (cm/s)	Angle with X-Axis (deg)	X vel (ft/s)	Y vel (ft/s)	Current Velocity (ft/s)	q (cfs/ft)	Q (cfs)
A	0.093	6.1	-4.9	-38.8	0.20	-0.16	0.26		0.00E+00
B1	0.110	20.1	-1.1	-3.1	0.66	-0.04	0.66		0.00E+00
B2	0.106	7.4	-1.8	-13.7	0.24	-0.06	0.25		0.00E+00
C1	0.200	24.6	-2.4	-5.6	0.81	-0.08	0.81		0.00E+00
C2	0.162	8.8	-1.5	-9.7	0.29	-0.05	0.29		0.00E+00
D1	0.243	19.4	-2.6	-7.6	0.64	-0.09	0.64		0.00E+00
D2	0.117	6.2	-5.2	-40.0	0.20	-0.17	0.27		1.36E-01
D3	0.106	2.6	-1.4	-28.3	0.09	-0.05	0.10		4.18E-02
E	0.169	31.9	-1.9	-3.4	1.05	-0.06	1.05		4.08E-01
F	0.130	18.0	-2.8	-8.8	0.59	-0.09	0.60		1.71E-01
G	0.109	3.1	-1.5	-25.8	0.10	-0.05	0.11		1.83E-02
H	0.172	31.6	-3.9	-7.0	1.04	-0.13	1.04		
I	0.240	23.2	1.9	4.7	0.76	0.06	0.76		
Down5	0.130	36.0	20.8	30.0	1.18	0.68	1.36	0.35	0.53
Down4	0.196	35.5	12.4	19.3	1.16	0.41	1.23	0.48	0.72
Down3	0.214	36.1	9.8	15.2	1.18	0.32	1.23	0.53	0.79
Down2	0.234	31.2	5.2	9.5	1.02	0.17	1.04	0.49	0.73
Down1	0.227	23.8	1.7	4.1	0.78	0.06	0.78	0.36	0.53

Table AII.5. Stage data - Baseline condition

Gaging Data - 2 Year Flood

Date		2/3/98		
Flow	Field	5700	Model	1.16
Manometer Displacement		4.91		
Gage F	Elevation	661.8	Depth	0.28

Gage Designation	Point Gage Depth (model, ft)	Water Depth (prototype, ft)	Bed Elevation (prototype, ft)	Water Surface (prototype, ft)
A	0.115	3.45	664.69	668.14
B1	0.142	4.26	664.06	668.32
B2	0.147	4.41	663.83	668.24
C1	0.331	9.93	658.20	668.13
C2	0.258	7.74	660.23	667.97
D1	0.419	12.57	655.94	668.51
D2	0.168	5.04	663.20	668.24
D3	0.138	4.14	664.06	668.20
E	0.296	8.88	659.77	668.65
F	0.195	5.85	662.42	668.27
G	0.151	4.53	663.52	668.05
H	0.146	4.38	657.74	662.12
I	0.284	8.52	653.52	662.04

Gaging Data - 10 Year Flood

Date		2/3/98		
Flow	Field	8500	Model	1.72
Manometer Displacement		10.91		
Gage F	Elevation	663.5	Depth	0.33

Gage Designation	Point Gage Depth (model, ft)	Water Depth (prototype, ft)	Bed Elevation (prototype, ft)	Water Surface (prototype, ft)
A	0.142	4.26	664.69	668.95
B1	0.17	5.1	664.06	669.16
B2	0.166	4.98	663.83	668.81
C1	0.352	10.56	658.20	668.76
C2	0.279	8.37	660.23	668.60
D1	0.449	13.47	655.94	669.41
D2	0.192	5.76	663.20	668.96
D3	0.164	4.92	664.06	668.98
E	0.307	9.21	659.77	668.98
F	0.215	6.45	662.42	668.87
G	0.171	5.13	663.52	668.65
H	0.185	5.55	657.74	663.29
I	0.32	9.6	653.52	663.12

Table AII.5. (Continued)

Gaging Data - 50 Year Flood

Date		2/3/98		
Flow	Field	12500	Model	2.54
Manometer Displacement		23.60		
Gage F	Elevation	665.6	Depth	0.40

Gage Designation	Point Gage Depth (model, ft)	Water Depth (prototype, ft)	Bed Elevation (prototype, ft)	Water Surface (prototype, ft)
A	0.17	5.1	664.69	669.79
B1	0.189	5.67	664.06	669.73
B2	0.191	5.73	663.83	669.56
C1	0.375	11.25	658.20	669.45
C2	0.304	9.12	660.23	669.35
D1	0.473	14.19	655.94	670.13
D2	0.214	6.42	663.20	669.62
D3	0.187	5.61	664.06	669.67
E	0.334	10.02	659.77	669.79
F	0.239	7.17	662.42	669.59
G	0.201	6.03	663.52	669.55
H	0.256	7.68	657.74	665.42
I	0.391	11.73	653.52	665.25

Gaging Data - 100 Year Flood

Date		2/3/98		
Flow	Field	13500	Model	2.74
Manometer Displacement		27.52		
Gage F	Elevation	666	Depth	0.42

Gage Designation	Point Gage Depth (model, ft)	Water Depth (prototype, ft)	Bed Elevation (prototype, ft)	Water Surface (prototype, ft)
A	0.172	5.16	664.69	669.85
B1	0.191	5.73	664.06	669.79
B2	0.202	6.06	663.83	669.89
C1	0.381	11.43	658.20	669.63
C2	0.315	9.45	660.23	669.68
D1	0.482	14.46	655.94	670.40
D2	0.221	6.63	663.20	669.83
D3	0.191	5.73	664.06	669.79
E	0.337	10.11	659.77	669.88
F	0.25	7.5	662.42	669.92
G	0.202	6.06	663.52	669.58
H	0.288	8.64	657.74	666.38
I	0.413	12.39	653.52	665.91

Table AII.5. (Continued)

Gaging Data - 500 Year Flood

Date		2/3/98		
Flow	Field	17630	Model	3.58
Manometer Displacement		46.94		
Gage F	Elevation	667.8	Depth	0.48

Gage Designation	Point Gage Depth (model, ft)	Water Depth (prototype, ft)	Bed Elevation (prototype, ft)	Water Surface (prototype, ft)
A	0.199	5.97	664.69	670.66
B1	0.217	6.51	664.06	670.57
B2	0.221	6.63	663.83	670.46
C1	0.403	12.09	658.20	670.29
C2	0.324	9.72	660.23	669.95
D1	0.502	15.06	655.94	671.00
D2	0.244	7.32	663.20	670.52
D3	0.22	6.6	664.06	670.66
E	0.362	10.86	659.77	670.63
F	0.266	7.98	662.42	670.40
G	0.226	6.78	663.52	670.30
H	0.354	10.62	657.74	668.36
I	0.48	14.4	653.52	667.92

Table AII.6. Model velocity data - Baseline condition

Velocity and Flow Spit Data - Calibration Flow

Location	Measurement Depth (ft)	X vel (cm/s)	Y vel (cm/s)	Angle with X-Axis (deg)	X vel (ft/s)	Y vel (ft/s)	Current Velocity (ft/s)	q (cfs/ft)	Q (cfs)
LLane1	0.089	7.5	0.2	1.5	0.25	0.01	0.25	0.04	0.06
LLane2	0.171	8.0	0.9	6.4	0.26	0.03	0.26	0.09	0.12
LLane3	0.162	8.2	1.0	7.0	0.27	0.03	0.27	0.09	0.13
LLane4	0.160	9.0	1.3	8.2	0.30	0.04	0.30	0.10	0.14
LLane5	0.192	8.9	1.0	6.4	0.29	0.03	0.29	0.11	0.16
LLane6	0.194	9.0	2.0	12.5	0.30	0.07	0.30	0.12	0.16
RLane1	0.161	6.0	-3.0	-26.6	0.20	-0.10	0.22	0.07	0.13
RLane2	0.174	5.5	-1.2	-12.3	0.18	-0.04	0.18	0.06	0.09
RLane3	0.140	5.0	-1.0	-11.3	0.16	-0.03	0.17	0.05	0.06
RLane4	0.113	5.1	-0.8	-8.9	0.17	-0.03	0.17	0.04	0.05
RLane5	0.083	5.0	-0.6	-6.8	0.16	-0.02	0.17	0.03	0.03
A	Insufficient Depth								
B1	Insufficient Depth								
B2	Insufficient Depth								
C1	0.168	9.9	-0.1	-0.6	0.32	0.00	0.32		
C2	0.132	5.2	0.5	5.5	0.17	0.02	0.17		
D1	0.219	5.4	-0.5	-5.3	0.18	-0.02	0.18		
D2	0.087	4.2	1.9	24.3	0.14	0.06	0.15		
D3	Insufficient Depth								
E	0.112	6.5	-1.0	-8.7	0.21	-0.03	0.22		
F	0.101	10.0	1.0	5.7	0.33	0.03	0.33		
G	Insufficient Depth								
H	0.082	15.2	4.5	16.5	0.50	0.15	0.52		
I	0.151	16.0	1.5	5.4	0.52	0.05	0.53		
Down5	Insufficient Depth								
Down4	0.098	21.0	12.0	29.7	0.69	0.39	0.79	0.16	0.47
Down3	0.118	31.0	15.0	25.8	1.02	0.49	1.13	0.27	0.40
Down2	0.141	22.0	8.0	20.0	0.72	0.26	0.77	0.22	0.32
Down1	0.142	15.5	1.5	5.5	0.51	0.05	0.51	0.14	0.22

Table AII.6. (Continued)

Velocity Data - 2 Year Flood

Location	Measurement Depth (ft)	X vel (cm/s)	Y vel (cm/s)	Angle with X-Axis (deg)	X vel (ft/s)	Y vel (ft/s)	Current Velocity (ft/s)	q (cfs/ft)	Q (cfs)
A	Insufficient Depth								
B1	0.071	4.4	-0.8	-10.3	0.14	-0.03	0.15		
B2	Insufficient Depth								
C1	0.166	9.1	-1.1	-6.9	0.30	-0.04	0.30		
C2	0.129	5.8	-0.2	-2.0	0.19	-0.01	0.19		
D1	0.210	6.2	-1.1	-10.1	0.20	-0.04	0.21		
D2	0.084	5.6	1.3	13.1	0.18	0.04	0.19		
D3	Insufficient Depth								
E	0.148	7.4	-1.2	-9.2	0.24	-0.04	0.25		
F	0.098	8.5	1.1	7.4	0.28	0.04	0.28		
G	0.076	0.8	1.2	56.3	0.03	0.04	0.05		
H	0.075	12.2	2.6	12.0	0.40	0.09	0.41		
I	0.147	15.1	1.3	4.9	0.50	0.04	0.50		
Down5	Insufficient Depth								
Down4	0.098	20.0	11.0	28.8	0.66	0.36	0.75	0.15	0.44
Down3	0.115	29.0	14.8	27.0	0.95	0.49	1.07	0.25	0.37
Down2	0.143	21.5	4.2	11.1	0.71	0.14	0.72	0.21	0.31
Down1	0.133	14.7	0.8	3.1	0.48	0.03	0.48	0.13	0.19

Table AII.6. (Continued)

Velocity Data - 10 Year Flood

Location	Measurement Depth (ft)	X vel (cm/s)	Y vel (cm/s)	Angle with X-Axis (deg)	X vel (ft/s)	Y vel (ft/s)	Current Velocity (ft/s)	q (cfs/ft)	Q (cfs)
A	0.071	1.6	-0.4	-14.0	0.05	-0.01	0.05		
B1	0.085	9.3	-0.4	-2.5	0.31	-0.01	0.31		
B2	0.083	6.3	-1.4	-12.5	0.21	-0.05	0.21		
C1	0.176	12.3	-1.7	-7.9	0.40	-0.06	0.41		
C2	0.140	6.8	-0.2	-1.7	0.22	-0.01	0.22		
D1	0.225	7.9	-1.2	-8.6	0.26	-0.04	0.26		
D2	0.096	6.0	2.6	23.4	0.20	0.09	0.21		
D3	0.082	1.7	-0.3	-10.0	0.06	-0.01	0.06		
E	0.154	10.4	-1.4	-7.7	0.34	-0.05	0.34		
F	0.108	12.7	0.8	3.6	0.42	0.03	0.42		
G	0.085	3.8	0.4	6.0	0.12	0.01	0.13		
H	0.093	15.2	1.3	4.9	0.50	0.04	0.50		
I	0.160	22.4	1.8	4.6	0.73	0.06	0.74		
Down5	Insufficient Depth								
Down4	0.111	42.4	17.1	22.0	1.39	0.56	1.50	0.33	0.67
Down3	0.132	35.0	22.3	32.5	1.15	0.73	1.36	0.36	0.54
Down2	0.149	27.4	8.4	17.0	0.90	0.28	0.94	0.28	0.42
Down1	0.150	22.4	2.2	5.6	0.73	0.07	0.74	0.22	0.33

Table AII.6. (Continued)

Velocity Data - 50 Year Flood

Location	Measurement Depth (ft)	X vel (cm/s)	Y vel (cm/s)	Angle with X-Axis (deg)	X vel (ft/s)	Y vel (ft/s)	Current Velocity (ft/s)	q (cfs/ft)	Q (cfs)
A	0.085	-1.4	1.0	-35.5	-0.05	0.03	0.06		
B1	0.094	11.6	-1.2	-5.9	0.38	-0.04	0.38		
B2	0.096	6.8	-1.9	-15.6	0.22	-0.06	0.23		
C1	0.188	17.7	-1.8	-5.8	0.58	-0.06	0.58		
C2	0.152	7.5	-0.4	-3.1	0.25	-0.01	0.25		
D1	0.237	10.8	-2.2	-11.5	0.35	-0.07	0.36		
D2	0.107	9.2	3.6	21.4	0.30	0.12	0.32		
D3	0.093	4.1	-0.7	-9.7	0.13	-0.02	0.14		
E	0.167	13.8	-2.5	-10.3	0.45	-0.08	0.46		
F	0.120	16.9	-0.9	-3.0	0.55	-0.03	0.56		
G	0.101	4.1	1.0	13.7	0.13	0.03	0.14		
H	0.128	17.7	2.5	8.0	0.58	0.08	0.59		
I	0.196	31.0	2.4	4.4	1.02	0.08	1.02		
Down5	0.074	4.5	-1.3	-16.1	0.15	-0.04	0.15	0.02	0.03
Down4	0.138	74.0	34.0	24.7	2.43	1.12	2.67	0.73	1.10
Down3	0.166	38.0	13.0	18.9	1.25	0.43	1.32	0.44	0.66
Down2	0.183	28.5	7.0	13.8	0.94	0.23	0.96	0.35	0.53
Down1	0.184	31.5	1.2	2.2	1.03	0.04	1.03	0.38	0.57

Table AII.6. (Continued)

Velocity Data - 100 Year Flood

Location	Measurement Depth (ft)	X vel (cm/s)	Y vel (cm/s)	Angle with X-Axis (deg)	X vel (ft/s)	Y vel (ft/s)	Current Velocity (ft/s)	q (cfs/ft)	Q (cfs)
A	0.086	2.2	-0.8	-20.0	0.07	-0.03	0.08		
B1	0.096	12.3	-0.6	-2.8	0.40	-0.02	0.40		
B2	0.101	6.5	-1.2	-10.5	0.21	-0.04	0.22		
C1	0.191	18.9	-2.5	-7.5	0.62	-0.08	0.63		
C2	0.158	9.2	-1.5	-9.3	0.30	-0.05	0.31		
D1	0.241	12.3	-1.8	-8.3	0.40	-0.06	0.41		
D2	0.111	6.3	-1.2	-10.8	0.21	-0.04	0.21		
D3	0.095	2.0	-0.4	-11.3	0.07	-0.01	0.07		
E	0.169	15.1	-2.3	-8.7	0.50	-0.08	0.50		
F	0.125	16.4	2.8	9.7	0.54	0.09	0.55		
G	0.101	3.5	1.0	15.9	0.11	0.03	0.12		
H	0.144	18.8	2.7	8.2	0.62	0.09	0.62		
I	0.207	31.0	0.9	1.7	1.02	0.03	1.02		
Down5	0.081	4.4	5.4	50.8	0.14	0.18	0.23	0.04	0.06
Down4	0.167	61.0	28.0	24.7	2.00	0.92	2.20	0.74	1.10
Down3	0.181	37.9	13.6	19.7	1.24	0.45	1.32	0.48	0.72
Down2	0.194	28.1	5.9	11.9	0.92	0.19	0.94	0.36	0.55
Down1	0.199	29.4	1.5	2.9	0.96	0.05	0.97	0.38	0.58

Table AII.6. (Continued)

Velocity Data - 500 Year Flood

Location	Measurement Depth (ft)	X vel (cm/s)	Y vel (cm/s)	Angle with X-Axis (deg)	X vel (ft/s)	Y vel (ft/s)	Current Velocity (ft/s)	q (cfs/ft)	Q (cfs)
A	0.100	4.4	-1.1	-14.0	0.14	-0.04	0.15		
B1	0.109	15.1	-2.0	-7.5	0.50	-0.07	0.50		
B2	0.111	2.0	-1.2	-31.0	0.07	-0.04	0.08		
C1	0.202	22.1	-4.8	-12.3	0.73	-0.16	0.74		
C2	0.162	10.4	-2.6	-14.0	0.34	-0.09	0.35		
D1	0.251	13.0	-2.9	-12.6	0.43	-0.10	0.44		
D2	0.122	7.2	-4.0	-29.1	0.24	-0.13	0.27		
D3	0.110	2.9	-1.0	-19.0	0.10	-0.03	0.10		
E	0.181	17.2	-4.1	-13.4	0.56	-0.13	0.58		
F	0.133	18.1	-2.0	-6.3	0.59	-0.07	0.60		
G	0.113	4.1	0.1	1.4	0.13	0.00	0.13		
H	0.177	18.0	-0.5	-1.6	0.59	-0.02	0.59		
I	0.240	31.0	0.5	0.9	1.02	0.02	1.02		
Down5	0.129	26.0	15.5	30.8	0.85	0.51	0.99	0.26	0.38
Down4	0.196	50.0	19.0	20.8	1.64	0.62	1.75	0.69	1.03
Down3	0.212	37.8	9.0	13.4	1.24	0.30	1.27	0.54	0.81
Down2	0.230	28.8	2.8	5.6	0.94	0.09	0.95	0.44	0.66
Down1	0.228	28.0	-0.2	-0.4	0.92	-0.01	0.92	0.42	0.63

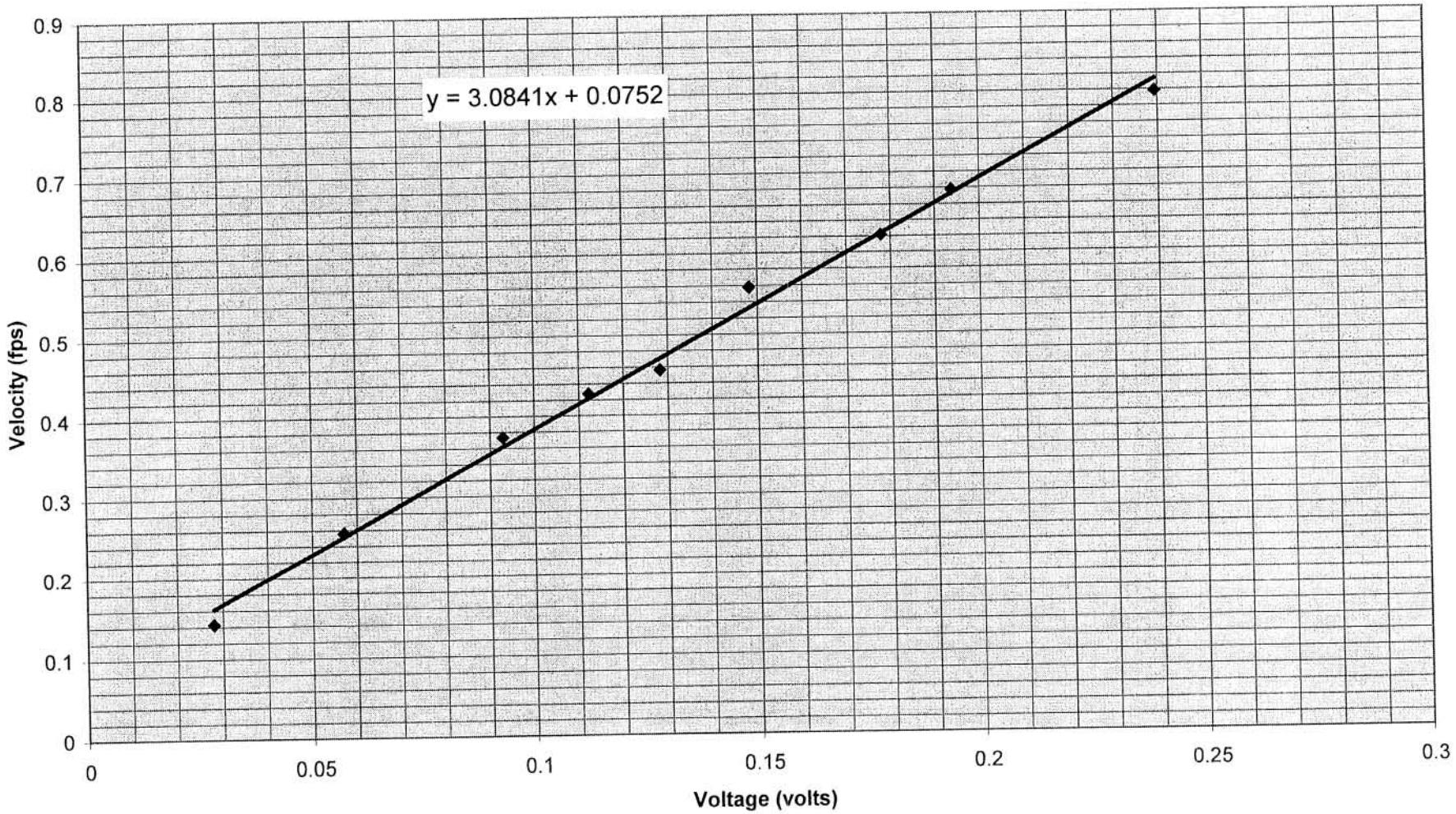

Figure AII.1. Propeller velocity meter calibration (X1), September 18. 1997

Appendix III

Table AIII.1 Bathtub spillway design - initial design parameters and control section design

KEY

Conditions on site	**BOLD**
Calculated values	normal
Design variables	
Matched conditions	

Spillway Length	
Existing headwater elevation (ft)	**667.75**
Dam crest elevation (ft)	**665**
Resulting head (ft)	2.75
Assumed C	3.6
q (cfs/ft)	16.41729
Required Length (ft)	347.1949
Approx circular length (ft)	84.623
Length of tub (ft)	131.2859

Control Section	
Rectangular channel exit width (ft)	53.90
Design Flow (cfs)	5700.00
Flow per unit width of channel (cfs/ft)	105.75
yc -critical depth (ft)	7.03
R - hydraulic radius (ft)	5.58
A - flow area (ft^2)	378.87
Mannings n	0.015
Critical slope	0.0023
Critical velocity (ft/s)	15.04
Critical velocity head (ft)	3.51
Exit channel Elevation (ft)	654.90
Energy grade line (ft)	665.44
Tailwater Condition @ exit (Station 0') (ft)	661.93
Existing tailwater condition (ft)	**661.92**
Water surface at entrance to control reach (Station -20') (ft)	663.97

Table AIII.2 Bathtub spillway design - approximate water surface profile along discharge channel centerline for design flow (5700 cfs)

1 Station (ft)	2 Delta X (ft)	3 Bottom (ft)	4 Trial Delta Y (ft)	5 W.S El (ft)	6 d (ft)	7 Width (ft)	8 A (sq ft)	9 Q (cfs)	10 V (ft/s)
-20.00		654.90		661.93	7.03	53.90	378.87	5700.00	15.04
0.00		654.95		663.97	9.02	53.90	526.86	5700.00	10.82
26.26	26.26	655.01	1.27	665.24	10.23	53.90	603.66	4837.86	8.01
52.51	26.26	655.07	0.71	665.95	10.88	53.90	645.50	3975.71	6.16
78.77	26.26	655.13	0.48	666.43	11.30	53.90	672.73	3113.57	4.63
105.03	26.26	655.19	0.32	666.75	11.56	53.90	689.66	2251.42	3.26
131.29	26.26	655.25	0.21	666.96	11.71	53.90	699.43	1389.28	1.99

11 Q1+Q2	12 Q1/(g*(Q1+Q2)	13 v1+v2	14 V2-V1	15 (Q2-Q1)	16 Q2-Q1/Q1	17 V2(Q2-Q1/Q1)	18 14+17	19 Calculated Delta Y 12*13*18
10537.86	0.01	18.83	2.80	862.14	0.18	1.93	4.73	1.27
8813.57	0.01	14.17	1.86	862.14	0.22	1.74	3.59	0.71
7089.28	0.01	10.79	1.53	862.14	0.28	1.71	3.24	0.48
5364.99	0.01	7.89	1.36	862.14	0.38	1.77	3.14	0.32
3640.71	0.01	5.25	1.28	862.14	0.62	2.03	3.30	0.21

Table AIII.3. Stage Data - Alternative I (Bathtub Spillway)

Gaging Data - 2 Year Flood

Date		12/10/97		
Flow	Field	5700	Model	1.16
Manometer Displacement		4.91		
Gage F	Elevation	661.8	Depth	0.28

Gage Designation	Point Gage Depth (model, ft)	Water Depth (prototype, ft)	Bed Elevation (prototype, ft)	Water Surface (prototype, ft)
A	0.098	2.94	664.69	667.63
B1	0.121	3.63	664.06	667.69
B2	0.127	3.81	663.83	667.64
C1	0.312	9.36	658.20	667.56
C2	0.236	7.08	660.23	667.31
D1	0.397	11.91	655.94	667.85
D2	0.149	4.47	663.20	667.67
D3	0.118	3.54	664.06	667.60
E	0.261	7.83	659.77	667.60
F	0.17	5.1	662.42	667.52
G	0.132	3.96	663.52	667.48
H	0.141	4.23	657.74	661.97
I	0.28	8.4	653.52	661.92

Gaging Data - 10 Year Flood

Date		12/10/97		
Flow	Field	8500	Model	1.72
Manometer Displacement		10.91		
Gage F	Elevation	663.5	Depth	0.33

Gage Designation	Point Gage Depth (model, ft)	Water Depth (prototype, ft)	Bed Elevation (prototype, ft)	Water Surface (prototype, ft)
A	0.116	3.48	664.69	668.17
B1	0.142	4.26	664.06	668.32
B2	0.148	4.44	663.83	668.27
C1	0.328	9.84	658.20	668.04
C2	0.261	7.83	660.23	668.06
D1	0.421	12.63	655.94	668.57
D2	0.176	5.28	663.20	668.48
D3	0.139	4.17	664.06	668.23
E	0.287	8.61	659.77	668.38
F	0.191	5.73	662.42	668.15
G	0.151	4.53	663.52	668.05
H	0.199	5.97	657.74	663.71
I	0.33	9.9	653.52	663.42

Table AIII.3. (Continued)

Gaging Data - 50 Year Flood

Date		12/10/97		
Flow	Field	12500	Model	2.54
Manometer Displacement		23.60		
Gage F	Elevation	665.6	Depth	0.40

Gage Designation	Point Gage Depth (model, ft)	Water Depth (prototype, ft)	Bed Elevation (prototype, ft)	Water Surface (prototype, ft)
A	0.15	4.5	664.69	669.19
B1	0.171	5.13	664.06	669.19
B2	0.17	5.1	663.83	668.93
C1	0.354	10.62	658.20	668.82
C2	0.283	8.49	660.23	668.72
D1	0.456	13.68	655.94	669.62
D2	0.197	5.91	663.20	669.11
D3	0.166	4.98	664.06	669.04
E	0.313	9.39	659.77	669.16
F	0.209	6.27	662.42	668.69
G	0.174	5.22	663.52	668.74
H	0.26	7.8	657.74	665.54
I	0.395	11.85	653.52	665.37

Gaging Data - 100 Year Flood

Date		12/10/97		
Flow	Field	13500	Model	2.74
Manometer Displacement		27.52		
Gage F	Elevation	666	Depth	0.42

Gage Designation	Point Gage Depth (model, ft)	Water Depth (prototype, ft)	Bed Elevation (prototype, ft)	Water Surface (prototype, ft)
A	0.154	4.62	664.69	669.31
B1	0.179	5.37	664.06	669.43
B2	0.181	5.43	663.83	669.26
C1	0.363	10.89	658.20	669.09
C2	0.292	8.76	660.23	668.99
D1	0.458	13.74	655.94	669.68
D2	0.201	6.03	663.20	669.23
D3	0.171	5.13	664.06	669.19
E	0.316	9.48	659.77	669.25
F	0.218	6.54	662.42	668.96
G	0.181	5.43	663.52	668.95
H	0.294	8.82	657.74	666.56
I	0.42	12.6	653.52	666.12

Table AIII.3. (Continued)

Gaging Data - 500 Year Flood

Date		12/10/97		
Flow	Field	17630	Model	3.58
Manometer Displacement		46.94		
Gage F	Elevation	667.8	Depth	0.48

Gage Designation	Point Gage Depth (model, ft)	Water Depth (prototype, ft)	Bed Elevation (prototype, ft)	Water Surface (prototype, ft)
A	0.18	5.4	664.69	670.09
B1	0.208	6.24	664.06	670.30
B2	0.202	6.06	663.83	669.89
C1	0.384	11.52	658.20	669.72
C2	0.314	9.42	660.23	669.65
D1	0.488	14.64	655.94	670.58
D2	0.23	6.9	663.20	670.10
D3	0.196	5.88	664.06	669.94
E	0.348	10.44	659.77	670.21
F	0.242	7.26	662.42	669.68
G	0.209	6.27	663.52	669.79
H	0.35	10.5	657.74	668.24
I	0.48	14.4	653.52	667.92

Table AIII.4. Model velocity data - Alternative I (Bathtub Spillway)

Velocity and Flow Spit Data - Calibration Flow

Location	Measurement Depth (ft)	X vel (cm/s)	Y vel (cm/s)	Angle with X-Axis (deg)	X vel (ft/s)	Y vel (ft/s)	Current Velocity (ft/s)	q (cfs/ft)	Q (cfs)
LLane1 (B1)	0.078	6.2	0.9	8.3	0.20	0.03	0.21	0.03	0.05
LLane2	0.163	6.7	1.1	9.3	0.22	0.04	0.22	0.07	0.10
LLane3	0.165	7.2	1.5	11.8	0.24	0.05	0.24	0.08	0.12
LLane4.	0.164	7.3	2.2	16.8	0.24	0.07	0.25	0.08	0.11
LLane5	0.189	7.4	2.0	15.1	0.24	0.07	0.25	0.10	0.14
LLane6	0.185	7.6	2.1	15.4	0.25	0.07	0.26	0.10	0.13
RLane1	0.155	7.5	-3.9	-27.5	0.25	-0.13	0.28	0.09	0.16
RLane2	0.166	6.0	-1.9	-17.6	0.20	-0.06	0.21	0.07	0.10
RLane3	0.133	6.3	-1.5	-13.4	0.21	-0.05	0.21	0.06	0.08
RLane4.	0.101	6.2	-1.4	-12.7	0.20	-0.05	0.21	0.04	0.06
RLane5	0.075	6.2	-1.3	-11.8	0.20	-0.04	0.21	0.03	0.04
A	Insufficient Depth								
B1	Insufficient Depth								
C1	0.157	7.2	0.8	6.3	0.24	0.03	0.24		
C2	0.118	6.2	-0.9	-8.3	0.20	-0.03	0.21		
D1	0.240	4.5	-0.5	-6.3	0.15	-0.02	0.15		
D2	0.076	4.9	1.0	11.5	0.16	0.03	0.16		
D3	0.062	1.1	-0.2	-10.3	0.04	-0.01	0.04		
E	0.136	4.9	-0.2	-2.3	0.16	-0.01	0.16		
F	0.086	8.6	10.0	49.3	0.28	0.33	0.43		
G	0.070	0.8	0.1	7.1	0.03	0.00	0.03		
H	0.081	5.5	3.9	35.1	0.18	0.13	0.22		
I	0.150	14.5	4.5	17.2	0.48	0.15	0.50		
Tub	0.098	43.0	23.0	28.1	1.41	0.75	1.60		
Down5	Insufficient Depth								
Down4.	0.095	12.5	8.5	34.2	0.41	0.28	0.50	0.09	0.28
Down3	0.105	24.5	13.0	28.0	0.80	0.43	0.91	0.19	0.29
Down2	0.107	34.0	16.0	25.2	1.12	0.52	1.23	0.26	0.40
Down1	0.135	13.0	3.0	13.0	0.43	0.10	0.44	0.12	0.18

Table AIII.4. (Continued)

Velocity Data - 2 Year Flood

Location	Measurement Depth (ft)	X vel (cm/s)	Y vel (cm/s)	Angle with X-Axis (deg)	X vel (ft/s)	Y vel (ft/s)	Current Velocity (ft/s)	q (cfs/ft)	Q (cfs)
A	Insufficient Depth								
B1	Insufficient Depth								
B2	Insufficient Depth								
C1	0.158	8.0	-1.2	-8.5	0.26	-0.04	0.27		
C2	0.124	5.0	-0.2	-2.3	0.16	-0.01	0.16		
D1	0.203	5.0	-1.0	-11.3	0.16	-0.03	0.17		
D2	0.075	6.0	-1.0	-9.5	0.20	-0.03	0.20		
D3	Insufficient Depth								
E	0.132	5.0	-1.2	-13.5	0.16	-0.04	0.17		
F	0.087	12.5	6.0	25.6	0.41	0.20	0.45		
G	Insufficient Depth								
H	0.042	5.2	3.1	30.8	0.17	0.10	0.20		
I	0.142	18.0	0.9	2.9	0.59	0.03	0.59		
Tub	0.099	45.0	7.0	8.8	1.48	0.23	1.49		
Down5	Insufficient Depth								
Down4.	0.093	16.0	3.5	12.3	0.52	0.11	0.54	0.10	0.30
Down3	0.110	31.0	5.0	9.2	1.02	0.16	1.03	0.23	0.34
Down2	0.129	37.0	4.0	6.2	1.21	0.13	1.22	0.32	0.47
Down1	0.127	14.0	1.0	4.1	0.46	0.03	0.46	0.12	0.18

Table AIII.4. (Continued)

Velocity Data - 10 Year Flood

Location	Measurement Depth (ft)	X vel (cm/s)	Y vel (cm/s)	Angle with X-Axis (deg)	X vel (ft/s)	Y vel (ft/s)	Current Velocity (ft/s)	q (cfs/ft)	Q (cfs)
A	Insufficient Depth								
B1	0.071	9.5	-1.5	-9.0	0.31	-0.05	0.32		
B2	0.074	6.8	-2.0	-16.4	0.22	-0.07	0.23		
C1	0.164	11.5	-2.9	-14.2	0.38	-0.10	0.39		
C2	0.131	6.9	-0.8	-6.6	0.23	-0.03	0.23		
D1	0.211	7.0	-2.0	-15.9	0.23	-0.07	0.24		
D2	0.088	6.5	-0.5	-4.4	0.21	-0.02	0.21		
D3	0.070	1.0	0.2	11.3	0.03	0.01	0.03		
E	0.144	8.1	-2.1	-14.5	0.27	-0.07	0.27		
F	0.096	16.6	8.2	26.3	0.54	0.27	0.61		
G	0.076	1.0	-1.2	-50.2	0.03	-0.04	0.05		
H	0.100	10.0	0.2	1.1	0.33	0.01	0.33		
I	0.165	16.0	-0.5	-1.8	0.52	-0.02	0.53		
Tub	0.121	60.0	9.0	8.5	1.97	0.30	1.99		
Down5	Insufficient Depth								
Down4.	0.119	52.0	14.0	15.1	1.71	0.46	1.77	0.42	0.84
Down3	0.137	34.0	3.0	5.0	1.12	0.10	1.12	0.31	0.46
Down2	0.153	45.0	2.0	2.5	1.48	0.07	1.48	0.45	0.68
Down1	0.145	12.0	-1.0	-4.8	0.39	-0.03	0.40	0.11	0.17

Table AIII.4. (Continued)

Velocity Data - 50 Year Flood

Location	Measurement Depth (ft)	X vel (cm/s)	Y vel (cm/s)	Angle with X-Axis (deg)	X vel (ft/s)	Y vel (ft/s)	Current Velocity (ft/s)	q (cfs/ft)	Q (cfs)
A	0.075	1.8	0.9	26.6	0.06	0.03	0.07		
B1	0.086	11.2	-0.3	-1.5	0.37	-0.01	0.37		
B2	0.085	7.1	-1.5	-11.9	0.23	-0.05	0.24		
C1	0.177	16.8	-1.9	-6.5	0.55	-0.06	0.55		
C2	0.140	9.2	0.3	1.9	0.30	0.01	0.30		
D1	0.228	8.5	-1.2	-8.0	0.28	-0.04	0.28		
D2	0.099	8.8	2.3	14.6	0.29	0.08	0.30		
D3	0.083	2.1	0.6	15.9	0.07	0.02	0.07		
E	0.157	12.0	-1.8	-8.5	0.39	-0.06	0.40		
F	0.104	19.1	10.6	29.0	0.63	0.35	0.72		
G	0.087	2.6	-0.8	-17.1	0.09	-0.03	0.09		
H	0.130	14.7	2.1	8.1	0.48	0.07	0.49		
I	0.198	21.8	1.8	4.7	0.72	0.06	0.72		
Tub	0.144	60.0	10.5	9.9	1.97	0.34	2.00		
Down5	0.076	3.3	4.2	51.8	0.11	0.14	0.18	0.03	0.04
Down4.	0.146	58.0	28.0	25.8	1.90	0.92	2.11	0.62	0.93
Down3	0.174	39.0	8.8	12.7	1.28	0.29	1.31	0.46	0.68
Down2	0.185	48.0	10.5	12.3	1.57	0.34	1.61	0.59	0.89
Down1	0.184	20.5	1.4	3.9	0.67	0.05	0.67	0.25	0.37

Table AIII.4. (Continued)

Velocity Data - 100 Year Flood

Location	Measurement Depth (ft)	X vel (cm/s)	Y vel (cm/s)	Angle with X-Axis (deg)	X vel (ft/s)	Y vel (ft/s)	Current Velocity (ft/s)	q (cfs/ft)	Q (cfs)
A	0.075	1.2	-1.2	-45.0	0.04	-0.04	0.06		
B1	0.089	15.1	0.3	1.1	0.50	0.01	0.50		
B2	0.091	7.0	-1.1	-8.9	0.23	-0.04	0.23		
C1	0.182	17.6	-1	-3.3	0.58	-0.03	0.58		
C2	0.146	11.1	0.8	4.1	0.36	0.03	0.37		
D1	0.229	11.7	-1.2	-5.9	0.38	-0.04	0.39		
D2	0.099	9.8	4.5	24.9	0.32	0.15	0.35		
D3	0.086	2.7	0.7	14.5	0.09	0.02	0.09		
E	0.158	12.1	-1.3	-6.1	0.40	-0.04	0.40		
F	0.109	20.8	12.5	31.0	0.68	0.41	0.80		
G	0.091	3.0	0.5	9.5	0.10	0.02	0.10		
H	0.147	14.8	3.2	12.2	0.49	0.10	0.50		
I	0.210	22.0	2.1	5.5	0.72	0.07	0.73		
Tub	0.153	63.0	21.5	18.8	2.07	0.71	2.18		
Down5	0.093	23.5	20.0	40.4	0.77	0.66	1.01	0.19	0.28
Down4.	0.171	33.8	14.0	22.5	1.11	0.46	1.20	0.41	0.62
Down3	0.183	39.0	8.3	12.0	1.28	0.27	1.31	0.48	0.72
Down2	0.200	39.0	8.6	12.4	1.28	0.28	1.31	0.52	0.79
Down1	0.203	19.8	1.6	4.6	0.65	0.05	0.65	0.26	0.40

Table AIII.4. (Continued)

Velocity Data - 500 Year Flood

Location	Measurement Depth (ft)	X vel (cm/s)	Y vel (cm/s)	Angle with X-Axis (deg)	X vel (ft/s)	Y vel (ft/s)	Current Velocity (ft/s)	q (cfs/ft)	Q (cfs)
A	0.090	6.0	-4.0	-33.7	0.20	-0.13	0.24		
B1	0.104	14.2	0.9	3.6	0.47	0.03	0.47		
B2	0.101	5.8	-1.8	-17.2	0.19	-0.06	0.20		
C1	0.192	22.8	-1.3	-3.3	0.75	-0.04	0.75		
C2	0.157	12.4	-1.1	-5.1	0.41	-0.04	0.41		
D1	0.244	12.6	-1.2	-5.4	0.41	-0.04	0.42		
D2	0.115	12.7	4.3	18.7	0.42	0.14	0.44		
D3	0.098	5.9	-0.4	-3.9	0.19	-0.01	0.19		
E	0.174	16.1	-1.2	-4.3	0.53	-0.04	0.53		
F	0.145	22.5	12.5	29.1	0.74	0.41	0.84		
G	0.105	5.2	2.1	22.0	0.17	0.07	0.18		
H	0.175	16.3	2.4	8.4	0.53	0.08	0.54		
I	0.240	29.7	3.0	5.8	0.97	0.10	0.98		
Tub	0.166	51.0	11.0	12.2	1.67	0.36	1.71		
Down5	0.117	24.7	17.3	35.0	0.81	0.57	0.99	0.23	0.35
Down4.	0.192	34.2	12.4	19.9	1.12	0.41	1.19	0.46	0.69
Down3	0.210	39.7	10.2	14.4	1.30	0.33	1.34	0.56	0.85
Down2	0.227	36.2	9.3	14.4	1.19	0.31	1.23	0.56	0.84
Down1	0.253	28.0	3.8	7.7	0.92	0.12	0.93	0.47	0.70

Table AIII.5. Stage Data - Alternative II (Rock Dam)

Gaging Data - 2 Year Flood

Date		2/10/98		
Flow	Field	5700	Model	1.16
Manometer Displacement		4.91		
Gage F	Elevation	661.8	Depth	0.28

Gage Designation	Point Gage Depth (model, ft)	Water Depth (prototype, ft)	Bed Elevation (prototype, ft)	Water Surface (prototype, ft)
A	0.105	3.15	664.69	667.84
B1	0.127	3.81	664.06	667.87
B2	0.129	3.87	663.83	667.70
C1	0.315	9.45	658.20	667.65
C2	0.244	7.32	660.23	667.55
D1	0.409	12.27	655.94	668.21
D2	0.152	4.56	663.20	667.76
D3	0.124	3.72	664.06	667.78
E	0.271	8.13	659.77	667.90
F	0.181	5.43	662.42	667.85
G	0.135	4.05	663.52	667.57
H	0.141	4.23	657.74	661.97
I	0.28	8.4	653.52	661.92

Gaging Data - 10 Year Flood

Date		2/10/98		
Flow	Field	8500	Model	1.72
Manometer Displacement		10.91		
Gage F	Elevation	663.5	Depth	0.33

Gage Designation	Point Gage Depth (model, ft)	Water Depth (prototype, ft)	Bed Elevation (prototype, ft)	Water Surface (prototype, ft)
A	0.135	4.05	664.69	668.74
B1	0.155	4.65	664.06	668.71
B2	0.164	4.92	663.83	668.75
C1	0.346	10.38	658.20	668.58
C2	0.273	8.19	660.23	668.42
D1	0.444	13.32	655.94	669.26
D2	0.186	5.58	663.20	668.78
D3	0.155	4.65	664.06	668.71
E	0.3	9	659.77	668.77
F	0.211	6.33	662.42	668.75
G	0.165	4.95	663.52	668.47
H	0.166	4.98	657.74	662.72
I	0.3	9	653.52	662.52

Table AIII.5. (Continued)

Gaging Data - 50 Year Flood

Date		2/10/98		
Flow	Field	12500	Model	2.54
Manometer Displacement		23.60		
Gage F	Elevation	665.6	Depth	0.40

Gage Designation	Point Gage Depth (model, ft)	Water Depth (prototype, ft)	Bed Elevation (prototype, ft)	Water Surface (prototype, ft)
A	0.168	5.04	664.69	669.73
B1	0.191	5.73	664.06	669.79
B2	0.194	5.82	663.83	669.65
C1	0.378	11.34	658.20	669.54
C2	0.307	9.21	660.23	669.44
D1	0.471	14.13	655.94	670.07
D2	0.215	6.45	663.20	669.65
D3	0.188	5.64	664.06	669.70
E	0.333	9.99	659.77	669.76
F	0.241	7.23	662.42	669.65
G	0.195	5.85	663.52	669.37
H	0.272	8.16	657.74	665.90
I	0.4	12	653.52	665.52

Gaging Data - 100 Year Flood

Date		2/10/98		
Flow	Field	13500	Model	2.74
Manometer Displacement		27.52		
Gage F	Elevation	666	Depth	0.42

Gage Designation	Point Gage Depth (model, ft)	Water Depth (prototype, ft)	Bed Elevation (prototype, ft)	Water Surface (prototype, ft)
A	0.176	5.28	664.69	669.97
B1	0.196	5.88	664.06	669.94
B2	0.202	6.06	663.83	669.89
C1	0.383	11.49	658.20	669.69
C2	0.314	9.42	660.23	669.65
D1	0.476	14.28	655.94	670.22
D2	0.222	6.66	663.20	669.86
D3	0.195	5.85	664.06	669.91
E	0.34	10.2	659.77	669.97
F	0.251	7.53	662.42	669.95
G	0.208	6.24	663.52	669.76
H	0.292	8.76	657.74	666.50
I	0.411	12.33	653.52	665.85

Table AIII.5. (Continued)

Gaging Data - 500 Year Flood

Date		2/10/98		
Flow	Field	17630	Model	3.58
Manometer Displacement		46.94		
Gage F	Elevation	667.8	Depth	0.48

Gage Designation	Point Gage Depth (model, ft)	Water Depth (prototype, ft)	Bed Elevation (prototype, ft)	Water Surface (prototype, ft)
A	0.204	6.12	664.69	670.81
B1	0.217	6.51	664.06	670.57
B2	0.227	6.81	663.83	670.64
C1	0.406	12.18	658.20	670.38
C2	0.336	10.08	660.23	670.31
D1	0.498	14.94	655.94	670.88
D2	0.243	7.29	663.20	670.49
D3	0.216	6.48	664.06	670.54
E	0.361	10.83	659.77	670.60
F	0.276	8.28	662.42	670.70
G	0.232	6.96	663.52	670.48
H	0.335	10.05	657.74	667.79
I	0.48	14.4	653.52	667.92

Table AIII.6 Model velocity data - Alternative II (Rock Dam)

Velocity and Flow Spit Data - Calibration Flow

Location	Measurement Depth (ft)	X vel (cm/s)	Y vel (cm/s)	Angle with X-Axis (deg)	X vel (ft/s)	Y vel (ft/s)	Current Velocity (ft/s)	q (cfs/ft)	Q (cfs)
LLane1	0.079	6.2	-0.6	-5.5	0.20	-0.02	0.20	0.03	0.05
LLane2	0.163	6.6	1.3	11.1	0.22	0.04	0.22	0.07	0.10
LLane3	0.155	6.7	1.0	8.5	0.22	0.03	0.22	0.07	0.11
LLane4	0.152	9.6	3.2	18.4	0.31	0.10	0.33	0.10	0.15
LLane5	0.184	9.7	3.1	17.7	0.32	0.10	0.33	0.12	0.18
LLane6	0.185	10.7	4.2	21.4	0.35	0.14	0.38	0.14	0.19
RLane1	0.153	6.4	-1.3	-11.5	0.21	-0.04	0.21	0.07	0.14
RLane2	0.169	6.1	-2.0	-18.2	0.20	-0.07	0.21	0.07	0.10
RLane3	0.133	5.8	-1.2	-11.7	0.19	-0.04	0.19	0.05	0.07
RLane4	0.103	5.2	-0.3	-3.3	0.17	-0.01	0.17	0.04	0.05
RLane5	0.077	3.2	-0.4	-7.1	0.10	-0.01	0.11	0.02	0.02
A	Insufficient Depth								
B1	0.068	7.8	-0.6	-4.4	0.26	-0.02	0.26		
B2	0.067	1.9	-1.9	-45.0	0.06	-0.06	0.09		
C1	0.161	9.9	-3.8	-21.0	0.32	-0.12	0.35		
C2	0.124	3.8	5.2	53.8	0.12	0.17	0.21		
D1	0.210	6.1	-3.8	-31.9	0.20	-0.12	0.24		
D2	0.079	3.8	5.8	56.8	0.12	0.19	0.23		
D3	Insufficient Depth								
E	0.140	8.5	-3.0	-19.4	0.28	-0.10	0.30		
F	0.093	6.7	3.1	24.8	0.22	0.10	0.24		
G	Insufficient Depth								
H	0.076	21.8	-1.3	-3.4	0.72	-0.04	0.72		
I	0.145	21.1	-2.3	-6.2	0.69	-0.08	0.70		
Down5	Insufficient Depth								
Down4	0.097	7.6	5.1	33.9	0.25	0.17	0.30	0.06	0.17
Down3	0.108	23.9	8.2	18.9	0.78	0.27	0.83	0.18	0.27
Down2	0.133	21.6	3.4	8.9	0.71	0.11	0.72	0.19	0.29
Down1	0.130	22.2	-2.4	-6.2	0.73	-0.08	0.73	0.19	0.29

Table AIII.6. (Continued)

Velocity Data - 2 Year Flood

Location	Measurement Depth (ft)	X vel (cm/s)	Y vel (cm/s)	Angle with X-Axis (deg)	X vel (ft/s)	Y vel (ft/s)	Current Velocity (ft/s)	q (cfs/ft)	Q (cfs)
A	Insufficient Depth								
B1	Insufficient Depth								
B2	0.065	3.2	2.8	41.2	0.10	0.09	0.14		
C1	0.158	8.2	1.9	13.0	0.27	0.06	0.28		
C2	0.122	4.9	3.8	37.8	0.16	0.12	0.20		
D1	0.205	5.6	1.3	13.1	0.18	0.04	0.19		
D2	0.076	3.9	4.2	47.1	0.13	0.14	0.19		
D3	0.062	1.3	5.1	75.7	0.04	0.17	0.17		
E	0.136	8.0	0.8	5.7	0.26	0.03	0.26		
F	0.091	7.4	5.3	35.6	0.24	0.17	0.30		
G	0.068	0.8	5.7	82.0	0.03	0.19	0.19		
H	0.071	19.8	0.4	1.2	0.65	0.01	0.65		
I	0.140	20.7	-1.6	-4.4	0.68	-0.05	0.68		
Down5	Insufficient Depth								
Down4	0.085	20.2	4.8	13.4	0.66	0.16	0.68	0.12	0.35
Down3	0.106	30.5	8.3	15.2	1.00	0.27	1.04	0.22	0.33
Down2	0.128	22.8	3.7	9.2	0.75	0.12	0.76	0.19	0.29
Down1	0.124	22.5	-0.4	-1.0	0.74	-0.01	0.74	0.18	0.27

Table AIII.6. (Continued)

Velocity Data - 10 Year Flood

Location	Measurement Depth (ft)	X vel (cm/s)	Y vel (cm/s)	Angle with X-Axis (deg)	X vel (ft/s)	Y vel (ft/s)	Current Velocity (ft/s)	q (cfs/ft)	Q (cfs)
A	0.067	4.8	0.3	3.6	0.16	0.01	0.16		
B1	0.077	11.3	3.3	16.3	0.37	0.11	0.39		
B2	0.082	4.1	3.2	38.0	0.13	0.10	0.17		
C1	0.173	14.3	4.1	16.0	0.47	0.13	0.49		
C2	0.137	6.2	3.5	29.4	0.20	0.11	0.23		
D1	0.224	8.2	4.8	30.3	0.27	0.16	0.31		
D2	0.093	1.9	1.0	27.8	0.06	0.03	0.07		
D3	0.078	1.0	4.4	77.2	0.03	0.14	0.15		
E	0.150	12.1	3.6	16.6	0.40	0.12	0.41		
F	0.106	10.6	4.2	21.6	0.35	0.14	0.37		
G	0.082	2.2	4.4	63.4	0.07	0.14	0.16		
H	0.083	26.7	11.4	23.1	0.88	0.37	0.95		
I	0.150	33.0	5.8	10.0	1.08	0.19	1.10		
Down5	Insufficient Depth								
Down4	0.100	17.5	14.7	40.0	0.57	0.48	0.75	0.15	0.30
Down3	0.117	36.7	17.4	25.4	1.20	0.57	1.33	0.31	0.47
Down2	0.137	32.2	21.0	33.1	1.06	0.69	1.26	0.35	0.52
Down1	0.134	33.6	6.2	10.5	1.10	0.20	1.12	0.30	0.45

Table AIII.6. (Continued)

Velocity Data - 50 Year Flood

Location	Measurement Depth (ft)	X vel (cm/s)	Y vel (cm/s)	Angle with X-Axis (deg)	X vel (ft/s)	Y vel (ft/s)	Current Velocity (ft/s)	q (cfs/ft)	Q (cfs)
A	0.084	6.5	2.5	21.0	0.21	0.08	0.23		
B1	0.095	14.0	4.7	18.6	0.46	0.15	0.48		
B2	0.097	6.2	5.8	43.1	0.20	0.19	0.28		
C1	0.189	17.5	5.3	16.8	0.57	0.17	0.60		
C2	0.154	8.3	4.9	30.6	0.27	0.16	0.32		
D1	0.236	9.9	4.9	26.3	0.32	0.16	0.36		
D2	0.108	7.4	2.3	17.3	0.24	0.08	0.25		
D3	0.094	2.2	5.8	69.2	0.07	0.19	0.20		
E	0.167	14.8	3.6	13.7	0.49	0.12	0.50		
F	0.121	11.6	5.4	25.0	0.38	0.18	0.42		
G	0.097	3.8	6.7	60.4	0.12	0.22	0.25		
H	0.136	22.3	9.3	22.6	0.73	0.31	0.79		
I	0.200	33.5	5.5	9.3	1.10	0.18	1.11		
Down5	0.080	1.4	14.5	84.5	0.05	0.48	0.48	0.08	0.11
Down4	0.148	49.0	21.6	23.8	1.61	0.71	1.76	0.52	0.78
Down3	0.173	29.6	15.8	28.1	0.97	0.52	1.10	0.38	0.57
Down2	0.194	31.7	10.8	18.8	1.04	0.35	1.10	0.43	0.64
Down1	0.187	30.4	5.3	9.9	1.00	0.17	1.01	0.38	0.57

Table AIII.6. (Continued)

Velocity Data - 100 Year Flood

Location	Measurement Depth (ft)	X vel (cm/s)	Y vel (cm/s)	Angle with X-Axis (deg)	X vel (ft/s)	Y vel (ft/s)	Current Velocity (ft/s)	q (cfs/ft)	Q (cfs)
A	0.088	4.4	6.0	53.7	0.14	0.20	0.24		
B1	0.098	17.8	5.5	17.2	0.58	0.18	0.61		
B2	0.101	4.9	5.3	47.2	0.16	0.17	0.24		
C1	0.192	19.2	5	14.6	0.63	0.16	0.65		
C2	0.157	5.0	6.3	51.6	0.16	0.21	0.26		
D1	0.238	12.3	4.8	21.3	0.40	0.16	0.43		
D2	0.114	7.9	5.5	34.8	0.26	0.18	0.32		
D3	0.098	3.0	6.8	66.2	0.10	0.22	0.24		
E	0.170	17.0	3.9	12.9	0.56	0.13	0.57		
F	0.126	13.8	4.9	19.5	0.45	0.16	0.48		
G	0.104	4.3	7.2	59.2	0.14	0.24	0.28		
H	0.146	23.3	8.3	19.6	0.76	0.27	0.81		
I	0.206	31.5	6.9	12.4	1.03	0.23	1.06		
Down5	0.087	7.2	10.8	56.3	0.24	0.35	0.43	0.07	0.11
Down4	0.166	59.0	34.0	30.0	1.94	1.12	2.23	0.74	1.11
Down3	0.180	30.4	15.2	26.6	1.00	0.50	1.12	0.40	0.60
Down2	0.201	33.8	11.2	18.3	1.11	0.37	1.17	0.47	0.70
Down1	0.198	24.7	7.3	16.5	0.81	0.24	0.85	0.33	0.50

Table AIII.6. (Continued)

Velocity Data - 500 Year Flood

Location	Measurement Depth (ft)	X vel (cm/s)	Y vel (cm/s)	Angle with X-Axis (deg)	X vel (ft/s)	Y vel (ft/s)	Current Velocity (ft/s)	q (cfs/ft)	Q (cfs)
A	0.102	7.3	5.1	34.9	0.24	0.17	0.29		
B1	0.109	18.1	3.5	10.9	0.59	0.11	0.60		
B2	0.114	6.3	4.0	32.4	0.21	0.13	0.24		
C1	0.203	17.8	1.8	5.8	0.58	0.06	0.59		
C2	0.168	9.4	5.0	28.0	0.31	0.16	0.35		
D1	0.249	14.2	1.1	4.4	0.47	0.04	0.47		
D2	0.122	6.2	8.2	52.9	0.20	0.27	0.34		
D3	0.108	3.8	4.9	52.2	0.12	0.16	0.20		
E	0.181	17.8	-0.8	-2.6	0.58	-0.03	0.58		
F	0.138	13.5	1.4	5.9	0.44	0.05	0.45		
G	0.116	5.1	8.6	59.3	0.17	0.28	0.33		
H	0.168	22.9	1.1	2.8	0.75	0.04	0.75		
I	0.240	28.3	-0.8	-1.6	0.93	-0.03	0.93		
Down5	0.125	23.3	14.5	31.9	0.76	0.48	0.90	0.23	0.34
Down4	0.194	40.0	14.7	20.2	1.31	0.48	1.40	0.54	0.81
Down3	0.211	28.2	5.9	11.8	0.93	0.19	0.95	0.40	0.60
Down2	0.231	32.8	1.6	2.8	1.08	0.05	1.08	0.50	0.75
Down1	0.223	24.9	-0.9	-2.1	0.82	-0.03	0.82	0.36	0.55

Table AIII.7. Stage Data - Alternative III (2-Sided Spillway)

Gaging Data - 2 Year Flood

Date		3/10/97		
Flow	Field	5700	Model	1.16
Manometer Displacement		4.91		
Gage F	Elevation	661.8	Depth	0.28

Gage Designation	Point Gage Depth (model, ft)	Water Depth (prototype, ft)	Bed Elevation (prototype, ft)	Water Surface (prototype, ft)
A	0.094	2.82	664.69	667.51
B1	0.119	3.57	664.06	667.63
B2	0.119	3.57	663.83	667.40
C1	0.304	9.12	658.20	667.32
C2	0.233	6.99	660.23	667.22
D1	0.382	11.46	655.94	667.40
D2	0.144	4.32	663.20	667.52
D3	0.108	3.24	664.06	667.30
G	0.12	3.6	663.52	667.12
H	0.153	4.59	657.74	662.33
I	0.28	8.4	653.52	661.92

Gaging Data - 10 Year Flood

Date		3/10/97		
Flow	Field	8500	Model	1.72
Manometer Displacement		10.91		
Gage F	Elevation	663.5	Depth	0.33

Gage Designation	Point Gage Depth (model, ft)	Water Depth (prototype, ft)	Bed Elevation (prototype, ft)	Water Surface (prototype, ft)
A	0.112	3.36	664.69	668.05
B1	0.128	3.84	664.06	667.90
B2	0.14	4.2	663.83	668.03
C1	0.323	9.69	658.20	667.89
C2	0.254	7.62	660.23	667.85
D1	0.4	12	655.94	667.94
D2	0.162	4.86	663.20	668.06
D3	0.126	3.78	664.06	667.84
G	0.145	4.35	663.52	667.87
H	0.203	6.09	657.74	663.83
I	0.33	9.9	653.52	663.42

Table AIII.7. (Continued)

Gaging Data - 50 Year Flood

Date		3/10/97		
Flow	Field	12500	Model	2.54
Manometer Displacement		23.60		
Gage F	Elevation	665.6	Depth	0.40

Gage Designation	Point Gage Depth (model, ft)	Water Depth (prototype, ft)	Bed Elevation (prototype, ft)	Water Surface (prototype, ft)
A	0.136	4.08	664.69	668.77
B1	0.166	4.98	664.06	669.04
B2	0.158	4.74	663.83	668.57
C1	0.345	10.35	658.20	668.55
C2	0.279	8.37	660.23	668.60
D1	0.419	12.57	655.94	668.51
D2	0.172	5.16	663.20	668.36
D3	0.157	4.71	664.06	668.77
G	0.166	4.98	663.52	668.50
H	0.268	8.04	657.74	665.78
I	0.4	12	653.52	665.52

Gaging Data - 100 Year Flood

Date		3/10/97		
Flow	Field	13500	Model	2.74
Manometer Displacement		27.52		
Gage F	Elevation	666	Depth	0.42

Gage Designation	Point Gage Depth (model, ft)	Water Depth (prototype, ft)	Bed Elevation (prototype, ft)	Water Surface (prototype, ft)
A	0.142	4.26	664.69	668.95
B1	0.171	5.13	664.06	669.19
B2	0.167	5.01	663.83	668.84
C1	0.354	10.62	658.20	668.82
C2	0.288	8.64	660.23	668.87
D1	0.437	13.11	655.94	669.05
D2	0.184	5.52	663.20	668.72
D3	0.162	4.86	664.06	668.92
G	0.171	5.13	663.52	668.65
H	0.286	8.58	657.74	666.32
I	0.42	12.6	653.52	666.12

Table AIII.7. (Continued)

Gaging Data - 500 Year Flood

Date		3/10/97		
Flow	Field	17630	Model	3.58
Manometer Displacement		46.94		
Gage F	Elevation	667.8	Depth	0.48

Gage Designation	Point Gage Depth (model, ft)	Water Depth (prototype, ft)	Bed Elevation (prototype, ft)	Water Surface (prototype, ft)
A	0.179	5.37	664.69	670.06
B1	0.196	5.88	664.06	669.94
B2	0.203	6.09	663.83	669.92
C1	0.39	11.7	658.20	669.90
C2	0.315	9.45	660.23	669.68
D1	0.466	13.98	655.94	669.92
D2	0.211	6.33	663.20	669.53
D3	0.199	5.97	664.06	670.03
G	0.211	6.33	663.52	669.85
H	0.349	10.47	657.74	668.21
I	0.48	14.4	653.52	667.92

Table AIII.8 Model velocity data - Alternative III (2-Sided Spillway)

Velocity and Flow Spit Data - Calibration Flow

Location	Measurement Depth (ft)	X vel (cm/s)	Y vel (cm/s)	Angle with X-Axis (deg)	X vel (ft/s)	Y vel (ft/s)	Current Velocity (ft/s)	q (cfs/ft)	Q (cfs)
LLane1	0.074	6.2	-0.9	-8.3	0.20	-0.03	0.21	0.03	0.05
LLane2	0.156	6.4	-1.0	-8.9	0.21	-0.03	0.21	0.07	0.10
LLane3	0.147	6.4	-1.1	-9.8	0.21	-0.04	0.21	0.06	0.09
LLane4	0.144	7.2	-0.3	-2.4	0.24	-0.01	0.24	0.07	0.10
LLane5	0.178	7.3	0.2	1.6	0.24	0.01	0.24	0.09	0.13
LLane6	0.179	8.0	0.5	3.6	0.26	0.02	0.26	0.09	0.19
RLane1	0.146	8.6	-3.8	-23.8	0.28	-0.12	0.31	0.09	0.14
RLane2	0.163	6.2	-2.9	-25.1	0.20	-0.10	0.22	0.07	0.11
RLane3	0.126	6.5	-2.1	-17.9	0.21	-0.07	0.22	0.06	0.08
RLane4	0.095	6.0	-2.1	-19.3	0.20	-0.07	0.21	0.04	0.06
RLane5	0.069	5.0	-1.4	-15.6	0.16	-0.05	0.17	0.02	0.04
A	Insufficient Depth								
B1	0.059	6.0	-0.9	-8.5	0.20	-0.03			
B2	Insufficient Depth								
C1	0.155	7.2	-1.0	-7.9	0.24	-0.03	0.24		
C2	0.119	6.1	-0.3	-2.8	0.20	-0.01	0.20		
D1	0.193	5.5	-0.5	-5.2	0.18	-0.02	0.18		
D2	0.073	7.9	2.1	14.9	0.26	0.07	0.27		
D3	Insufficient Depth								
G	0.062	0.2	0.8	76.0	0.01	0.03	0.03		
H	0.078	16.5	-0.2	-0.7	0.54	-0.01	0.54		
I	0.145	20.3	-1.4	-3.9	0.67	-0.05	0.67		
Down5	Insufficient Depth								
Down4	0.104	19.0	1.9	5.7	0.62	0.06	0.63	0.13	0.39
Down3	0.119	18.9	1.6	4.8	0.62	0.05	0.62	0.15	0.22
Down2	0.141	23.9	1.8	4.3	0.78	0.06	0.79	0.22	0.33
Down1	0.134	20.0	-1.9	-5.4	0.66	-0.06	0.66	0.18	0.26

Table AIII.8. (Continued)

Velocity Data - 2 Year Flood

Location	Measurement Depth (ft)	X vel (cm/s)	Y vel (cm/s)	Angle with X-Axis (deg)	X vel (ft/s)	Y vel (ft/s)	Current Velocity (ft/s)	q (cfs/ft)	Q (cfs)
A	Insufficient Depth								
B1	Insufficient Depth								
B2	Insufficient Depth								
C1	0.152	7.1	1.1	8.8	0.23	0.04	0.24		
C2	0.117	7.5	2.2	16.3	0.25	0.07	0.26		
D1	0.191	4.9	1.9	21.2	0.16	0.06	0.17		
D2	0.072	8.1	3.0	20.3	0.27	0.10	0.28		
D3	Insufficient Depth								
G	0.060	2.0	0.8	21.8	0.07	0.03	0.07		
H	0.077	15.3	2.9	10.7	0.50	0.10	0.51		
I	0.140	22.1	1.1	2.8	0.73	0.04	0.73		
Down5	Insufficient Depth								
Down4	0.099	20.6	4.2	11.5	0.68	0.14	0.69	0.14	0.41
Down3	0.114	21.7	4.9	12.7	0.71	0.16	0.73	0.17	0.25
Down2	0.135	25.1	3.1	7.0	0.82	0.10	0.83	0.22	0.34
Down1	0.129	21.8	1.1	2.9	0.72	0.04	0.72	0.18	0.28

Table AIII.8. (Continued)

Velocity Data - 10 Year Flood

Location	Measurement Depth (ft)	X vel (cm/s)	Y vel (cm/s)	Angle with X-Axis (deg)	X vel (ft/s)	Y vel (ft/s)	Current Velocity (ft/s)	q (cfs/ft)	Q (cfs)
A	Insufficient Depth								
B1	0.064	8.5	0.9	6.0	0.28	0.03	0.28		
B2	0.070	7.8	2.4	17.1	0.26	0.08	0.27		
C1	0.162	10.6	0.2	1.1	0.35	0.01	0.35		
C2	0.127	14.2	2.9	11.5	0.47	0.10	0.48		
D1	0.200	7.2	1.9	14.8	0.24	0.06	0.24		
D2	0.081	11.0	3.9	19.5	0.36	0.13	0.38		
D3	0.063	2.0	3.0	56.3	0.07	0.10	0.12		
G	0.073	1.5	3.0	63.4	0.05	0.10	0.11		
H	0.102	21.1	1.9	5.1	0.69	0.06	0.70		
I	0.165	27.0	1.7	3.6	0.89	0.06	0.89		
Down5	Insufficient Depth								
Down4	0.126	28.2	5.1	10.3	0.93	0.17	0.94	0.24	0.47
Down3	0.140	28.2	5.1	10.3	0.93	0.17	0.94	0.26	0.39
Down2	0.156	30.3	4.5	8.4	0.99	0.15	1.00	0.31	0.47
Down1	0.155	24.9	1.9	4.4	0.82	0.06	0.82	0.25	0.38

Table AIII.8. (Continued)

Velocity Data - 50 Year Flood

Location	Measurement Depth (ft)	X vel (cm/s)	Y vel (cm/s)	Angle with X-Axis (deg)	X vel (ft/s)	Y vel (ft/s)	Current Velocity (ft/s)	q (cfs/ft)	Q (cfs)
A	0.068	6.3	1.2	10.8	0.21	0.04	0.21		
B1	0.083	13.7	-1.7	-7.1	0.45	-0.06	0.45		
B2	0.079	8.3	-0.8	-5.5	0.27	-0.03	0.27		
C1	0.173	15.0	-1.1	-4.2	0.49	-0.04	0.49		
C2	0.140	10.5	1.1	6.0	0.34	0.04	0.35		
D1	0.210	9.7	-0.6	-3.5	0.32	-0.02	0.32		
D2	0.086	12.4	1.8	8.3	0.41	0.06	0.41		
D3	0.079	0.8	1.2	56.3	0.03	0.04	0.05		
G	0.083	2.9	2.4	39.6	0.10	0.08	0.12		
H	0.134	22.6	1.4	3.5	0.74	0.05	0.74		
I	0.200	28.0	-0.3	-0.6	0.92	-0.01	0.92		
Down5	0.095	26.7	-0.4	-0.9	0.88	-0.01	0.88	0.17	0.25
Down4	0.165	32.4	3.1	5.5	1.06	0.10	1.07	0.35	0.53
Down3	0.175	30.6	4.1	7.6	1.00	0.13	1.01	0.35	0.53
Down2	0.194	28.8	2.4	4.8	0.94	0.08	0.95	0.37	0.55
Down1	0.191	24.4	-0.5	-1.2	0.80	-0.02	0.80	0.31	0.46

Table AIII.8. (Continued)

Velocity Data - 100 Year Flood

Location	Measurement Depth (ft)	X vel (cm/s)	Y vel (cm/s)	Angle with X-Axis (deg)	X vel (ft/s)	Y vel (ft/s)	Current Velocity (ft/s)	q (cfs/ft)	Q (cfs)
A	0.071	6.8	1.0	8.4	0.22	0.03	0.23		
B1	0.085	16.6	1.9	6.5	0.54	0.06	0.55		
B2	0.084	8.5	1.2	8.0	0.28	0.04	0.28		
C1	0.177	17.9	1.2	3.8	0.59	0.04	0.59		
C2	0.144	12.1	2.2	10.3	0.40	0.07	0.40		
D1	0.219	12.2	3.0	13.8	0.40	0.10	0.41		
D2	0.092	13.0	3.5	15.1	0.43	0.11	0.44		
D3	0.081	1.3	3.3	68.5	0.04	0.11	0.12		
G	0.086	3.4	3.2	43.3	0.11	0.10	0.15		
H	0.143	26.1	3.9	8.5	0.86	0.13	0.87		
I	0.210	29.8	-0.4	-0.8	0.98	-0.01	0.98		
Down5	0.095	30.5	1.4	2.6	1.00	0.05	1.00	0.19	0.29
Down4	0.168	37.1	4.0	6.2	1.22	0.13	1.22	0.41	0.62
Down3	0.184	33.9	2.3	3.9	1.11	0.08	1.11	0.41	0.62
Down2	0.202	31.8	1.8	3.2	1.04	0.06	1.04	0.42	0.63
Down1	0.194	31.3	1.2	2.2	1.03	0.04	1.03	0.40	0.60

Table AIII.8. (Continued)

Velocity Data - 500 Year Flood

Location	Bottom (ft)	Top (ft)	Measurement Depth (ft)	X vel (cm/s)	Y vel (cm/s)	Angle with X-Axis (deg)	X vel (ft/s)	Y vel (ft/s)	Current Velocity (ft/s)	q (cfs/ft)	Q (cfs)
A	1.232	1.411	0.090	7.2	-0.3	-2.4	0.24	-0.01	0.24		
B1	1.227	1.423	0.098	19.5	-1.0	-2.9	0.64	-0.03	0.64		
B2	1.188	1.391	0.102	9.9	0.2	1.2	0.32	0.01	0.32		
C1	1.043	1.433	0.195	18.5	-1.2	-3.7	0.61	-0.04	0.61		
C2	1.089	1.404	0.158	14.1	1.0	4.1	0.46	0.03	0.46		
D1	0.947	1.413	0.233	14.9	0.2	0.8	0.49	0.01	0.49		
D2	1.222	1.433	0.106	15.0	2.5	9.5	0.49	0.08	0.50		
D3	1.186	1.385	0.100	6.9	0.7	5.8	0.23	0.02	0.23		
G	1.205	1.416	0.106	6.9	3.6	27.6	0.23	0.12	0.26		
H	1.000	1.349	0.175	22.6	1.5	3.8	0.74	0.05	0.74		
I	0.839	1.319	0.240	33.8	2.8	4.7	1.11	0.09	1.11		
Down5	1.055	1.310	0.128	36.8	11.5	17.4	1.21	0.38	1.26	0.32	0.48
Down4	0.917	1.323	0.203	37.2	9.2	13.9	1.22	0.30	1.26	0.51	0.77
Down3	0.893	1.328	0.218	39.9	7.7	10.9	1.31	0.25	1.33	0.58	0.87
Down2	0.852	1.326	0.237	34.3	4.9	8.1	1.13	0.16	1.14	0.54	0.81
Down1	0.867	1.327	0.230	31.1	3.1	5.7	1.02	0.10	1.03	0.47	0.71

Appendix IV

Table AIV.1. Summary of spillway dimensions and bedrock flow contributions

	Alternative I (Bathtub Spillway)	Alternative II (Rock Dam)	Alternative III (2-Sided Spillway)
Spillway Cross-Sectional Dimensions (ft)			
Crest Elevation	665.0	665.9	665.5
Toe Elevation	659.0	656.1	657.0
Height	6.0	9.8	8.5
Width	14.0	39.0	13.5
Spillway Length (ft)			
Left Side Straight	169		289
Right Side Straight	122		297
Bathtub Sides	264		
Bathtub Head	113		
Total	**668**	**373**	**586**
***Length of Bedrock Flow Contribution (ft)**			
2 Year	**140	**156	0
10 Year	**152	**237	0
50 Year	**230	**270	95
100 Year	**250	**277	110
500 Year	**278	**308	180

* Data for Alternative I and II estimated from photographic material.

** Includes length of flow over existing, broken retaining wall (~115 ft).